A SHORT COURSE IN
FOUNDATION ENGINEERING

2ND EDITION

NOEL SIMONS and BRUCE MENZIES

Thomas Telford

First published 1975 by IPC Science and Technology Press, and then in 1977 by Butterworth Scientific
This edition published by Thomas Telford Publishing, Thomas Telford Ltd, 1 Heron Quay, London E14 4JD.
URL: http://www.t-telford.co.uk

Reprinted 2001

Distributors for Thomas Telford books are
USA: ASCE Press, 1801 Alexander Bell Drive, Reston, VA 20191-4400, USA
Japan: Maruzen Co. Ltd, Book Department, 3–10 Nihonbashi 2-chome, Chuo-ku, Tokyo 103
Australia: DA Books and Journals, 648 Whitehorse Road, Mitcham 3132, Victoria

Cover photograph of the Tower of Pisa by kind permission of Professor John Burland

A catalogue record for this book is available from the British Library

ISBN: 0 7277 2751 6

Typeset by Academic + Technical, Bristol
Printed and bound in Great Britain by MPG Books, Bodmin

Dedication

Laurits Bjerrum
1918–1973

Mentor and friend whose outstanding contributions to geotechnical engineering have influenced the lives of many of us.

Preface (first edition)

This book is based on a series of lectures given to practising civil engineers attending residential courses on foundation engineering at the University of Surrey, UK. Attention has been concentrated on methods for predicting the failure loads, and the deformations at working loads, of piled and non-piled foundations. It must be emphasized that a knowledge of these methods alone will not enable an engineer to become a reliable practitioner of the art of foundation engineering. Peck (1962) has listed the attributes necessary for the successful practice of subsurface engineering as follows:

- a knowledge of precedents,
- a working knowledge of geology,
- familiarity with soil mechanics.

By concentrating on the third point (because of time and space limitations) the authors are not suggesting that it is the most significant factor. Without doubt, a knowledge of precedents is by far the most important; such experience is a necessary and priceless asset of a good foundation engineer. Also, a working knowledge of geology is as basic to foundation engineering as is familiarity with soil mechanics' methods. It makes one aware of the departures from reality inherent in simplifying assumptions which have to be made before computations can be performed. The geology of a site must be understood before any reasonable assessment can be made of the errors involved in calculations and predictions. Moreover, intelligent subsurface exploration is impossible without a working knowledge of geology.

It is hoped that this book will reflect the authors' experience of teaching, research and consulting and may, therefore, appeal to both students and practising engineers.

The book is written in the belief that brevity is a virtue. To facilitate the extraction and use of information the authors have endeavoured to concentrate information in tables and in charts.

The book uses SI units. Gravitational units have been used throughout with weight per unit volume being expressed as unit weight (kN/m^3) rather than in terms of mass density (Mg/m^3). As a helpful simplification, the unit weight of water is taken as 10 kN/m^3.

The authors are most grateful to Margaret Harris who did the drawings, and to Corrie Niemantsverdriet and Carole Cox who typed the script.

Noel Simons, Bruce Menzies
University of Surrey
Guildford 1975

Preface (second edition)

Since we wrote the first edition some 25 years ago, the single biggest change in design offices has been the appearance of PCs on design engineer's desks. There are now a large number of computer programs for solving all sorts of foundation design problems from bearing capacity and slope stability to settlement prediction and pile group design. In our view, the need for engineers to be able to carry out calculations by hand is as important as ever. There has always been a responsibility on the design engineer to verify test data and soil parameters. Now design engineers must be able to verify the results of quite sophisticated computer programs. For these reasons we continue to concentrate data and information in the form of tables and charts as well as illustrate design methods with worked examples. We have extended and updated the content to include major new sections on short term and long term stability, critical state interpretation of peak strength, seismic methods for measuring ground stiffness in situ, and offshore pile design: total stress and effective stress approaches. Above all, it is the prime aim of this book to provide engineers with the means to check that ground properties (inputs) and design predictions (outputs) collectively pass the 'sanity test'!

Noel Simons, Bruce Menzies
University of Surrey
Guildford 1999

Acknowledgements

We warmly thank our colleagues at the University of Surrey for all their help and advice over many years: Chris Clayton, Marcus Matthews, Mike Huxley, Mike Gunn, Vicki Hope and Rick Woods. We also gratefully acknowledge the help of Suzanne Lacasse, Toralv Berre, Ken Been, John Atkinson, Shamsher Prakash, Diego Lo Presti, Charles Ng and Dick Chandler – without whom our 'Fifteen Commandments of Triaxial Testing' would have numbered ten! We also thank William Powrie for permission to reproduce material from his book *Soil Mechanics: Concepts and Applications*. We are most grateful to Mark Randolph, John Pelletier, Kjell Karlsrud, and Mark Finch for advice on offshore pile design. Of course, the comments expressed in this book are those of the authors and do not necessarily reflect the views of any of the above.

We acknowledge permission from Taylor & Francis Books Ltd to publish Figures 2.21 and 2.25 and sections of pages 57 and 60 from *Soil Mechanics: Concepts and Applications* by William Powrie, published by E & FN Spon, 1997.

We acknowledge permission from The Offshore Technology Conference to publish Figures 1 and 2 and extracts from pages 255, 256, 257 and 263 of OTC 7157 *Historical development and assessment of the current API design methods for axially loaded piles* by J. H. Pelletier, J. D. Murff and A. C.Young presented at the 25th Annual OTC in Houston, Texas, USA, 3–6 May 1993.

Contents

Recommended list of units, unit abbreviations, quantity symbols and conversion factors for use in soil and rock mechanics.

Part 1. SI base units, derived units and multiples.

Quantity and symbol	Units and multiples	Unit abbreviations	Conversion factors for existing units	Remarks
Length (various)	kilometre metre millimetre micrometre	km m mm μm	1 mile = 1.609 km 1 yard = 0.9144 m 1 ft = 0.3048 m 1 in = 25.40 mm	 1 micrometre = 1 micron
Area (A)	square kilometre square metre square millimetre	km^2 m^2 mm^2	1 $mile^2$ = 2.590 km^2 1 yd^2 = 0.8361m^2 1 ft^2 = 0.09290 m^2 1 in^2 = 645.2 mm^2	
Volume (V)	cubic metre cubic centimetre cubic millimetre	m^3 cm^3 mm^3	1 yd^3 = 0.7646 m^3 1 ft^3 = 0.02832 m^3 1 in^3 = 16.39 cm^3 1 UK gallon = 4546 cm^3	 To be used for solids and liquids
Mass (m)	megagram (or tonne) kilogram gram	Mg (t) kg g	1 ton = 1.016 Mg 1 lb = 0.4536 kg	 Megagram is the SI term
Unit weight (γ)	kilonewton per cubic metre	kN/m^3	100 lb/ft^3 = 15.708 kN/m^3 (62.43 lb/ft^3 pure water = 9.807 kN/m^3 = specific gravity 1.0 approx.)	Unit weight is weight per unit volume
Force (various)	Meganewton kilonewton Newton	MN kN N	1 tonf = 9.964 kN 1 lbf = 4.448 N 1 kgf = 9.807 N	
Pressure (p, u)	Meganewton per square metre Megapascal	MN/m^2 MPa	1 $tonf/in^2$ = 15.44 MN/m^2 (1 MN/m^2 = 1 N/mm^2)	To be used for shear strength, compressive strength, bearing capacity, elastic moduli and laboratory pressures of rock
Stress (σ, τ) and Elastic moduli (E, G, K)	kilonewton per square metre kilopascal	kN/m^2 kPa	1 lbf/in^2 = 6.895 N/m^2 1 lbf/ft^2 = 0.04788 kPa 1 $tonf/ft^2$ = 107.3 kPa 1 bar = 100 kPa 1 kgf/cm^2 = 98.07 kPa	Ditto for soils

Quantity and symbol	Units and multiples	Unit abbreviations	Conversion factors for existing units	Remarks
Coefficient of volume compressibility (m_v) or swelling (m_s)	square metre per meganewton square metre per kilonewton	m^2/MN m^2/kN	$1\,ft^2/tonf = 9.324\,m^2/MN = 0.009324\,m^2/kN$	
Coefficient of water permeability (kw)	metre per second	m/s	$1\,cm/s = 0.01\,m/s$	This is a velocity, depending on temperature and defined by Darcy's law $V = k_w \frac{\delta h}{\delta s}$ V = velocity of flow $\frac{\delta h}{\delta s}$ = hydraulic gradient
Absolute permeability (k)	square micrometre	μm^2	$1\,Darcy = 0.9869\,\mu m^2$	This is an area which quantifies the seepage properties of the ground independently of the fluid concerned or its temperature $V = \frac{kpg}{\eta} \frac{\delta h}{\delta s}$ p = fluid density g = gravitational acceleration η = dynamic viscosity
Dynamic viscosity (η)	millipascal second (centipoise)	mPas (cP)	$1\,cP = 1\,mPas$ ($1\,Pa = 1\,N/m^2$)	Dynamic viscosity is defined by Stokes' Law. A pascal is a kilonewton per square metre
Kinematic viscosity (ν)	square millimetre per second (centistoke)	mm^2/s (cSt)	$1\,cSt = 1\,mm^2/s$	$\nu = \eta/\rho$
Celsius temperature (t)	degree Celsius	°C	$t°F = 5(t - 32)/9°C$	The Celsius temperature t is equal to the difference $t = T - T_0$ between two thermodynamic temperatures T and T_0 where $T_0 = 273.15\,K$ (K = Kelvin)

Part 2. Other units

Quantity and symbol	Units and multiples	Unit abbreviations	Conversion factors for existing units	Remarks
Plane angle (various)	Degree Minute second (angle)	$^\circ$ $'$ $''$		To be used for angle of shearing resistance (ϕ) and for slopes
Time (t)	year	year	$1\,\text{year} = 31.557 \times 10^6\,\text{s}$	'a' is the abbreviation for year
	day	d	$1\,\text{d} = 86.40 \times 10^3\,\text{s}$	
	hour	h	$1\,\text{h} = 3600\,\text{s}$	
	second (time)	s		The second (time) is the SI unit
Coefficient of consolidation (c_v) or swelling (c_s)	square metre per year	m^2/year	$1\,ft^2/\text{year} = 0.09290$ m^2/year	

Dedication

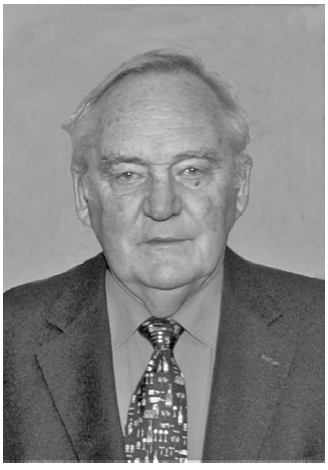

Professor Noel Simons FREng, 1931–2006

Noel Simons, who developed the University of Surrey into one of the UK's leading centres of geotechnical learning and research, and who inspired the *Short Course Series* of geotechnical books, died on August 10th 2006. He was aged 75.

He was not only a wonderful teacher, mentor, colleague and co-author, but was also a dear friend. This book is dedicated to his memory.

CHAPTER ONE

Effective stress and short term and long term stability

> *'The stresses in any point of a section through a mass of soil can be computed from the* total principal stresses σ_1, σ_2, σ_3 *which act in this point. If the voids of the soil are filled with water under a stress u, the total principal stresses consist of two parts. One part, u, acts in the water* and *in the solid in every direction with equal intensity. It is called the* neutral stress *(or the pore water pressure). The balance* $\sigma'_1 = \sigma_1 - u$, $\sigma'_2 = \sigma_2 - u$, *and* $\sigma'_3 = \sigma_3 - u$ *represents an excess over the neutral stress u and it has its seat exclusively in the solid phase of the soil.*
>
> *This fraction of the total principal stresses will be called the* effective principal stresses *. . . . A change in the neutral stress u produces practically no volume change and has practically no influence on the stress conditions for failure . . . . Porous materials (such as sand, clay and concrete) react to a change of u as if they were incompressible and as if their internal friction were equal to zero. All the measurable effects of a change of stress, such as compression, distortion and a change of shearing resistance are* exclusively *due to changes in the effective stresses* σ'_1, σ'_2, *and* σ'_3. *Hence every investigation of the stability of a saturated body of soil requires the knowledge of both the total and the neutral stresses.'*
>
> **Karl Terzaghi (1936).**

Definition of effective stress

Effective stress in any direction is defined as the difference between the total stress in that direction and the pore-water pressure. The term *effective stress* is, therefore, a misnomer, its meaning being a stress difference.

As pointed out by Skempton (1960), even the work of the great pioneers of soil mechanics like Coulomb, Collin, Rankine, Rasal, Bell and Forchheimer was of limited validity owing to the absence of the unifying principle of effective stress. Like all truly basic ideas the concept of effective stress is deceptively simple and yet its full significance has become apparent quite

slowly. The concept was glimpsed by Lyell (1871), Boussinesq (1876) and Reynolds (1886) and observed by Fillunger (1915), Bell (1915), Westerberg (1921) and Terzaghi and Rendulic (1934). It was Terzaghi (1936) who clearly stated for the first time this basic law governing the mechanical properties of porous materials. It is remarkable therefore that even to this day the principle of effective stress is imperfectly and cursorily explained in many undergraduate textbooks and, probably as a result of this, imperfectly known and understood by many practising engineers.

The nature of effective stress

Soil is a skeletal structure of solid particles in contact, forming an interstitial system of interconnecting voids or pores. The pores are filled partially or wholly with water. The interaction between the soil structure and the pore fluid determines the unique time-dependent engineering behaviour of the soil mass.

The deformability of a soil subjected to loading or unloading is, in the main, its capacity to deform the voids, usually by displacement of water. The strength of a soil is its ultimate resistance to such loading.

Shear stresses can be carried only by the structure of solid particles, the water having no shear strength. On the other hand, the normal stress on any plane is the sum of two components: owing to both the load transmitted by the solid particles of the soil structure and to the pressure in the fluid in the void space (Bishop and Henkel, 1962).

The deformability and strength of a soil are dependent on the difference between the applied external total loading stress, σ, and the pore water pressure, u. This difference is termed the *effective stress* and is written $(\sigma - u)$.

The physical nature of this parameter may be intuitively understood by considering the saturated soil bounded by a flexible impermeable membrane as shown in Fig. 1.1 The external applied total pressure is σ normal to the boundary. The pore water pressure is u $(<\sigma)$ which, being

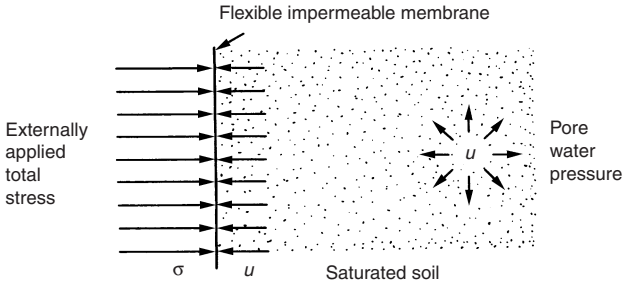

Fig. 1.1 Intuitive soil model demonstrating the nature of effective stress

a hydrostatic pressure, acts with equal intensity in all directions, giving a pressure of u normal to the boundary. By examining the stresses normal to the boundary it may be seen by inspection that the disparity in stresses $(\sigma - u)$ is transmitted across the boundary into the soil structure, assuming an equilibrium condition. Thus, *the effective stress* $(\sigma - u)$ *is a measure of the loading transmitted by the soil structure*.

The principle of effective stress

The principle of effective stress was stated by Bishop (1959) in terms of two simple hypotheses:

- Volume change and deformation in soils depends on the difference between the total stress and the pressure set up in the fluid in the pore space, not on the total stress applied. This leads to the expression

  $$\sigma' = \sigma - u \tag{1.1}$$

  where σ denotes the total normal stress, u denotes the pore pressure, and σ' is termed the effective stress.
- Shear strength depends on the effective stress, not on the total normal stress on the plane considered. This may be expressed by the equation

  $$\tau_f = c' + \sigma' \tan \phi' \tag{1.2}$$

  where τ_f denotes the shear strength, σ' the effective stress on the plane considered, c' the cohesion intercept, ϕ' the angle of shearing resistance, with respect to effective stress.

The principle of effective stress, as expressed above, has proved to be vital in the solution of practical problems in soil mechanics.

To explore more rigorously the physical nature of effective stress, consider the forces acting across a surface X–X in the soil which approximates to a plane but passes always through the pore space and points of contact of the soil particles (Bishop, 1959) as shown in Fig. 1.2.

Normal stress is then equal to the average force perpendicular to this plane, per unit area, and areas are considered as projected onto the plane.

Let

σ denote the total normal stress on this plane,
σ'_i the average intergranular normal force per unit area of the plane,
u the pore water pressure,
a the effective contact area of the soil particles per unit area of the plane.

It follows that $\sigma = \sigma'_i + (1 - a)u$ whence

$$\sigma'_i = (\sigma - u) + au \tag{1.3}$$

Thus the effective stress $(\sigma - u)$ is not exactly equal to the average intergranular force per unit area of the plane, σ'_i, and is dependent on the contact

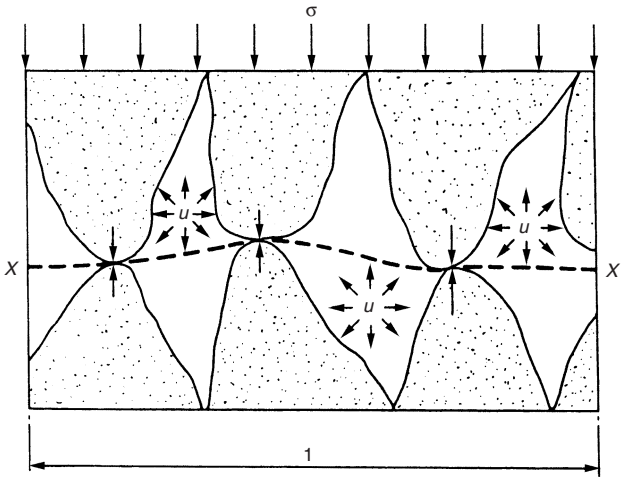

Fig. 1.2 Interparticle forces acting across a surface X–X

area between the particles. Although this area may be small it cannot be zero as this would imply infinite local contact stresses between the particles.

Consider now the deformations at the contact between two soil particles also acted on by pore water pressure (Fig. 1.3).

The force system may be regarded as being made up of two components. If P is the average force per contact and there are N contacts per unit area, then the intergranular force per unit area of the plane X–X space is

$$\sigma'_{\mathrm{i}} = NP \tag{1.4}$$

Now if a homogeneous isotropic soil particle is subjected to an isotropic stress, u, over its whole surface, the deformation incurred is a small elastic reduction in particle volume without any change in shape. The soil skeleton as a whole, therefore, also reduces slightly in volume without change in shape.

The compressibility of the skeletal structure of the soil, however, is very much greater than the compressibility of the individual soil particles of which it is comprised. Hence it is only that part of the local contact stress which is in excess of the pore water pressure that actually causes

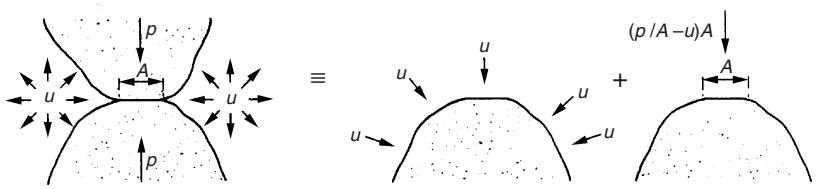

Fig. 1.3 Separation of interparticle force components

a structural deformation by volumetric strain or by shear strain or by both. This excess stress which controls structural deformation is equal to $(P/A - u)$ where A is the area of the particular contact. By summing the corresponding components of excess inter particle force an expression is obtained for σ' defined as that part of the normal stress which controls volume change due to deformation of the soil structure, whence the excess force per unit of the plane X–X is

$$\begin{aligned}\sigma' &= N((P/A) - u)A \\ &= NP - uNA \\ &= NP - ua \quad (\text{since } NA = a) \\ &= \sigma_i - au \end{aligned} \tag{1.5}$$

Substituting for σ_i' from equation (1.3) gives

$$\sigma' = (\sigma - u) + au - au$$

or

$$\sigma' = (\sigma - u) \tag{1.6}$$

i.e. the effective stress is that part of the normal total stress which controls deformation of the soil structure, irrespective of the interparticle contact areas. This leads to the interesting conclusion that although the average intergranular force per unit area depends on the magnitude of 'a', volume changes due to deformation of the soil structure depend simply on the stress difference $(\sigma - u)$, whatever the nature of 'a' (Bishop, 1959).

To understand better the nature of effective stress, it is instructive to consider what it is not! It is not the intergranular stress or the intergranular force per unit cross sectional area. To illustrate this point, let the average intergranular stress be σ_g.

For force equilibrium in the vertical direction

$$\sigma A = \sigma_g aA + u(1 - a)A$$

whence

$$\sigma_g = (\sigma - u(1 - a))/a \tag{1.7}$$

To use realistic numbers let $\sigma = 100\,\text{kPa}$, $u = 50\,\text{kPa}$, and let $a = 0.01$ (clay) and 0.3 (lead shot), respectively.

From equation (1.3) $\sigma_i' = 50.5\,\text{kPa}$ and $65\,\text{kPa}$, respectively.

From equation (1.7) $\sigma_g = 5050\,\text{kPa}$ and $216.7\,\text{kPa}$, respectively.

The effective stress is $\sigma' = (\sigma - u) = 50\,\text{kPa}$.

These values are summarized in Table 1.1. It can clearly be seen from Table 1.1 that effective stress is *not* the average intergranular stress and *not* the average intergranular force per unit area. It is simply and *exactly* equal to the total stress less the pore pressure.

Table 1.1 Intergranular force per unit area, intergranular stress and effective stresses for clay and lead shot

Soil type	Intergranular contact area per unit area	Intergranular force per unit area σ_i' kPa	Intergranular stress σ_g kPa	Effective stress $\sigma' = (\sigma - u)$ kPa
Clay	0.01	50.5	5050	50
Lead shot	0.3	65	216.7	50

In an elegant experiment performed on lead shot, Laughton (1955) showed clearly that, in spite of significant contact areas between the particles, volume change and shear strength were still governed by the simple expression for effective stress, namely, $\sigma' = (\sigma - u)$.

The important implication the principle of effective stress has on the strength is that a change in effective stress results in a change of strength, and the corollary follows, that if there is no change in effective stress, then there is no change in strength. While it is true that a change in volume will always be accompanied by a change in effective stress, it is not necessarily true, however, that a change in effective stress will produce a change in volume.

Consider, for example, the undrained triaxial test on a saturated soil. During the test, while there is no change in water content and therefore in volume, the pore pressures do change and alter the vertical or horizontal effective stress, or both. At failure, the effective stress throughout the sample will have changed considerably from that pertaining before the axial loading stage of the test. These changes in effective stress are accompanied by specimen deformation by the change of shape. It follows, therefore, that *the sufficient and necessary condition for a change in the state of effective stress to occur is that the soil structure deforms.* Deformation may occur by volumetric strain, by shear strain or by both. The corollary follows that deformation is induced by a change in the state of effective stress, whether or not there is a change in volume.

This implication of the principle of effective stress is of interest. Consider for example, the interrelation of stress changes in the oedometer or under uniform global loading conditions in the field, for a saturated clay.

Let $\Delta\sigma_v$ be the change in vertical total stress, $\Delta\sigma_h$ be the change in horizontal total stress, and Δu be the change in pore-water pressure. At the moment of applying the vertical stress increment there is no deformation, and it thus follows that there is no change in effective stress in any direction and therefore

$$\Delta u = \Delta\sigma_v = \Delta\sigma_h \tag{1.8}$$

This expression has been proved by Bishop (1958) for soft soils. Bishop (1973) has shown that, for porous materials of very low compressibility, equation (1.8) is modified. Equation (1.8) is valid, of course, independently of the value of the pore pressure parameter, A.

As a consequence of this, during drainage the stress path followed in the oedometer is quite complex. At the start of the consolidation stage, it has been shown that the oedometer ring applies a stress increment to the sample equal to the increment in vertical stress. During consolidation, however, the horizontal stress decreases to a value, at the end of pore pressure dissipation, equal to K_0 times the vertical stress (Simons and Menzies, 1974).

The computation of effective stress

The computation of effective stress requires the separate determination of the total stress, σ, and of the pore water pressure, u. The effective stress is then found as

$$\sigma' = \sigma - u$$

The determination of vertical total stress

Consider the typical *at rest* ground condition shown in Fig. 1.4. This is a *global* loading condition.

Consider an element of soil at a depth D metres. The water level is at the surface. The bulk unit weight of the soil (i.e. including solids and water) is $\gamma\,\text{kN/m}^3$. The total vertical stress σ_v is computed by finding the total weight of a vertical column subtended by unit horizontal area ($1\,\text{m}^2$) at depth D. The weight of this column divided by its base area is $\gamma D\,\text{kPa}$ and is the vertical total stress acting on a horizontal plane at depth D.

The vertical total stress σ_v, and the horizontal total stress σ_h are principal stresses. In general, $\sigma_v \neq \sigma_h$.

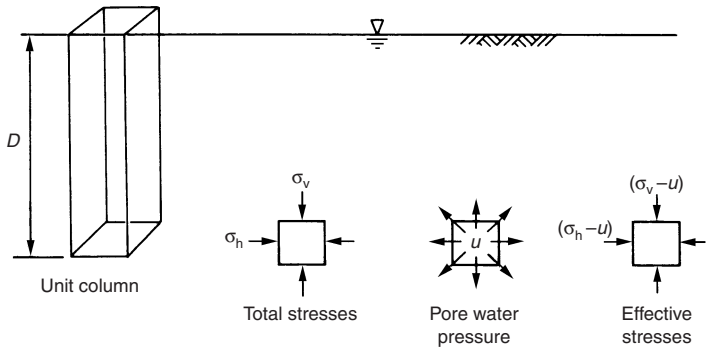

Fig. 1.4 'At rest' in situ stresses due to self-weight of soil

For local loading, the total stresses may be estimated using elastic theory as discussed in Chapter 3.

The determination of pore-water pressure

Referring to Fig. 1.4, the pore-water pressure, u, is found by considering a vertical unit column of water only. The presence of the soil structure has no effect on the pore water pressure. Thus, $u = \gamma_w D$, where γ_w, is the unit weight of water. A helpful approximation is to take $\gamma_w = 10\,\text{kN/m}^3$ (more accurately, $\gamma_w = 9.807\,\text{kN/m}^3$).

For a clay layer rapidly loaded locally, the viscous retardation of pore-water flow in the fine-grained soil gives a build-up of pore pressure. Water will eventually flow out of the zone of loading influence to the ground surface and into surrounding soil unaffected by the loading. This flow or consolidation takes place under the load-induced hydraulic gradient which is itself reduced by the flow as the consolidation of the soil structure allows it to support more load. The law of diminishing returns thus applies and there is an exponential decay in the excess or load-generated pore pressure. This effect is illustrated in Fig. 1.5 where a saturated clay layer is rapidly loaded by the building-up of an embankment. The distribution of pore pressure with time (isochrones) is shown by the relative heights of piezometric head in the piezometers.

In real soils subjected to rapid local loading, the effects of deformation of the soil structure at constant volume, the compressibility of the pore fluid in practice and the dependence of the structural properties of the soil skeleton upon the mean stress, all mean that initially the loading

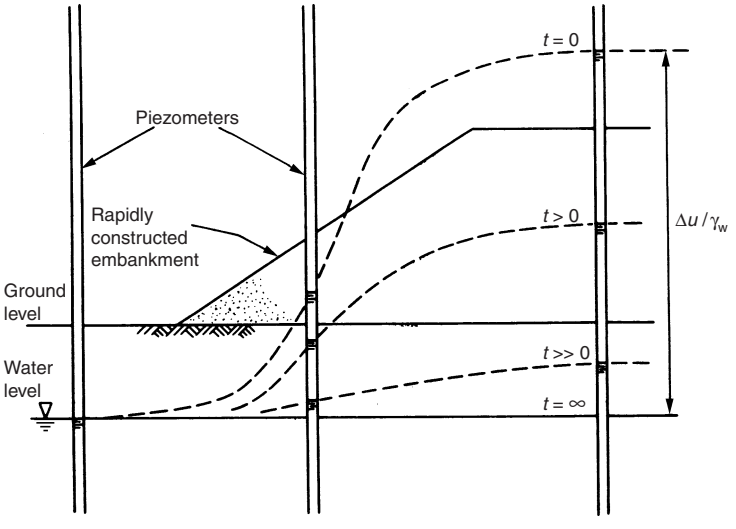

Fig. 1.5 Pore pressure response of a saturated clay to rapid local loading

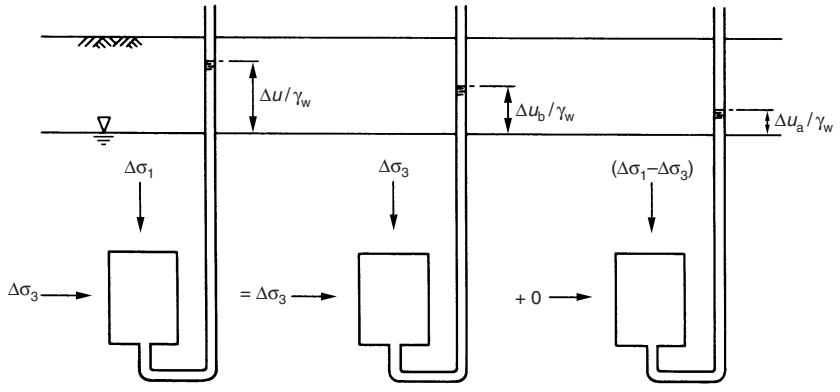

Fig. 1.6 Components of excess pore pressure generated by a loading increment ($\Delta\sigma_1 > \Delta\sigma_2 = \Delta\sigma_3$)

change is shared between the soil structure and the generated pore-pressure change. The generated pore-pressure change is thus not only a function of the loading change but also a function of the soil properties. These properties are experimentally determined and are called the *pore pressure parameters A* and *B*.

Consider the loading increment applied to a cylindrical soil element shown in Fig. 1.6. The loading change is in triaxial compression, the major principal total stress increasing by $\Delta\sigma_1$, while the minor principal (or radial) total stress increases by $\Delta\sigma_3$. An excess pore pressure, i.e. greater than the existing pore pressure, of Δu is generated by the loading increment.

The generalized loading system of Fig. 1.4 may be split into two components consisting of an isotropic change of stress $\Delta\sigma_3$ generating an excess pore pressure Δu_b and a uniaxial change of stress $(\Delta\sigma_1 - \Delta\sigma_3)$ generating an excess pore pressure Δu_a.

By the principle of superposition

$$\Delta u = \Delta u_b + \Delta u_a \tag{1.9}$$

Assuming that the excess pore pressure generated by the loading increment is a simple function of that loading increment we have,

$$\Delta u_b = B\Delta\sigma_3 \tag{1.10}$$

and

$$\Delta u_a = \bar{A}(\Delta\sigma_1 - \Delta\sigma_3) \tag{1.11}$$

where $\bar{A}$ and B are experimentally determined pore-pressure parameters.

Thus, the total pore pressure change is made up of two components: one that is B times the isotropic stress change, and the other that is $\bar{A}$ times the change in principal stress difference.

Hence,

$$\Delta u = B\Delta\sigma_3 + \bar{A}(\Delta\sigma_1 - \Delta\sigma_3) \tag{1.12}$$

(Note that Skempton (1954) gives $\Delta u = B[\Delta\sigma_3 + A(\Delta\sigma_1 - \Delta\sigma_3)]$, i.e. $\bar{A} = AB$)

The pore pressure parameters may be measured in the triaxial compression test where a cylindrical soil sample is tested in two stages. In the first stage, the sample is subjected to an increment of all-round pressure and the pore pressure increase measured. In the second stage, the sample is loaded axially and the pore pressure increase measured. For a saturated soil, $B = 1$ and $\bar{A} = A$.

WORKED EXAMPLE

Question The strata in the flat bottom of a valley consist of 3 m of coarse gravel overlying 12 m of clay. Beneath the clay is fissured sandstone of relatively high permeability.

The water table in the gravel is 0.6 m below ground level. The water in the sandstone is under artesian pressure corresponding to a standpipe level of 6 m above ground level.

The unit weights of the soil are:

Gravel	above water table	16 kN/m^3
	below water table (saturated)	20 kN/m^3
Clay	saturated	22 kN/m^3

1 Plot total stresses, pore water pressures and effective vertical stresses against depth:
   (a) With initial ground water levels,
   (b) Assuming that the water level in the gravel is lowered 2 m by pumping, but the water pressure in the sandstone is unchanged,
   (c) Assuming that the water level in the gravel is kept as for (b), but that relief wells lower the water pressure in the sandstone by 5.5 m,
   (d) Assuming that the relief wells are then pumped to reduce the water level in the sandstone to 15 m below ground level.

Note that for (b), (c) and (d), stresses are required both for the short-term and the long-term conditions.

2 To what depth can a wide excavation be made into the clay before the bottom *blows up* (neglect side shear) assuming the initial ground water level.
   (a) With initial artesian pressure in sandstone?

(b) With relief wells reducing the artesian pressure to 0.6 m above ground level?

(c) With relief wells pumped to reduce the pressure to 15 m below ground level?

3 An excavation 9 m in depth (below ground level) is required. If a ratio of total vertical stress to uplift pressure of 1.3 is required for safety, to what depth must the piezometric head in the sandstone be lowered?

4 If the coefficient of volume change of the clay is $0.0002\,m^2/kN$ to what extent would the clay layer in the locality eventually decrease in thickness if the artesian pressure were permanently lowered by this amount?

5 If, on the other hand, the water level in the sandstone were raised to 15 m above ground level owing to the impounding behind a dam upstream of the site, at what depth in the undisturbed clay would the vertical effective stress be least and what would this value be?

Answers 1 See Fig. 1.7. Note that rapid changes of global total stress do not cause immediate changes in effective stress within the clay layer.

2 (a) Let the excavation proceed to a depth D below ground level. The bottom will blow up when the total stress, diminished by excavation, equals the water pressure in the sand stone, that is, when $(15 - D)22 = 21 \times 10$ assuming the excavation is kept pumped dry.

(b) Thus, $D = 5.454$ m.

(c) Similarly, $(15 - D)22 = 15.6 \times 10$. Thus, $D = 7.909$ m.

(d) By inspection, $D = 15$ m.

3 By inspection, $(6 \times 22)/10p = 1.3$, where p is the total piezometric head in the sandstone, whence $p = 10.153$ m, i.e. the piezometric head in the sandstone must be lowered to $(15 - 10.153) = 4.847$ m below ground level.

4 The change in effective stress is $(21 - 10.153)10/2 = 54.235$ kPa, whence the change in thickness of the clay layer is $0.0002 \times 54.235 \times 12 = 0.130$ m.

5 The pore pressure at the base of the clay layer will be $(15 + 15)10 = 300$ kPa giving a minimum vertical effective stress of 21.6 kPa at 15 m depth.

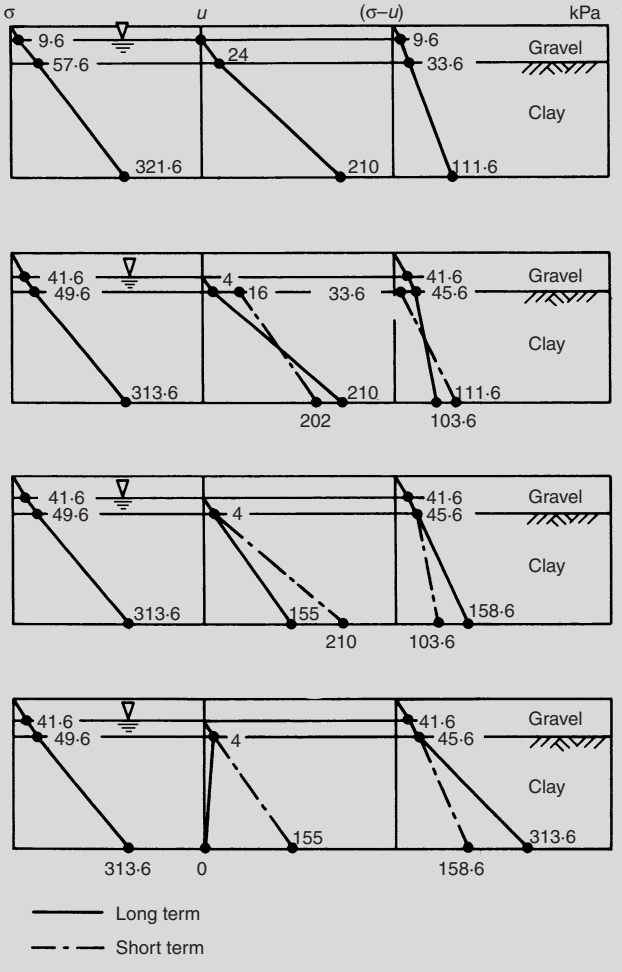

Fig. 1.7. Solution to worked example, Section 1

Short-term and long-term stability

'One of the main reasons for the late development of soil mechanics as a systematic branch of civil engineering has been the difficulty in recognizing that the difference between the shear characteristics of sand and clay lies not so much in the difference between the frictional properties of the component particles, as in the very wide difference – about one million times – in permeability. The all-round component of a stress change applied to a saturated clay is thus not effective in producing any change in the frictional component of strength until a sufficient time has elapsed for water to

> *leave (or enter), so that the appropriate volume change can take place.'*
> **Bishop & Bjerrum (1960)**

The interaction of soil structure and pore water

The uniquely time-dependent engineering behaviour of fine-grained saturated soils is derived from the interaction of the compressible structural soil skeleton and the relatively incompressible pore water. Rapid changes in external loading do not immediately bring about a volume change due to the viscous resistance to pore water displacement. Therefore, the soil structural configuration does not immediately change and thus, by Hooke's Law, the structural loading does not change.

However, while the compressible soil structure requires a volume change to change its loading, the relatively incompressible pore water may change its pressure without much volume change. The external loading change is therefore reflected by a change in pore pressure. With time, this 'excess' pore pressure will dissipate, volume change occurring by pore-water flow until the consequent change in structural configuration brings the structural loading into equilibrium with the changed external loading.

This process may be examined by the spring–dashpot analogy demonstrated in Fig. 1.8.

The soil structure is modelled by a spring, the soil voids modelled by the chamber under the piston and the soil permeability modelled by the lack of fit of the piston in the cylinder – thus a soil of high permeability is modelled by a piston which allows a lot of leakage whereas a soil of low permeability is modelled by a piston which allows very little leakage. It is assumed the piston is frictionless. Pore pressure is indicated by the water level in a standpipe whose bore is very much less than that of the piston. Initially the piston is uniformly loaded by a loading intensity p including the weight of the piston.

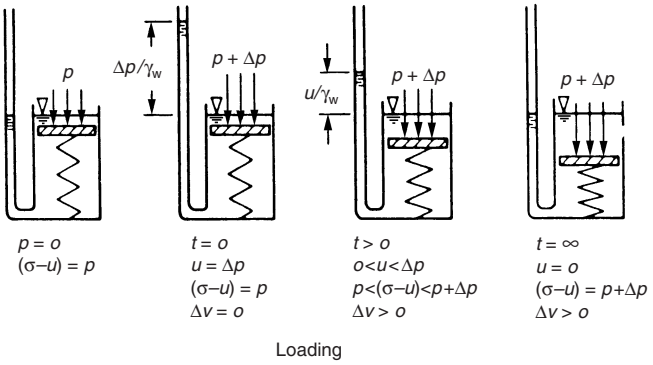

Fig. 1.8 Spring–dashpot analogy for soil consolidation

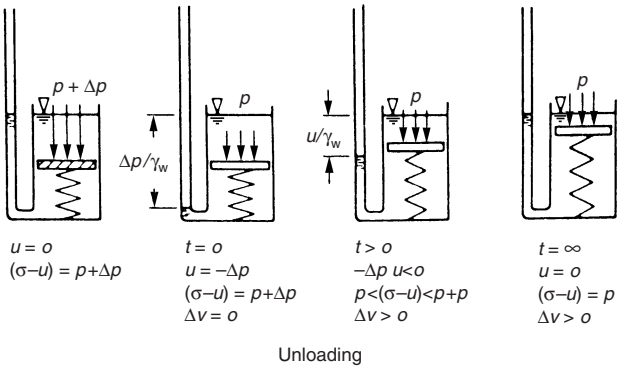

Fig. 1.9 Spring–dashpot analogy for soil swelling

The instant immediately after $(t = 0)$ rapidly increasing the loading by Δp, the spring (soil structure) is unaffected because insufficient time has elapsed for viscous flow past the piston to reduce the volume of the chamber (pores) under the piston and thus allow the spring to compress further and carry some more load. The loading increment, Δp, is thus initially carried by an equal increase in pore pressure. As time elapses, flow takes place, the piston displacing downwards, the applied loading increment Δp being shared between the spring and the pore pressure. The hydraulic gradient causing flow from the area of high pore pressure under the piston to the area of zero pore pressure over the piston, is itself reduced by the flow as the spring is allowed to compress further and take more load. The law of diminishing returns thus applies and there is an exponential decay in pore pressure and change in length of the spring. Ultimately, the pore pressure dissipates to the equilibrium value and the total load is fully supported by the spring.

The instant immediately after rapidly decreasing the loading by Δp, as shown in Fig. 1.9, the spring is again unaffected because insufficient time has elapsed for viscous flow past the piston to increase the volume of the chamber under the piston and thus allow the spring to expand and shed some load.

The loading reduction Δp is thus initially reflected by a numerically equal decrease in pore pressure. As before, as time elapses, flow takes place, the piston displacing upwards, the loading reduction Δp being shared between the spring and the pore pressure. Ultimately, the negative pore pressure increases to the equilibrium value and the loading in the spring reduces to p.

The generation of pore pressure in the loading of real soils

The stability considerations of foundations and earthworks in saturated fine grained soils are highly time dependent. This is because the average

Table 1.2 Effective stress strength parameters and permeabilities for soils of widely varying particle size (after Bishop & Bjerrum, 1960).

Soil	Permeability m/sec	c' kPa	ϕ' degrees
Rockfill	5	0	45
Gravel	5×10^{-4}	0	43
Medium sand	–	0	33
Fine sand	1×10^{-6}	0	20–35*
Silt	3×10^{-7}	0	32
Normally-consolidated clay of low plasticity	1.5×10^{-10}	0	32*
Normally-consolidated clay of high plasticity	1×10^{-10}	0	23
Over-consolidated clay of low plasticity	1×10^{-10}	8	32
Over-consolidated clay of high plasticity	5×10^{-11}	12	20

size of the inter-connecting pores are so small that the displacement of pore water is retarded by viscous forces. The resistance that a soil offers to water flow is its 'permeability' which is the velocity of flow under a unit hydraulic gradient. It can be seen from Table 1.2 that permeability is the largest quantitative difference between soils of different time dependent stability (as pointed out by Bishop & Bjerrum (1960).

Note that the sand and normally-consolidated clay marked thus '*' have similar shear strength parameters but the permeability of the clay is several orders of magnitude lower, thereby accounting for its unique time-dependency whereas the more permeable sand reacts to loading changes almost immediately.

The time-dependent behaviour of fine grained soils whose in situ total stresses are subject to change may be usefully considered under conditions of unloading and loading as discussed below.

The unloading condition

If a saturated clay is unloaded, such as may occur in an excavation or cutting, an overall reduction in mean total stress occurs. In a fine-grained soil like clay, the viscous resistance to pore-water flow prevents the soil structure, partially relieved of its external loading, from rapidly expanding and sucking in pore water from the surrounding soil. With time, this suction is dissipated by drainage into the area of lowered pore pressure from the surrounding area of higher pore pressure unaffected by the excavation. This migration of pore water causes an increase in soil volume in the zone of influence, the soil swelling and the soil structure softening, giving rise to a reduction in strength. The minimum factor of safety occurs at the equilibrium long-term condition.

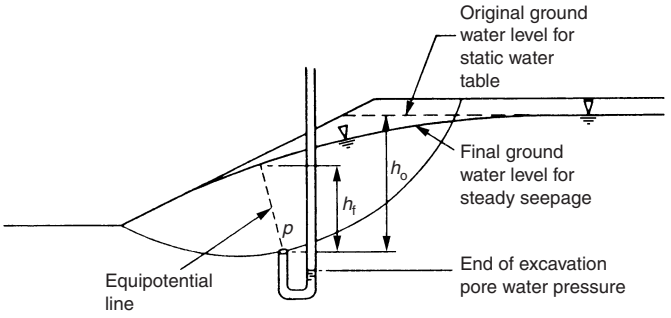

Fig. 1.10 Short-term and long-term pore pressures in a cutting

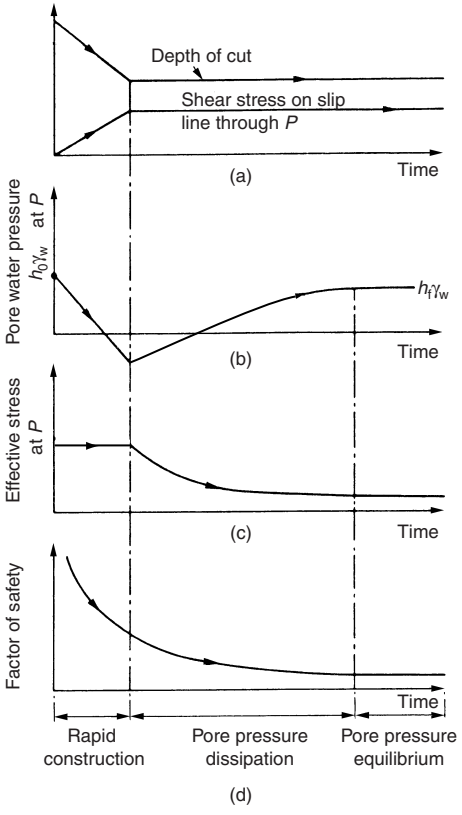

Fig. 1.11 Variation with time of the shear stress, local pore pressure, local effective stress, and factor of safety for a saturated clay excavation (after Bishop & Bjerrum, 1960)

For example, consider the time-dependent stability of a cutting as represented in Fig. 1.10.

The reduction in the in situ total stresses (Fig. 1.11(a)) causes a reduction in pore-water pressure dependent on the actual change in principal stress difference and the appropriate value of A (Fig. 1.11(b)). The consequent migration of pore water causes the soil structure to swell reducing the strength and hence stability (Fig. 1.11(d)).

The loading condition

If a saturated clay is loaded, such as may occur in soils supporting building foundations and earth embankments (Fig. 1.12), an overall increase in mean total stress occurs (Fig. 1.13(a)). In a fine-grained soil like clay, the viscous resistance to pore water expulsion prevents the soil structure from rapidly contracting. In the short-term loading condition, therefore, there is a change in effective stress due to shear strain only together with an increase in pore pressure (Fig. 1.13(b) and (c)). With time, this excess pore pressure is dissipated by drainage away from the area of increased pore pressure into the surrounding area of lower pore pressure unaffected by the construction. This flow of pore water causes a time-dependent reduction in volume in the zone of influence, the soil consolidating and the soil structure stiffening, giving rise to decreasing settlement and increasing strength. The minimum factor of safety occurs in the short-term undrained condition when the strength is lowest (Fig. 1.13(d)).

In this undrained condition the stressed zone does not immediately change its water content or its volume. The load increment does, however, distort the stressed zone. The effective stresses change along with the change in the shape of the soil structure. Eventually the changes in the structural configuration may no longer produce a stable condition and the consequent instability gives rise to a plastic mechanism or plastic flow and failure occurs.

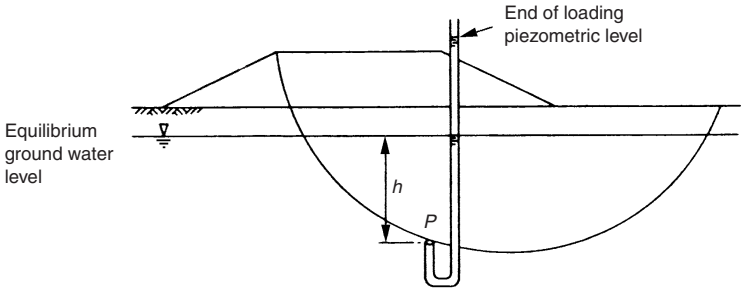

Fig. 1.12 Pore pressure generated on a potential slip surface by embankment loading

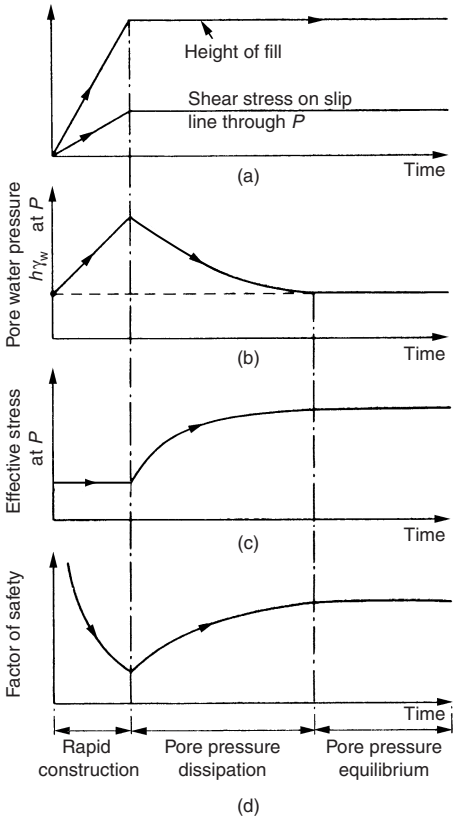

Fig. 1.13 Variation with time of the shear stress, local pore pressure, local effective stress, and factor of safety for a saturated clay foundation beneath an embankment fill (after Bishop & Bjerrum, 1960)

The strength is determined by the local effective stresses at failure normal to the failure surfaces. These are conditioned by and generated from the structural configuration of the parent material (which is itself conditioned by the preloading in situ stresses) and its undrained reaction to deformation. A first step, therefore, in fulfilling the complex similitude requirements that accordingly arise is to ensure that the shear test used to find the strength is effectively undrained.

The undrained shear test may be used to give a direct measure of shear strength, namely the undrained shear strengths s_u, or it may be used to give an indirect measure of shear strength, if the pore water pressures are measured, by providing c' and $\tan \phi'$. It is therefore possible to analyse the stability of the loaded soil by:

(i) using the undrained shear strength, s_u, in a total stress analysis, or

(ii) using the effective stress shear strength parameters c' and $\tan\phi'$ in an effective stress analysis.

The use of (ii) requires an estimation of the end of construction pore pressures in the failure zone at failure, whereas the use of (i) requires no knowledge of the pore pressure whatsoever.

In general civil engineering works, the soil loading change is applied gradually during the construction period. The excess pore pressures generated by the loading are thus partially dissipated at the end of construction. The end of construction pore pressures and the increased in situ shear strength can be measured on site if the resulting increased economy of design warrants the field instrumentation and testing. On all but large projects this is rarely the case. In addition, the loading is localized, allowing the soil structure to strain laterally, the soil stresses dissipating and the principal stresses rotating within the zone of influence.

In the absence of sound field data on the end of construction shear strengths and pore pressures and in the face of analytical difficulties under local loading, an idealized soil model possessing none of these difficulties is usually invoked for design purposes. This consists of proposing that the end of the construction condition corresponds to the idealized case of the perfectly undrained condition. Here the soil is considered to be fully saturated with incompressible water and is sufficiently rapidly loaded that, in the short term, it is completely undrained. Prefailure and failure distortions of the soil mass in the field are, by implication if not by fact, simulated by the test measuring the undrained shear strength. It follows that if the shear strength of the soil structure is determined under rapid loading conditions prior to construction, this undrained shear strength may be used for short-term design considerations. No knowledge of the pore pressures is required, the undrained shear strength being used in a total stress analysis (the so-called $\phi = 0$ analysis).

A note on the $\phi = 0$ analysis

'It is a simple task to place a clay specimen in a shearing apparatus and cause a shear failure. A numerical value of shearing strength, which has acceptable precision, may readily be obtained if proper technique, a representative sample, and a satisfactory apparatus are used. The point which has too often been insufficiently appreciated by testing engineers is that the shearing strength, both in the laboratory specimen and in the clay in nature, is dependent on a number of variables. Before meaning can be attached to shearing strengths determined in the laboratory, the engineer who is to interpret the test results must have at his command an understanding of the factors or variables on which the strength is dependent, and he

> *must make adjustments for every factor which occurs differently in the test than in nature.'*
> **D. W. Taylor (1948)**

The concept of the $\phi = 0$ analysis

The $\phi = 0$ analysis is a stability analysis which derives its name from the total stress interpretation of the unconsolidated–undrained triaxial test. In this test, three test specimens of saturated soil taken from the same core barrel (usually clay, but it may be any soil) are tested in unconsolidated–undrained triaxial compression at three different cell pressures. The resulting compression strengths (deviator stresses at failure) are the same because the initial isotropic state of effective stress of each test specimen is unchanged by applying cell pressure. Plotting Mohr's circles in terms of total stress (the effective stresses are not known) give circles of the same diameter (Fig. 1.14). An envelope to the circles is, of course, a horizontal straight line. Interpreting these results using Coulomb's (1773) equation,

$$\tau_f = c + \sigma \tan \phi \tag{1.13}$$

$$\text{gives } \tau_f = c = c_u \ (= s_u \text{ the undrained shear strength}) \tag{1.14}$$

$$\text{and } \phi = \phi_u = 0 \tag{1.15}$$

This apparent insensitivity of shear strength to loading changes led Skempton (1948) to conclude that shear strength was uniquely dependent on water content and if water content did not change then strength did not change. Accordingly, it was believed at that time that as soil strength was unaffected by loading changes in the short term, the strength measured before construction could be used to predict the stability after construction. Thus, the $\phi = 0$ analysis emerged and appeared to work well for both foundations and cuts. Analysis of failed cuts using the $\phi = 0$ method (Lodalen, Norway; Frankton, New Zealand; Eau Brink, England) gave factors of safety of unity thereby apparently confirming the validity of the method. Amazingly, these early case histories gave fortuitously atypical results and it was eventually realized that the critical long term stability of cuts could not be predicted using the $\phi = 0$ analysis because the strength diminishes with long term swelling.

Thus for cuts, long term or 'drained' strengths must be used and this can be predicted in terms of effective stress using the Terzaghi–Coulomb equation:

$$s_d = c' + (\sigma - u) \tan \phi' \tag{1.16}$$

provided the long term pore-water pressures are known which they normally are because the ground-water regime, initially disturbed by the construction activity, has regained a steady state.

For foundations, however, critical stability is in the short term because the strength increases with consolidation in the long term. In the short term the pore water pressures are unknown and thus an effective stress analysis cannot be made unless pore pressures can be estimated. Accordingly, a $\phi = 0$ analysis must be carried out using the undrained shear strength s_u.

The applicability of the $\phi = 0$ analysis

From the principle of effective stress it is known that effective stress (and hence strength) will not change provided the soil structure does not deform. This is the case in the unconsolidated–undrained triaxial test during the cell pressure increment stages which are isotropic. The combination of the undrained condition (no volumetric strain) and the isotropic stress change (no shear strain) ensures no deformation and hence no change in the initial state of effective stress. Thus, the $\phi = 0$ condition corresponds to a 'no change in the initial state of effective stress' condition. Of course, the strength of the soil skeleton is mobilized in the unconsolidated–undrained triaxial test by axial deformation changing the effective stresses – it is just that this strength is dependent on the initial state of effective stress.

From the principle of similitude it follows that the concept inherent in the $\phi = 0$ condition (i.e. no change in strength if initial state of effective stress is unchanged), and demonstrated in the unconsolidated–undrained triaxial test, must be matched to a corresponding field condition if the s_u measured in this way is to be used in a $\phi = 0$ analysis to predict the field stability. This means that the analysis is only wholly appropriate to a field condition where the construction activity is both undrained and causes an isotropic increase in total stress. This occurs in the laboratory, for example, in the oedometer at the instant of loading change. In the field this condition may be approximated by rapid global loading such as may occur in the short term at shallow depth beneath the centre of a wide embankment. Towards the toe of the embankment shear strain will occur with consequent change in effective stress, thereby progressively invalidating the

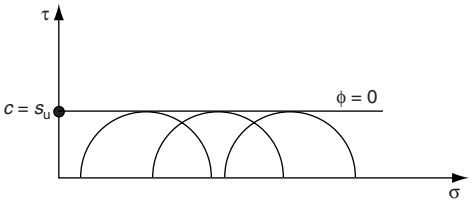

Fig. 1.14 Unconsolidated–undrained triaxial test Mohr's circles showing $\phi = 0$ failure envelope

concept inherent in the $\phi = 0$ analysis. The extent to which this occurs may or may not be significant. Certainly, where narrow foundations such as strip footings are concerned, shear strains will occur throughout the zone of influence and so make the $\phi = 0$ analysis not strictly appropriate. Accordingly, high factors of safety on shear strength (typically $F = 3$) are taken to deal with this discrepancy and with any other factors causing a lack of similitude.

CHAPTER TWO

Shear strength

The definition of shear strength

The shear strength of a soil in any direction is the maximum shear stress that can be applied to the soil structure in that direction. When this maximum has been reached, the soil is regarded as having *failed*, the strength of the soil having been fully mobilized.

The nature of shear strength

When soil fails it does so by means of some plastic failure mechanism involving shear. The shear strength of a soil is derived from the structural strength alone, the pore water having no shear strength. The resistance of the soil structure to shear arises from the frictional resistance, F, generated by the interparticle forces, N (Fig. 2.1). In the soil mass, the loading transmitted by the soil structure normally to the shear surface is an integrated measure of these interparticle forces. The shear strength, τ_f (shear stress at failure), on any plane in a soil, is some function of the effective stress normal to that plane. Assuming a linear relationship gives

$$\tau_f = k_1 + k_2(\sigma_n - u) \tag{2.1}$$

where σ_n is the total stress normal to the plane, u is the pore-water pressure, and k_1, and k_2 are two experimentally determined constants.

Experiment has shown this expression to be substantially correct over a wide range of soils for a limited range of stresses.

Common usage has

$$k_1 = c' \tag{2.2}$$

$$k_2 = \tan\phi' \tag{2.3}$$

whence

$$\tau_f = c' + (\sigma_n - u)\tan\phi' \tag{2.4}$$

where c' is the cohesion intercept and ϕ' is the angle of shearing resistance, with respect to effective stress.

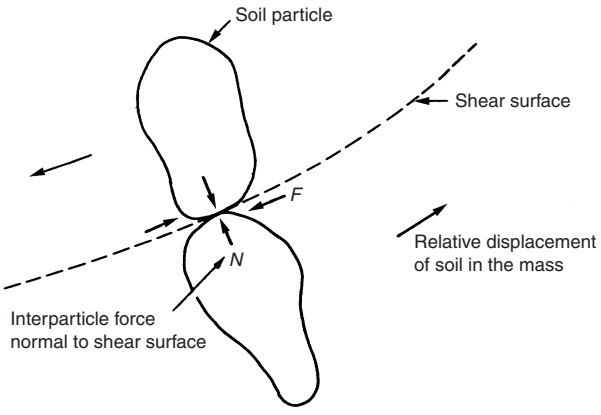

Fig. 2.1 Forces arising at inter-particle slip

The measurement of shear strength

Direct and indirect measurements

If the effective stress shear strength parameters c' and $\tan\phi'$ are known, the shear strength on any plane may be estimated from a knowledge of the effective stress normal to that plane $(\sigma_n - u)$. In this way, the shear strength is evaluated indirectly by using the experimentally determined values of c' and $\tan\phi'$, and estimating or measuring the total normal stress σ_n and the pore water pressure u, whence $\tau_f = c' + (\sigma_n - u)\tan\phi'$.

It is possible to measure the peak shear strength, τ_f, directly. A device which does this is the direct shear box (Fig. 2.2) which tests a prismoidal specimen of soil contained in a rigid box which is split in a horizontal mid-section. The top half of the box is free to move relative to the bottom half. The box is open at the top where the soil specimen is loaded vertically by a horizontal rigid platen. By constraining one half of the box to move relative to the other half, the soil specimen is sheared on a horizontal plane. The peak shear strength is found directly by measuring the maximum shear stress required for the relative displacement.

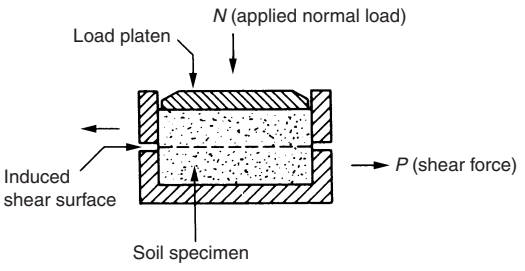

Fig. 2.2 A schematic section through the direct shear box

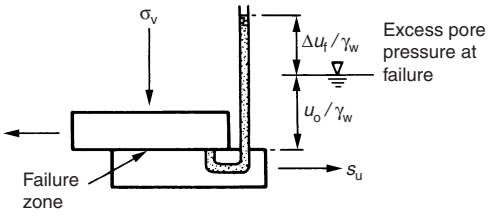

Fig. 2.3 Stresses at undrained failure in the direct shear box

The relationship between the direct and indirect measurements of shear strength may now be examined in more detail.

Consider a saturated clay specimen confined in a direct shear box and loaded vertically on a horizontal midsection with a total stress of σ_v (Fig. 2.3). The box is contained in an open cell which is flooded to a constant depth. The pore pressure has the equilibrium value, u_0. The shear strength may be found directly by shearing the specimen. By shearing the specimen rapidly, the undrained condition is simulated, that is, there is no change in water content and therefore no change in overall volume, owing to the viscous resistance to rapid displacement of pore water in a fine grained soil.

The shearing distortion of the soil structure in the shear zone generates an excess pore-water pressure, which at failure is Δu_f.

The shear strength directly obtained is, therefore, the undrained shear strength,

$$s_u = c' + (\sigma_v - u_0 - \Delta u_f) \tan \phi' \tag{2.5}$$

It can be seen, therefore, that the undrained shear strength, s_u, simply provides a direct measure of the shear strength of a soil structure which is rapidly sheared. This strength may also be deduced from a knowledge of the effective stress at failure and the relationship between effective stress and shear strength for the soil embodied in the parameters c' and $\tan \phi'$.

Drained and undrained measurements

If a fine-grained saturated soil is rapidly loaded (e.g. rapidly filling a large oil tank), in the short term the soil is effectively undrained because of the viscous forces resisting pore-water flow within the soil. The excess pore pressure generated by the *sudden* application of load dissipates by drainage or consolidation over a period of time which may, in the case of clays, extend for many tens or even hundreds of years. Hence, the terms *short* and *sudden* are relative and a load application over several months during a construction period may be relatively rapid with the short-term, end-of-construction, condition approximating

to the undrained case. In positive loading conditions such as embankments and footings, the subsequent consolidation under the influence of the increased load gives rise to increased strength and stability. The lowest strength and, therefore, the most critical stability condition consequently holds at the end of construction when loading is completed. The critical strength is thus the undrained shear strength before consolidation. One way of measuring the strength is to build up rapidly the load in a full scale field test until the soil fails and this is sometimes done, particularly in earthworks, by means of trial embankments. However, such full-scale testing is very expensive and only really applicable to large and costly projects where the subsoil is uniform. For variable subsoils and cases where large expenditure on soil testing is unlikely to effect large economies in design, small-scale testing is more appropriate. A rapid test in the direct shear box, for example, presents a convenient, though vastly simplified small-scale simulation or model of the likely full-scale field or prototype failure. It was seen in the preceding section that this rapid direct measure of shear strength gave the undrained shear strength, s_u. However if the test is carried out slowly, the distortion of the soil structure in the shear zone produces an insignificantly small excess pore-water pressure. This is because any slight increase in pore pressure has time to dissipate by drainage; that is, the slow test is *drained* as opposed to *undrained* in the quick test. Hence, the pore pressure remains at almost u_0 throughout the test (Fig. 2.4). The soil structure in the shear zone is able to change its volume by drainage. Hence the shear distorted structure in the drained test will be different from that of the undrained test, giving a different strength, the drained shear strength,

$$s_d = c' + (\sigma_v - u_0) \tan \phi' \tag{2.6}$$

The essential feature is that, generally

$$s_u \neq s_d$$

for although it is the one soil which is being tested, the soil structures in the failure zones are different in each case.

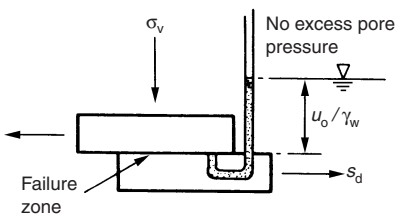

Fig. 2.4 Stresses at drained failure in the direct shear box

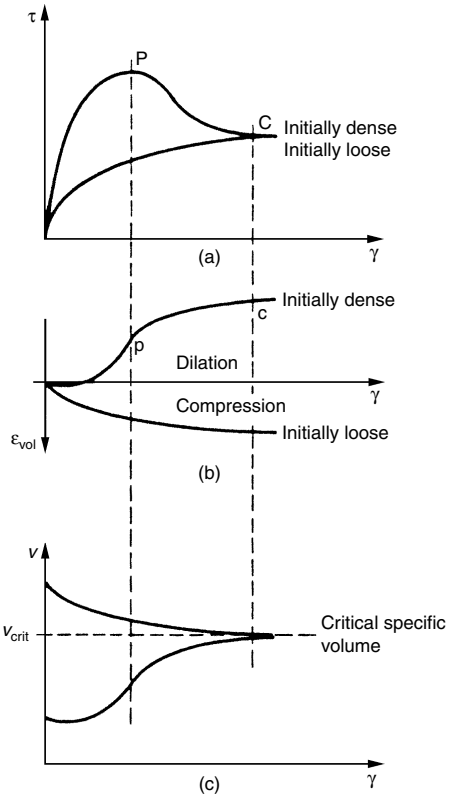

Fig. 2.5 Typical shearbox test results: (a) τ versus γ; (b) ε_{vol} versus γ; (c) υ versus γ (Powrie, 1997)

In the drained direct shear test therefore, the pore pressure is almost zero and therefore the effective stresses are known. From this, the effective stress shear strength parameters c' and $\tan\phi'$ may be deduced from two or more such tests. Hence this test not only directly measures the drained shear strength for the particular consolidation pressures, σ_v, of each test but, in furnishing c' and ϕ', it also allows the shear strength to be estimated for any loading condition.

Critical states

The achievement of a critical void ratio or specific volume, at which continued shear can take place without change in volume, is illustrated by the typical results from shear box tests on dense and loose samples of sand shown in Fig. 2.5. The normal effective stress p' is the same in each test.

In the test on the initially dense sample, the shear stress gradually increases with shear strain, γ (Fig. 2.5(a)). The shear stress increases to a peak at P, before falling to a steady value at C which is maintained as

the shear strain is increased. The initially dense sample may undergo a very small compression at the start of shear, but then begins to dilate (Fig. 2.5(b)). The curve of ε_{vol} (volumetric strain) versus γ becomes steeper, indicating that the rate of dilation (or expansion) $d\varepsilon_{vol}/d\gamma$ is increasing. The slope of the curve reaches a maximum at P, but with continued shear strain the curve becomes less steep until at C it is horizontal. When the curve is horizontal $d\varepsilon_{vol}/d\gamma$ is zero, indicating that dilation has ceased. The peak shear stress at P in Fig. 2.5(a) coincides with the maximum rate of dilation at P in Fig. 2.5(b). The steady-state shear stress at C in Fig. 2.5(a) corresponds to the achievement of the critical specific volume at C in Fig. 2.5(c).

The initially loose sample displays no peak strength, but eventually reaches the same critical shear stress as the initially dense sample (Fig. 2.5(a)). Figure 2.5(b) shows that the initially loose sample does not dilate, but gradually compresses during shear until the critical specific volume is reached (i.e. the volumetric strain remains constant). Figure 2.5(c) shows that the critical specific volume is the same in each case. The curves shown in Fig. 2.5 indicate that, when sheared, a soil will eventually reach a critical void ratio, at which continued deformation can take place without further change in volume or stress. This condition, at which unlimited shear strain can be applied without further changes in specific volume v, shear stress τ and normal effective stress σ', is known as a critical state. The critical state concept was originally recognised by Casagrande (1936), and was developed considerably by Roscoe *et al.* (1958).

The use of peak strength in design

In some respects, the peak strength of a soil should be of academic interest only. A peak strength is a transient thing, sustainable only while the soil is dilating. A soil cannot carry on dilating for ever, and sooner or later its strength must fall to the critical state value, ϕ'_{crit} Furthermore, the peak strength is not a soil property in the same way that the critical state strength is. The peak strength depends on the potential for dilation, and will therefore (for a soil of given initial specific volume) decrease as the normal effective stress increases.

This point may be reinforced by plotting the peak strength data on a graph of τ against σ'. Fig. 2.6(a) shows that the envelope formed by the peak strength data is curved. In contrast to the critical state strength also shown in Fig. 2.6(a), the peak strength data cannot accurately be described by means of a simple equation. Unfortunately, this does not stop some people from trying. In some books, you will find peak strength data described by means of a 'best-fit' straight line, having an equation of the form

$$\tau_p = c' + \sigma' \tan \phi'_{tgt} \tag{2.7}$$

(Fig. 2.6(b)), where c' is the intersection of the line with the τ-axis, and

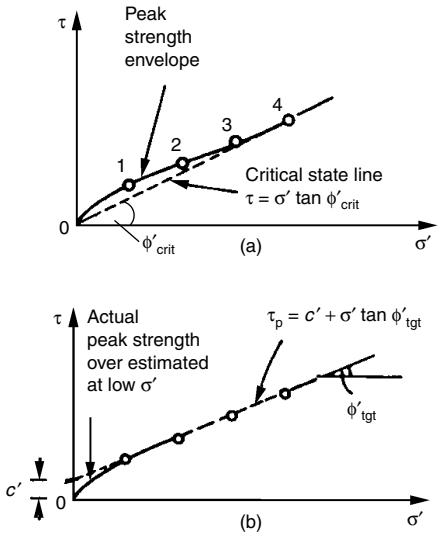

Fig. 2.6 (a) Peak strength data, plotted as τ versus σ', showing curved failure envelope; (b) how not to interpret peak strength data (Powrie, 1997)

$\tan \phi'_{tgt}$ is its slope. Such an approach is conceptually flawed. For at least three reasons, it is also potentially dangerous:

1. It can lead to the overestimation of the actual peak strength at either low (Fig. 2.6(b)) or high effective stresses, depending on where the 'best fit' straight line is drawn. (The position of the best fit straight line will depend on the available data points, which – if the testing programme has not been specified with care – may be predominantly at either high or low normal effective stresses.)
2. The designer of a geotechnical engineering structure cannot guarantee that the peak strength will be uniformly mobilised everywhere it is needed at the same time. It is much more likely that only some soil elements will reach their peak strength first. If any extra strain is imposed on these elements, they will fail in a brittle manner as their strength falls towards the critical value. In doing so, they will shed load to their neighbours, which will then also become overstressed and fail in a brittle manner. In this way, a progressive collapse can occur, which – like the propagation of a crack through glass – is sudden and catastrophic. (Experience suggests that progressive failure is potentially particularly important with embankments and slopes, and perhaps less of a problem with retaining walls and foundations.)
3. Quite apart from the possibility of progressive collapse, many of the design procedures used in geotechnical engineering assume that the soil can be relied on to behave in a ductile manner. When a ductile

material fails, it will undergo continued deformation at constant load. This is in contrast to a brittle material, which at failure breaks and loses its load-carrying capacity entirely. At the critical state, the behaviour of the soil is ductile: the definition of the critical state is that unlimited shear strain can be applied *without further changes in stress* or specific volume. Between the peak strength and the critical state, however, the behaviour of the soil is essentially brittle. In design, it is safer to use the critical state strength. It is also simpler mathematically. It must be appreciated, however, that this has not always been standard practice. This means that procedures which have led to acceptable designs on the basis of the peak strength might err on the conservative side when used unmodified with the critical state strength. In cases where it is really necessary, the peak strength can be quantified with reference to the slope of the line joining the origin to the peak stress state $(\tau_{\text{peak}}, \sigma')$.

$$\phi'_{\text{peak}} = \tan^{-1}(\tau/\sigma')_{\text{peak}} \tag{2.8}$$

The value of ϕ'_{peak} defined in this way will gradually diminish with increasing normal effective stress σ', until it eventually falls to ϕ'_{crit} (for example at test 4 in Fig. 2.6(a)).

Note: this section *Critical states* is reproduced by kind permission from Powrie (1997).

Methods of measurement

The direct shear box

The direct shear box test, introduced in the preceding section, represents a simple and direct shear test. As shown in Fig. 2.7, the relationship

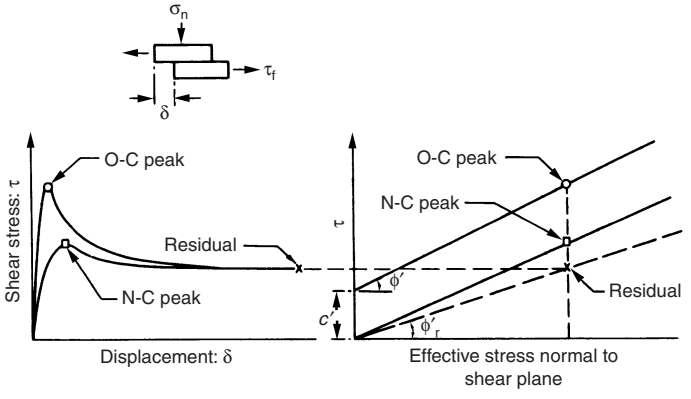

Fig. 2.7 Relation of peak shear strengths to residual shear strengths as measured in the direct shear box of over-consolidated (O–C) and normally-consolidated (N–C) clays

between strength and effective stress,

$$\tau_f = c' + (\sigma_n - u_f)\tan\phi' \tag{2.9}$$

plots as a straight line in τ, $(\sigma - u)$ co-ordinates, with a slope of $\tan\phi'$ and an intercept on the shear stress axis of c'. This line or *failure envelope* may be evaluated by the drained direct shear test by applying a different vertical stress in each test and measuring the shear stress up to and beyond the peak value.

After exceeding the peak shear strength clays strain-soften to a residual value of strength that corresponds to the resistance to sliding on an established shear plane. Large displacements are necessary to achieve this minimum ultimate strength requiring multiple reversals in the direct shear box or, more appropriately, use of the ring shear apparatus (Bishop *et al.,* 1971). As shown in Fig. 2.7, the peak and residual strengths may be displayed as failure and post-failure envelopes giving the residual shear strength

$$s_r = c'_r + (\sigma_n - u)\tan\phi'_r \tag{2.10}$$

where c'_r is the residual cohesion intercept and ϕ'_r is the residual angle of shearing resistance. Soft, silty clays may show little difference between the peak and residual strengths. As the plasticity index of the clay increases, the difference tends to increase, even in the normally consolidated condition, and the decrease in strength is associated with re-orientation of the clay particles along the slip surface. Most over-consolidated clays show a marked decrease in strength from peak to residual, resulting partly from particle orientation and partly from an increase in water content owing to dilation within the zone of shearing. These effects increase with clay content and the degree of over-consolidation.

In a field failure, the average shear strength is the integrated sum of all the elements around the slip surface. This strength will lie between the peak and residual strengths. It is assessed from field failures and expressed in terms of a *residual factor* (Skempton, 1964),

$$R = \frac{s_f - \bar{s}}{s_f - s_r} \tag{2.11}$$

where s_f is the peak shear strength, s_r is the residual shear strength, and $\bar{s}$ is the average shear strength around the failure surface.

In clays, the fall-off in strength from the peak to the residual value may be expressed in terms of a *brittleness index*, I_B, which is the ratio of the reduction in strength from peak to residual to the peak strength and is written

$$I_B = \frac{s_f - s_r}{s_f} \tag{2.12}$$

As shown in Fig. 2.7, the soft plastic normally consolidated soil has a low brittleness index whereas the stiff over-consolidated soil has a high brittleness index.

The consequence of this strain-softening behaviour of stiff clays is the practical phenomenon of *progressive failure.* If for any reason a clay is forced to exceed the peak strength at some particular point within its mass, the strength at that point will decrease. This action will put additional stress on to the clay at some other point along the potential failure surface, causing the peak to be passed at that point also. In this way a progressive failure can be initiated and, in the limit, the strength along the entire length of a slip surface will fall to the residual value.

The *ring shear apparatus* (Bishop *et al.*, 1971) may be used to determine the full shear-stress displacement relationship of an annular ring-shaped soil specimen subjected to a constant normal stress, confined laterally and ultimately caused to rupture on a horizontal plane of relative rotary motion. The apparatus may be considered as a conventional direct shear box extended round into a ring. Each revolution of one half of the specimen relative to the other represents a displacement of one perimeter. Consequently, large actual displacements may be obtained in the one direction, and, indeed, large displacements may be necessary to realize the residual shear strength.

The triaxial compression test

A more versatile soil testing apparatus than the direct shear box is the triaxial cell (Fig. 2.8(a)).

In this test, a right cylindrical column of saturated soil is tested in triaxial compression with $\sigma_1 > \sigma_2 = \sigma_3$, the axial principal stress acting vertically. Triaxial extension, $\sigma_1 = \sigma_2 > \sigma_3$, is also possible. The stress system is mixed, σ_1, being generated by the displacement of a rigid platen, whereas σ_3 is directly applied by hydrostatic fluid pressure against a flexible rubber membrane.

The specimen, enclosed in a rubber membrane, is mounted on a saturated porous disc resting on the base pedestal of the cell. The cell water, which applies σ_3, is isolated from the pore water by the rubber membrane. The porous disc allows the pore water to communicate with the saturated water ducts in the base of the cell. One of these ducts is connected to the pore-pressure transducer, the other duct being connected to a back-pressure of $p < \sigma_3$ which is the datum of pore pressure measurement. The back pressure ensures both saturation of the specimen by dissolving any residual air and also that any pore-pressure reduction owing to incipient dilation of the soil does not give rise to a negative gauge pressure and cause cavitation. However, if these considerations do not arise, then $p = 0$ may be obtained during drainage by connecting the pore-pressure duct to

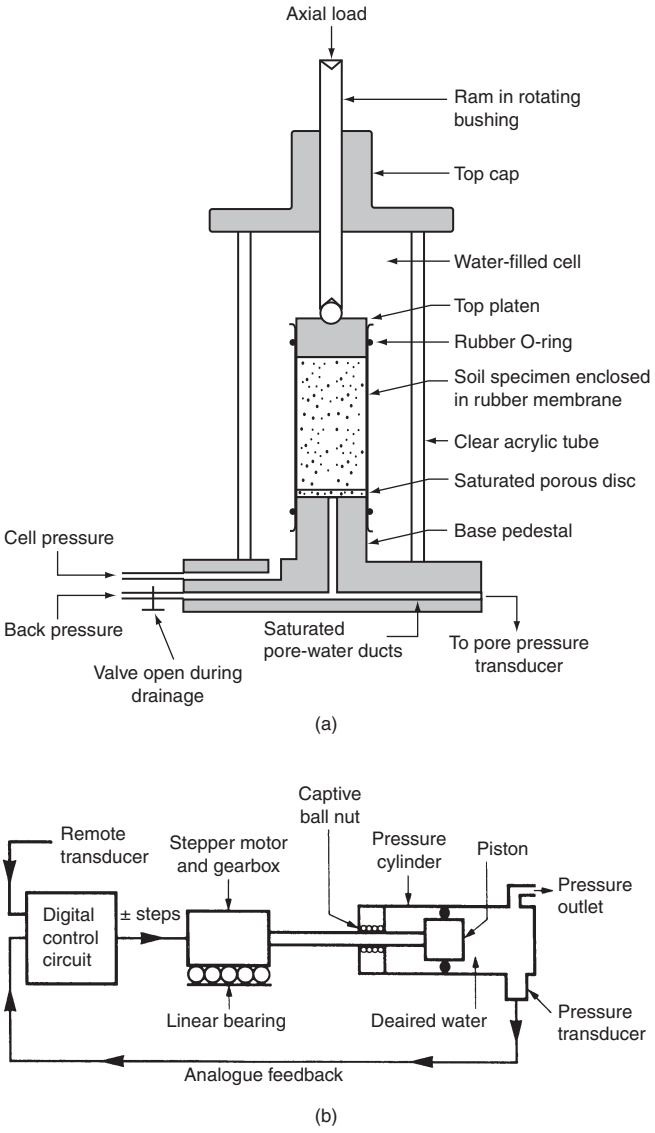

Fig. 2.8(a) Typical set-up for triaxial compression tests; (b) closed loop control screw pump schematic (permission of GDS Instruments Ltd.)

a free water surface in a burette level with the mid-height of the test specimen. Where volume-change measurement is important, for example for the correction of cross-sectional area of the test specimen, the application of positive back pressure is desirable to dissolve any air bubbles (see also our 'Fifteen Commandments of Triaxial Testing' which follow). The cell pressure is maintained at a constant pressure of σ_3. The soil structure is thus consolidated to an effective stress of $(\sigma_3 - p)$.

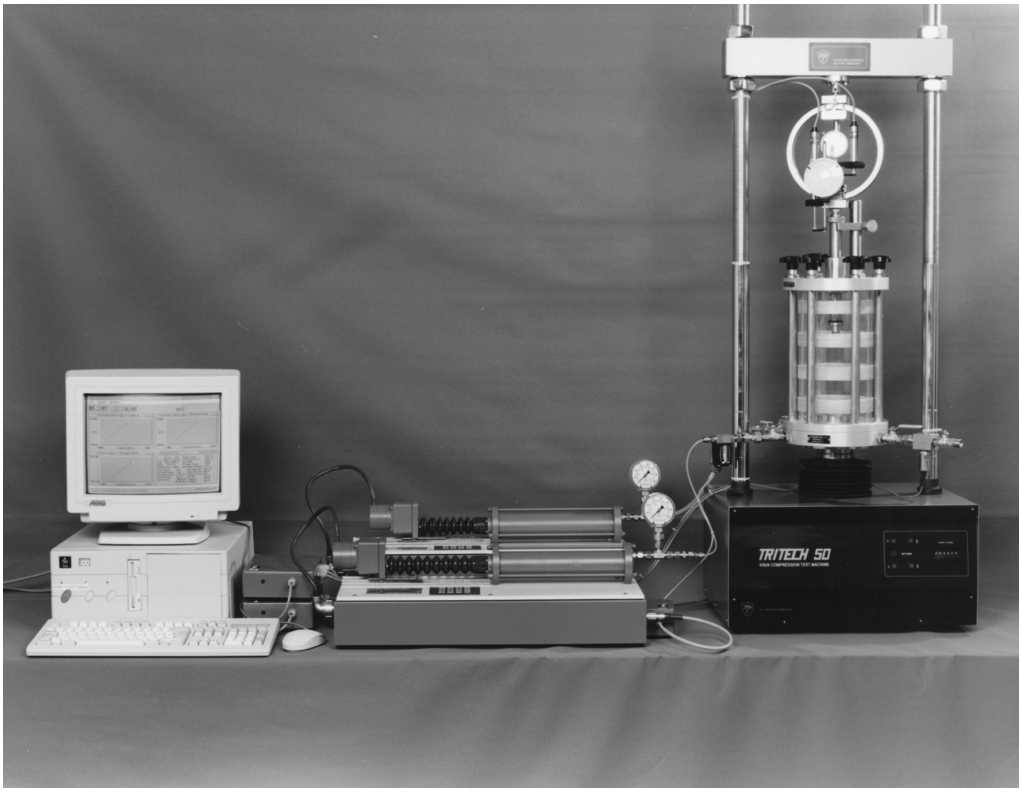

Fig. 2.8 (c) Computer-automated triaxial testing system (permission of GDS Instruments Ltd.)

The specimen is tested at a constant strain rate by a motorized loading frame. The cell is driven upwards, the loading ram bearing against a proving ring or load cell fixed to the testing frame. The load measured per unit specimen cross-sectional area is the principal stress difference or *deviator stress*, $(\sigma_1 - \sigma_3)$.

Cell pressure and back pressure are normally applied by means of compressed air–water bladder devices or by a closed-loop control screw pump of the GDS type shown schematically in Fig. 2.8(b). As well as not requiring a compressed air supply, the microprocessor-controlled screw pump has the added advantage that it provides a measurement of volume change by counting the steps to the stepping motor. In addition, the device has a computer interface. When the loading frame has a computer interface as well, computer automation of the triaxial test is enabled as shown in Fig. 2.8(c). See also Menzies *et al.* (1977), Menzies (1988) and Menzies and Hooker (1992).

The great advantage of the triaxial cell over the shear box is the control of drainage through the base pore-water ducts. It is therefore possible to

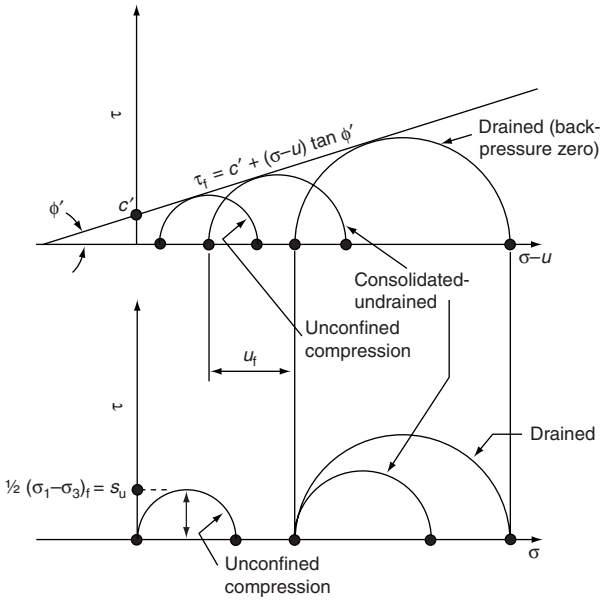

Fig. 2.9 Correlation between axial compression tests

measure the total specimen volume change by measuring the water imbibed or expelled in the drained case, or, in the undrained case, it is possible to measure the pore pressure. Another advantage of the triaxial test is that the applied stresses are principal stresses. This is not true near the specimen ends because of the frictional *end restraint* of the rigid platens.

The triaxial test gives an indirect measure of shear strength. It does this by providing the undrained shear strength from a Mohr's circle construction in terms of total stress from unconsolidated–undrained tests. It also provides the effective stress-shear strength parameters c' and $\tan \phi'$ from consolidated–undrained or drained tests, by invoking the Mohr–Coulomb failure criterion in terms of effective stress. The inter-relationships of various triaxial and uniaxial tests are demonstrated in Fig. 2.9. It can be seen that the Mohr–Coulomb failure criterion requires the Mohr's circles at failure to be tangential to the failure envelope.

WORKED EXAMPLE

The triaxial compression test

Consider nine identical saturated clay specimens removed from the same borehole at the same depth where, for example, it is assumed that the mean effective stress is 50 kPa. The specimens are removed

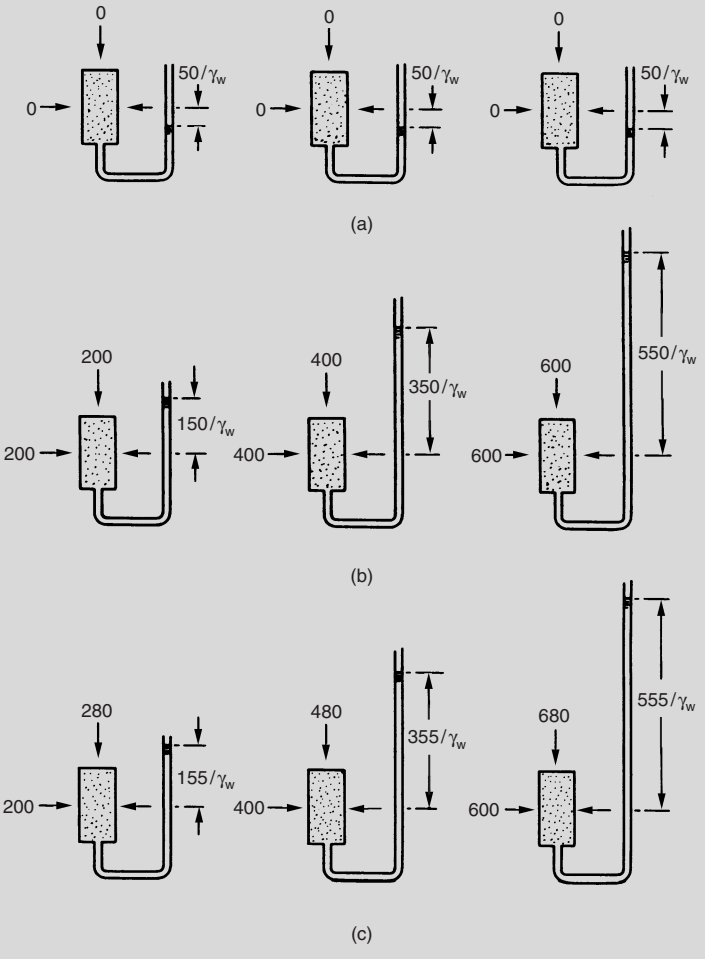

Fig. 2.10 Stress diagrams for the undrained test. (a) total stresses and pore pressures after removal from ground; (b) application of cell pressure, undrained; (c) application of axial load to failure, undrained

from their capped sampling tubes and immediately encased in impermeable rubber sheaths. In the transition from the ground to the laboratory bench, the water content has remained unaltered while the external total stresses have been reduced to zero. Assuming the sampling disturbance has not significantly distorted the specimens, the constant water content and therefore constant volume suggests that the state of effective stress has changed little, the pore pressure being reduced to give a suction of about −50 kPa gauge pressure (Fig. 2.10(a)).

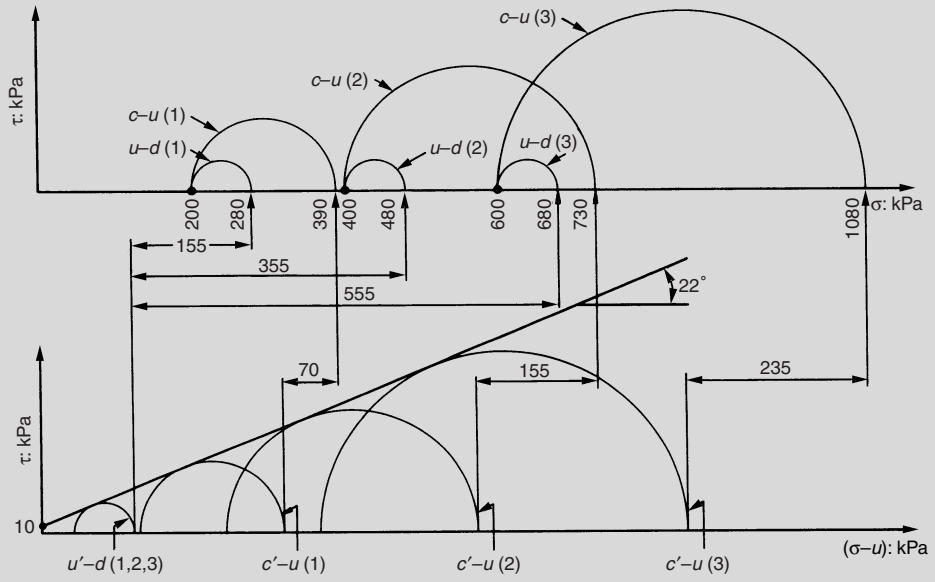

Fig. 2.11 Typical undrained (u–d) and consolidated–undrained (c–u) triaxial compression test Mohr's circles in terms of total stress and effective stress

Undrained test

The specimens are now placed in three identical triaxial cells at cell pressures of 200, 400 and 600 kPa, still undrained. Because the soil structure is saturated with relatively incompressible water (relative to the soil skeleton), the cell pressure is transmitted across the flexible impermeable rubber membrane increasing the pore pressure by the respective cell pressures. The specimen volume and shape remain the same as no drainage is permitted and the effective stress is unaltered at 50 kPa (Fig. 2.10(b)).

The still identical specimens are then loaded axially to failure. As the load-deformation properties of soil depend uniquely on the effective stress the specimens originally possessing the same structure and therefore effective stress, undergo the same changes in shape, generating the same changes in effective stress and therefore pore pressure (Fig. 2.10(c)). Thus, the structural strengths are the same for each specimen to give a unique Mohr's circle in terms of effective stress (Fig. 2.11).

It can be seen that undrained isotropic changes in stress do not alter the effective stress; this only happens for a saturated specimen, when one of the two principal stresses is changed with respect to the other

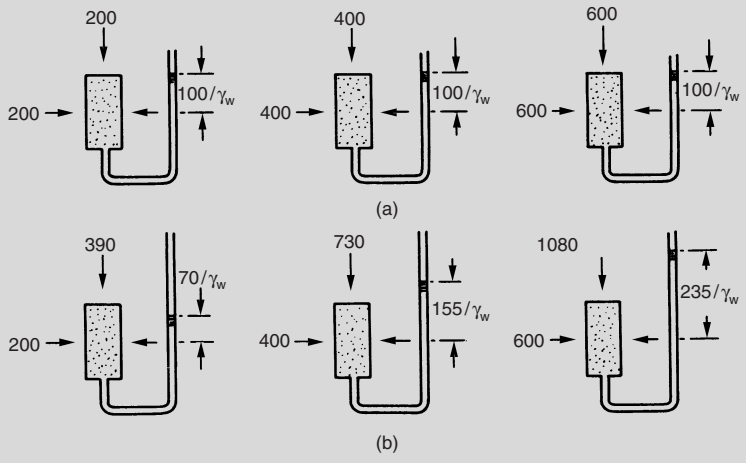

Fig. 2.12 Stress diagrams for the consolidated–undrained test. (a) application of cell pressure. Drainage to back pressure of 100 kPa; (b) application of axial load to failure, undrained

to give rise to a principal stress difference of $(\sigma_1 - \sigma_3)$. The compressive strength of the soil specimen is $(\sigma_1 - \sigma_3)_f$, that is, the principal stress difference at failure.

Because only one Mohr's circle with respect to effective stress results, an envelope cannot be obtained. In order to separate the Mohr's circles and obtain an envelope, the consolidated–undrained test is used.

Consolidated–undrained test

Each originally identical specimen has its structure altered in turn by allowing it to drain under the cell pressure against a back pressure of 100 kPa (Fig. 2.12(a)).

This consolidation stage increases the effective stresses to the difference between the respective cell pressures and the back pressure, the pore volume decreasing by drainage of pore water out of the specimen, increasing the stiffness and strength of the consequently denser structure.

When the consolidation stage is completed, drainage during axial loading is not allowed and the specimens are loaded axially to failure in the undrained condition as before (Fig. 2.12(b)). However, in this case, the different soil structures respond to the deformation with different strengths giving rise to Mohr's circles of different location and diameter (Fig. 2.11).

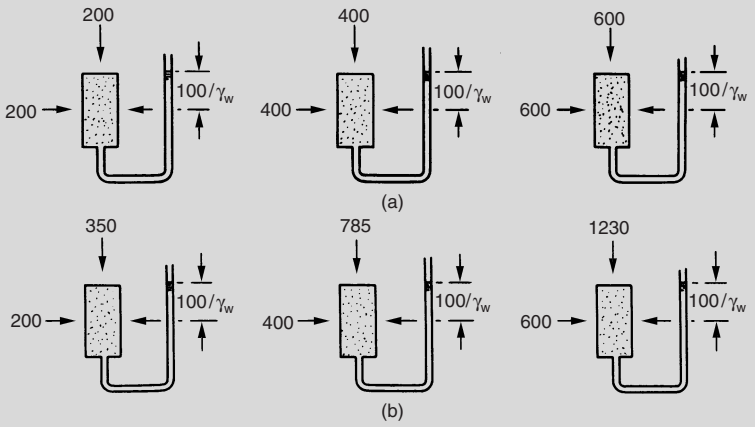

Fig. 2.13 Stress diagrams for drained test. (a) application of cell pressure. Drainage to back pressure of 100 kPa; (b) application of axial load to failure. Drainage to back pressure of 100 kPa

Drained test

The effective stress shear strength parameters may also be obtained by carrying out drained tests. Here, as the name suggests, the specimen is drained the whole time, that is during the cell pressure application (Fig. 2.13(a)) and during axial loading to failure (Fig. 2.13(b)). As the pore pressures are set to the back pressure, the effective stresses are readily obtained from the total stresses (Fig. 2.14).

The correlation between the various tests may be seen by considering, say, specimen number 2 (Fig. 2.15).

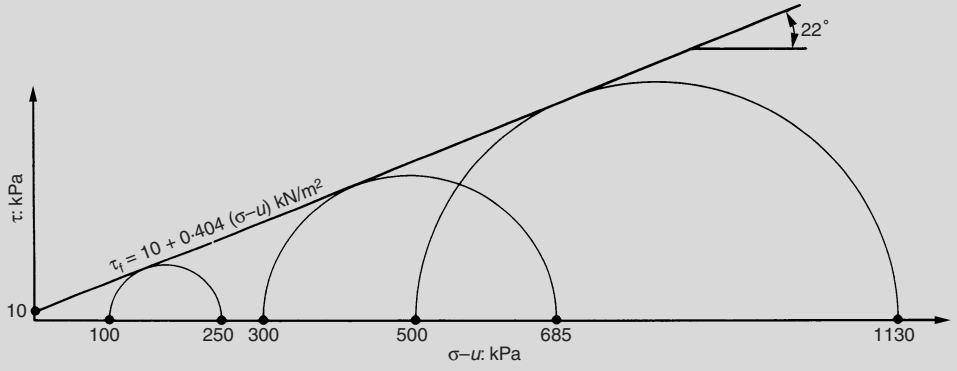

Fig. 2.14 Failure envelope for drained triaxial compression test

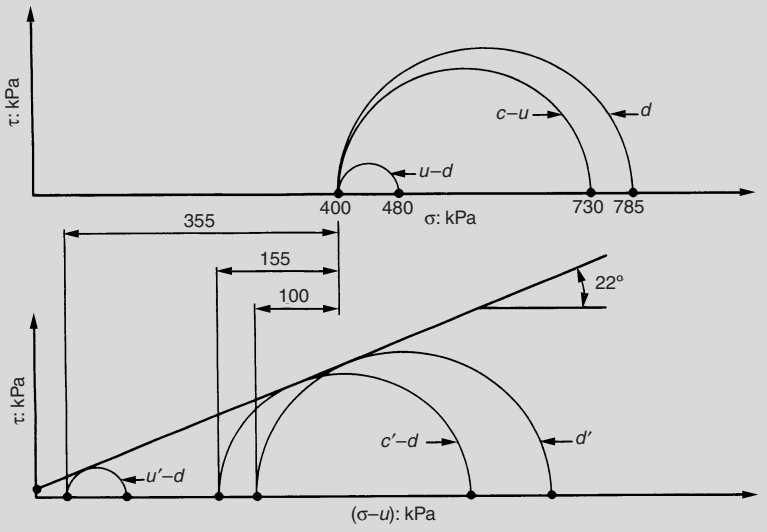

Fig. 2.15 Correlation between undrained (u–d), consolidated–undrained (c–u) and drained (d) triaxial compression tests for specimen number 2

Unconfined compression test

A further axial compression test is unconfined compression which may be regarded as a forerunner of the triaxial compression test. The cylindrical specimen of saturated clay is rapidly loaded axially but is not sheathed in a rubber membrane and is not confined by a cell pressure, that is, $\sigma_3 = 0$. The test is undrained and the undrained shear strength is $s_u = \tau_{max} = \sigma_1/2$ as shown in Fig. 2.9.

Stress paths in the triaxial test

The plotting of several Mohr's circles to determine the failure envelope can lead to a confusing number of circles. One way of overcoming this problem is to plot one point only. It is useful to plot the topmost point of the Mohr's circle as shown in Fig. 2.16. Typical effective stress paths for soft and stiff soils in the consolidated–undrained triaxial test are given in Fig. 2.17.

To obtain the effective stress shear strength parameters a *failure line is* drawn tangential to the *failure* portion of the stress path. Taking the slope of this line as θ and the intercept of the maximum shear stress axis as K gives

$$c' = K \sec \phi' \tag{2.13}$$

$$\phi' = \sin^{-1}(\tan \theta) \tag{2.14}$$

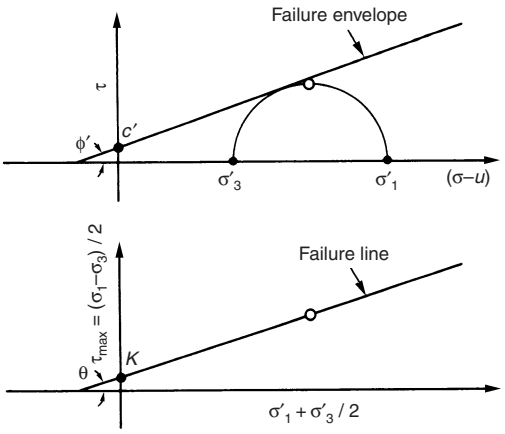

Fig. 2.16 Stress-path representation of top point of Mohr's circle at failure

Plotting triaxial test results in this way gives a clear and unambiguous indication of failure.

The fifteen commandments of triaxial testing

1. Obtain good quality 'undisturbed' samples by using the best available technique in relation to soil type, e.g. thin-walled piston samplers jacked (not hammered) into place in soft clays, block samples for stiff clays. Ensure good quality storage and transport of samples.
2. Test immediately on sampling or as soon as possible thereafter to minimise time-dependent sampling disturbance.
3. Use dry porous stones to avoid take up of water by soil suction (this does depend on soil type, overconsolidation ratio, etc). Raise cell pressure until pore water pressure is zero (see 4).

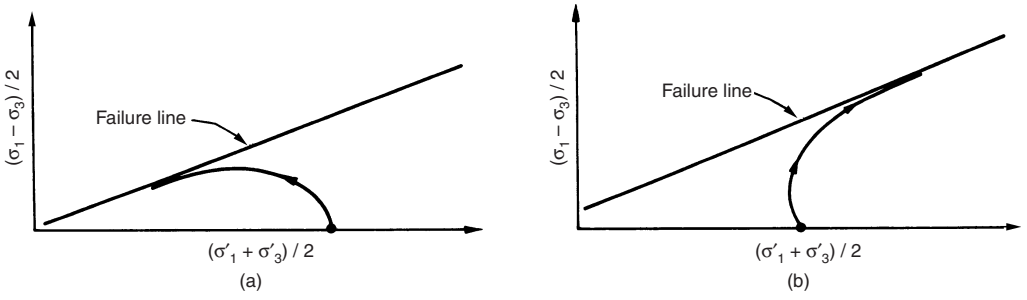

Fig. 2.17 Typical effective stress paths for undrained triaxial compression tests on (a) loose sand/soft clay; (b) dense sand/stiff clay

Then flush stones with de-aired water. Then slowly (see 7) restore in situ stresses.

4. Use a mid-plane pore pressure probe. Not only does this measure pore pressure in the zone of maximum shear strain, but it also measures original suction as well as detecting the zero pore pressure condition sought in 3. Control drained testing rate using pore pressure gradient. Using the mid-plane pore pressure probe, this can apply to undrained tests as well.
5. Use local strain transducers to measure axial and radial deformations directly on the test specimen (normally used to measure the small strain stiffness of stiff soils). These measurements do not include bedding errors and machine compliance and so provide small strain Young's modulus and Poisson's ratio appropriate to ground movements around real structures.
6. Use internal submersible load cell to measure axial force. This measurement does not include ram friction. Take care you use the correct range of load cell (see 10). Use extension top caps so you can apply stress paths simulating unloading, e.g. excavation. Better still, use a triaxial cell with internal tie rods so you can fix the loading ram and top cap together.
7. Saturate test specimens slowly. This minimises 'destructuration' (sample damage) which can occur when actual pore pressure changes lag behind back-pressure changes and so the effective stress state is different from that intended. Measure volume change carefully and correct the cross-sectional area of the test specimen to give accurate deviator stress. Remember that the sample must be fully saturated at failure also.
8. Soil is a stress path-dependent material so use testing regimes (frequencies and amplitudes, stress paths, strain paths, etc.) which mirror actual geological conditions (e.g. earthquake), construction sequences (e.g. excavation followed by installation of foundations), and in-service processes (e.g. filling and emptying oil storage tanks). This may be less important for undrained tests on saturated test specimens.
9. Do not do just one test where you can do two. Do not do just two tests where you can do three, etc. Above all, demonstrate repeatability of your test procedures and hence your test results.
10. Have a numerate appreciation of the accuracy and resolution (they are different!) of the measurements you are making. Do not use high range transducers to carry out low range measurements – the Golden Rule of instrumentation!

11. Understand the theoretical soil mechanics involved. Know roughly what the answer should be. Realize that if a result is unexpected it is more likely to be because there was something wrong with the test than because the soil was unusual. Critically examine the results to ensure that they are physically reasonable. Do they pass the 'sanity test'?
12. Define the purpose of the test and ensure that the proposed test is suitable for the purpose. This normally means you select the appropriate drainage conditions and stress path as well as appropriate instrumentation, e.g. low range load cell for soft soils, local strain transducers for the measurement of small strain stiffness of stiff soils, mid-plane pore pressure probe to measure pore pressure parameter B for stiff soils, etc.
13. Maintain all the equipment and instruments in perfect working order. Calibrate the instruments frequently and determine the error of all readings. Note that 'error' is the sum of 'accuracy' (property of a transducer and its calibration) and 'resolution' (usually property of the measuring/logging system for transducers having infinite resolution like a pressure transducer, e.g. a 12 bit A/D converter has a resolution of 1 in 4096). Conduct a test with known constant loads and pressures and demonstrate that no changes of stress were recorded. Use a rigid steel block as a test specimen and demonstrate that no strains were measured. The duration of these tests should exceed the duration of a typical triaxial test.
14. Demonstrate that the rate of loading is sufficiently slow to ensure that all measurements are correct. You do this by reducing the testing rate until the results (e.g. c' and ϕ') do not change. In undrained tests with pore pressure measurement, the rate of loading must be slow enough to ensure that the measured pore pressures are representative of the sample. Be wary of high reported values of c'. Remember: ''no c' too low, no phi too high''.
15. Set up the steady-state condition prior to the test and demonstrate that your readings are not changing (you may have to wait to the end of a consolidation or swelling period). Record everything during the test itself. Continue the test until the test specimen has reached the state required by the purpose of the test. Continue to record the steady-state readings for a short period after the test is over. If the readings then change significantly or randomly then your measuring and logging system has probably broken down during the test and the test data should be rejected.

Field measurements of undrained shear strength

The triaxial and unconfined compression tests and the laboratory direct shear box test rely on obtaining samples of soil from the ground by sampling from boreholes or trial pits and sealing and transporting these samples to the laboratory. The degree of disturbance affecting the samples will vary according to the type of soil, sampling method and skill of the operator. At best, there will be some structural disturbance simply from the removal of the in situ stresses during sampling and laboratory preparation even if these in situ stresses are subsequently reapplied as a first stage of the test. There is, therefore, considerable attraction in measuring shear strength in the field, in situ.

The determination of the undrained shear strength is only appropriate in the case of clays which, in short term loading, may approximate in the field to the undrained condition. A typical variation of undrained shear strength with depth is shown in Fig. 2.18, for both normally consolidated and heavily over-consolidated clay.

An indication of undrained shear strength may be obtained from plasticity tests. For example, Fig. 2.19 shows the relationship between the ratio of the undrained shear strength to the effective overburden pressure, s_u/p' and the plasticity index, PI, for several normally consolidated marine clays.

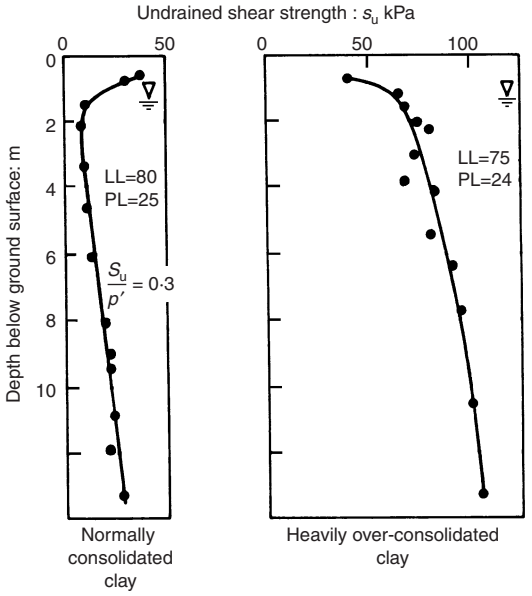

Fig. 2.18 Typical variations of undrained shear strength with depth, after Bishop and Henkel (1962)

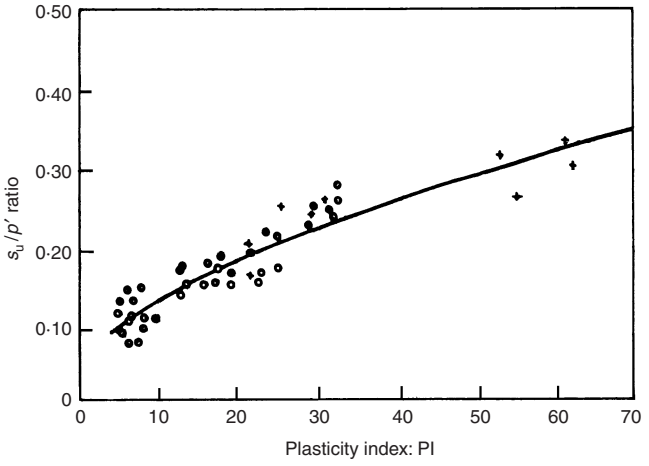

Fig. 2.19 Relationship between s_u/p' and plasticity index, after Bjerrum and Simons (1960)

As shown in Table 2.1, the relationship between consistency and strength may be generalized to give a rough guide of strength from field inspection.

The in situ shear vane

The field shear vane is a means of determining the in situ undrained shear strength. This consists of a cruciform vane on a shaft (Fig. 2.20). The vane is inserted into the clay soil and a measured increasing torque is applied to the shaft until the soil fails as indicated by a constant or dropping torque by shearing on a circumscribing cylindrical surface. The test is carried out rapidly. Now, if s_{u_v} is the undrained shear strength in the vertical direction, and s_{u_h} is the undrained shear strength in the horizontal direction,

Table 2.1 Consistency-strength relationship from field inspection (after BS 8004: 1986)

Consistency	Field indications	Undrained shear strength (kPa)
Very stiff	Brittle or very tough	>150
Stiff	Cannot be moulded in the fingers	75–150
Firm	Can be moulded in the fingers by strong pressure	40–75
Soft	Easily moulded in the fingers	20–40
Very soft	Exudes between the fingers when squeezed in the fist	<20

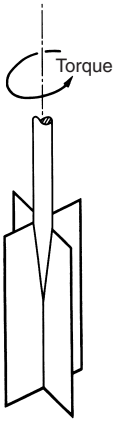

Fig. 2.20 Representation of the shear vane

then the maximum torque is

$$T = \frac{\pi D^2}{2}\left(Hs_{u_v} + \frac{D}{3}s_{u_h}\right) \tag{2.15}$$

where H is the vane height and D is the vane diameter, and assuming peak strengths are mobilized simultaneously along all vane edges.

This equation in two unknowns, s_{u_v} and s_{u_h} can only be solved if the torque is found for two vanes with different height to diameter ratios.

It is often incorrectly assumed that the soil is isotropic and

$$s_{u_v} = s_{u_h} = s_u$$

whence,

$$T = \frac{\pi D^2}{2}\left(H + \frac{D}{3}\right)s_u = ks_u$$

where k is a geometrical constant of the vane.

The in situ shear vane may be used in inspection pits and down boreholes for the extensive determination of in situ strength profiles as part of a site investigation programme.

Some types of shear vane equipment have the extension rods in an outer casing with the vane fitting inside a driving shoe. This type of vane may be driven or pushed to the desired depth and the vane extended from the shoe and the test carried out. The vane may then be retracted and driving continued to a lower depth.

It must be emphasized that the in situ vane provides a direct measure of shear strength and because the torque application is usually hand-operated, it is a relatively rapid strength measure, therefore giving the undrained shear strength.

The large diameter plate-loading test

In some over-consolidated clays such as London clay, the release of previous overburden pressure allows the soil mass to expand vertically causing cracks or fissures to form. In stiff fissured clay of this kind, therefore, the difficulty in shear testing is to ensure that the specimen or zone tested is representative of the fissured soil mass as a whole and not reflecting the behaviour of intact lumps. Small scale testing can, in these circumstances, be dangerously misleading, as demonstrated in Fig. 2.21. In the penetration test, a penetrometer with a conical point is loaded in a standard way. The penetration is measured and this provides indications of strength of intact lumps. The triaxial compression tests on 38 mm and 98 mm diameter specimens fail to include sufficiently the effect of the fissures. Only the large diameter (865 mm) in situ plate loading tests, carried out in the bottom of a borehole, tests a truly representative zone of soil. In this test, the plate is loaded and its deflection measured to give bearing pressure settlement relationships. At failure, bearing capacity theory is invoked to provide the field undrained shear strength. The line representing this undrained shear strength in Fig. 2.21 is the *lower bound* of the scatter of the triaxial test results and is the most appropriate value to use in a bearing capacity calculation.

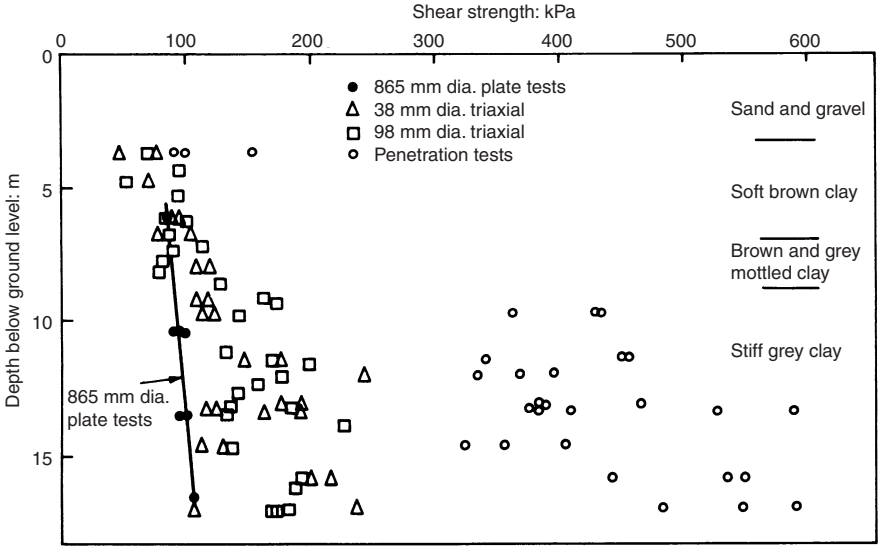

Fig. 2.21 Comparison of undrained shear strengths estimated from 865 mm diameter plate tests and triaxial tests on 38 mm and 98 mm diameter specimens in London clay at Chelsea, after Marsland (1971a)

Factors affecting the measurement of shear strength

The factor which most significantly affects the measurement of shear strength is the mode of test, that is, whether the test is drained or undrained and this has been considered previously. Further significant factors which affect the measurement of shear strength, particularly undrained shear strength, are the type of test, that is, whether by direct shear box, triaxial compression, in situ shear vane, etc; the effects of the orientation of the test specimen or test zone, that is, the effect of anisotropy; time to failure; sampling disturbance and size of test specimen or test zone; time between sampling and testing. These factors are now discussed.

Strength anisotropy

Soil-strength anisotropy arises from the two interacting anisotropies of geometrical anisotropy, that is, preferred particle packing; and of stress anisotropy. The geometrical anisotropy arises at deposition when the sedimented particles tend to orientate with their long axes horizontal seeking packing positions of minimum potential energy. The horizontal layering or bedding which results is further established by subsequent deposition which increases the overburden pressure. The stress anisotropy arises because of a combination of stress history and the geometrical anisotropies of both the particles themselves and of the packed structure they form. The net effect is a clear strength and stress–strain anisotropy.

Consider, for example, the drained triaxial compression tests carried out on a dense dry rounded sand in a new cubical triaxial cell described by Arthur and Menzies (1972). The cubical specimen was stressed on all six faces with flat, water-filled, pressurized rubber bags. The test specimen was prepared by pouring sand through air into a tilted former. In this way, it was possible to vary the direction of the bedding of the particles which was normal to the direction of deposition. A clear stress–strain anisotropy was measured, the strain required to mobilize a given strength being greater for the bedding aligned in the vertical major principal stress direction than for the conventional case of the bedding aligned horizontally in the test specimen.

Parallel tests were carried out by Arthur and Phillips (1972) in a conventional triaxial cell testing a prismatic specimen with lubricated ends. It can be seen from Fig. 2.22(a) that remarkably similar anisotropic strengths have been measured in different apparatus. The major differences in type of apparatus include the control of deformation (one stress control, the other, displacement control), the geometric proportions of the specimens, and the application of the boundary stresses (one with uniform pressures on each face and one with rigid ends). It would appear, therefore, that drained triaxial compression tests on a dry, rounded sand give

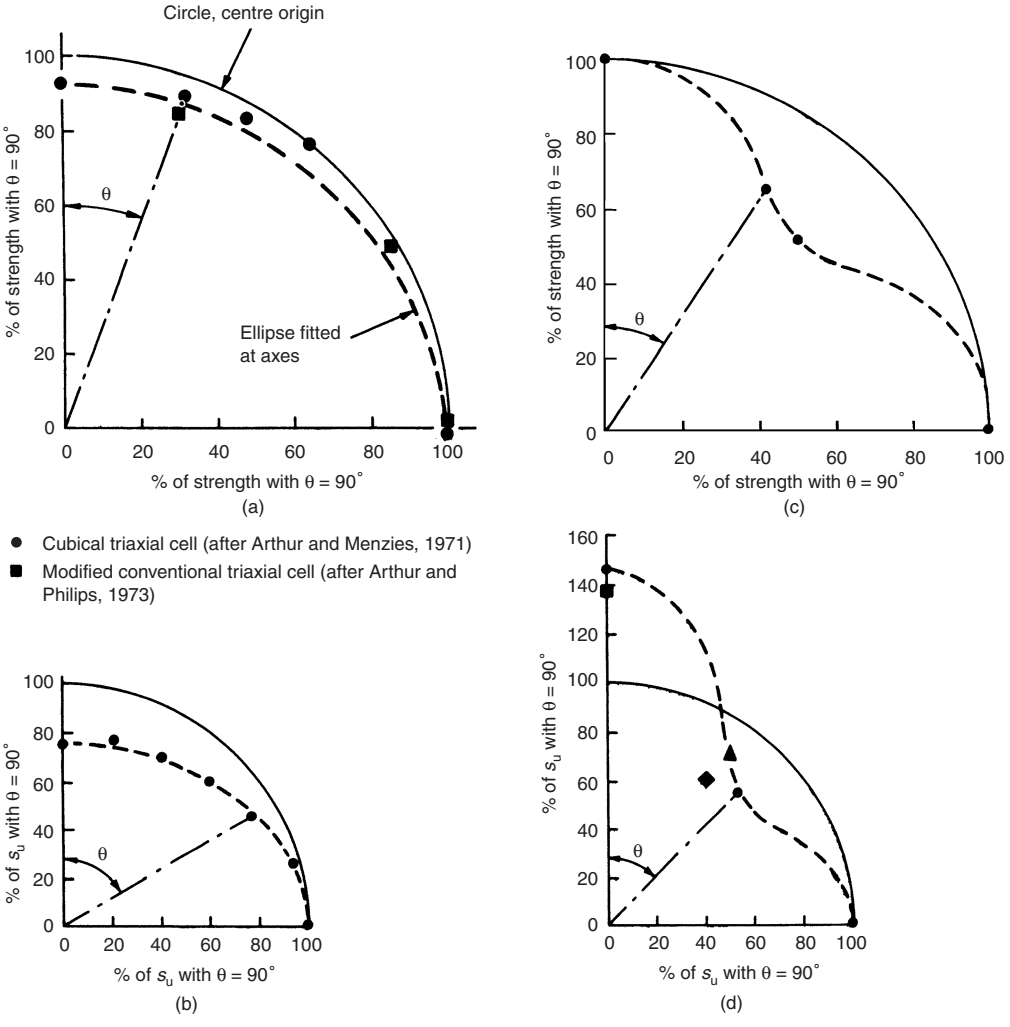

Fig. 2.22 Polar diagrams showing variations of soil strength measured in compression tests; θ denotes inclination of bedding with respect to vertical axis of test specimen. (a) drained tests on dense rounded Leighton Buzzard sand, after Arthur and Menzies (1971); (b) undrained tests on lightly over-consolidated Welland clay, after Lo (1965); (c) undrained tests on heavily over-consolidated blue London clay, after Simons (1967); (d) undrained tests on heavily over-consolidated London clay, after Bishop (1967)

similar measures of the strength anisotropy despite fundamental differences in the type of triaxial apparatus used. It is of interest to note that fitting an ellipse to the strength distribution of Fig. 2.22(a) adequately represents the variation. An elliptical variation of strength with direction was first proposed by Casagrande and Carillo (1944) in a theoretical

treatment. Lo (1965) found an elliptical-like variation in the undrained shear strength of a lightly over-consolidated Welland clay (Fig. 2.20(b)). Simons (1967) on the other hand, found a non-elliptical variation in the undrained shear strength of a heavily over-consolidated London clay (Fig. 2.22(c)). Results summarized by Bishop (1966) are similar (Fig. 2.22(d)).

Geometrical anisotropy, or *fabric* as it is sometimes called, not only gives rise to strength variations with orientation of the test axes but is also probably partly the cause of undrained strength variations between test type. Madhloom (1973) carried out a series of undrained triaxial

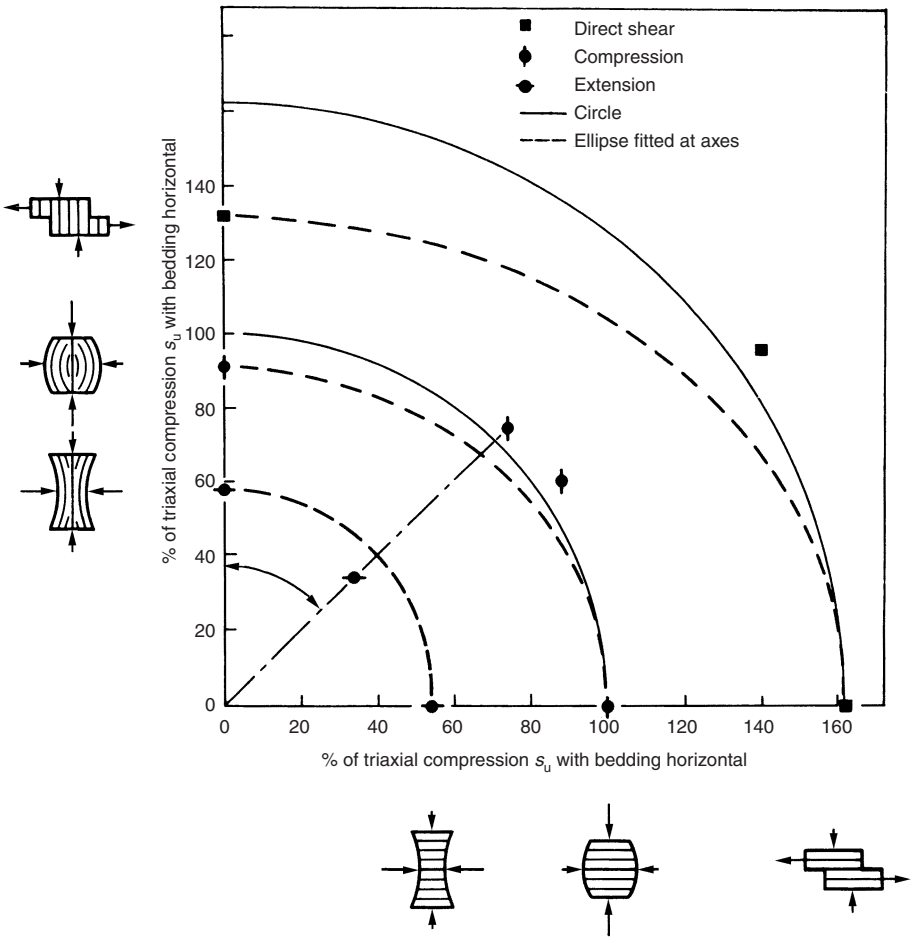

Fig. 2.23 Polar diagram showing the variation in undrained shear strength with test type and specimen orientation for a soft clay from Kings Lynn, Norfolk, after Madhloom (1974)

compression tests, triaxial extension tests and direct shear box tests using specimens of a soft, silty clay from Kings Lynn, Norfolk. The soil was obtained by using a Geonor piston sampler. Samples were extruded in the laboratory and hand-trimmed to give test specimens in which the bedding was orientated at different angles to the specimen axes. A polar diagram showing the variation of undrained shear strength with test type and specimen orientation is given in Fig. 2.23.

It is clear that the magnitude of undrained strength anisotropy in clays is much greater than drained strength anisotropy in sands. It can be seen that generally for this type of clay the triaxial compression test indicates a strength intermediate between that indicated by the triaxial extension test and the direct shear box test. This was not the case, however, in tests on soft marine clays reported by Bjerrum (1972a) and given in Table 2.2. Here the direct shear box (and the corrected shear vane) indicated strengths intermediate between the triaxial extension and compression tests.

Bjerrum (1972) found that using the undrained shear strength measured by the vane in a conventional limit analysis gave varying estimates of the

Table 2.2 Comparison between the results of compression and extension tests, direct simple shear tests, and in situ vane tests on soft clay, after Bjerrum (1972(a))

Type of soil	Index properties %			
	Water content, w	Liquid limit w_l	Plastic limit w_p	Plasticity index I_p
Bangkok clay	140	150	65	85
Matagami clay	90	85	38	47
Drammen plastic clay	52	61	32	29
Vaterland clay	35	42	26	16
Studentertunden	31	43	25	18
Drammen lean clay	30	33	22	11

Table 2.2 Continued

Type of soil	Triaxial test τ/p'_0		Simple shear test τ_f/p'_0	Vane tests s_u/p'_0	
	Compression	Extension		Observed	Corrected for rate
Bangkok clay	0.70	0.40	0.41	0.59	0.47
Matagami clay	0.61	0.45	0.39	0.46	0.40
Drammen plastic clay	0.40	0.15	0.30	0.36	0.30
Vaterland clay	0.32	0.09	0.26	0.22	0.20
Studentertunden	0.31	0.10	0.19	0.18	0.16
Drammen lean clay	0.34	0.09	0.22	0.24	0.21

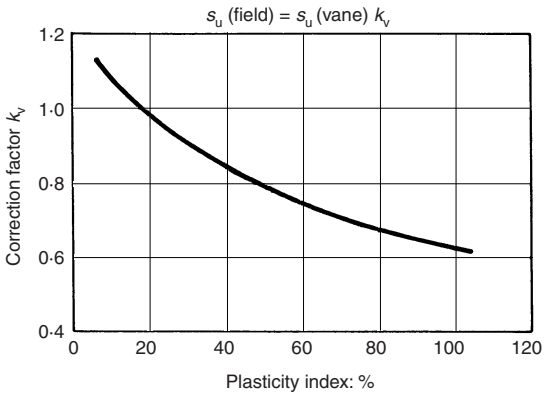

Fig. 2.24 Vane strength correction factor for soft clays, after Bjerrum (1973)

actual stability depending on the plasticity of the clay. The disparity between $s_{u_{(field)}}$ and $s_{u_{(vane)}}$ may be partly accounted for by the combined effects of anisotropy and testing rate. The correlation

$$s_{u_{(field)}} = s_{u_{(vane)}} k_v$$

for soft clays is given in Fig. 2.24.

Time to undrained failure

As demonstrated by Bjerrum, Simons and Torblaa (1958), the greater the time to undrained failure, the lower will be undrained strength (Fig. 2.25(a)). It is therefore necessary to take this factor into account when using the results of in situ vane tests or undrained triaxial compression tests, with a failure time of the order of 10 min, to predict the short term stability of cuttings and embankments, where the shear stresses leading to failure may be gradually applied over a period of many weeks of construction.

The greater the plasticity index of the clay, the greater is the reduction factor which should be applied to the results of the tests with small times to failure. As shown in Fig. 2.25(b) most of the reduction in undrained shear strength is because of an increase in the pore water pressure as the time to failure increases.

A further factor to be considered is the elapsed time between taking up a sample, or opening a test pit, and performing strength tests. No thorough study of this aspect has been made to date but it is apparent that the greater the elapsed time, for a stiff, fissured clay, the smaller is the measured strength. Marsland (1971b) noted that from loading tests made on 152 mm diameter plates at Ashford Common, strengths measured 4–8 hours and 2.5 days after excavation were approximately 85% and 75%,

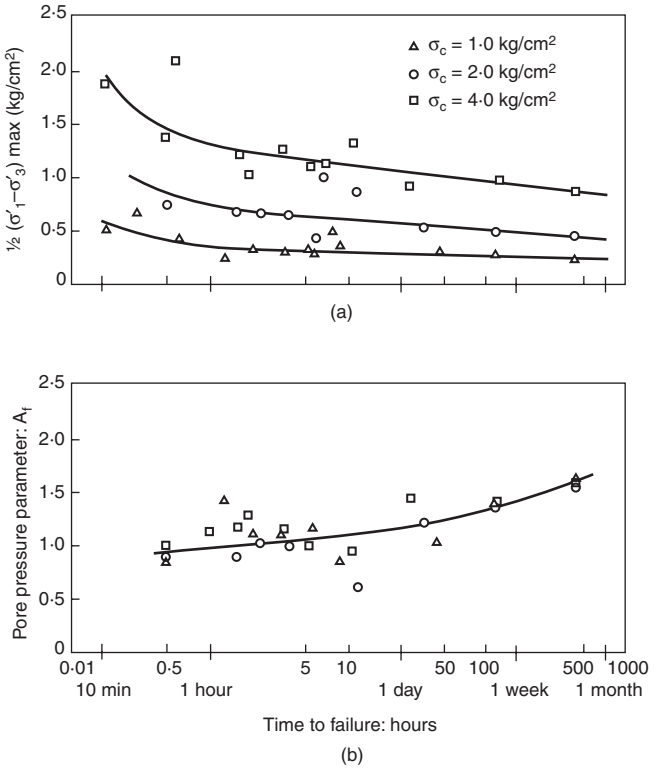

Fig. 2.25 The effect of time to failure on undrained shear strength and pore pressure generation, after Bjerrum, Simons and Torblaa (1958); (a) undrained shear strength plotted against time to failure; (b) pore-pressure parameter A_f plotted against time to failure

respectively, of those measured 0.5 hour after excavation. Other evidence was provided by laboratory tests on 38 mm dia. specimens cut from block samples of fissured clay from Wraysbury, which were stored for different periods before testing. Strengths of specimens cut from blocks stored for about 150 days before testing were only about 75% of the strengths of specimens prepared from blocks within 5 days of excavation from the shaft. This could be attributed to a gradual extension of fissures within the specimens.

Sampling disturbance and test specimen size

If the test specimen is disturbed by the sampling process, the measured undrained shear strength will generally be lower than the in situ value for a given test apparatus and procedure. Thin-walled piston samples jacked into the ground cause very little disturbance and this technique, together with careful handling in the field, during transit, and in the

laboratory, are believed to give reasonably reliable measurements of the undrained shear strength of clay. Equally well, hand-cut block samples of clay taken from open excavation may be used. In Table 2.3, which shows results reported by Simons (1967), the undrained shear strength of various sized test specimens of London clay is compared with that obtained from the customary 38 mm dia. × 76 mm triaxial specimens extracted from a U-4 sampling tube. The strength of 38 mm dia. × 76 mm triaxial specimens taken from hand-cut blocks is 143% of the strength obtained from 38 mm dia. × 76 mm specimens taken from U-4 sampling tubes. This difference results from the greater disturbance caused by using the U-4 sampling tubes.

From Table 2.3 it may also be seen that the size of specimen is of crucial importance. With stiff, fissured clays, the size of the test specimen must be large enough to ensure that the specimen is fully representative of the structure of the clay in the mass. If specimens are too small, the measured strength will be greater than that which can be relied on in the field.

In addition to the laboratory tests given in Table 2.3, Simons (1967) compared the results obtained from an analysis of a slip on the same site with 610 mm × 610 mm square in situ shear box tests, the 305 mm dia. × 610 mm vertical triaxial specimens and the 38 mm dia. × 76 mm vertical specimens from U-4 samples, the latter representing standard practice. These results are given in Table 2.4. Corrections have been made for the different water contents and times to failure, assuming purely undrained shear. The main points to note are:

- The standard 38 mm dia. × 76 mm specimens give a strength 185% times that indicated by an analysis of the slip. If no corrections are made for water content and time to failure, this ratio would be 310%;
- The 305 mm dia. × 610 mm triaxial specimens show a strength 21% higher than that indicated by the slip analysis. Of course, part of this

Table 2.3 Effect of test specimen size and time to failure on undrained shear strength of triaxial compression test specimens cut from intact blocks of blue London clay, after Simons (1967)

Size of triaxial test specimen (mm)	Number of tests	Water content w%	Time to failure t_f min.	s_u kPa	s_u ($w = 28$%) kPa	Strength ratio
305 × 610	5	28.2	63	48.8	50.7	0.62
152 × 305	9	27.1	110	51.5	46.0	0.56
102 × 203	11	27.7	175	47.9	46.4	0.57
38 × 76 (U-4)	36	26.9	8	93.4	81.9	1.00
38 × 76 (blocks)	12	28.1	7	116.3	117.3	1.43
13 × 25 (intact)	19	26.6	10	262.4	219.3	2.68

Table 2.4 Comparison of undrained shear tests on London clay, with strength estimated from a field failure, after Simons 1967)

Test	w% Water content	t_f Time to failure (min)	s_u kPa	s_u ($w = 28\%$) kPa	s_u ($w = 28\%$) ($t_f = 4000$ min) kPa	Strength ratio
Slip	29.3	4000	30.1	35.4	35.4	1.00
610 mm × 610 mm shear box	28.1	71	47.9	48.3	41.2	1.16
305 mm × 610 mm triaxial	28.2	63	48.8	50.8	43.1	1.21
38 mm × 76 mm triaxial	26.9	8	93.4	81.8	65.6	1.85

difference is due to the different inclinations of the failure surfaces as discussed later.

The 610 mm × 610 mm in situ shear box tests give a strength 16% higher than that from slip analysis.

Bearing in mind the approximate nature of the corrections made for water content and time to failure, and the possibility that slight restraint imposed by the shear box may have resulted in a higher measured strength, reasonable agreement between the in situ shear box tests and the slip analysis is indicated.

To summarize, the standard undrained triaxial tests carried out on 38 mm dia. × 76 mm specimens taken from U-4 samples greatly overestimates the in situ strength of the London clay as indicated by an analysis of the end of construction slip. Much better agreement is obtained from the results of triaxial specimens 100 mm dia. × 200 mm high and larger, and 610 mm × 610 mm in situ shear tests.

CHAPTER THREE

Immediate settlement

Introduction

Generally, the settlement of foundations may be regarded as consisting of three separate components of settlement, giving

$$\delta = \delta_i + \delta_c + \delta_s \tag{3.1}$$

where

- δ = total ultimate settlement,
- δ_i = immediate settlement resulting from the constant volume distortion of the loaded soil mass,
- δ_c = consolidation settlement resulting from the time dependent flow of water from the loaded area under the influence of the load generated excess pore pressure which is itself dissipated by the flow,
- δ_s = secondary settlement, or creep which is also time dependent but may occur at essentially constant effective stress.

This chapter covers the most convenient methods currently used to estimate the magnitude of the immediate or *undrained* settlement, δ_i. As a useful aside, some methods for estimating vertical foundation stresses are also given. The methods for estimating foundation settlement and stresses are based on the results of elastic theory.

The use of elastic theory in soil mechanics

In soil mechanics, foundation settlement and stresses under local loading (as against uniform global loading) conditions are determined from the established procedures of the mathematical theory of elasticity. Changes in foundation stresses caused by changes in applied loading are obtained in terms of total stress and the measured or computed pore pressure changes must be subtracted to yield the resulting changes in effective stress. The mathematical theory of elasticity furnishes the engineer with displacements and distributions of stresses caused by loads covering flat, flexible and rigid areas of various geometrical shapes, either on or in the horizontal surfaces of semi-infinite or layered elastic solids of wide extent. The procedure uses the assumption of constant soil parameters: Young's modulus, E, and Poisson's ratio, ν. These parameters

vary with time from the undrained values at the instant of loading ($\nu = 0.5$ for the idealized undrained case) to the drained values at the end of dissipation of the excess pore pressure. As pointed out by Davis and Poulos (1968) the assumption of constant elastic soil parameters does not imply that real soil behaves as an ideal elastic solid. Nevertheless, similarities exist between the behaviour of real soil and ideal elastic solids. Elastic-type behaviour may be simulated at small strains, that is, under loading conditions which ensure a high factor of safety against failure. This is reasonably true, for example, for foundations where the factor of safety is of the order of three, but is unlikely for embankments where the factor of safety is of the order of 1.5. In addition, at stresses less than the preconsolidation pressure, p'_c (also called 'maximum past pressure'), strains are very nearly recoverable (or 'elastic') whereas at stresses beyond p'_c, strains are permanent (or 'plastic'), i.e. p'_c is a *yield stress*.

Generally, however, soil stresses will decrease away from the loading in much the same way as in an elastic medium. The elastic *soil constants* must be experimentally determined under conditions which simulate the range of stresses and type of deformation encountered in the field, thereby justifying the use of the elastic analytical model for predicting stresses and settlements. Distributions of stress and displacement in an elastic solid caused by a distributed load are based on integrations of the effect of a vertical point load. There are solutions to various problems and most of these may be found in the comprehensive digests by Lysmer and Duncan (1972) and by Poulos and Davis (1974).

In the following sections, a limited selection may be found of the results for vertical loadings applied to an elastic solid of wide extent. From these results, foundation settlements and distributions of vertical stresses beneath foundations may be estimated.

Elastic stress distributions

Stress distributions may be obtained in the form of contours of equal stresses (Fig. 3.1) or *pressure bulbs* which serve as a useful qualitative conceptual aid. For example, it can be seen from Fig. 3.1(a) that the influence of a flexible strip footing does not extend much beyond a depth of about twice the footing width.

The distribution of contact pressure under a uniformly loaded, flexible circular area usually produces a bowl-shaped settlement of the loaded area (Fig. 3.2(a)). This is not always the case. The deformed shape will depend on the variation with depth of the moduli and on the relative magnitudes of the horizontal and vertical moduli (see Fig. 3.14).

In order to produce a uniform settlement, the unit load on a circular area must be very much greater at the rim than at the centre. Hence, if a

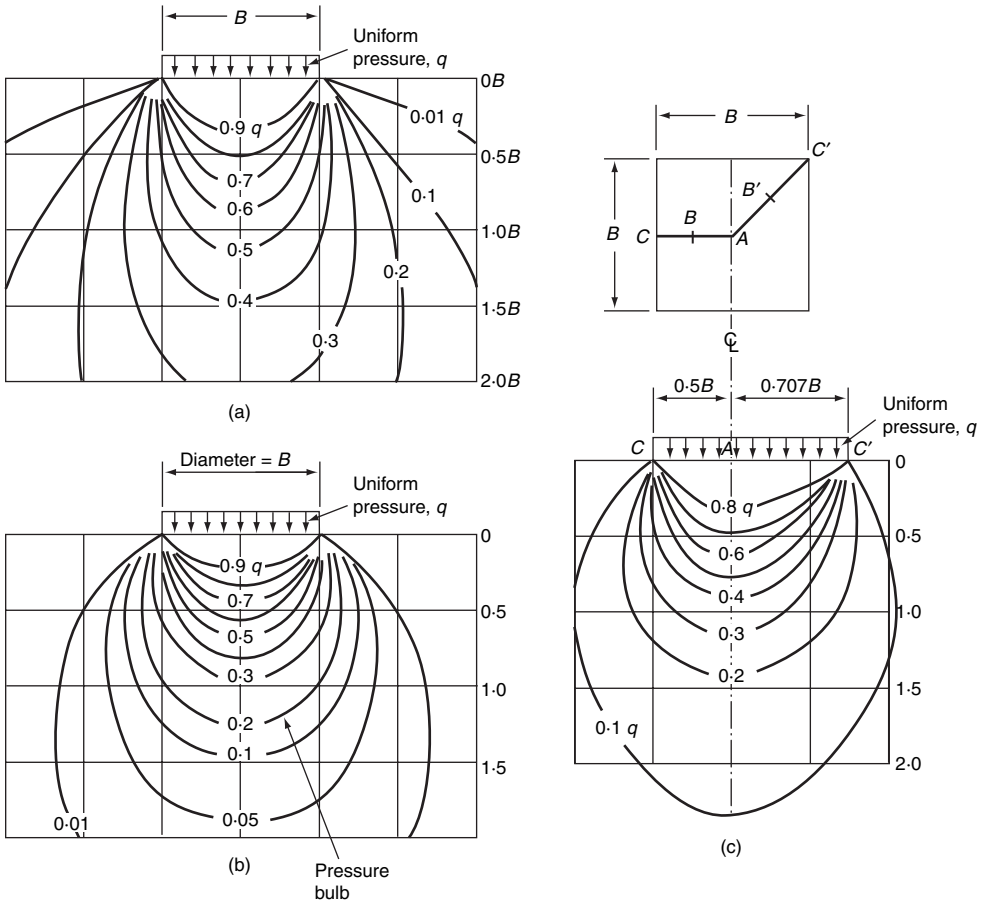

Fig. 3.1 Vertical stresses under uniformly loaded flexible footing resting on a deep wide homogenous isotropic elastic solid, after Teng (1962); (a) strip footing; (b) circular footing; (c) square footing

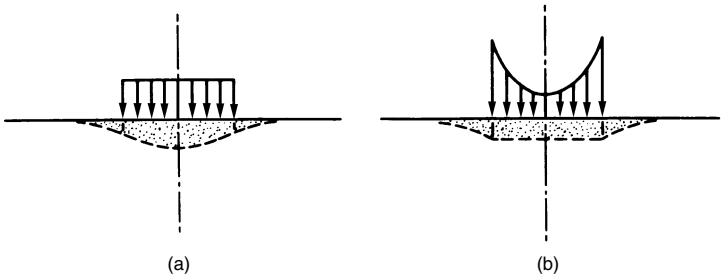

Fig. 3.2 Settlement and contact stresses for uniformly loaded circular areas resting on a deep wide homogeneous isotropic elastic solid. (a) flexible footings; (b) rigid footings

perfectly uniform settlement is enforced by the absolute rigidity of a footing, the contact pressure must increase from the centre of the base of the footing toward the rim, provided the supporting material is perfectly elastic (Fig. 3.2(b)). Thus the contact pressure of real rigid footings will be different from that of the idealized flexible footings. By St. Venant's principle, however, the stress distributions will be much the same.

> ***St. Venant's Principle***
> *If forces acting on a small portion of the surface of an elastic body are replaced by another statically equivalent system of forces acting on the same portion of the surface, this redistribution of loading produces substantial changes in the stresses locally but has a negligible effect on the stresses at distances which are large in comparison with the linear dimensions of the surface on which the forces are changed.*
> **Timoshenko and Goodier (1951)**

Design charts for estimating foundation stresses

Probably the most useful design chart for estimating foundation stresses is that given by Janbu, Bjerrum and Kjaernsli (1956) and shown in Fig. 3.3. This chart gives the increase in vertical stress beneath the *centre* of a uniformly loaded flexible area of strip, rectangular or circular shape.

The design chart of Fadum (1948) given in Fig. 3.4 is of classical interest. It provides estimates of vertical stress beneath the *corner* of uniformly loaded flexible rectangular areas. It may also be used for stress determination beneath any point on a uniformly loaded area of a shape amenable to subdivision into rectangular areas. The subdivision is carried out in such a way that the point under consideration forms a common corner. The contribution from each area is computed and summed, invoking the principle of superposition. The technique may be extended to include a point outside the area. In this case, the area is extended to include the point with subdivision and computation carried out as before except that the contribution of the fictitious area is subtracted.

For estimating vertical stresses beneath flexible, uniformly loaded areas of shapes not amenable to treatment by Figs. 3.3 or 3.4, the chart given by Newmark (1942) and shown in Fig. 3.5 may be used. In this case, the area is drawn to scale on transparent paper such that the depth at which the stress change is required equals the scale datum AB (Fig. 3.5). The scale drawing is positioned on the chart with the point in question (either inside or outside the area) located on the centre spot. An estimate is then made of the number of segments and fractions of segments, N, of the chart enclosed by the boundary of the scaled area. If the loading

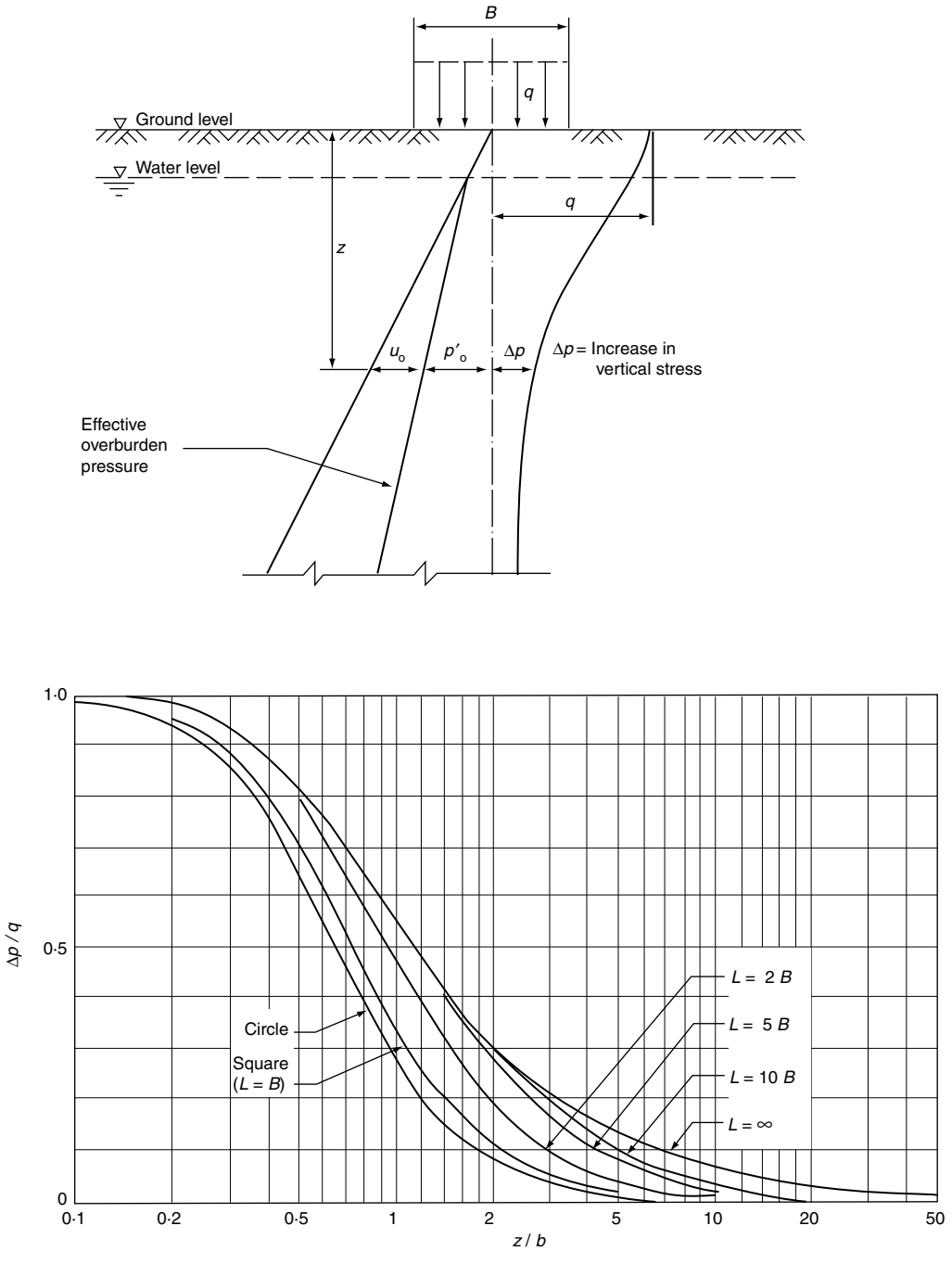

Fig. 3.3 Determination of increase in vertical stress under the centre of uniformly loaded flexible footings, after Janbu, Bjerrum and Kjaernsli (1956)

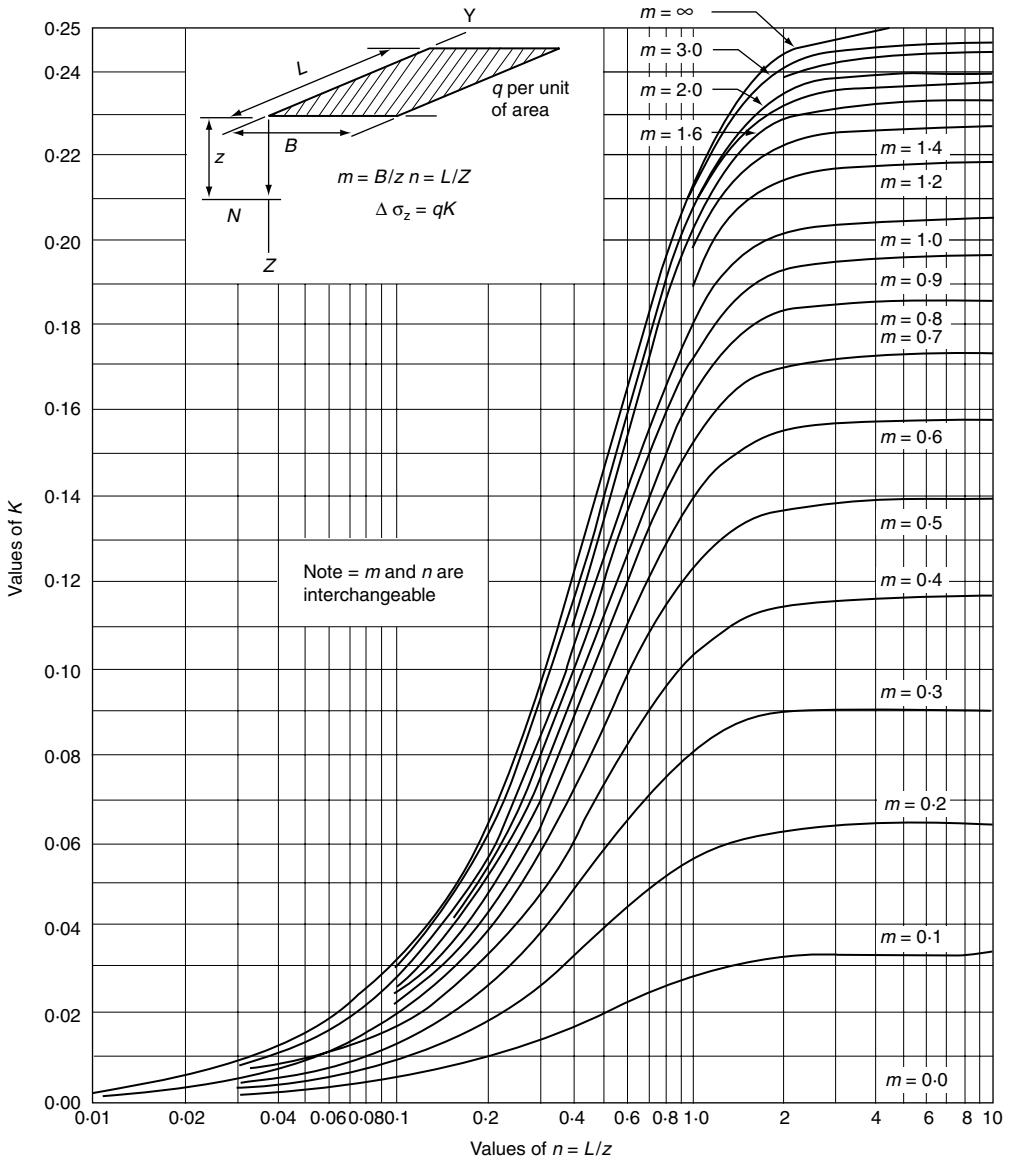

Fig. 3.4 Influence coefficients for the increase in vertical stress under the corner of a uniformly loaded flexible rectangular footing, after Fadum (1948)

intensity is q kPa, then the stress at the required depth below the point in question is computed as $\sigma_v = 0.001Nq$ kPa.

Elastic settlements

As pointed out by Davis and Poulos (1968), in a layered soil the total final settlement may be obtained by summation of the vertical strains in each

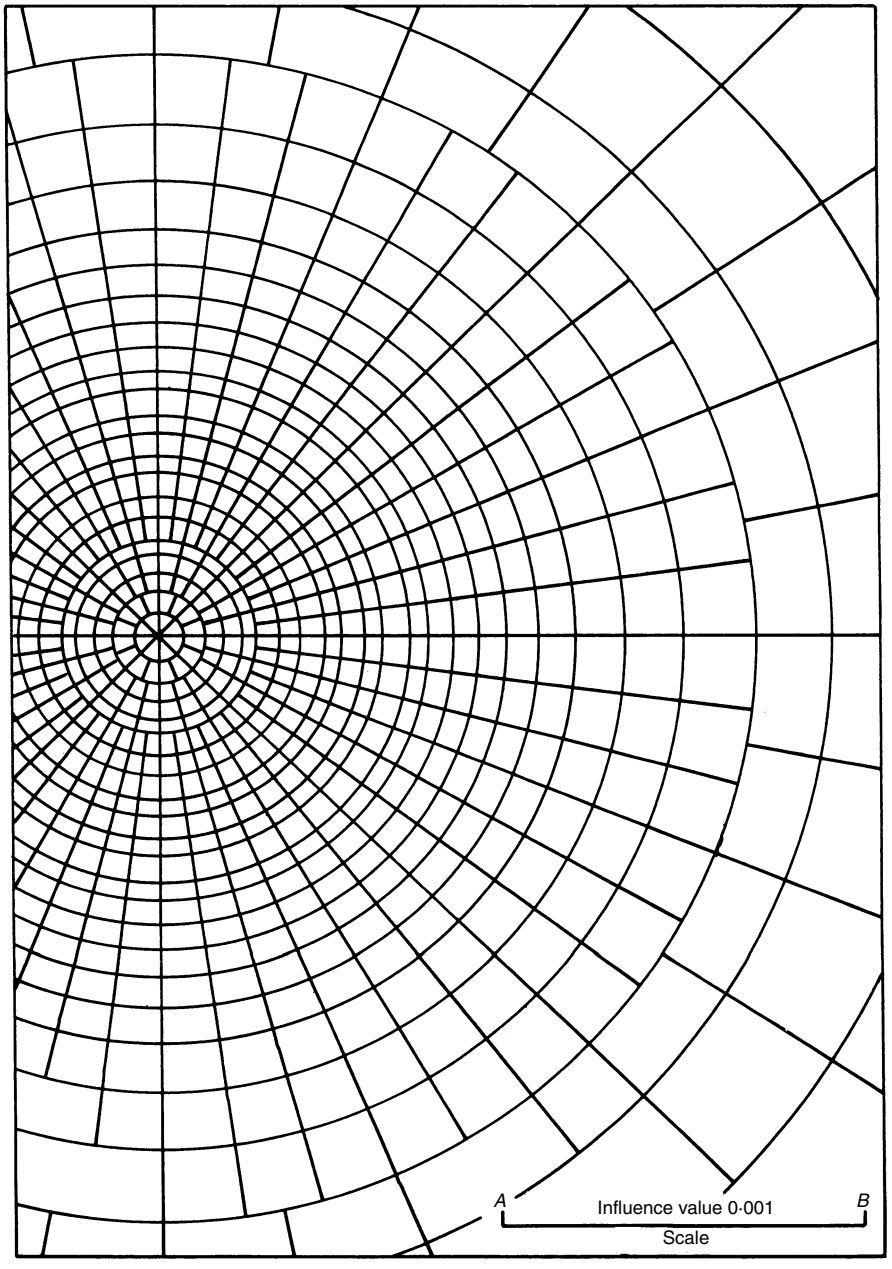

Fig. 3.5 Influence chart for the increase in vertical stress under a uniformly loaded flexible footing, after Newmark (1942)

layer whence generally

$$\delta_z = \sum \frac{1}{E'}(\sigma_z - \nu'\sigma_x - \nu'\sigma_y)\delta h \tag{3.2}$$

where E' and ν' are the elastic parameters for the soil structure appropriate to the stress changes in each layer; σ_x, σ_y and σ_z, are the stresses owing to the foundation, and δh is the thickness of each layer.

If, however, the soil profile is, for example, a reasonably homogeneous clay stratum, then appropriate values of E' and ν' can be assigned to the clay for the whole depth of the stratum, giving

$$\delta_z = \frac{qBI}{E'} \tag{3.3}$$

where q is the foundation pressure, B is some convenient dimension of the foundation and I is an influence factor given by elastic theory.

Undrained or immediate settlements

If an incompressible elastic solid of wide extent is locally loaded, local deformations will occur at constant volume. If a saturated clay layer is rapidly loaded locally, the low permeability of the clay retards drainage of water out of the pores and the clay deforms in the undrained or constant volume mode. The similarity is thus apparent between a loaded incompressible (i.e. $\nu = 0.5$) elastic solid and a loaded *end of construction* saturated clay. The appropriate form, therefore, of equation (3.3) is

$$\delta_i = \delta_u = \frac{qBI_u}{E_u} \tag{3.4}$$

where I_u is the influence factor for $\nu = \nu_u = 0.5$ and E_u is the modulus determined from undrained triaxial tests.

Design charts for estimating immediate settlements

Probably the most useful chart is that given by Janbu, Bjerrum and Kjaernsli (1956) and reinterpreted by Christian and Carrier (1978) and shown in Fig. 3.6. The chart provides estimates of the *average* immediate settlement of uniformly loaded, flexible areas, rectangular or circular in shape, embedded in soils that can be assumed to be elastic and incompresible. The average settlements are obtained from equation (3.4) putting $I_u = \mu_0\mu_1$.

Generally, real soil profiles which are deposited naturally consist of layers of soils of different properties underlain ultimately by a *hard* stratum. Within these layers, strength and moduli generally increase with depth. Gibson (1967) has shown that the variation of modulus with

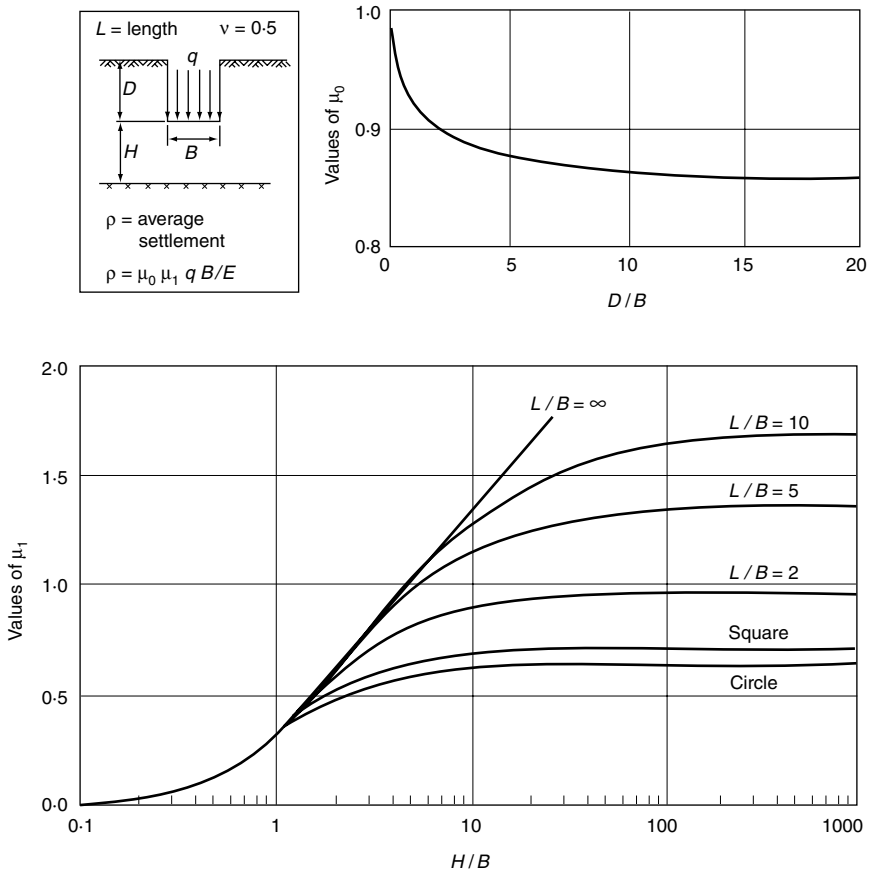

Fig. 3.6 Diagrams for the factors μ_0 and μ_1 used in the calculation of the immediate average settlement of uniformly loaded flexible areas on homogeneous isotropic saturated clay, after Janbu, Bjerrum and Kjaernsli (1956), as reinterpreted by Christian and Carrier (1978)

depth has little effect on the distribution of stresses but has a marked effect on surface displacements which are concentrated within the loaded area for an incompressible medium. The chart given in Fig. 3.6 may be used to accommodate a variation of E with depth by replacing the multi-layered system with one hypothetical layer on a rigid base. The depth of this hypothetical layer is successively extended to incorporate each *real* layer, the corresponding values of E being ascribed in each case and settlements calculated. By subtracting the effect of the hypothetical layer above each *real* layer, the separate compression of each layer may be found and summed to give the overall total settlement.

WORKED EXAMPLE

Consider the typical example given in Fig. 3.7. Referring to Fig. 3.6, $D/B = 0.3$, whence $\mu_0 = 0.96$. For layer (1) $L/B = 4$ and $H/B = 1$, whence $\mu_1 = 0.3$.

The compression of layer (1) if it had a rigid base is therefore,

$$\delta_{(1)_{20}} = 0.3 \times 0.96 \times \frac{0.05 \times 10}{20} = 0.0072\,\text{m}$$

Assuming that layer (2) extends to the surface and has a rigid base gives $H/B = 1.5$ whence $\mu_1 = 0.5$.

The combined compression of layer (1) and (2) if $E_1 = E_2 = 30\,\text{MPa}$ and if layer (2) had a rigid base is, therefore,

$$\delta_{(1,2)_{30}} = 0.5 \times 0.96 \times \frac{0.05 \times 10}{30} = 0.0080\,\text{m}$$

The compression of layer (1) if $E_1 = E_2 = 30\,\text{MPa}$ and if it had a rigid base is

$$\delta_{(1)_{30}} = 0.3 \times 0.96 \times \frac{0.05 \times 10}{30} = 0.0048\,\text{m}$$

Assuming that layer (3) extends to the surface gives $H/B = 2.5$ whence $\mu_1 = 0.75$.

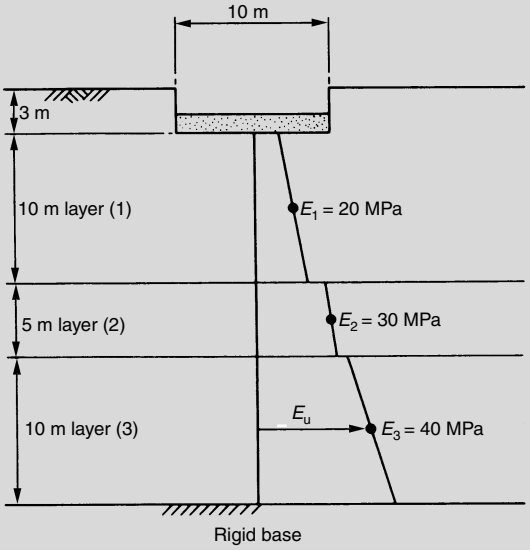

Fig. 3.7 Rectangular footing, 10 m × 40 m, uniformly loaded with net intensity 50 kPa

The compression of layers (1), (2) and (3) if $E_1 = E_2 = E3 = 40\,\text{MPa}$ is, therefore,

$$\delta_{(1,2,3)_{40}} = 0.75 \times 0.96 \times \frac{0.05 \times 10}{40} = 0.0090\,\text{m}$$

The combined compression of layers (1) and (2) if $E_1 = E_2 = 40\,\text{MPa}$ and if layer (2) has a rigid base is

$$\delta_{(1,2)_{40}} = 0.5 \times 0.96 \times \frac{0.05 \times 10}{40} = 0.0060\,\text{m}$$

The overall total settlement is, therefore,

$$\begin{aligned}\delta_{(1)_{20}(2)_{30}(3)_{40}} &= \delta_{(1)_{20}} + \delta_{(1,2)_{30}} - \delta_{(1)_{30}} + \delta_{(1,2,3)_{40}} - \delta_{(1,2)_{40}} \\ &= 0.0072 + 0.0080 - 0.0048 + 0.0090 - 0.0060\,\text{m} \\ &= 13.4\,\text{mm}\end{aligned}$$

Butler (1974) has adopted a similar approach using a simple extrapolation of Steinbrenner's (1934) approximation. The Boussinesq (1885) displacements for an infinite depth of soil are used. The effect of the rigid base is simulated by the approximation that the compression of a finite layer of depth z metres on a rigid base is the same as the compression within the top z metres of an infinitely deep deposit.

Butler gives charts which enable estimates to be made of the settlement of the corner of a uniformly loaded, flexible rectangular area resting on the surface of a heterogeneous elastic layer. It is assumed that the modulus increases linearly with depth. Butler's charts for immediate (undrained) settlement are given in Fig. 3.8(a), (b) and (c).

The result of the following worked example tends to confirm the rough guide relating the relative settlements given by the expression

$$\delta_{(\text{flexible, average})} \approx 0.9\delta_{(\text{flexible maximum})} \approx 1.1\delta_{(\text{rigid})}$$

Davis and Poulos (1968) give the following expressions effectively relating rigid footing settlements to flexible footing settlements.

For a circle,

$$\delta_{\text{rigid}} \approx \tfrac{1}{2}(\delta_{\text{centre}} + \delta_{\text{edge}})_{\text{flexible}}$$

For a rectangle,

$$\delta_{\text{rigid}} \approx \tfrac{1}{3}(2\delta_{\text{centre}} + \delta_{\text{corner}})_{\text{flexible}}$$

For a strip,

$$\delta_{\text{rigid}} \approx \tfrac{1}{2}(\delta_{\text{centre}} + \delta_{\text{edge}})_{\text{flexible}}$$

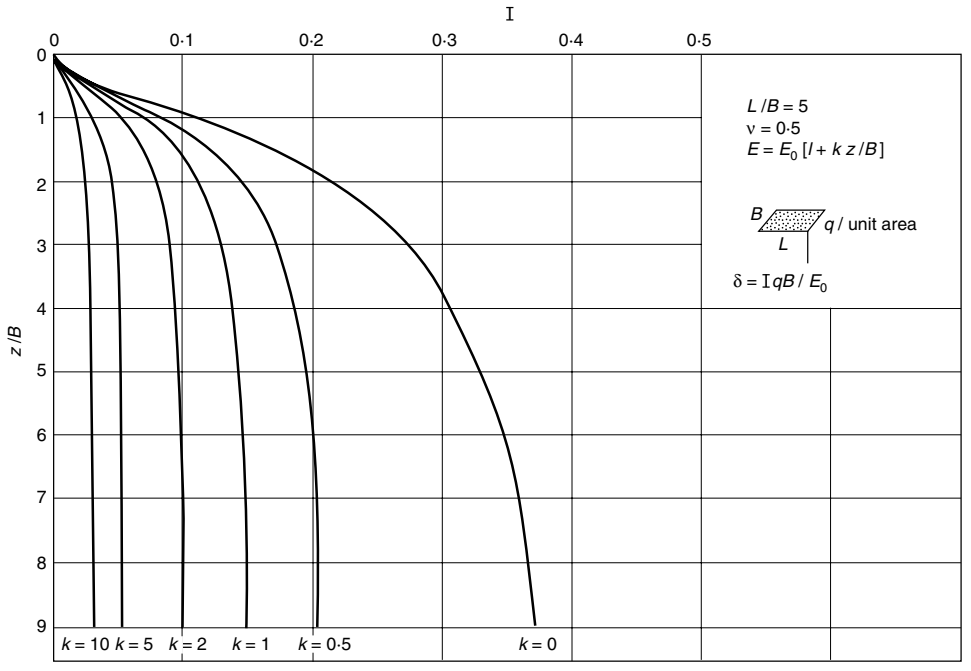

(a)

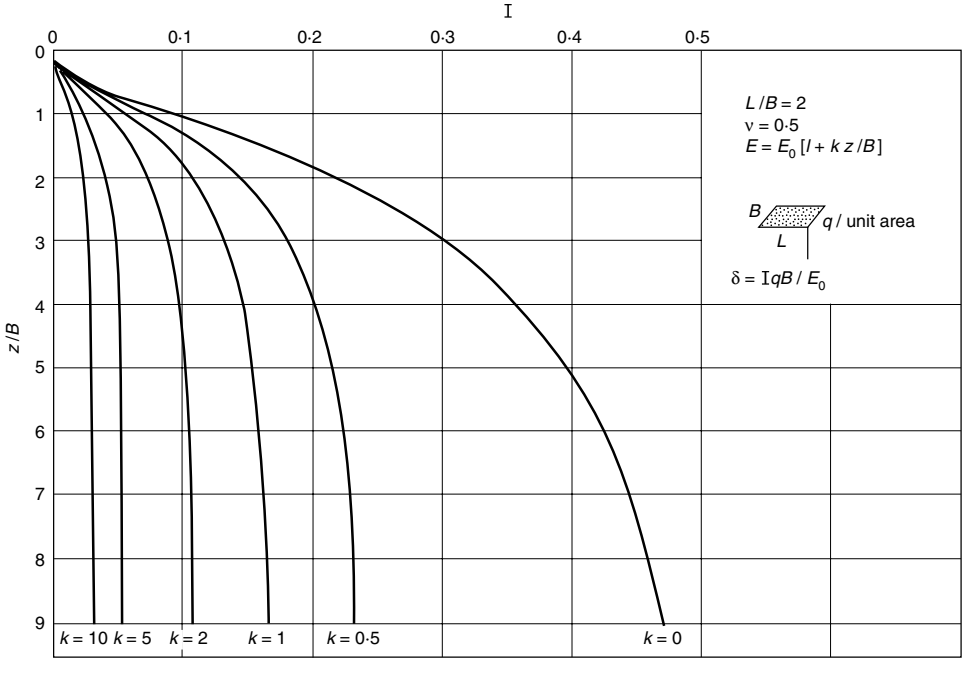

(b)

Fig. 3.8 (a) and (b)

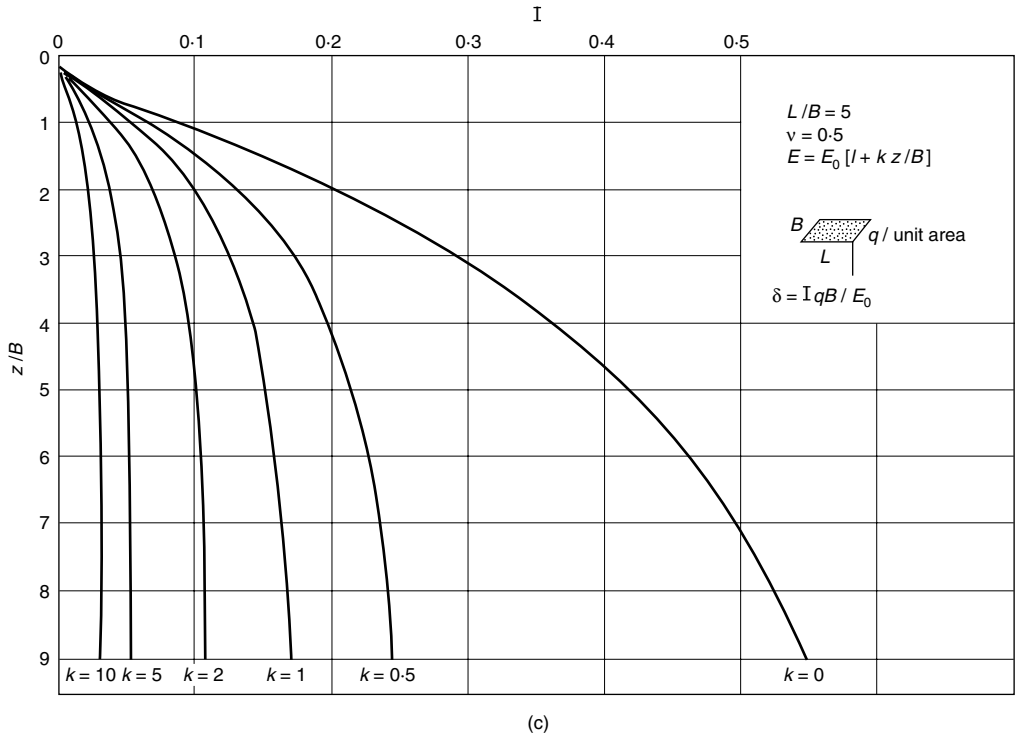

Fig. 3.8 Influence coefficients for immediate settlement of the corner of a flexible uniformly loaded rectangle on the surface of a saturated clay with Young's modulus increasing linearly with depth, after Butler (1975); (a) length to breadth ratio $L/B = 1$; (b) length to breadth ratio $L/B = 2$; (c) length to breadth ratio $L/B = 5$

As far as the footing roughness is concerned, it should be noted that an analysis of a rigid circular plate resting on a heterogeneous elastic half-space (Carrier and Christian, 1973) showed that for most practical problems the solution for a rough plate was the same as the solution for a smooth plate.

WORKED EXAMPLE

Consider the case shown in Fig. 3.9. The settlement at the centre may be found by subdividing the loaded area as shown and using superposition.

Referring to Fig. 3.8, for $L/B = 2$, $k = 0.5$, $z/b = 8$, we have $I = 0.23$.

The settlement of the corner of a rectangle 5 m × 10 m is

$$\delta_{\text{corner}} = \frac{BqI}{E_0} = \frac{5 \times 0.05}{10} \times 0.23 = 0.00575\,\text{m}$$

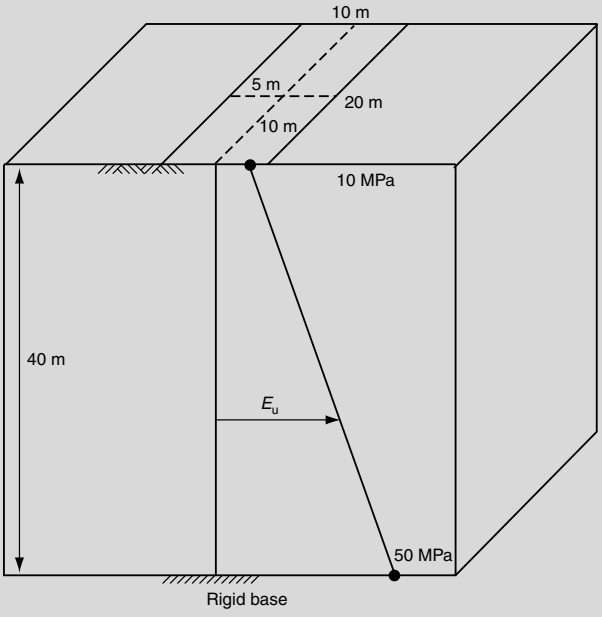

Fig. 3.9 Subdivision of rectangular area loaded uniformly with intensity 50 kPa

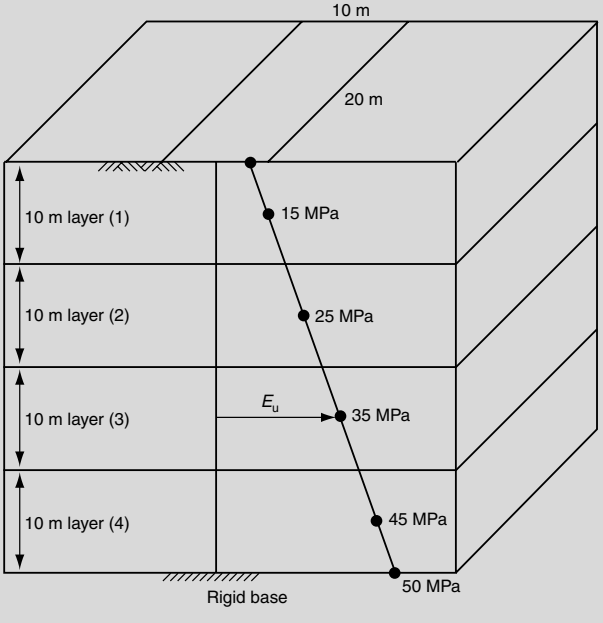

Fig. 3.10 Layering of soil profile beneath rectangular area uniformly loaded with intensity 50 kPa

By superposition, the settlement in the centre of a rectangle 10 m × 20 m is

$$\delta_{\text{centre}} = 4\delta_{\text{corner}} = 4 \times 0.00575 = 0.023\,\text{m}$$

This kind of problem may be dealt with using the chart given in Fig. 3.6 and *layering* the soil as shown in Fig. 3.10.

Noting that $L/B = 2$, $D/B = 0$, i.e. $\mu_0 = 1$, then for the four layers shown we have by Fig. 3.6

H/B	μ_1
1	0.3
2	0.65
3	0.75
4	0.8

Therefore,

$$\delta_{\text{average}} = 0.05 \times 10\left[\frac{0.3}{15} + \left(\frac{0.65}{25} - \frac{0.3}{25}\right) + \left(\frac{0.75}{35} - \frac{0.65}{35}\right) + \left(\frac{0.8}{45} - \frac{0.75}{45}\right)\right]$$

$$= 0.019\,\text{m}$$

Heave of excavations

When an excavation is opened, load is removed from the soil and *heave* may therefore be expected. This heave can be considered as occurring without change in volume of the soil, provided that no water is allowed to accumulate in the excavation, and that the excavation is kept open for a reasonably short period. The calculations of immediate heave may therefore be made in exactly the same way as for immediate settlement, considering the soil weight removed as a negative load. If water is allowed to remain in an excavation in clay for even a short time, not only will a greater heave be experienced owing to the soil increasing in volume by taking up water, but the shear strength, and hence the bearing capacity, will also be reduced.

There are two additional points to bear in mind when considering immediate heave:

- The value for E_u for unloading is generally greater than the value of E_u for loading.
- Any de-watering has a very great effect on the magnitude of the heave. Lowering the ground water table increases the effective stresses in the

underlying soil and this leads to settlement which tends to reduce the magnitude of the elastic heave.

Reference may be made to Serota and Jennings (1959).

Estimates of undrained modulus

Clearly, the success of the preceding methods in predicting undrained settlements rests crucially on the use of appropriate values of the undrained modulus, E_u. Indeed, the analytical sophistication of many methods presupposes, by implication, unrealistically accurate values of E_u.

Traditionally, E_u has been estimated from conventional undrained triaxial tests, where E_u is determined over a range of axial loading equal to half the ultimate. A worthwhile refinement is to determine E_u over the range of stress relevant to the particular problem, because the experimental stress–strain relationship may not be linear even for stresses less than 50% of the ultimate. Davis and Poulos (1968) suggest that the *undisturbed* triaxial specimen is given a preliminary consolidation under K_0 conditions and with an axial stress equal to the effective overburden pressure at the sampling depth. This procedure attempts to return the specimen to its original state of effective stress in the ground, assuming that the horizontal effective stress in the ground was the same as that produced by the laboratory K_0 condition. There is some evidence (Skempton and Sowa, 1963) to suggest that is not generally the case. Simons and Som (1970) have shown that triaxial tests on London clay in which the specimens are brought back to their original in situ stresses give elastic moduli which are much higher than those determined from conventional undrained triaxial tests. This has been confirmed by Marsland (1971) who carried out 865 mm diameter plate loading tests in 900 mm diameter bore holes in London clay. Marsland found that the average moduli determined from the loading tests on 865 mm diameter plates in well-prepared boreholes were between 1.8–4.8 times those obtained from undrained triaxial tests (see Fig. 3.11).

Sample disturbance is known to affect considerably the value of modulus obtained (Simons, 1957; Ladd, 1969; Raymond *et al.,* 1971). For example, it was found that for two structures in Norway (Simons, 1957), the E_u values obtained by carefully conducted, unconfined compression tests carried out on samples obtained by a 54 mm thin-walled stationary piston sampler, were about one-third of the values which could be estimated from the settlement observations. Ladd (1969) suggested that sample disturbance can be partly overcome by proper reconsolidation in the laboratory.

It has been suggested that more realistic determinations of E_u will be obtained if:

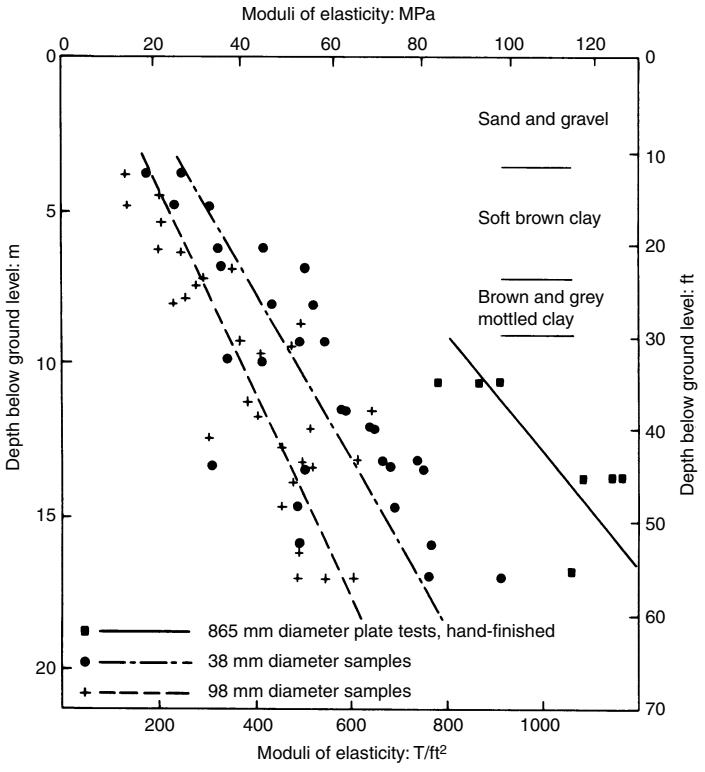

Fig. 3.11 Moduli determined from triaxial tests on 38 mm and 98 mm diameter specimens, and from 865 mm diameter plate tests on London clay at Chelsea, after Marsland, (1971c)

- Samples are reconsolidated under a stress system equal to that existing in the field, e.g. Simons (1957) and Berre (1973) or
- Samples are reconsolidated isotropically to a stress equal to 1/2 to 2/3 of the in situ vertical stress, Raymond *et al.* (1971).

However, if samples of sensitive clays in particular are significantly disturbed, then reconsolidation may well lead to changes in moisture content, and hence a stiffer soil structure, with E_u determinations which are on the high side.

Factors which should be considered when using consolidated undrained tests to estimate the deformation are: type of consolidation, that is, whether isotropic or anisotropic; the stress level; consolidation period; the stress path followed; the rate of strain; the elapsed times between opening up a test pit or drilling a borehole, taking a sample, and then testing it; the size of the sample; orientation of the sample.

Reference may be made to Marsland (1971), Ward (1971), Berre and Bjerrum (1973), Bjerrum (1973) and Lambe (1973a,b).

Of particular importance is the shear stress level. The field loading tests which have been carried out in Norway have yielded invaluable information. Two field loading tests on a soft quick clay were carried out at Asrum by Høeg, Andersland and Rolfsen (1969), another at Mastermyr by Frimann Clausen (1969, 1970) and two at Sunderland by Engesgaar (1970).

These tests showed clearly that for surface loads up to approximately one-third to one-half of the failure load, the measured undrained settlements (and the induced pore water pressures) were small; as the loading approached failure much larger settlements were naturally observed. The corresponding E_u values were thus shown to be very sensitive to the shear stress level. Even though the filling was placed on peat and soft quick clay with a total thickness of some 19 m, very small settlements were recorded during the early stages of the test at Mastermyr.

Carefully conducted laboratory tests on a variety of clays by Berre (1973), confirm the conclusion. In addition, Berre found that the undrained stress–strain relationships were somewhat anisotropic and also time-dependent, the smaller the strain rate the smaller the E_u value by a factor of approximately one third per log-cycle of time. It should, however, be pointed out that the E_u value for the Fornebu clay was not found to be dependent on the strain rate. Bjerrum, Simons and Torblaa (1957), and Madhloom (1973) found an increase in E_u with increasing time to failure.

Because of the many difficulties faced in selecting a modulus value from the results of laboratory tests, it has been suggested that a correlation between the deformation modulus and the undrained shear strength, may provide a basis for a settlement calculation. Different authors have quoted different values for the ratio of E_u/s_u, for example Bjerrum (1964), 250–500; and Bjerrum (1972), 500–1500.

Table 3.1 shows values of the E_u/s_u ratio for a number of structures on normally and slightly over-consolidated clay, and the ratio ranges from 40–3000. As discussed earlier, the shear stress level is a factor which has great influence on E_u; low values of E_u/s_u would be expected for highly plastic clays with a high shear stress level, and higher values for lightly-loaded clays of small plasticity (Ladd, 1964; Bjerrum, 1972).

The use of the Menard pressuremeter has also been advocated for the determination of the undrained modulus of clay (Hobbs, 1971; Calhoon, 1972). In principle, the pressuremeter, which tests a comparatively large volume of soil in situ, should provide a reliable basis for calculating the initial settlement, provided the soil is not greatly anisotropic with respect to E_u. It is of interest to note that Calhoon (1972) found that initial settlements computed from pressuremeter data are of the same order of magnitude as initial settlements computed for E_u values in the range 500–1000 times the undrained shear strength.

Table 3.1 Values of the ratio of undrained modulus to undrained shear strength, after Simons (1974)

Site	E_u/s_u	Reference
Test embankment	40	Wilkes (1974)
Oil tanks, Arabian Gulf	50–70 (depending on factor of safety)	Meigh and Corbett (1970)
Skabo Office Building Oslo	150	Simons (1957)
Turnhallen (Heavy) Drammen	190	Simons (1957)
Tank, Shellhaven	220	Bjerrum (1964)
Northeast Test Embankment, Boston	240	Lambe (1973a)
Preload test, Lagunillas	250	Lambe (1973a)
Preload test, Amuay	250	Lambe (1973a)
Loading test, Skå Edeby	340	Bjerrum (1964)
Storage tanks South Portland	400	Liu and Dugan (1974)
Satellite antenna tower Fucino plains	450	D'Elia and Grisolia (1974)
Loading test, Fornebu	500	Bjerrum (1964)
Loading test, Åsrum	1000	Høeg Andersland and Rolfsen (1969)
Økernbråken, Oslo	1500	Simons (1963)
Loading test, Mastemyr	3000	Frimann Clausen (1969, 1970)

The Norwegian field compressometer (Janbu and Senneset, 1973), provides a reliable method for obtaining the undrained deformation modulus when used in sands and silts.

An investigation into the undrained deformation properties of a clay crust has been carried out by Bauer, Scott and Shields (1973). They found that in situ plate loading tests, using a rigid 460 mm diameter steel plate, gave a good correlation with the results from a 3.1 m × 3.1 m heavily reinforced rigid footing, 660 mm thick, although values deduced from laboratory tests were generally too low and erratic.

For London clay, Wroth (1971) demonstrated that deformation moduli measured in a consistent way are dependent on the mean stress at the start of shear (p'_0) and, to a lesser extent, on the over-consolidation ratio (or OCR = p'_m/p'_0 where p'_m is the maximum mean stress experienced by the soil). Burland (1974) has emphasized the usefulness of field observations from which in situ properties may be back-analysed.

Atkinson (1974) has compared the in situ E_u values calculated in the above way with the values determined from undrained cylindrical compression tests. As shown in Fig. 3.12 the relationship suggested by Wroth is well-defined but the moduli determined from field measurements are approximately five times the moduli determined from laboratory measurements.

Values for the field E_u were obtained from plate loading tests at Chelsea and Hendon (Marsland, 1971); from observations of the heave of a deep

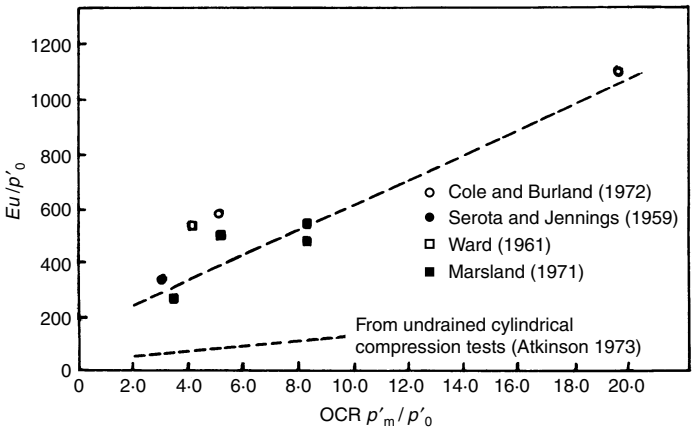

Fig. 3.12 Values of E_u/p'_0 plotted against OCR, after Atkinson (1974)

excavation (Serota and Jennings, 1959); from the deflections of a retaining wall (Cole and Burland, 1972); and from the deflections of a tunnel below an excavation (Ward, 1961). With the exception of the Hendon plate loading tests, these sites were in or near central London.

Atkinson (1974) observes that the significant difference between the laboratory and field measured values of the same soil parameter, E_u, can be partly explained by allowing for elastic anisotropy in analysing the field data. By assuming a degree of undrained anisotropy of 0.6 (Atkinson, 1973) the field moduli could be reduced by about 30%. The balance of the disparity between laboratory and field measured E_u may be attributed to sampling disturbance, test machine interference, and an isotropic starting state of stress in the laboratory tests.

Apart from difficulties in obtaining undisturbed, representative, triaxial specimens and restoring them to their in situ effective stresses prior to testing, there is the problem of carrying out appropriate measurements of axial strain during the test. The frictional restraint of the end platens cause the specimen to deform under axial loading in the characteristically *barrelled* fashion, with the deformation concentrated in the middle third of the specimen. To base axial strain measurements, therefore, on the displacement of the top platen, gives a low estimate of the true axial strain (Arthur and Menzies, 1968) giving an overestimate of E_u. Even using lubricated *free end* platens (Rowe and Barden, 1965) does not exclude the possibility of local strains exceeding the integrated value (Arthur and Phillips, 1972). Methods of strain measurement in the triaxial test include bedding errors which exaggerate the amount of measured deformation, giving artificially low stiffness readings (Menzies, 1997). Axial strains must therefore be measured locally (Jardine *et al.*, 1986).

The choice of stiffness parameter may depend upon the drainage conditions (i.e. whether or not the soil is permitted to change in volume) as well as the strain level. This is the case when using Young's modulus, E'. The drained values of Young's modulus, E', incorporate volumetric strains as well as shear distortion and hence are not the same as the undrained equivalent, E_u, which simply involves shear distortion. The use of Young's modulus to describe the stiffness of soil is attractive because the constants are more easily understood and because direct experimental measurement is straightforward. In many ways, however, it is more fundamental to use an alternative pair of elastic constants. These are the bulk modulus, K, and the shear modulus, G, which divide the deformation into the volumetric part (change in size with no shear distortion) and a distortional part (change in shape at constant volume), respectively. The shear modulus G is independent of drainage conditions and hence for isotropic materials $G_u = G'$. In terms of numerical analysis, when moving from an undrained loading stage to a drained loading stage G remains constant whereas E must be updated from E_u to E' (Matthews *et al.*, 1996).

The effects of heterogeneity and anisotropy

Although the use of an average value of E_u may, with experience, give a reasonable estimate of the average initial settlement of a structure, if it is necessary to predict the initial deflected shape, then heterogeneity and anisotropy must be taken into account. The effects of heterogeneity and anisotropy have been considered, for example, by Lambe (1964), Gibson (1967), Davies and Poulos (1968), Gibson and Sills (1971), Burland, Sills and Gibson (1973), Carrier and Christian (1973), and solutions to a limited number of problems are available.

An example of the influence of heterogeneity is given in Fig. 3.13, taken from Burland, Sills and Gibson (1973). The theoretical deflected shapes of the ground surface for the Mundford tank, founded on chalk (Ward, Burland and Gallois, 1968) are compared with the observed displacements. It can be seen that the settlement of the ground surface is localized around the loaded area much more than the simple elastic Boussinesq theory predicts – an effect accounted for almost entirely by the influence of inhomogeneity.

The deformed shape of the ground surface depends on the variation of the moduli with depth and the relative magnitudes of the horizontal and vertical moduli. Rodrigues (1975), for example, has shown (Fig. 3.14) by a finite element stress analysis that the maximum settlement of a flexible loaded area may occur nearer the edges than in the middle; an effect predicted by Gibson (1974).

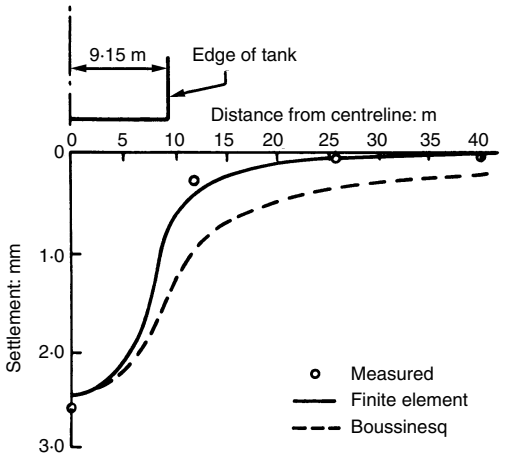

Fig. 3.13 Effect of heterogeneity on ground surface deformation, after Burland, Sills and Gibson (1973)

Two important points to emerge are:

- The vertical settlement is generally very sensitive to the horizontal modulus E_h.

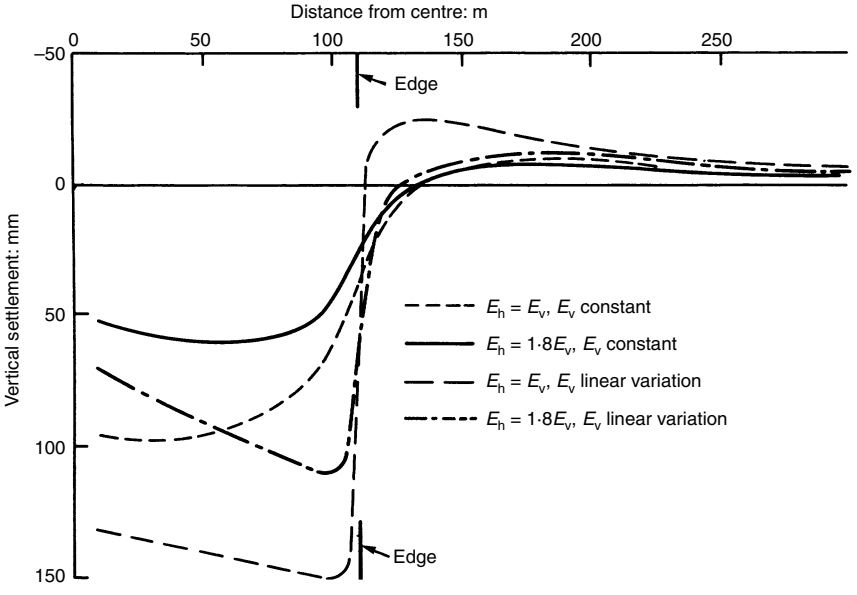

Fig. 3.14 Vertical settlement of a uniformly loaded flexible circular area resting on a wide deep elastic solid of specified anisotropy and heterogeneity, after Rodrigues (1975)

- For $E_v = 0$ at the surface and E_v increasing with depth, the maximum settlement is near the edge because of the large lateral strains existing at the edge.

Seismic methods for measuring ground stiffness

Why seismic methods?

In many geotechnical engineering problems, evaluation of deformation properties of soils and rocks is required for the prediction of ground movements. Traditionally in situ loading tests and laboratory tests have been employed for this purpose.

During the past decade, however, there have been important developments in the understanding of stress–strain behaviour of geomaterials which have closed the gap between static and very small strain dynamic measurements of stiffness. This has resulted in the increasing use of seismic methods to measure the shear modulus G as part of site investigations.

The use of seismic methods are attractive since they are not affected by sample disturbance or insertion effects and are capable of sampling a representative volume of the ground even in difficult materials such as fractured rock. These in situ non-destructive methods can be very usefully applied to measuring properties for the monitoring of soil improvements.

Stiffness in geotechnical engineering

The typical variation of shear or bulk stiffness with strain for most soils is given in Fig. 3.15. It is believed that most soils behave elastically at very small strains (i.e. <0.00l%) giving rise to a constant stiffness. The strain induced by the propagation of seismic waves is within this range and hence provides a measure of the upper bound for stiffness (E_{max} or G_{max}). It is also now generally accepted that ground strains associated with most soil–structure interaction problems are less than 0.l% and hence small strain stiffness values are required to make reasonable predictions of deformation (Jardine *et al.*, 1986).

Numerical models used in geotechnical design now take account of the stiffness–strain relationship as well as kinematic yield surfaces. In most cases however; the data provided for such models are laboratory-measured stiffness profiles at operational strain levels rather than upper bound stiffnesses. Current research into the stiffness–strain behaviour of geomaterials will eventually provide an accurate means of characterising the 'S'-shaped curve of Fig. 3.15.

The upper bound stiffness is clearly a fundamental parameter in defining this curve and hence the use of in situ seismic measurements of stiffness will become even more important in the future. At the present time these measurements may be used in conjunction with laboratory measurements for soil and in situ loading test measurements in rock

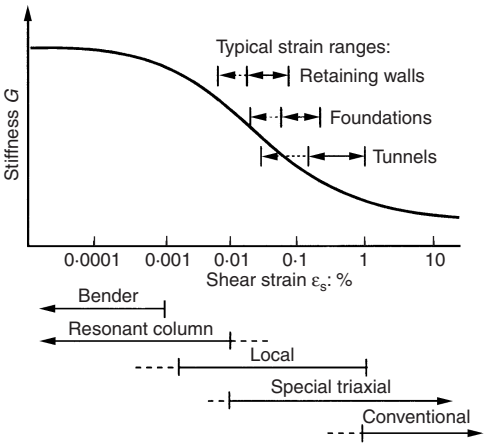

Fig. 3.15 Typical variation of stiffness with strain for most soils

which provide a lower bound for stiffness. In the area of monitoring ground improvements, however, the seismic methods offer an immediate measure of a fundamental engineering parameter G_{max}.

Seismic methods for stiffness measurement

Seismic methods utilize the propagation of elastic waves through the ground. There are two categories of seismic waves: body waves, comprising compressional (*P*) and shear (*S*) waves, and surface waves, which include Rayleigh (*R*) waves. The modes of propagation of these wave types are well known and are described in most texts on seismic methods (e.g. Telford *et al.*, 1990). The waves propagate at velocities which are a function of the density and elastic properties of the ground. The Rayleigh wave is a surface wave that travels parallel to the ground surface at a depth of approximately one wavelength. In an isotropic elastic medium the velocity of a shear wave, V_s, is:

$$V_s = \sqrt{G/\rho} \tag{3.5}$$

where G is the shear modulus and ρ the density. According to the theory of elasticity, Young's modulus E is related to G by:

$$G = \frac{E}{2(1 + \nu)} \tag{3.6}$$

where ν is the Poisson's ratio. Thus G can be obtained from measurements of V_s alone.

Surface waves may also be used to determine shear stiffness in soils and rocks. Approximately two-thirds of the energy from an impact source propagates away in the form of surface waves of the type first described by Rayleigh in 1885. These waves travel at speeds governed by the

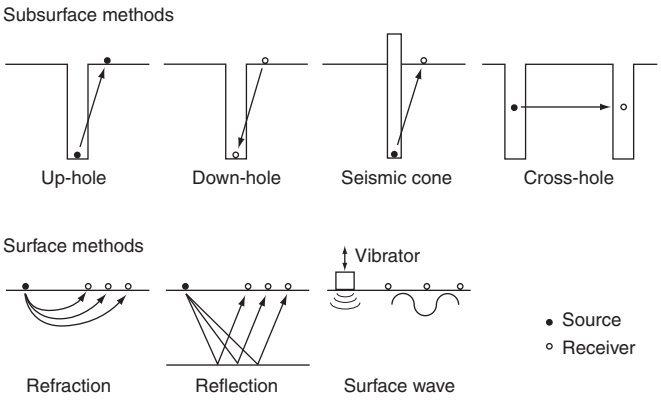

Fig. 3.16 Subsurface and surface geophysical methods for determining stiffness

stiffness–depth profile of the near surface material. It can be shown from the theory of elasticity that the relationship between the characteristic velocity of shear waves V_s and Rayleigh waves V_r in an elastic medium is given by:

$$V_r = CV_s \tag{3.7}$$

where C is a function of Poisson's ratio ν. The range of C is from 0.911 to 0.955 for the range of Poisson's ratio associated with most soils and rocks if anisotropy is ignored. The maximum error in G arising from an erroneous value of C is therefore less than 10%.

The seismic methods employed to determine stiffness–depth profiles may be divided into subsurface and surface methods as shown schematically in Fig. 3.16. Most of the subsurface methods require one or more boreholes which need to be cased with special plastic casing which adds to the cost of the survey.

These methods are most useful where the depth of investigation is greater than l5 m and involve the measurement of the transit times of seismic waves over known distances. The seismic cone has the advantage of providing both strength and stiffness data and does not require a borehole since the cone is pushed into the ground. However, the depth of penetration is limited by the strength of the ground and any obstructions such as boulders, claystones or rock layers.

A simple and cost-effective surface method makes use of surface waves. Surface wave methods exploit the dispersive nature of Rayleigh waves. The speed of propagation of a Rayleigh wave travelling at the surface of inhomogeneous ground depends on its wavelength (or frequency) as well as the material properties of the ground. Measurements of phase velocity of Rayleigh waves of different frequencies (or wavelengths) can

be used to determine a velocity–depth profile. Reference may be made to Matthews (1993), Matthews (1994), Matthews *et al.* (1996) and Matthews *et al.* (1997).

The surface wave method

Two distinct surface wave methods are available. The Spectral Analysis of Surface Waves (SASW) method makes use of a hammer as an energy source. The Continuous Surface Wave (CSW) method makes use of a vibrator as an energy source. Both techniques are described in detail by Matthews *et al.* (1996).

The SASW method relies on the frequency spectrum of the energy source used. In most cases a range of hammers of different mass are employed to achieve the necessary frequency range (3–200 Hz). It is inevitable, however, that certain frequencies will be missing from the spectra of these sources, which may result in gaps in the stiffness profile data. This disadvantage may be overcome by replacing the hammers with a frequency-controlled vibrator. This is the basis of the CSW method.

The process of converting a field dispersion curve (which plots phase velocity against wavelength) to a Rayleigh wave velocity–depth relationship is known as inversion. There are two principal ways of approaching this; either by the wavelength–depth method, or by using any of a number of finite element approaches.

The wavelength–depth method is the simplest, but least exact of the methods. It is of practical value because it offers a quick way of processing data on-site and so enables preliminary assessment. It also provides a useful initial estimate of the velocity–depth profile to input in the algorithms of the other approaches. In the wavelength–depth method, the representative depth, D, is taken to be a fraction, z, of the wavelength, λ, and λ/z is assumed to be constant. Gazetas (1982) recommended that $D = \lambda/4$ is used at sites where the stiffness increases significantly with depth, and that $D = \lambda/2$ is suitable at more homogeneous sites. Gazetas also suggested that taking $D = \lambda/3$ is a reasonable compromise.

Typical shear modulus–depth profiles for a coastal alluvial site and a chalk site using the CSW method where depth is taken as $D = \lambda/3$ are given in Fig. 3.17.

Monitoring ground improvement

Seismic methods, particularly the methods based on surface waves, provide a good method for monitoring ground improvement works. In many types of ground improvement there is some uncertainty concerning the effectiveness of the improvement method.

In particular it is difficult to assess the degree of improvement brought about by dynamic compaction and vibroflotation while the ground is

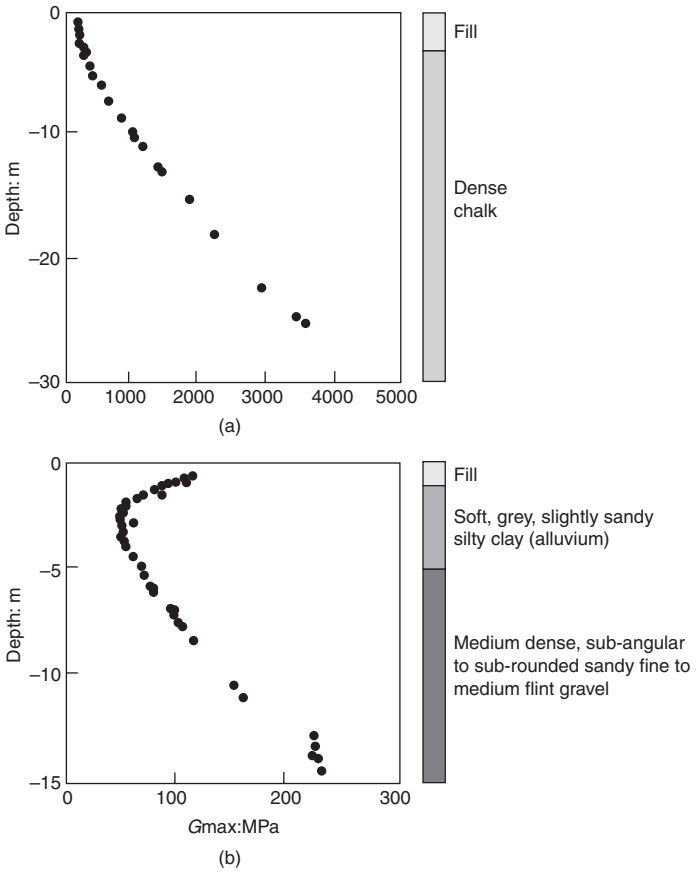

Fig. 3.17 Typical shear modulus–depth profiles from CSW tests (permission of GDS Instruments Ltd)

being treated. The result is either that too much work is carried out for little gain in ground stiffness after a certain point or that the improvement is insufficient and further remedial action is required.

In both cases extra costs are involved. Ideally a rapid and direct measure of improvement is required during the treatment process. Surface wave geophysics can provide such a direct measurement. A survey of the site can be carried out prior to ground improvement to give a set of baseline stiffness profiles. During the improvement process further stiffness profiles can be obtained rapidly and compared directly with the baseline measurements. In this way the amount of improvement can be quantified in terms of stiffness. This has the added benefit that the effective depth of the improvement can be determined.

Cuellar (1997) discusses the use of surface wave geophysics to assess the efficiency of some ground treatments such as grouted backfill and

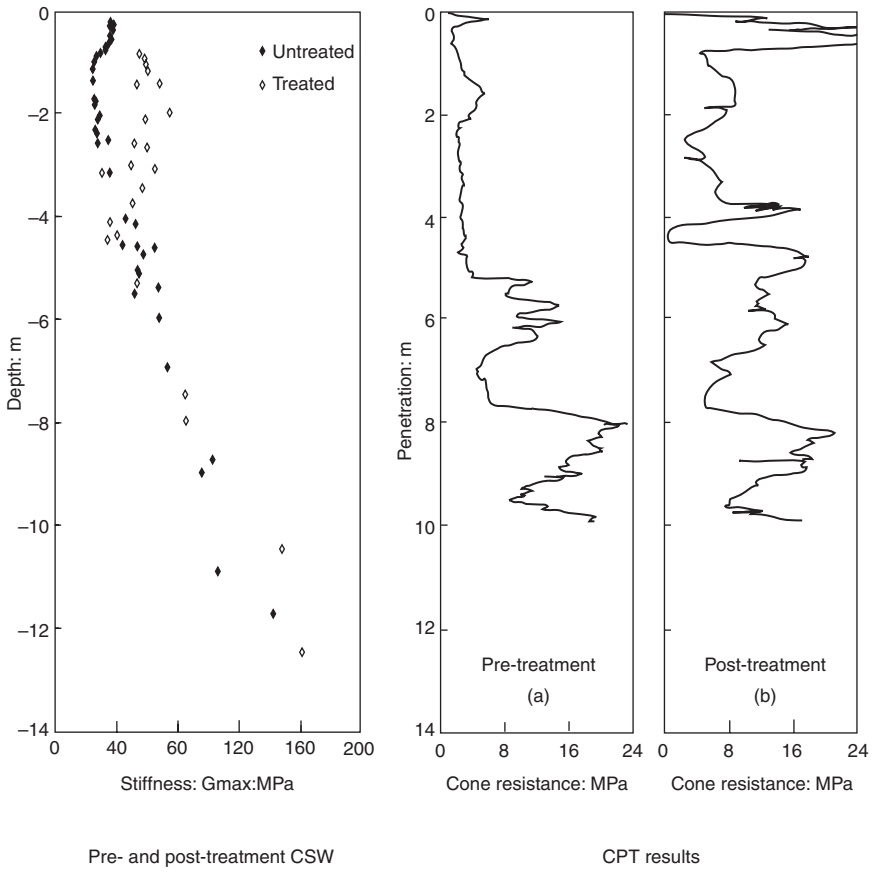

Fig. 3.18 Comparison of 'before and after' CSW stiffness–depth profiles and CPT cone resistance–depth profiles for loose sandy fill between vibro-stone columns for a site in the UK (Menzies, 2000)

stone columns. In both examples the improvement in stiffness is clearly shown in the surface wave data.

Hooker (1998) has carried out trials using the CSW technique to evaluate the effects of the use of stone columns inserted by vibro replacement. A doubling of the average maximum shear modulus was observed between columns in a test taking less than 1 h to perform. Menzies (2000) has correlated these results with CPT (Fig. 3.18). The increase in stiffness in the treated zone measured by the CSW system is clearly verified by the CPT cone resistance readings.

Advantages of geophysical methods for stiffness measurement

Like all methods of parameter determination, field geophysical techniques have both advantages and disadvantages. For most engineers,

Table 3.2 Examples of stiffness degradation for different geomaterials (after Heymann, 1998)

Material	$E_{0.01}/E_0$	$E_{0.1}/E_0$	$E_{1.0}/E_0$
Intact chalk	0.87–0.93	0.42	failed
London clay	0.83–0.97	0.35–0.58	0.11–0.20
Bothkennar clay	0.75–0.81	0.36–0.55	0.11–0.21

the primary difficulty has been a belief that geophysics measures dynamic stiffness at very small strain levels, and that this stiffness is very different from that required for geotechnical design. This is not the case. Matthews (1993) suggests that for fractured chalk the ratio between stiffnesses predicted using geophysics and those from large-diameter plate loading tests is close to unity and that geophysics provides the best way to determine stiffness.

For clays it has also been found that the maximum stiffness in highest quality laboratory specimens is close to that determined from field geophysics (Clayton and Heymann, in press). Table 3.2 shows the stiffness degradation with strain level for a soft clay (Bothkennar clay), a stiff fissured clay (London clay) and an intact weak rock (Chalk) determined in the triaxial apparatus using local strain instrumentation described by Heymann *et al.* (1997). It is clear from Table 3.2 that the stiffness at operational strain levels, E_{op}, is between 40 and 80% of the maximum stiffness, E_0. Given the rates of stiffness degradation discussed above, it would seem entirely reasonable to estimate operational stiffness, E_{op}, from field geophysical results in combination with some (perhaps conservative) reduction factor to take account of the expected strain level around the proposed construction. Referring to Table 3.2, notional values for factoring E_0 could be as follows:

$E_{op} \approx 0.50E_0$ for soft clays, and

$E_{op} \approx 0.85E_0$ for stiff clays and weak rocks

Values of stiffness estimated in this way can be expected to be far superior to many techniques routinely used today. For example, oedometer testing, external strain triaxial testing, and penetration testing, where poor performance in predicting stiffness has been known for decades (e.g. Burland and Hancock, 1977; Clayton *et al.*, 1988; Izumi *et al.*, 1997). As an example, Fig. 3.19 shows not only stiffness back-figured from ground movements around a number of major structures in the London area, but also the very much lower values from routine oedometer and triaxial tests conducted on samples from the Grand Buildings site. It can be seen that these stiffnesses are about an order of magnitude too

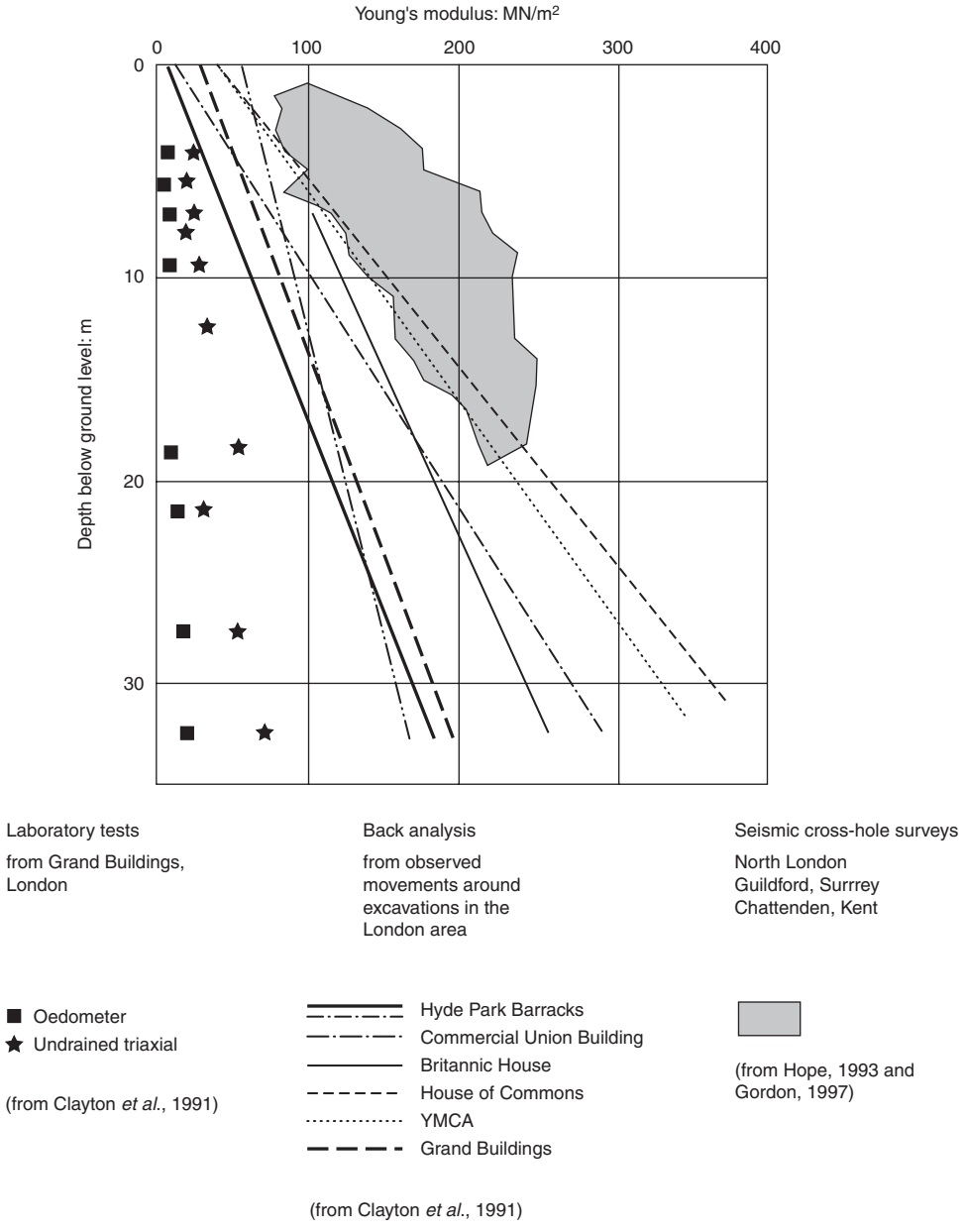

Fig. 3.19 Stiffness profiles for various London clay sites (Matthews et al., 2000)

low. In contrast, the cross-hole stiffnesses for the London clay sites are close to those derived from back analysis.

Geophysics has other advantages. For example, although it may be necessary to install cased holes for sources and receivers, the vast bulk of the ground tested remains at its in situ stress and saturation level, and

undisturbed. In contrast, laboratory tests require that samples be taken. Sample disturbance involves not only mechanical disturbance to the soil structure, but also stress relief. In addition, field geophysical results are representative of a large volume of ground, so that layering and fracturing are taken into account. And some techniques (for example CSW and SASW) are non-invasive. Because boreholes are not required such tests are very fast, and the results can be obtained relatively cheaply, and avoid significant contact with contaminated land (Matthews *et al.*, 2000). Because the CSW/SASW method is an inherently averaging technique (e.g. see Fig. 3.18), minor variations such as thin seams are overlooked, but the mass properties of the ground (i.e. including jointing, fissuring, etc.) are well represented and usually in foundation engineering it is this average value which matters (Menzies, 2000).

CHAPTER FOUR

Bearing capacity of footings

Introduction

Foundation engineering may be defined as the art of applying – economically – structural loads to the ground in such a manner as to avoid excessive deformations. It should be noted that unless foundations are placed on hard sound rock, some measurable settlement will always occur. In particular, differential settlements must be kept within tolerable bounds, although if total settlements become too large, damage to services may occur, and tall buildings may tilt.

When designing foundations, there are two criteria which must be considered and satisfied separately:

- There must be an adequate factor of safety against a bearing capacity failure in the soil.
- The settlements, and particularly the differential settlements, must be kept within reasonable limits.

For foundations on clays, either bearing capacity or settlement may govern the foundation design; it will be found that with foundations on granular soils, however, the choice of allowed bearing pressure will, on virtually every occasion, be controlled by settlement.

Deformation of an element of soil is a function of a change in effective stress, not a change in total stress. Various causes of deformation of a structure are listed as follows:

- Application of structural loads
- Lowering of the ground water table
- Collapse of soil structure on wetting
- Heave of swelling soils
- Fast growing trees on clay soils
- Deterioration of the foundation (sulphate attack of concrete, corrosion of steel piles, decay of timber piles)
- Mining subsidence
- Sinkholes
- Vibrations in sandy soils
- Heave of clay soils after clearance of trees

- Seasonal moisture movements
- The effects of frost action.

The settlement of a foundation on a saturated soil may be considered as consisting of three different types:

- The immediate, elastic, or initial settlement which occurs immediately upon load application, under conditions of no change in volume.
- The primary consolidation settlement which develops as the volume changes as a consequence of the dissipation of excess pore-water pressures.
- The secondary settlement, which is a creep phenomenon and occurs under conditions of practically zero excess pore water pressure.

The bearing capacity of a soil is related to shear failure in the ground. For foundations on clays, the undrained shear strength is usually the controlling factor, because clays are of low permeability and the construction of the structure generally occurs under undrained conditions. The clay will then consolidate with time, gain strength and so the bearing capacity will increase with time. The *end of construction* case is almost always critical. Granular soils are of high permeability, however, and by the end of construction, the drained condition has already been reached. The applied structural load, therefore, increases not only the shear stresses in the soil, but also the effective stresses and hence the strength. This is the main reason why sands and gravels have higher bearing capacities than clays.

It is vital to distinguish between gross and net foundation pressures. The *gross* foundation pressure, q, at foundation level is the total applied load divided by the area of the foundation. The *net* foundation pressure, q_n (or the net loading intensity) is the net increase in pressure at foundation level, and is the pressure causing consolidation settlement, and shear failure in the soil.

WORKED EXAMPLE

Determine the gross and net foundation pressures for the example shown in Fig. 4.1. The initial total overburden pressure at foundation level is

$$p_0 = 2 \times 20 = 40\,\text{kPa}$$

For simplicity it is assumed that the soil is fully saturated above the water table to the ground surface and hence the bulk unit weight is the same above and below the water table. The water table is the line where the water pressure equals atmospheric pressure and fine-grained soils

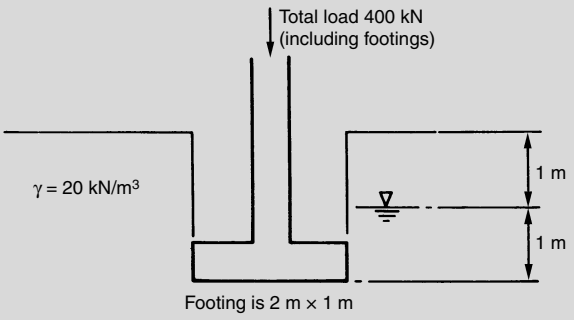

Fig. 4.1 Example of gross and net pressures

can be fully saturated above the water table, the water being held by capillary tension.

The gross foundation pressure $= q = 400/2 = 200\,\text{kPa}$.

The net foundation pressure $= q_n = q - p_0 = 200 - 40 = 160\,\text{kPa}$. It can be seen that this is the net increase in effective stress at foundation level.

The final effective stress at foundation after dissipation of excess pore-water pressure is

$$p'_f = q - u = 200 - 10 = 190\,\text{kPa}$$

Since $p'_0 = 30\,\text{kPa}$, the net increase in effective stress at foundation level is $190 - 30 = 160\,\text{kPa}$.

Various definitions

The ultimate bearing pressure, q_f, is the value of the bearing pressure at which the ground fails in shear.

The maximum safe bearing pressure, q_s, is the intensity of applied pressure that the soil will safely support without risk of a shear failure, irrespective of the settlement which may develop, that is

$$q_s = q_f/F$$

where F is the load factor, which generally varies from 1.75 to 3.0. A value of 1.75 would be chosen where there is considerable experience of the soil under consideration and where strict settlement criteria do not apply. A figure of 3.0 would be taken where little is known of the field behaviour of the soil and where settlements must be kept to a minimum.

The allowable bearing pressure, q_a, is the allowed intensity of applied pressure, taking into account both bearing capacity and settlement.

In this chapter, methods of determining the *safe* bearing pressure (i.e. governed by the strength of the soil) of footings are outlined.

Charts for estimating the distribution of vertical stresses below a foundation are given in Chapter 3, together with procedures for estimating initial undrained settlements.

Settlement analysis is covered in Chapter 5.

The 'indentation problem'

Upper bound approach

The mathematical theory of plasticity can be used to adopt a very simple approach to the soil mechanics of bearing capacity (Calladine, 1985). Consider the so-called 'indentation problem' shown in Fig. 4.2. This corresponds to the 'kinematically admissible state', i.e. only mechanisms of failure are considered and compatibility of stresses is ignored.

Referring to Fig. 4.2(a), a work equation can be written thus

external work done = internal work done

$$F \times b/2 \times \theta = kb\theta\pi \times b$$

where $kb\theta\pi$ is the strength k acting around the perimeter of the half circle at a lever arm of b, i.e. $F/b = q = (\pi + \pi)k = 6.29k$.

As shown in Fig. 4.2(b), this assumes that all the material is ideally rigid-plastic (i.e. no movement takes place until the strength is reached when large strains can then occur at constant shear stress), and that internal dissipation of energy takes place at interfaces between rigid blocks. Therefore we require the relative sliding displacements between adjacent blocks of the mechanism.

Consider the classical punching of a die problem shown in Fig. 4.3(a). Here the mechanism of failure is more feasible (and more complex). To obtain relative movements between adjacent blocks requires the use of a velocity diagram given in Fig. 4.3(b).

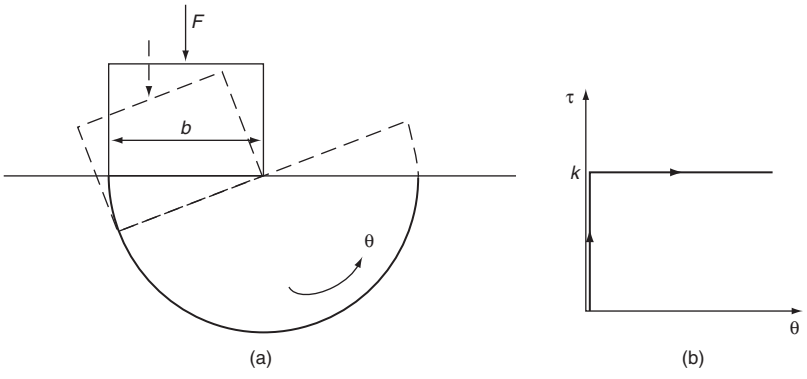

Fig. 4.2(a) Simple mechanism for indentation problem; (b) rigid–plastic material properties

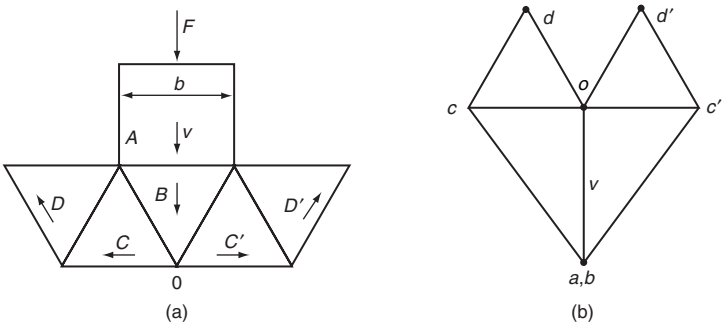

Fig. 4.3 Complex mechanism for indentation problem and associated velocity (relative movement) diagram

The work equation is

$$F \times \boldsymbol{oa} = 2k(\boldsymbol{bc} \times L_{\mathrm{BC}} + \boldsymbol{co} \times L_{\mathrm{CO}} + \boldsymbol{cd} \times L_{\mathrm{DC}} + \boldsymbol{do} \times L_{\mathrm{DO}})$$

Noting that the ratio of vectors $\boldsymbol{oc}/\boldsymbol{oa} = 1/\sqrt{3}$ and that the lengths between adjacent sliding blocks $L_{\mathrm{BC}} = L_{\mathrm{CO}} = L_{\mathrm{DC}} = L_{\mathrm{DO}} = b$, then

$$F = 2kb(2/\sqrt{3} + 1/\sqrt{3} + 1/\sqrt{3} + 1/\sqrt{3}) \quad \text{whence}$$

$$F/b = q = (10/\sqrt{3})k = 5.76k$$

Thus as the mechanism is made more feasible, the punching force (bearing capacity) is reduced, i.e. we are approaching an *upper bound*.

Lower bound approach

This is the 'statically admissible state' where mechanisms are ignored and compatibility of stresses is ensured. As shown in Fig. 4.4 a stress discontinuity is proposed. Here equilibrium is maintained *within* each block and *across* each discontinuity, i.e. $\sigma_{\mathrm{n}}^{\mathrm{I}} = \sigma_{\mathrm{n}}^{\mathrm{II}}$. As shown in Fig 4.4, the Mohr's circles representing stress zones I and II share a common point. If the material on both sides of the discontinuity is at yield (i.e. a slip plane) then both circles will have the same maximum diameter (Fig. 4.4).

Consider that zone I is stress-free, i.e. like a vertical cliff face. The corresponding Mohr's circle diagram is shown in Fig. 4.4(a) where the 'circle' for zone I is vanishingly small and plots as a point at the origin. Here by inspection

$$q = 2k$$

Consider now that both zones I and II are at yield as shown in Fig. 4.4(b). By inspection

$$q = 4k$$

This load is only about 2/3 of the upper bound indenter load already found.

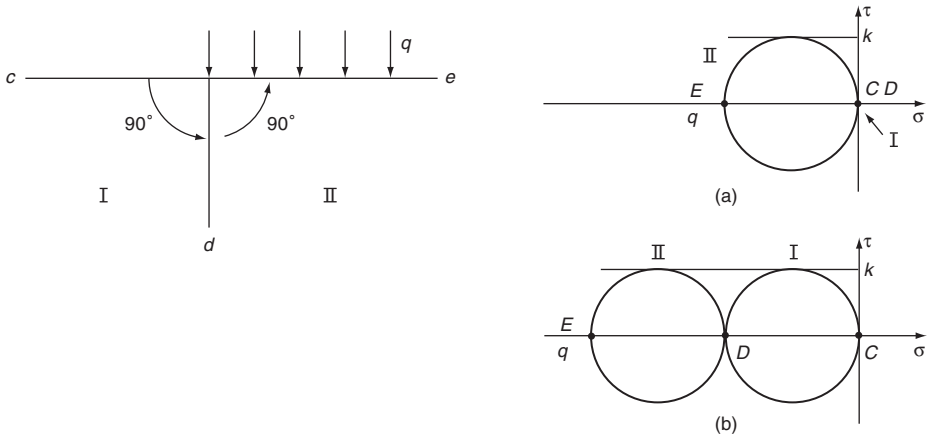

Fig. 4.4 Vertical discontinuity. (a) Zone I stress free; (b) Zone I and Zone II at yield

Now explore the possibility of improving the lower bound solution by using more than one plane of discontinuity. For example, in Fig. 4.5, the vertical plane considered in Fig. 4.4 is replaced by two planes inclined to the vertical at a small angle, ϕ, thus enclosing a third zone. Clearly, two planes of discontinuity are better than one as the two 'original' circles are 'pushed' apart by the circle corresponding to the newly-formed zone. As ϕ increases, the new circle becomes larger and when $\phi = 22.5^\circ$ the new circle has grown to its largest allowable radius, k, as shown in Fig. 4.5 whence

$$q = (2 + 2\sqrt{2})k = 4.83k$$

This is a substantial increase (20%) on the previous value.

As shown in Fig. 4.6, three planes give four circles separated by $k \sin 30^\circ = k/2$ whence

$$q = k + 6 \times k/2 + k = 5k$$

which is a further improvement of about 3% on the previous lower bound.

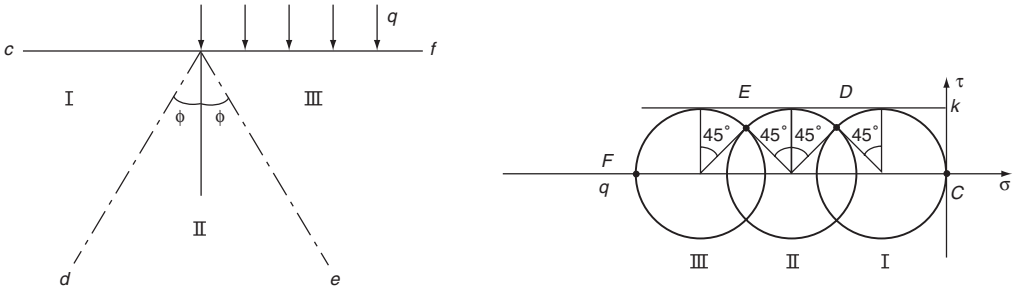

Fig. 4.5 Two discontinuities, all three zones at yield

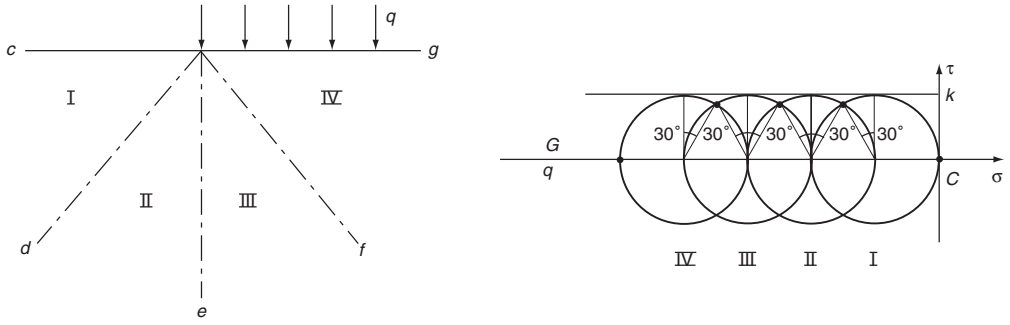

Fig. 4.6 Three discontinuities, all four zones at yield

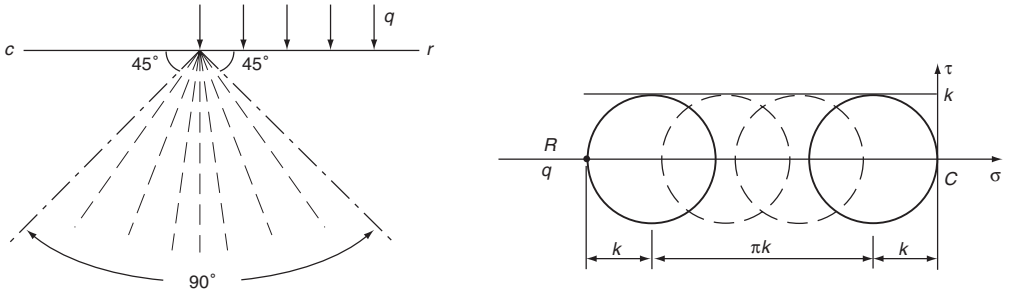

Fig. 4.7 Fan of discontinuities, all zones at yield

A *fan* of planes as shown in Fig. 4.7 gives

$$q = k(2 + \pi) = 5.14k$$

Thus as the feasibility of the stress discontinuities is improved a greater value is achieved, i.e. we are approaching a *lower bound*.

In summary, as shown in Fig. 4.8, the solution lies somewhere between upper and lower bounds which are approached with increasing feasibility of mechanisms on the one hand (upper bound) and increasing feasibility of stress discontinuities (lower bound) on the other hand.

Soil mechanics interpretation

For soils, the indentation problem considered above corresponds to the short term stability condition of a positive loading on a saturated clay. From a consideration of short term and long term stability (see Chapter 1), we know that stability is critical in the short term for loading soils of low permeability. The excess pore pressure generated by the loading is dissipated with time leading to consolidation with an increase in strength. This means the worst case is at the end of construction corresponding to the undrained state. Thus we can use the undrained shear strength s_u

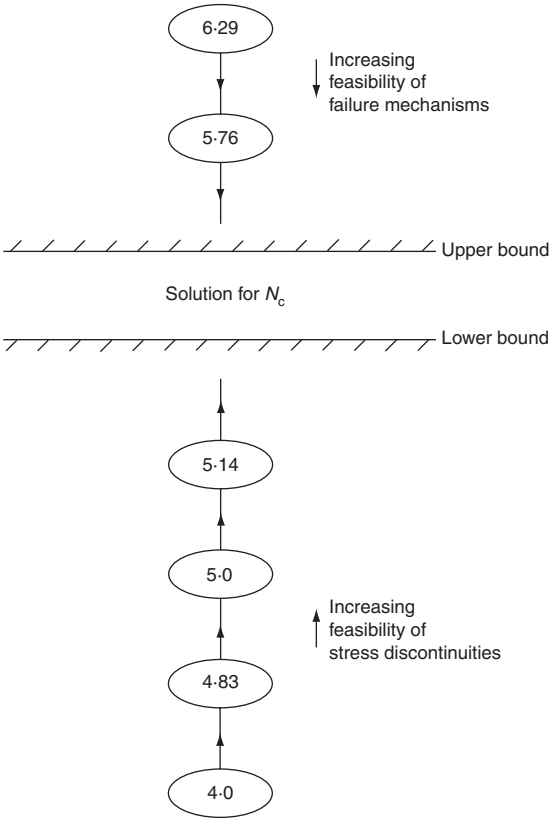

Fig. 4.8 Summary of upper and lower bound approaches to solving the indentation problem, $q = N_c k$.

and find the bearing capacity as

$$q_u = N_c s_u$$

where $N_c = 5.14$ which is on the safe side (being a lower bound) for strip footings on the surface of the ground.

Ultimate bearing capacity

The ultimate bearing capacity of a footing may be determined using bearing theory, whereby a failure mechanism is postulated and the pressure causing failure in the soil is expressed in terms of the shear strength mobilized at failure and the geometry of the problem. Several bearing capacity theories have been proposed and the one most commonly adopted for shallow footings is that of Terzaghi (1943).

By considering a strip footing, neglecting the strength of the soil above foundation level, Terzaghi arrived at the following solution for a strip footing for a soil having a cohesion intercept, c, and an angle of shearing

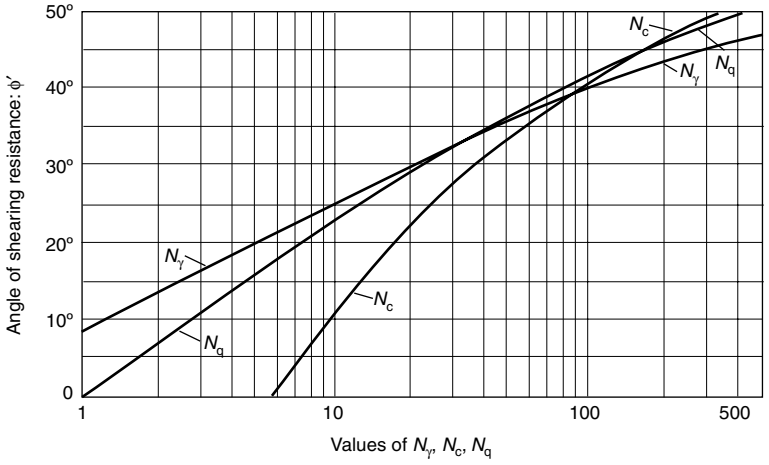

Fig. 4.9 Bearing capacity factors, N_c, N_q, N_γ, after Terzaghi (1943)

resistance, ϕ.

$$q_f = cN_c + \gamma DN_q + \tfrac{1}{2}B\gamma N_\gamma \tag{4.1}$$

where N'_c, N_q, and N_γ are bearing capacity factors depending on the value of ϕ, and are reproduced in Fig. 4.9. These factors are valid for strip footings and require to be adjusted for rectangular and circular footings as follows:

Rectangular footings:

N_c rect $= N_c$ strip $(1 + 0.2(B/L))$

N_γ rect $= N_\gamma$ strip $(1 - 0.2(B/L))$

N_q rect $= N_q$ strip

Circular footings:

N_c circle $= 1.3 \times N_c$ strip

N_γ circle $= 0.6 \times N_\gamma$ strip

N_q circle $= N_q$ strip

In the form presented by Terzaghi, the bearing capacity solution can be applied strictly only to cases where the ground water table is deep; total stresses equal effective stresses everywhere and the shear stress parameters should be expressed in terms of effective stress.

The Terzaghi solution could also be applied to an undrained, total stress condition, using in this case, shear strength parameters in terms of total stress, c_u and ϕ_u.

For free draining soils, that is the excess pore water pressures under the footing are zero at the end of load application, the bearing capacity equation is most usefully expressed as follows for the case of high ground

water table:

$$q_f = c'N_c + p'(N_q - 1) + \tfrac{1}{2}B\gamma'N_\gamma + p \tag{4.2}$$

where p' = initial effective overburden pressure at foundation level, p = initial total overburden pressure at foundation level, and γ' = submerged unit weight.

If the ground water table is low then the equation can be written:

$$q_f = c'N_c + p(N_q - 1) + \tfrac{1}{2}B\gamma N_\gamma + p \tag{4.3}$$

When using the bearing capacity equation to solve a problem in practice, it is necessary to consider whether the material is so permeable that the excess pore pressures dissipate immediately the load is applied, that is, consolidation and gain in strength are complete at the end of the construction period, or whether the permeability is so low that very little pore pressure dissipation occurs during construction, no gain in soil strength can be relied upon and the condition is essentially undrained. The first possibility will apply to sands and gravels and can be analysed using a drained analysis in terms of effective stress; and the second applies to clays and can be analysed using an undrained analysis in terms of total stress. Of course, with time, a clay under load will consolidate and gain in strength and the long term bearing capacity will, in general, be greater than the short term undrained bearing capacity, and if necessary could be determined from an effective stress analysis. Examples are given below.

Granular soils

Consider a strip loading applied at a depth D below the surface of a sand deposit with the ground water table at the ground surface. Equation 4.2 can then be written as follows:

$$q_f = p'(N_q - 1) + \tfrac{1}{2}B\gamma'N_\gamma + p \tag{4.4}$$

The following points should be noted:

- The ultimate bearing pressure, q_f, depends on the initial effective overburden pressure, p', at foundation level; for a greater depth of footing or if ground water is absent (both increasing p'), then q_f will be increased.
- q_f depends on the submerged unit weight, γ'. If the ground water table is deep, greater than for example, $2B$, below the foundation level and will always remain below that depth, then the bulk unit weight, γ, can be inserted instead of γ', resulting in increased bearing capacity.
- q_f is very sensitive to ϕ', particularly for large values of ϕ'; small increases in ϕ will lead to large increases in N_q and N_γ and hence to large increases in q_f. For this reason, caution must be exercised when estimating the value of ϕ' to be used.

WORKED EXAMPLE

Consider a strip footing 2 m wide founded at a depth of 1.5 m below the surface of a dense sand with $\phi' = 42^\circ$. The ground water table is at foundation level, and $\gamma = 20\,\text{kN/m}^3$ and $\gamma' = 10\,\text{kN/m}^3$, see Fig. 4.10. Determine the safe bearing pressure for $\phi' = 42^\circ$, $N\gamma = 140$ and $N_q = 110$, from Fig. 4.9

$$q_f = 1.5 \times 20(110 - 1) + \tfrac{1}{2} \times 2 \times 10 \times 140 + 1.5 \times 20$$
$$= 4700\,\text{kPa}$$

Applying a load factor of two to determine the working load gives

$$q_s = 2350\,\text{kPa}$$

If, at a particular location along the strip footing, the sand is locally a little looser, with an angle of shearing resistance 10% less than the 42° used in the calculations, i.e. 37.8°, what is the load factor for the design loading of 2105 kPa? For $\phi' = 37.8^\circ$, $N_\gamma = 75$, $N_q = 63$, from Fig. 4.9

$$q_f = 1.5 \times 20 \times (63 - 1) + \tfrac{1}{2} \times 2 \times 10 \times 75 + 1.5 \times 20$$
$$= 2640\,\text{kPa}$$

The load factor is therefore

$$\frac{2640}{2350} = 1.12$$

i.e. close to 1.0!

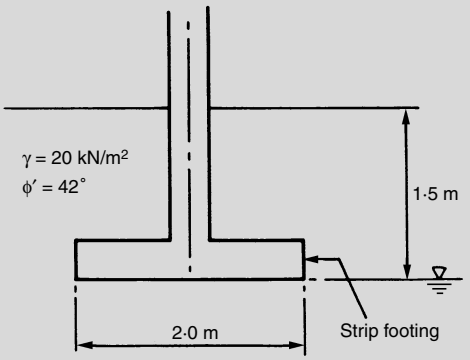

Fig. 4.10 Example of bearing capacity calculation

This example has been chosen to illustrate two main points:

- For most footings on granular materials, the bearing pressure is extremely high in terms of bearing capacity, so that the allowed bearing pressure in a practical problem is determined by consideration of

settlement, rather than strength. The only possible exception to this statement would be a very narrow foundation, founded just below the surface of a loose sand with a very high ground water table.

- In bearing capacity calculations, the load factor is by no means equal to the factor of safety on shear strength. The example shows that even if a load factor of two is adopted, soil failure can be approached if the shearing resistance is only 10% less than that used in the design calculation. Since difficulties lie in assessing correctly soil strength, a more practical and safer approach is to place a factor of safety on the shear strength of the soil and to use the factored strength in bearing capacity calculations to obtain safe bearing pressures. This point is also particularly relevant when making passive earth pressure calculations, particularly for high values of shearing resistance and wall friction.

Consider the end of construction stability of a saturated clay owing to foundation loading. This is the undrained condition and the problem is analysed in terms of total stress, taking $\phi = 0$.

Equation 4.2 can be written as follows:

$$q_f = cN_c + p \tag{4.5}$$

or

$$q_f = s_u N_c + \gamma D$$

where s_u = undrained shear strength, γ = bulk unit weight, D = depth of footing below ground surface, and N_c = bearing capacity factor depending only on the geometry, and is given in Fig. 4.11. The ultimate bearing capacity is independent of the breadth, B.

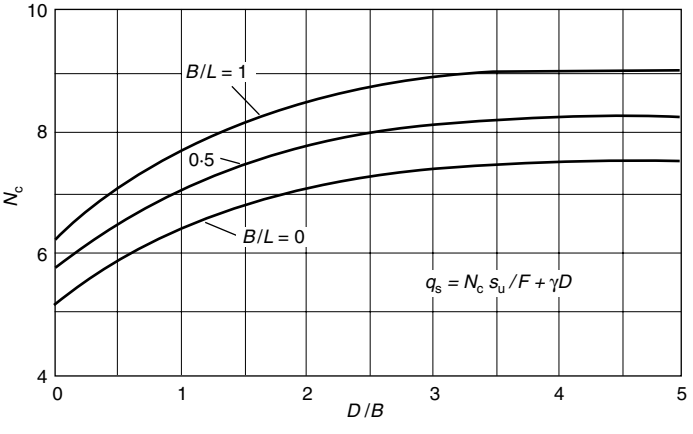

Fig. 4.11 Bearing capacity factor, N_c, for undrained analysis, after Skempton (1951)

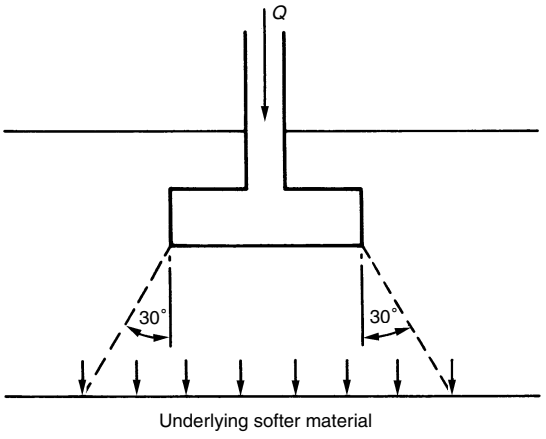

Fig. 4.12 Spread of load onto underlying layer

In many practical cases, the undrained shear strength varies with depth below a foundation. In this case, the average value of s_u should be taken over a depth below foundation level equal to $\frac{2}{3}B$, provided the shear strength of any layer does not depart from the average strength by more than $\pm 50\%$. If a softer layer is present under a foundation, its effect can be assessed by assuming a spread of load from the foundation down to the surface of the softer material, as shown in Fig. 4.12, and then carrying out a bearing capacity calculation in the usual way.

A particular problem which must be treated with caution is the case of an oil tank on a soft clay deposit. Because of the flexibility of the base, it is possible for a local failure to occur, for example, along a strip near the edge. In such cases, the shear strength must not be averaged over a depth equal to 2/3 of the tank diameter. Local failure must be considered and trial strips analysed until a minimum factor of safety is obtained. The procedure is indicated in Fig. 4.13.

A classic paper covering the failure of an oil tank in detail has been published by Bjerrum and Øverland (1957). By back-analysing the failure of an oil tank at Frederikstad the authors found that the minimum calculated factor of safety against a local failure was 1.05, whereas a value of 1.72 was found for an overall failure of the tank.

Eccentric loading

Meyerhof (1953) has shown that, as a reasonably good approximation, the influence of an eccentric load with eccentricity, e, measured from the axis of symmetry of a foundation of width B, can be accounted for by using a reduced width, B', in the bearing capacity calculations, where

$$B' = B - 2e \tag{4.6}$$

and then considering the loading to be symmetrical.

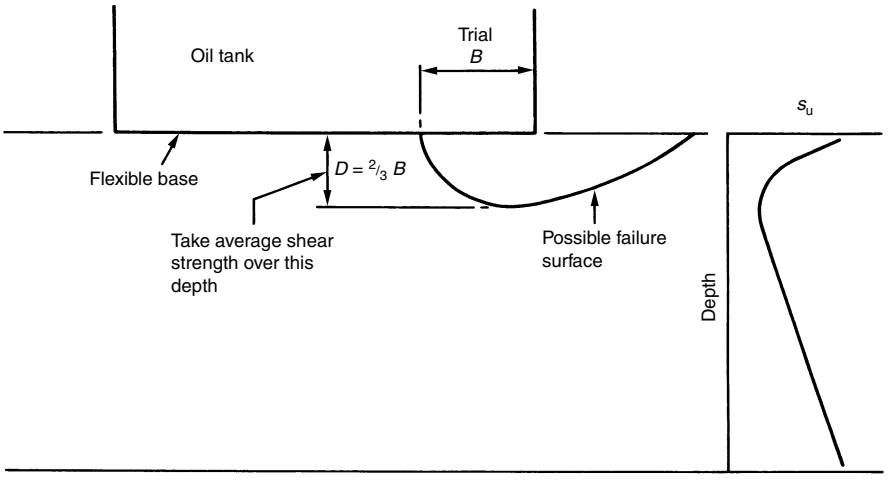

Fig. 4.13 Bearing capacity calculations for an oil tank, after Bjerrum and Øverland (1957)

Inclined loading

For the case of inclined loading, with a vertical component P_v and a horizontal component P_h, Brinch Hansen (1955) proposed operating with an equivalent vertical applied foundation pressure, q_e, where

$$q_e = \frac{P_v + \lambda P_h}{A} \tag{4.7}$$

where A = area of the base and λ = dimensionless constant depending on the angle of shearing resistance. Values of λ are given in Table 4.1.

Table 4.1 λ factor for inclined loading bearing capacity calculations, after Brinch Hansen (1955)

$\tan\phi'/F$	0	0.2	0.4	0.6	0.8	1.0
λ	1.4	1.8	2.3	2.8	3.3	3.9

WORKED EXAMPLE

Determine the short-term, undrained, and the long-term, fully drained, bearing capacities of the square footing shown in Fig. 4.14.

Short term condition:

$s_u = 70\,\text{kPa}$, $\phi_u = 0$, $\gamma = 20\,\text{kN/m}^3$, $N_c = 7.2$ (Fig. 4.11 for $D/B = 0.67$), whence:

$$q_f = s_u N_c + \gamma D = 70 \times 7.2 + 20 \times 1 = 524\,\text{kPa}$$

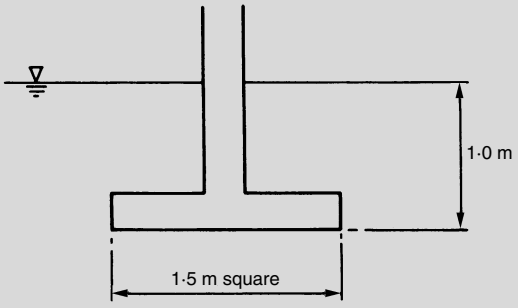

Fig. 4.14 Example of short term and long term bearing capacity calculations

Long term condition:

Values of N_c, N_q, and $N\gamma$, from Fig. 4.9, and adjusted for the square footing are:

$$c' = 10\,\text{kPa}, \quad \phi' = 30^\circ, \quad \gamma = 20\,\text{kN/m}^3, \quad \gamma' = 10\,\text{kN/m}^3$$

$$N_c = 36 \times (1 + 0.2)43.2$$

$$N_q = 22 \times 1 = 22$$

$$N\gamma = 20 \times (1 - 0.2) = 16$$

whence

$$\begin{aligned} q_f &= c'N_c + p'(N_q - 1) + \tfrac{1}{2}B\gamma'N_\gamma + p \\ &= 10 \times 43.2 + 1 \times 10 \times 21 + \tfrac{1}{2} \times 1.5 \times 10 \times 16 + 1 \times 20 \\ &= 702\,\text{kPa} \end{aligned}$$

This calculation merely confirms that, in general, the long-term bearing capacity of a clay foundation after consolidation is greater than the short-term bearing capacity. Possible exceptions to this general proposition are:

- Where lateral dissipation of excess pore-water pressure from under a large loaded area, e.g. an oil tank or an embankment, may give rise to increases in pore pressure outside the loaded area, reaching a critical value some time after the end of construction.
- In a thick clay deposit where a decrease in the undrained shear strength with time (Chapter 2) may be greater than the gain in strength because of consolidation near the drainage boundaries.

WORKED EXAMPLE

Design a strip footing to carry the loading system, shown in Fig. 4.15, in a saturated clay.

Data:

Minimum depth of footing	= 1 m
Undrained shear strength	= 100 kPa
Required factor of safety	= 2
Bulk unit weight	= 20 kN/m^3
Eccentricity	= 0.2 m
Vertical component, P_v	= 400 kN/m
Horizontal component, P_h	= 75 kN/m

Calculation:

$B' = B - 2e = 2 - 2 \times 0.2 = 1.6\,\text{m}$

$N_c = 6.0$ (for $D/B = (1.0/1.6) = 0.625$, Fig. 4.11)

Safe foundation pressure $= N_c s_u / F + \gamma D$

$$= \frac{6.0 \times 100}{2} + 20 \times 1$$

$$= 320\,\text{kPa}$$

Equivalent applied pressure $= \dfrac{P_v + \lambda P_h}{A}$ (λ from Table 4.1)

$$= \frac{400 + 1.4 \times 75}{1.6 \times 1}$$

$$= 316\,\text{kPa}$$

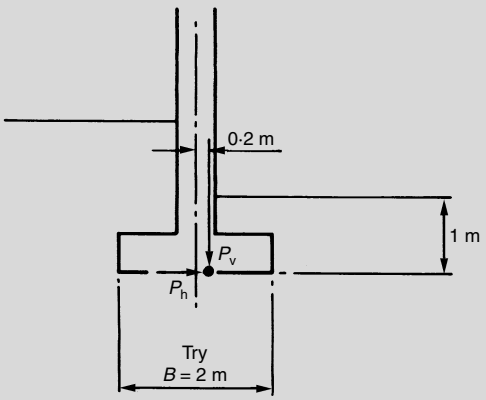

Fig. 4.15 Example of bearing capacity calculations for inclined and eccentric loading

This is satisfactory.

The resistance to sliding along the base may be assessed as follows (neglecting the passive resistance of the soil which may be affected by softening, etc.):

$$\begin{aligned}\text{Sliding resistance} &= \text{base area} \times \text{adhesion between base and clay} \\ &= 2 \times 1 \times 100 \times 0.75 \\ &= 150\,\text{kN}\end{aligned}$$

This assumes that the adhesion between the underside of the base and the clay is 0.75 times the undrained shear strength. For further discussion on adhesion between clay and concrete, see Chapter 6.

Factor of safety against sliding = 150/75 = 2. This is satisfactory.

Side adhesion for footings in clay

Additional support to a footing at depth in clay may be obtained from side adhesion of the clay to the foundation. Particular care must be taken when making an allowance for tension or shrinkage cracks. Because of the difficulty of estimating the depth of such cracks, side adhesion is generally neglected for shallow foundations.

In the case of a bridge pier, for example, extending deep into a clay layer, a considerable contribution to the load-carrying capacity will derive from side adhesion and this should be allowed for in design. The problem is similar to the design of a large diameter pile which is considered in Chapter 6.

Allowable bearing pressures

Approximate allowable bearing pressures for preliminary design only, are given in Table 4.2, taken from BS 8004: 1986.

Table 4.2 Approximate allowable bearing values, after BS 8004: 1986

Group	Types of rocks and soils	Approximate bearing value (kPa)	Remarks
1 Rocks	Hard igneous and gneissic rocks in sound condition	10 000	These values are based on the assumption that the foundations are carried down to unweathered rock
	Hard limestones and hard sandstones	4000	
	Schists and slates	3000	
	Hard shales, hard mudstones and soft sandstones	2000	
	Soft shales and soft mudstones	600 to 1000	
	Hard sound chalk, soft limestone	600	
	Thinly bedded limestones, sand-stones, shales Heavily shattered rocks	To be assessed after inspection	
2 Non-cohesive soils	Compact gravel, or compact sand and gravel	>600	Width of foundation (B) not less than 1 m. Ground water level assumed to be a depth not less than B below the base of the foundation
	Medium dense gravel, or medium dense sand and gravel	200 to 600	
	Loose gravel, or loose sand and gravel	<200	
	Compact sand	>300	
	Medium dense sand	100 to 300	
	Loose sand	<100	
3 Cohesive soils	Very stiff boulder clays and hard clays	300 to 600	Group 3 is susceptible to long-term consolidation settlement
	Stiff clays	150 to 300	
	Firm clays	75 to 150	
	Soft clays and silts	<75	
	Very soft clays and silts	Not applicable	

WORKED EXAMPLES

Example 1: short term and long term bearing capacity

A long strip foundation is 2 m wide and is located at a depth of 1 m in a soil of unit weight $\gamma = 20\,\text{kPa}$. Estimate the bearing capacity of the soil for the short and long terms. The water table is at a depth of 1 m.

The undrained parameters are: shear strength is $s_u = 50\,\text{kPa}$, $\phi_u = 0$, bearing capacity factor $N_c = 5.9$.

The drained parameters are: cohesion intercept with respect to effective stress $c' = 5\,\text{kPa}$, angle of shearing resistance with respect to effective stress is $\phi' = 28^\circ$. Bearing capacity factors are $N_c = 32$, $N_q = 19$, $N_\gamma = 15$.

Short term:

$$q_{ult} = s_u \times N_c + \gamma \times D$$
$$= 50 \times 5.9 + 20 \times 1$$
$$= 315\,\text{kPa}$$

Long term:

$$q_{ult} = c' \times N_c + p'(N_q - 1) + \tfrac{1}{2} \times B \times \gamma' \times N_\gamma + p$$
$$= 5 \times 32 + 20 \times 18 + \tfrac{1}{2} \times 2 \times (20 - 10) \times 15 + 15$$
$$= 690\,\text{kPa}$$

Example 2: effect of differing unit weights above and below the water table

A long strip foundation is 15 m wide and located at a depth of 2 m in a dense sand of dry unit weight $\gamma_d = 18\,\text{kPa}$ and saturated unit weight $\gamma_{sat} = 20\,\text{kPa}$. The water table is at foundation level.

The drained parameters are: cohesion intercept with respect to effective stress $c' = 0$, angle of shearing resistance with respect to effective stress is $\phi' = 40^\circ$. Bearing capacity factors are $N_c = 90$, $N_q = 80$, $N_\gamma = 100$.

$$q_f = c' \times N_c + p'(N_q - 1) + \tfrac{1}{2} \times B \times \gamma' \times N_\gamma + p$$
$$= 0 + 2 \times 18 \times 79 + \tfrac{1}{2} \times 15 \times 10 \times 100 + 2 \times 18$$
$$= 10\,380\,\text{kPa}$$

Example 3: effect of water level on submerged foundation

A bridge pier applies a total load of 120 000 kN including self weight and is founded at a depth of 7 m in silty clay of unit weight $\gamma = 20\,\text{kPa}$ and undrained shear strength $s_u = 110\,\text{kPa}$. The plan dimensions of the pier are 30 m × 8 m. The river level fluctuates between a depth of 3 m in the dry season and 8 m in the wet season. Estimate the factors of safety of bearing capacity for the dry and wet seasons. Take the side adhesion factor $\alpha = 0.45$.

The bearing capacity factor is $N_c = 6.7$.
The bearing area is $A_b = 30 \times 8 = 240\,\text{m}^2$.
The side shearing area is $A_s = 2 \times (30 + 8) \times 7 = 532\,\text{m}^2$.

Let the factor of safety be F. Then:

$$120\,000 = (6.7 \times 240 \times 110 + 532 \times 0.45 \times 110)/F$$
$$+ (7 + 20 \times 240) + ((3\,\text{or}\,8) \times 10 \times 240)$$

whence $F_3 = 2.57$ and $F_8 = 3.02$.

Example 4: difference between factor of safety on ultimate bearing capacity and factor of safety on shear strength

A long strip footing is 3 m wide and located at a depth of 2 m in loose dense sand. The water level can vary from (a) a depth below ground of 2 m in the dry season to (b) a height above ground of 1 m in the wet season. The dry unit weight $\gamma_d = 16\,\text{kPa}$ and saturated unit

weight $\gamma_{sat} = 20\,\text{kPa}$. The angle of shearing resistance with respect to effective stress is $\phi' = 33^\circ$.

For both wet and dry seasons estimate the ultimate bearing capacity and the allowable bearing capacity for a factor of safety on shear strength of 1.5.

Allowable bearing pressure:

For $\phi' = \tan^{-1}((\tan 33^\circ)/1.5) = 23.4^\circ$, $N_q = 11$, $N_\gamma = 7.5$.

$$q_f = c' \times N_c + p'(N_q - 1) + \tfrac{1}{2} \times B \times \gamma' \times N_\gamma + p$$

$$= 2 \times 16(11 - 1) + \tfrac{1}{2} \times 3 \times 10 \times 75 + 2 \times 16 = 464\,\text{kPa}$$

$$= 2 \times 10(11 - 1) + \tfrac{1}{2} \times 3 \times 10 \times 75 + (10 + 2 \times 20) = 362\,\text{kPa}$$

Ultimate bearing capacity:

For $\phi' = 33^\circ$, $N_q = 32$, $N_\gamma = 32$.

$$q_f = c' \times N_c + p'(N_q - 1) + \tfrac{1}{2} \times B \times \gamma' \times N_\gamma + p$$

$$\text{(a)} = 2 \times 16 \times 31 + \tfrac{1}{2} \times 3 \times 10 \times 32 + 2 \times 16 = 1504\,\text{kPa}$$

$$\text{(b)} = 2 \times 10 \times 31 + \tfrac{1}{2} \times 3 \times 10 \times 32 + (10 + 2 \times 20) = 1150\,\text{kPa}$$

i.e. $F \approx 3.2$ on ultimate loading, but $F = 1.5$ on strength.

Example 5: difference between general and local failure

A large diameter oil tank applying a pressure of 120 kPa to the ground is to be founded on the surface of a soft to firm deposit of saturated clay. The undrained shear strength of the clay varies linearly from 40 kPa at the surface to 20 kPa at a depth of 3 m, is constant at 20 kPa from 3 m to 5 m, and then increases linearly from 20 kPa at 5 m to 95 kPa at a depth of 20 m below the ground surface.

The clay rests on a thick deposit of dense sand. Taking reasonable values for any parameters not given, estimate the factor of safety against a bearing capacity failure, considering both general and local failure.

Note: $N_c = 6.2$ for a circle on the ground surface, and $N_c = 5.2$ for a strip on the ground surface.

General failure:

Average strength over the full depth of the clay is 33.1 kPa.
Factor of safety $F = (33.1 \times 6.2)/120 = 1.71$.

Local edge failure:

Minimum average strength is 25.4 kPa.
Factor of safety $F = (25.4 \times 5.2)/120 = 1.10$.

CHAPTER FIVE

Settlement analysis

Introduction

This chapter deals with the prediction of the settlement of structures, and concentrates on factors affecting significantly the accuracy of such predictions.

Initial, undrained settlement has been covered in Chapter 3, and settlements related to volume change are discussed below.

There may be a temptation to believe that settlement prediction has become an exact science, because of the advances that have been made in recent years, and the availability of the powerful finite element method of analysis. This is not true and the following quotation is particularly relevant and valid.

> *'Whoever expects from soil mechanics a set of simple, hard-and-fast rules for settlement computation will be deeply disappointed. He might as well expect a simple rule for constructing a geological profile from a single test boring record. The nature of the problem strictly precludes the possibility of establishing such rules. If a supervising or construction engineer wants to enjoy the benefits of recent developments in this field he should first of all study the rules for securing reliable settlement records, and then start to observe the buildings of his district. After he has done this for a certain period he will discover for himself the value of the information which he can obtain from soil mechanics.'*
> **Karl Terzaghi (1936).**

Consolidation settlements of clays

It should be made clear that although initial, primary consolidation and secondary settlements are discussed separately, this does not imply that they are separate components taking place at different times. The settlement at the end of construction is sometimes taken as being equal to the initial settlement but, even if the construction period is short, this will include some part of the primary consolidation settlement. Secondary settlement also, considered to be the settlement occurring after changes in effective stress have taken place, will also develop during the primary

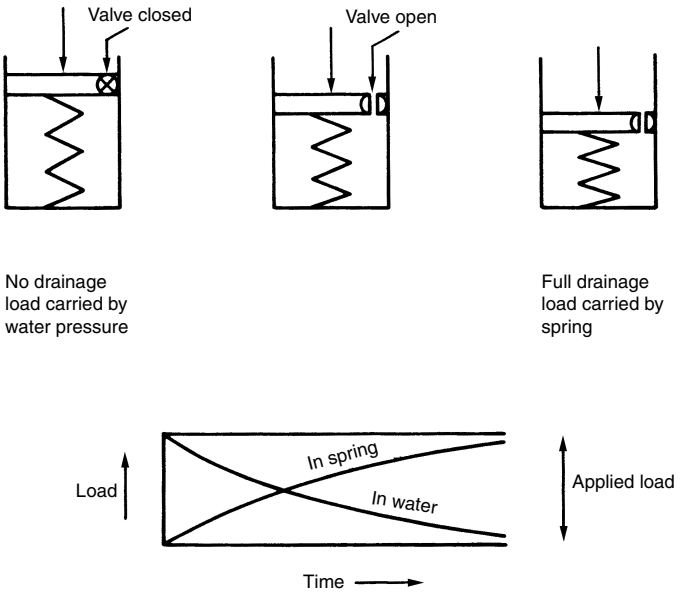

Fig. 5.1 Piston and spring analogy

consolidation period as the pore-water pressure dissipates and the effective stresses increase.

Terzaghi's theory of consolidation

The process of consolidation is illustrated by the piston and spring analogy shown in Fig. 5.1. At the instant the load is applied, because the system is not allowed to drain, the spring cannot deform and the loading is carried by the excess pore water pressure. If, now, slow drainage is allowed, water will leak out and the load will be transferred from the water to the spring until finally, after sufficient time has elapsed and the spring has deformed sufficiently to carry the applied loading, the deformation ceases and the excess pore water pressure is zero. In the corresponding soil element, the spring is replaced by the soil structure, and the rate of water expulsion is governed by the permeability of the soil and the length of the drainage path.

It is necessary, then, to calculate both the magnitude and the rate of the consolidation settlement and in practice, use is generally made of the Terzaghi theory of one-dimensional consolidation, which considers the situation shown in Fig. 5.2. The main assumptions on which the theory is based are:

- the soil is saturated,
- the water and the clay particles are incompressible,
- Darcy's law is valid,

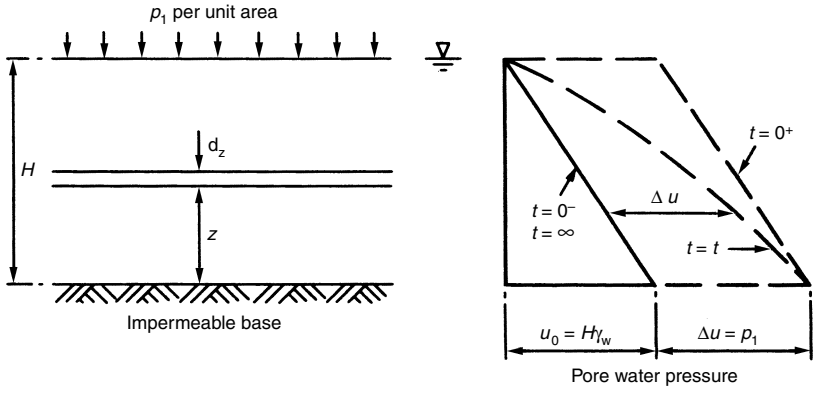

Fig. 5.2 Key figure for one-dimensional consolidation

- for a change in voids ratio corresponding to a given increment in effective stress, the permeability, k, and the coefficient of volume change, m_v, remain constant,
- the time taken for the clay to consolidate depends entirely on the permeability of the clay,
- the clay is laterally confined,
- the flow of water is one-dimensional,
- effective and total stresses are uniformly distributed over any horizontal section.

These assumptions correspond to the oedometer test in the laboratory and to a clay layer in the field subjected to uniform global loading, that is, a uniformly distributed loading applied over an infinite area.

Based on these assumptions, the governing differential equation relating excess pore water pressure, position and time can be derived as

$$\frac{\partial u}{\partial t} = c_v \frac{\partial^2 u}{\partial z^2} \tag{5.1}$$

where

$$c_v = \frac{k}{m_v \gamma_w} = \text{coefficient of consolidation}$$

and

$$m_v = \frac{\Delta V}{V} \Big/ \Delta p = \frac{\Delta H}{H} \Big/ \Delta p = \text{coefficient of volume compressibility}$$

Equation 5.1 must be solved for the following boundary conditions:

$\Delta u = p_1$ for $t = 0$ and $0 < z < H$

$\Delta u = 0$ for $t > 0$ and $z = H$

$\Delta u = 0$ for $t = \infty$ and $0 < z < H$

The solution may be expressed in the form:

$$\Delta u = \frac{4p_1}{\pi} \sum_{N=0}^{N=\infty} \frac{(-1)^N}{2N+1} e^{-(2N+1)^2\pi^2(T_v/4)} \cos\left[\frac{(2N+1)\pi z}{2H}\right] \tag{5.2}$$

where

$$T_v = \frac{c_v t}{H^2}$$

is an independent dimensionless variable known as the time factor.

It follows that the degree of consolidation, $\bar{U}$, at any time (equal to the settlement at that time, δ_t, expressed as a percentage of the total final settlement, δ_c, at the end of consolidation) is given by:

$$\bar{U} = \frac{\delta_t}{\delta_c} = 1 - \frac{8}{\pi^2} \sum_{N=0}^{N=\infty} \frac{1}{(2N+1)^2} e^{-(2N+1)^2\pi^2 T_v/4} \tag{5.3}$$

Solutions relating $\bar{U}$ and T_v for various distributions of initial excess pore water pressure, and single and double drainage are given in Fig. 5.3. Using these solutions, it should be noted that the total thickness of the consolidating layer is always used in the computations. The solution relating $\bar{U}$ and T_v is then taken, corresponding to the drainage conditions of the particular problem.

Further points on consolidation

Voids ratio and effective pressure

A typical relationship between voids ratio and effective pressure is shown on Fig. 5.4(a) and between voids ratio and the logarithm of effective pressure on Fig. 5.4(b).

Final consolidation settlement

The final consolidation settlement can be calculated using any of the following expressions:

$$\delta_c = \frac{\Delta e}{1+e_0} H \tag{5.4}$$

$$\delta_c = m_v H \Delta p \tag{5.5}$$

$$\delta_c = \frac{C_c}{1+e_0} H \log_{10} \frac{p_0' + \Delta p}{p_0'} \tag{5.6}$$

where C_c = compression index and is the slope of the $e - \log p'$ line. It is convenient to use C_c when dealing with normally consolidated clays and m_v for over-consolidated clays.

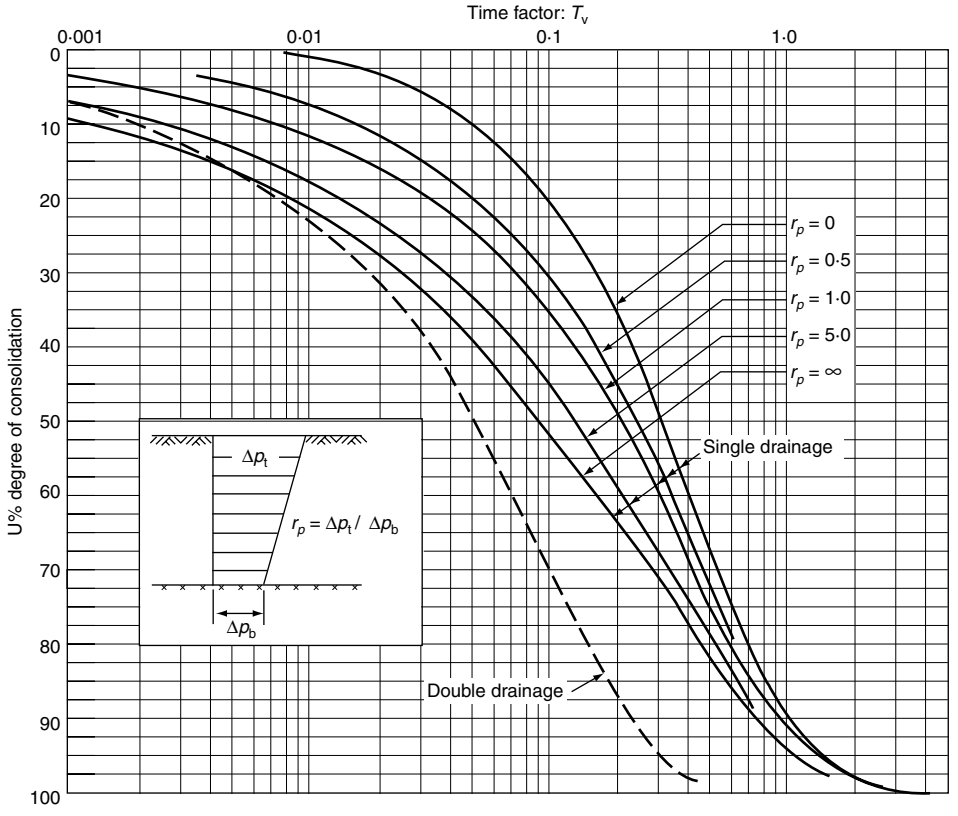

Fig. 5.3 Relationship between degree of consolidation and time factor, after Janbu, Bjerrum and Kjaernsli (1956)

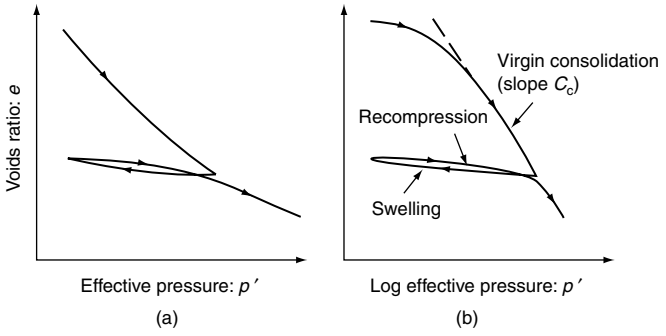

Figure 5.4(a) Relationship between voids ratio and effective pressure; (b) relationship between voids ratio and the logarithm of effective pressure

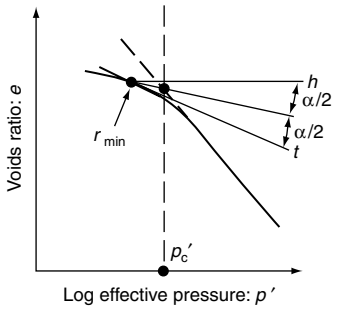

Fig. 5.5 Construction for determining the preconsolidation pressure, p'_c, after Casagrande (1936)

Settlement for a given load increment

It can be seen from Fig. 5.4 that the settlement for a given load increment is much greater for a normally consolidated clay than for an over-consolidated clay. It is vital therefore to determine whether or not a clay is over-consolidated. This can be determined from:

- a knowledge of the geological history of the clay, that is, whether previous overburden has been removed or the ground water table is now higher than in the past,
- the Casagrande construction, illustrated in Fig. 5.5, which gives the pre-consolidation pressure p'_c (the greatest effective pressure the clay has carried in the past). If $p'_c > p'_0$, the clay is over-consolidated. If $p'_c = p'_0$, the clay is normally consolidated,
- comparing the measured undrained shear strength with that to be expected for a normally consolidated clay having a similar plasticity index, see Fig. 2.17. If the measured strength is greater than that anticipated for a normally consolidated clay the clay is probably over-consolidated,
- comparing C_c corresponding to p'_0 with the value predicted for a normally consolidated clay, $C_c = 0.009(LL - 10)$. If C_c at p'_0 is less than that expected for a normally consolidated clay, the clay is probably over-consolidated,
- a determination of the liquidity index (LI), of the clay where

$$LI = \frac{w_c - PL}{LL - PL}$$

and LL is the liquid limit and PL is the plastic limit, determined according to BS 1377. Normally consolidated clays have a liquidity index varying from about 0.6 to 1.0, and over-consolidated clays have a liquidity index varying from 0 to about 0.6. This gives a rough guide only.

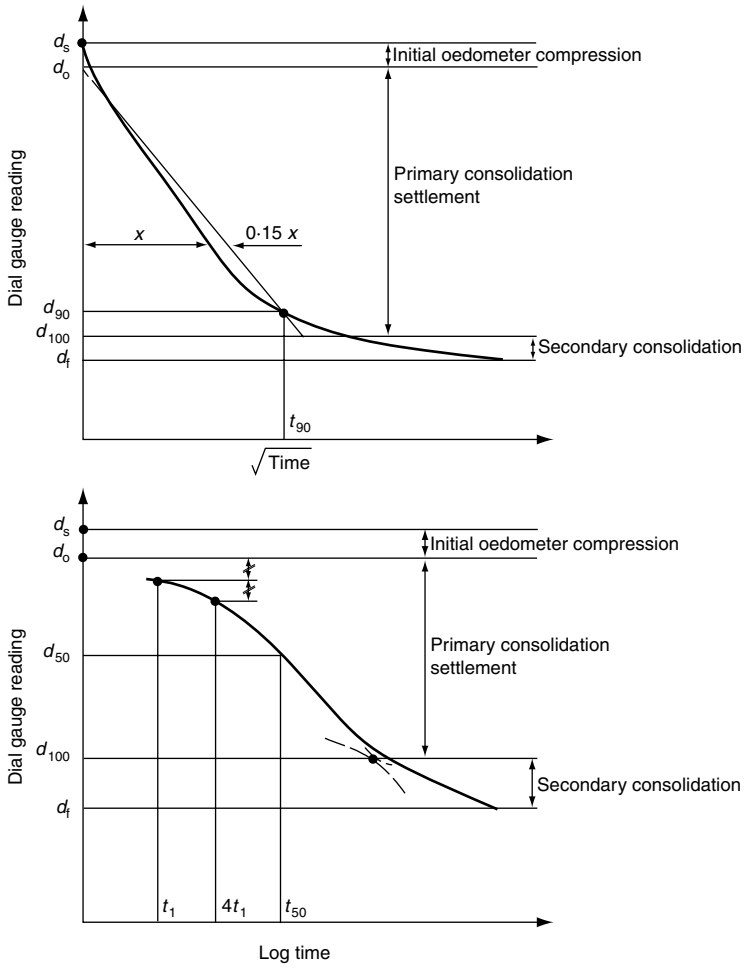

Fig. 5.6 Determination of the coefficient of consolidation, c_v; (a) square root of time method, $c_v = T_{90}$. $H^2/t_{90} = 0.212H^2/t_{90}$ (H = sample thickness); (b) logarithm of time method, $c_v = T_{50}$. $H^2/t_{50} = 0.0492H^2/t_{50}$ (H = sample thickness)

Coefficient of consolidation

The coefficient of consolidation is calculated using either the square root of time plot or the logarithm of time plot; the procedures are illustrated in Fig. 5.6.

Correction of measured compressibility

It is important, particularly for stiff clays having low compressibilities, to correct the measured compressibility for the initial compression in the oedometer, otherwise values very much on the high side may result,

that is, the deformation $(d_0 - d_s)$ must be excluded when determining m_v; d_0 is the corrected zero reading and d_s is the observed initial reading.

WORKED EXAMPLE

The problem is to calculate the total primary consolidation settlement for the example shown in Fig. 5.7, and to determine the time for 50% and 90% of this settlement to develop.

For the purposes of settlement calculation, the clay will be subdivided into two layers, *A* and *B*, of thickness 3 m and 4 m respectively.

The net increase in foundation stress at foundation level is $100 - 2 \times 20 = 60\,\text{kPa}$. The net increase in vertical stress under the centre of *layer A* $= 60 \times 0.75 = 45\,\text{kPa}$ (for $z/B = 4.5/10$, Fig. 3.3) and *layer B* $= 60 \times 0.46 = 27.6\,\text{kPa}$ (for $z/B = 8/10$, Fig. 3.3)

$$\delta_c = m_v H_A \Delta\sigma_A + m_v H_B \Delta\sigma_B \text{ (using equation 5.5)}$$

$$= (0.0001 \times 3000 \times 45 + 0.0001 \times 4000 \times 27.6)\,\text{mm}$$

$$= (13.5 + 11.0)\,\text{mm} = 24.5\,\text{mm}$$

Making an allowance for the rigidity of the footing by taking a rigidity factor of 0.8, the total consolidation settlement of the rigid footing is $0.8 \times 24.5 = 19.6\,\text{mm}$.

For $U = 50\%$, $T_v = 0.049$, from Fig. 5.3 therefore $t_{50} = (0.049 \times 7^2)/1 = 2.4$ years.

For $U = 90\%$, $T_v = 0.21$, from Fig. 5.3 therefore $t_{90} = (0.21 \times 7^2)/1 = 10.3$ years.

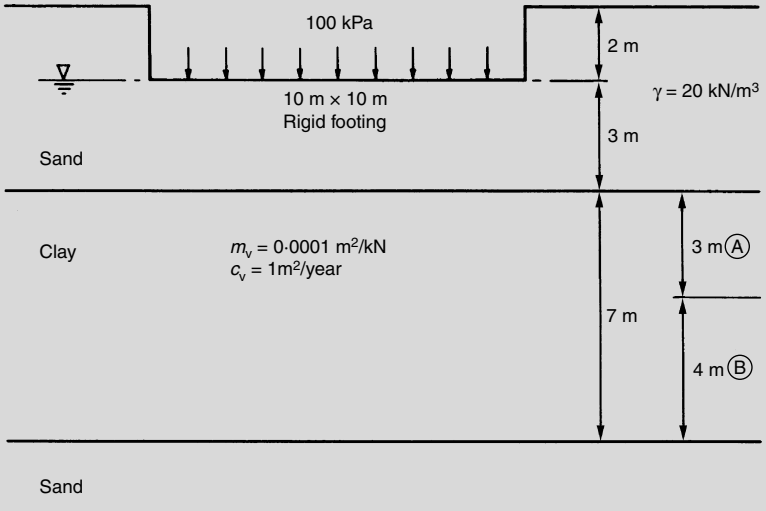

Fig 5.7 Example of calculation of primary consolidation settlement

Prediction of primary consolidation settlement

Prediction of the magnitude and rate of the primary consolidation settlement of saturated clay strata was first made possible by Terzaghi about 50 years ago when the theory of one-dimensional consolidation was developed. In addition, an oedometer was designed which allowed the determination of the parameters, c_v and m_v or C_c which were necessary for the calculation procedure.

Considerable progress has been made in refining the computation process, and the authors have attempted to isolate some of the factors of particular importance which influence the accuracy of settlement predictions.

Net increase in stress

Consolidation settlement calculations are based on the assumption that the settlement is a function of the net increase in foundation pressure; if this net increase is zero, it is assumed that the consolidation settlement will be zero. The view has been expressed that, because the changes in pore water pressure for equal unloading and loading stages may well be different (Bishop and Henkel, 1953), it is possible that residual pore water pressures could be set up owing to an unloading and reloading cycle, particularly in cases when the factor of safety against a bottom heave failure during excavation is small, which is very often the case. It appears, however, that there is a considerable body of evidence to show that only very small settlements are experienced with fully floating foundations (Casagrande and Fadum, 1942; Aldrich, 1952; Bjerrum, 1964; Golder, 1965; Bjerrum and Eide, 1966; Bjerrum, 1967; D'Appolonia and Lambe, 1971). The data given by Bjerrum. and Eide (1966) are summarized in Table 5.1.

It can be seen that the settlement during reloading was approximately equal to the heave. In addition, it was noted that the settlements terminated a short time after the end of construction. It can therefore be concluded that it is satisfactory to perform consolidation settlement calculations based on net increases in foundation pressure only.

Sample disturbance

The importance of sample disturbance has been recognized for many years, for example, Terzaghi, 1941; Rutledge, 1944; Schmertmann, 1953 and 1955; and procedures have been suggested to correct laboratory stress–strain relationships for such disturbance. For normally consolidated clays, sample disturbance will lead to measured oedometer compressibilities which are too low, whereas for over-consolidated clays, the measured compressibilities may be too high.

Table 5.1 Observed vertical movements of compensated foundations, after Bjerrum and Eide (1966)

Structure	Date completed	Undrained shear strength (kPa)	Net foundation pressure (kPa)	Heave (mm)	Total settlement (mm)
Håndverk Industri, Drammen	1958	7–15	1	26	34
Werringgården, Drammen	1956	6–15	0	29	30
Norløff, Drammen	1955	6–15	0	–	c. 30
Park Hotel, Drammen	1961	10–15	0	–	40
Idunbygg, Drammen	1963	30	0–5	–	45

Bjerrum (1967) pointed out that the measurement of the pre-consolidation pressure was particularly sensitive to sample disturbance and that only the highest standards of sampling and laboratory technique would result in consistent and reliable determinations.

Berre, Schjetne and Sollie (1969) compared values of $C_c/(1+e_o)$ and p'_c/p'_0 obtained from a new 95 mm piston sampler and from the 54 mm piston sampler (itself a very high quality instrument) which has been in use for many years. They found more scatter in the results from the 54 mm sampler, and, in addition, the average value of p'_c/p'_0 derived from the 95 mm sampler was some 5% higher than that obtained from the smaller tube. In addition, they noted that chemical changes may take place in a clay if stored for several months in steel sampling tubes, and that these changes could well alter the geotechnical properties of the soil.

Bjerrum (1973) noted that several types of soft and sensitive clays at very small strain show a critical shear stress which in many cases governs their behaviour. This small strain behaviour is destroyed if the clay is subjected to even relatively small strains either during the sampling operations or during handling in the laboratory. Furthermore, sample disturbance leading to redistribution of moisture content, may lead to significant errors in measured parameters.

A method of correcting an $e - \log p'$ curve for sample disturbance is shown in Fig. 5.8 (Schmertmann, 1953).

Considering first a normally consolidated clay, the correction for sample disturbance is outlined on Fig. 5.8(a). The straight line through e_o, p'_0 intersecting the straight line portion of the laboratory curve at $e = 0.42e_o$ is taken as representing the field relationship between voids ratio and log pressure. It should be noted that if the correction for sample disturbance is not made, then the calculated settlements would underestimate the true field settlement.

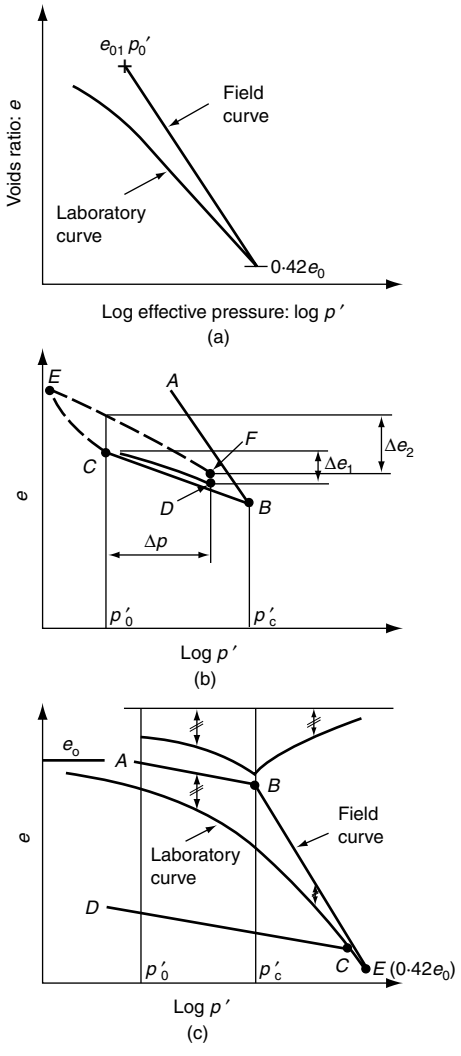

Fig. 5.8 Correction of voids ratio–log effective pressure curve for sample disturbance, after Schmertmann (1953)

If the clay is over-consolidated, however, a different situation exists. Referring to Fig. 5.8(b), allow a clay to first be consolidated to a higher pressure p_c', point B, and then as a consequence of the removal of glaciers or surface erosion, for example, let it swell to a smaller pressure, p_0' point C which represents the condition of the over-consolidated soil in the field. If a loading of Δp is applied to the soil in the field, it will consolidate along the full line curve to point D, and the change in void ratio will be Δe_1. If the soil is sampled at C, and a standard oedometer test carried out, the sample will swell to point E under the first loading increment in the oedometer

and then consolidate along line *EF*. If this curve is used to predict settlement, the change in voids ratio will be Δe_2 which is greater than Δe_1 and thus the field settlement will be overestimated. A better test procedure, which should be applied to all clays, either normally consolidated or over-consolidated, is not to add water to the sample until the applied loading is approximately equal to p'_0. Care must be taken, however, to ensure that the sample cannot dry out. Even if this procedure is followed, it will still be necessary to correct for sample disturbance, and Schmertmann's procedure is as follows (referring to Fig. 5.8(c)):

- plot (e_o, p'_0), point A,
- determine p'_c, the maximum pre-consolidation pressure,
- through A draw a straight line AB parallel to the rebound curve, CD, to intersect the vertical line through p'_c at B,
- through B draw a straight line BE to intersect the straight line portion of the laboratory curve at E, where $e = 0.42e_o$.

The curve ABE then represents the field relationship between voids ratio and pressure.

The determination of p'_c is clearly of great importance and Schmertmann has suggested that the use of 'voids ratio reduction patterns' gives a more precise estimate of p'_c than the Casagrande construction. A voids ratio reduction pattern is simply the difference in voids ratio between the laboratory curve and any estimate field curve plotted against log pressure. Evidence suggests that the voids ratio reduction pattern is symmetrical about p'_c. Various values for p'_c are assumed, the field curves are constructed, and the value which gives the most symmetrical voids ratio reduction pattern is most probably the correct field pre-consolidation pressure.

In his paper, Schmertmann (1953) shows, first, that for good undisturbed samples, the slope of the $e - \log p'$ curve in the range of over-consolidation is approximately equal to the slope of the rebound curve, and this has often been confirmed in the laboratory. Second, the slope of the rebound curve is not very sensitive to the amount of sample disturbance. These two factors form the basis of Schmertmann's construction.

There can be no doubt that high standards of sampling and testing must be adopted if reliable settlement predictions are to be obtained.

Induced pore-water pressures under a structure

A most important contribution to settlement analysis was made by Skempton and Bjerrum (1957). They pointed out that an element of soil underneath a foundation undergoes lateral deformation as a result of applied loading and that the induced pore-water pressure is, in general, less than the increment in vertical stress on the element, because it is

dependent on the value of Skempton's pore pressure parameter, A. The consolidation of a clay results from the dissipation of pore water pressure. But a given set of stresses will set up different pore water pressures in different clays if the A values are different. Thus two identical foundations carrying identical loads, resting on two clays with identical compressibilities, will experience different consolidation settlement if the A values of the clay are unequal. This is true despite the fact that no difference would be seen in oedometer test results. For the special case of the oedometer test, however, where the sample is laterally confined, then, irrespective of the A value, the pore water pressure set up is equal to the increment in vertical stress (Simons and Menzies, 1974). Skempton and Bjerrum (1957) proposed that a correction factor should be applied to the settlement, calculated on the basis of oedometer tests and showed that the factor was a function of the geometry of the problem and the A value, the smaller the A value, the smaller the correction factor. The factor μ is shown in Fig. 5.9 and the field settlement is then equal to μ times the settlement calculated on the basis of oedometer tests (see equation 5.14).

For heavily over-consolidated clays, A values less than 1 would be expected and the Skempton–Bjerrum correction factor is usually applied in such cases. It should be noted that in the working range of stress for normally consolidated clays, particularly when there is no question of

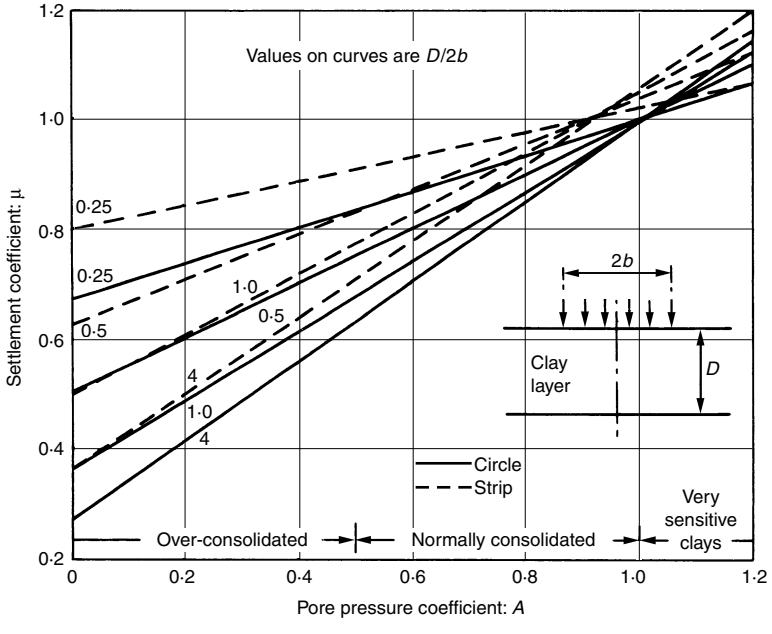

Fig. 5.9 Correction factor for pore pressures set up under a foundation, after Skempton and Bjerrum (1957)

over-stressing occurring, A values less than 1 can arise, and the correction factor should then be applied.

Stress path settlement analysis

As discussed above, Skempton and Bjerrum (1957) recognized that an element of soil underneath a foundation undergoes lateral deformation as a result of applied foundation loading and that the subsequent consolidation would be a function of the excess pore water pressures set up in situ. It was assumed, however, that the relationship between axial compressibility and effective stress could be determined in the standard oedometer, that is, the influence of lateral stresses on the stress deformation characteristics of the soil was not taken into account. A better laboratory procedure to predict the deformation of a soil under a given foundation loading, would be to test the soil by applying as closely as possible the same stress changes as those to which the soil will be subjected in the field. Moreover, because soil behaviour is generally non-linear, deformation properties, such as the undrained elastic modulus, Poisson's ratio, and the drained compressibility, will vary with stress level. It is also desirable that a soil specimen, after sampling, be first brought back to the stress system initially prevailing in the ground, before subjecting it to the stress changes it is likely to undergo on loading. Thus the concept of stress path testing (Simons and Som, 1969 and 1970; Simons, 1971) logically follows.

A stress path is essentially a line drawn through points on a plot of stress changes and shows the relationship between components of stress at various stages in moving from one stress point to another. Stress paths can be plotted in a variety of ways, and in studying the deformation of soils, a simple plot of vertical stress (effective or total) has been found to be convenient. It should also be noted that in this discussion, consideration is only given to cases where, by virtue of symmetry, the intermediate and minor principal stresses are equal and where the vertical and horizontal stresses are the principal stresses.

Consider how an element of over-consolidated clay under the centre line of a circular loaded area may be stressed. Before the application of the surface loading, the in situ vertical and horizontal effective stresses will be p' and $K_0 p'$, respectively, where K_0 is greater than unity (Skempton, 1961). The in situ effective stresses (p' and $K_0 p'$) are represented by the point A and the corresponding total stresses by A_1 in Fig. 5.10. Owing to the applied foundation pressure, q, the stresses on the element will increase by $\Delta\sigma_v$, and $\Delta\sigma_{h1}$. If the foundation pressure is applied sufficiently quickly so that no drainage occurs during the load application, the element will deform without any volume change and any vertical compression will be associated with a lateral expansion.

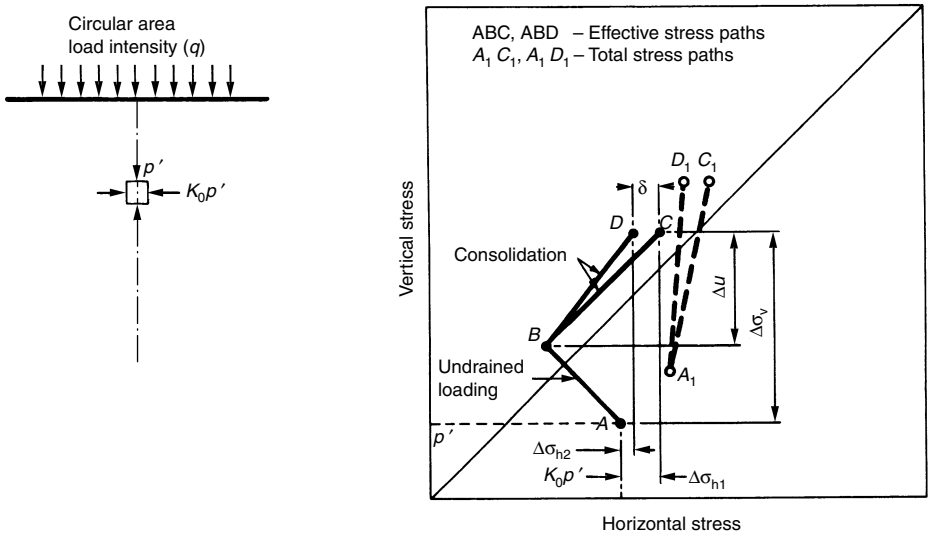

Fig. 5.10 Stress path during undrained and drained loading, after Simons and Som (1969)

Now, the increase in stresses $\Delta\sigma_v$, and $\Delta\sigma_{h1}$ will set up an excess pore-water pressure in the element of saturated clay ($B = 1$) (Skempton, 1954), where

$$\Delta u = \Delta\sigma_{h1} + A(\Delta\sigma_v - \Delta\sigma_{h1}) \tag{5.7}$$

Therefore, immediately after load application, the effective stresses are:

$$(\sigma'_v)_o = p' + \Delta\sigma_v - \Delta u \tag{5.8}$$

$$(\sigma'_h)_o = K_0 p' + \Delta\sigma_{h1} - \Delta u \tag{5.9}$$

Since for most clays, and certainly for London clay, the value of A is positive and less than unity in the range of stresses normally encountered in practice, Δu is greater than $\Delta\sigma_{h1}$. Consequently, the effective vertical stress increases and the effective horizontal stress decreases during load application, and the stress point moves from A to B. The vertical strain during undrained loading is, therefore, a function of the stress path, AB. The element now begins to consolidate. During the early stages, the increase in effective horizontal stress is a re-compression until the original value $K_0 p'$ is restored, beyond which the further increase of effective horizontal stress is net, while the element is subjected to a net increase in effective vertical stress during the entire process of consolidation.

During load application under undrained conditions, a saturated clay behaves as an incompressible medium with Poisson's ratio equal to 0.5. As the excess pore water pressure dissipates, however, Poisson's ratio

decreases and finally falls to its fully drained value at the end of consolidation. This change in Poisson's ratio is unlikely to affect significantly the vertical stress (for an elastic, isotropic, homogeneous medium, the vertical stress increases are independent of the material parameters) but the horizontal stress will decrease by an amount δ to a new value $K_0 p' + \Delta\sigma_{h2}$ where

$$\Delta\sigma_{h2} = \Delta\sigma_{h1} - \delta \tag{5.10}$$

Therefore during consolidation, the element will follow the effective stress path *BD*, which will govern the vertical strain during drained loading.

An ideal settlement analysis should take into account the complete patterns of stress changes to which typical elements of soil will be subjected in the field, and a summation of the corresponding vertical strains would give the predicted settlement of the structure.

The stages of an idealized experimental programme are outlined in Fig. 5.11. When a sample is removed from the ground without significant mechanical disturbance or change in water content, the total stresses are reduced to zero and a negative pore-water pressure is set up (Skempton and Sowa, 1963). In the first stage, therefore, the in situ stresses should be restored to obtain the condition before sampling. Then a set of stresses equal to those to which the sample will be subjected owing to the foundation loading, should be applied under undrained conditions, and both the vertical strain and the pore-water pressure measured. The sample should then be allowed to consolidate against a back-pressure equal to the equilibrium pore water pressure u_o, and, at the same time, the horizontal stress

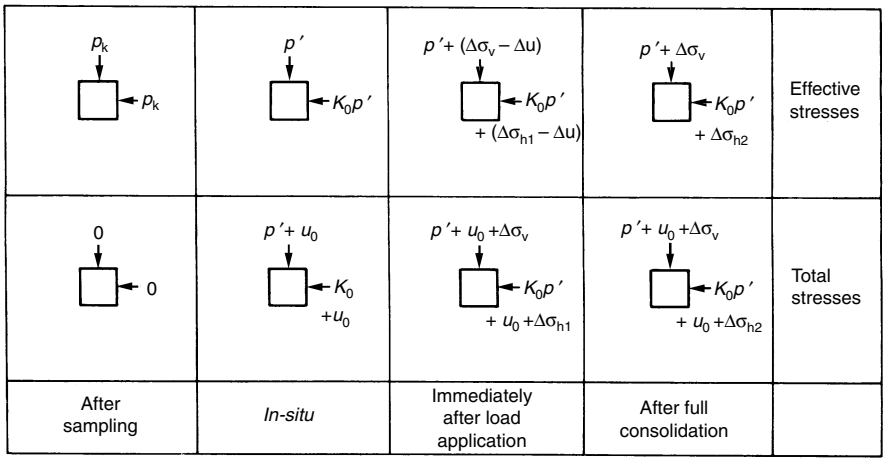

Fig. 5.11 Idealized experimental programme for predicting settlement, after Simons and Som (1960)

should be decreased to its final value. The vertical strain recorded during this final stage together with that observed during the undrained loading, gives the total strain of the element in the field and the total settlement can be obtained by summation.

The stress path method of settlement analysis has been applied to London clay (Som, 1968, Simons and Som, 1969 and 1970; Simons, 1971).

The most important conclusions resulting from this work are as follows.

- The actual stress path for an element of soil beneath a foundation in the field is in general quite different from that implied in standard methods of settlement computation based on the oedometer test. Because the axial deformation of an element of soil is dependent on the stress path followed, standard methods of settlement analysis cannot be expected to yield accurate predictions.
- In a foundation problem, the elastic modulus of the soil varies with depth as a consequence of increasing effective stresses before construction, and also because of different stress levels that are imposed by the applied foundation pressure. To measure correctly the variation of the elastic modulus with depth, it is necessary that an undisturbed sample be first brought back to the stress system prevailing in the ground before sampling and then be subjected under undrained conditions to the actual stress increments that are likely to be applied in the field. For London clay, the elastic modulus so obtained differs considerably from, and is generally larger than, that determined from standard undrained tests.
- The *volumetric* compressibility of London clay is primarily a function of effective vertical stress and is largely independent of the lateral stresses, at least within the range of stresses covered by the testing programme. However, the *vertical strain is* greatly influenced by the relative magnitude of the vertical and lateral stress increments during consolidation. Direct use of oedometer test results will not therefore result in accurate predictions of settlement, even if account is taken of the different excess pore water pressures set up in the oedometer and in the field.
- The volumetric compressibility of London clay can, for practical purposes, be determined from either triaxial or oedometer tests, the latter giving satisfactory results only when initial swelling is positively prevented, and apparatus and bedding errors are eliminated. It is then possible to use the oedometer volume compressibility, together with a relationship between K' $(= \Delta\sigma_3'/\Delta\sigma_1')$ and $\varepsilon_1/\varepsilon_v$ (the ratio of the axial to volumetric strain) to calculate the settlement of a structure. This relationship can be predicted with sufficient accuracy by assuming the soil to be a cross-anisotropic elastic material.

WORKED EXAMPLE

It has been shown that both the undrained and drained deformation moduli vary with the stress path followed and, therefore, significant errors in settlement calculations can develop if procedures are adopted which do not satisfactorily take into account the influence of stress path. Purely as an illustrative example, the settlement of a typical foundation on London clay has been calculated by three different methods, and the results are compared below.

The example is a circular, flexible, smooth footing, 12.2 m in diameter and founded at a depth of 6.1 m at a site for which the soil profile has been assumed to be the same as at Bradwell (Skempton, 1961), and settlement analyses have been made for the centre of this circular foundation. The Bradwell data have been chosen simply because the effective stress–depth relationships, necessary for the stress path method of analysis, have been established to a considerable depth at this site.

From a knowledge of bearing capacity, a net foundation pressure of 140 kPa and a gross pressure 198 kPa have been adopted, to give a factor of safety against failure of more than three. The buried footing effect has not been taken into account in the comparative analyses that follow.

The immediate undrained settlement has been calculated in the conventional manner using an average Young's modulus of 38 500 kPa obtained from stress–strain relationships of standard undrained tests, and the settlement is obtained by the equation:

$$\delta_{\mathrm{i}} = \frac{qB\mu_0\mu_1}{E} \tag{5.11}$$

where q = net foundation pressure, 140 kPa; B = diameter of circle = 12.2 m; and μ_0, μ_1 are dimensionless influence factors obtained from Fig. 3.6.

The immediate undrained settlement following the stress path method is given by:

$$\delta_{\mathrm{i}} = \sum \frac{\Delta\sigma_{\mathrm{v}} - \Delta\sigma_h}{E(\mathrm{z})}\,\mathrm{dz} \tag{5.12}$$

where $\Delta\sigma_{\mathrm{v}}$ and $\Delta\sigma_{\mathrm{h}}$ are the increments in total vertical and horizontal stresses at any depth z, respectively, and $E(\mathrm{z})$ is the corresponding deformation modulus, taking into account the initial and final (under undrained conditions) vertical and horizontal effective stresses.

The results of the calculations are given in Table 5.2 and show an immediate settlement of 32.7 mm by the conventional method and 17.2 mm by the stress path method.

Table 5.2 Example of settlement calculations, after Simons (1971)

Type of settlement	Conventional method (mm)	Skempton and Bjerrum's method (mm)	Stress path method (mm)
Immediate	32.7	32.7	17.2
Consolidation	109.0	75.1	40.9
Total	141.7	107.8	58.1

The consolidation settlement, δ_c has been calculated using the conventional method, the Skempton and Bjerrum (1957) approach, and the stress path method.

In the conventional method, the settlement is given by:

$$\delta_c = \int_0^z (m_{v)_1} \Delta\sigma_v \, dz \tag{5.13}$$

where (m_v) is the volume compressibility determined in the standard oedometer test, and $\Delta\sigma_v$ the increase in total vertical stress.

Following the Skempton and Bjerrum method, the settlement is:

$$\delta_c = \mu \int_0^z (m_v)_1 \Delta\sigma_v \, dz \tag{5.14}$$

where $(m_v)_1$ and $\Delta\sigma_v$ are as before and μ is a function of the soil type and the geometry of the foundation.

In the present case, μ is 0.69, corresponding to $A = 0.55$ and $z/B = 1.5$, from Fig. 5.9.

For the stress path method, the settlement is:

$$\delta_c = \int_0^z \lambda (m_v)_3 \, \Delta u \, dz \tag{5.15}$$

where Δu is the increase in pore water pressure under undrained loading which dissipates, resulting in the consolidation settlement; $(m_v)_3$ is the coefficient of volume compressibility for three-dimensional strain, which has been shown to be independent of the type of test for practical purposes; λ is the ratio of vertical strain to the volumetric strain which has been shown to be highly sensitive to the stress increment ratios.

The results of the calculations are given in Table 5.2 and show $\delta_c = 109$ mm by the conventional method, $\delta_c = 75.1$ mm by Skempton and Bjerrum's method, and $\delta_c = 32.7$ mm by the stress path method. It can be seen that conventional methods overestimate the stress path settlement by 240% (Menzies, 1997)!

The conventional method gives the highest calculated settlement, because it assumes that $\Delta u = \Delta\sigma_v$ and that the relationship between axial compressibility and effective vertical stress is given by the standard oedometer. The Skempton and Bjerrum method takes into account the fact that Δu is not equal to $\Delta\sigma_v$ in the field, although it is in the oedometer, but assumes again that the relationship between axial compressibility and effective vertical stress can be obtained from the oedometer test.

The relative magnitudes of the settlements as calculated by the different methods depend on the conditions existing at any particular site, and are not, therefore, in general, the same as those indicated by the example above. It is clear that the Skempton and Bjerrum approach is a great improvement on the conventional method, but will not necessarily give a precise estimate of the true field settlement.

The stress path method represents an improvement on the Skempton and Bjerrum procedure. With computer controlled triaxial testing systems (e.g. see Fig. 2.8(c)), stress path testing is now routine. Because, however, it has been shown (Som, 1968; Simons and Som, 1969) that, for practical purposes, the volumetric compressibility can be determined from either triaxial or oedometer tests, it is possible to use the oedometer volume compressibility together with a relationship, which can be obtained experimentally or predicted theoretically, between the ratio of the axial to the volumetric strain and the ratio of applied effective horizontal to vertical stress.

Pre-consolidation pressure

An excellent example of the importance in practice of determining the pre-consolidation pressure is given by Vargas (1955) who showed from settlement observations of a number of buildings in Sao Paulo that:

- Where the applied foundation stress did not exceed the difference between the pre-consolidation pressure and the in situ effective pressure, the observed settlements were generally less than 10 mm, and were very much smaller than those computed directly from oedometer curves, on occasions equalling only 10% of the computed values.
- Where the applied foundation stress exceeded $p'_c - p'_0$, albeit only marginally, much larger settlements were measured. Reasonable agreement between calculated and observed settlement was obtained only if the calculations were based on stress increases in excess of p'_c, not p'_0.

Detailed studies of the properties of various clays by a number of investigators have shown that there are different factors which can give rise to a pre-consolidation pressure greater than the present effective overburden pressure, for example:

- removal of overburden
- fluctuations in the groundwater table
- cold-welding of mineral contact points between particles
- exchange of cations
- precipitation of cementing agents
- geochemical processes caused by weathering
- delayed compression.

It is well known that the determination of p'_c is partly a function of the test procedure adopted in the laboratory, for example, the rate of loading adopted, whether or not rest periods have been permitted, and the effects of sample disturbance. The value of p'_c determined in the laboratory may well be different from that which can be relied upon in the field.

The development of pre-consolidation pressure resulting from delayed compression and the effects of such pre-consolidation on the settlements of structures has been discussed in detail by Bjerrum (1967 and 1973).

The concept of instant and delayed compression as proposed by Bjerrum is illustrated in Fig. 5.12; instant compression is the settlement which would result if the excess pore water pressures set up by a foundation loading could dissipate instantaneously with load application; delayed compression is the settlement then developing at constant effective stress.

A clay which has recently been deposited and come to equilibrium under its own weight but has not undergone significant secondary consolidation may be classified as a young normally consolidated clay. Such a clay is characterized by the fact that it is just capable of carrying the overburden weight of soil, and any additional load will result in relatively large settlements. If an undisturbed sample of a young clay is tested in an oedometer, the resulting $e - \log p$ curve will show a sharp bend exactly at the effective overburden pressure p'_0 which the sample carried in the field. A consolidation curve of this type is shown in Fig. 5.13 marked young, being characterized by the fact that $p'_c = p'_0$. Thus, to this group of clays belongs only the clays which are geologically recent. A clay which has just consolidated under an additional load as, for instance, a fill, will also be classified with respect to its compressibility as a young clay deposit.

If a young clay is left under constant effective stresses for hundreds or thousands of years, it will continue to settle. The result of this secondary or delayed consolidation is a more stable configuration of the structural arrangement of the particles which means greater strength and reduced compressibility. With time, a clay undergoing delayed consolidation will thus develop a reserve resistance against a further compression. It can carry a load in addition to the effective overburden pressure without significant volume change. If an undisturbed sample of such an *aged* normally consolidated clay is subjected to a consolidation test, the resulting

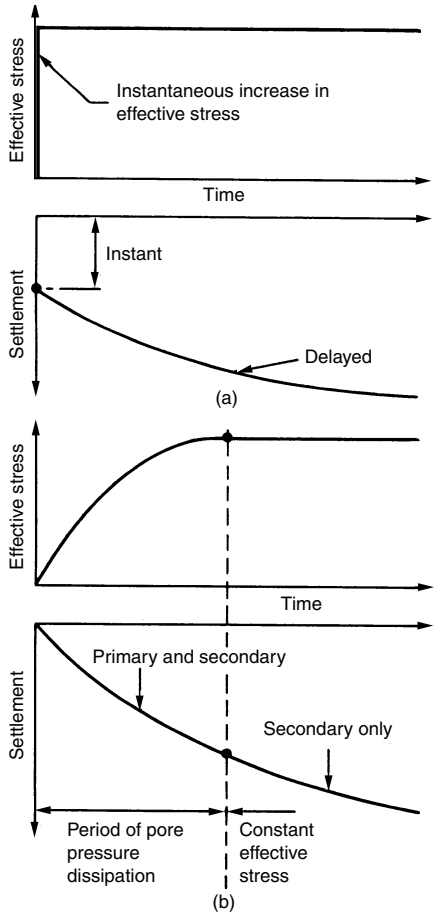

Fig. 5.12 Instant and delayed compression, after Bjerrum (1967)

$e - \log p$ curve will follow the curve marked *aged* on Fig. 5.13. The curve shows an abrupt increase in compressibility at a pressure p'_c which is greater than p'_0.

As pointed out by Bjerrum (1972), considerable patience is required to determine experimentally in the laboratory the basic information necessary for constructing such a diagram as Fig. 5.13. The only diagrams existing originate from areas where long term observations of settlement are available.

A p'_c effect developed as a result of a delayed consolidation is characterized by the fact that the developed value of p'_c increases proportionally with p'_0, the effective overburden pressure the clay carried in the period it experienced delayed consolidation. In a homogeneous clay deposit, the ratio p'_c/p'_0 is consequently constant with depth and this ratio can conveniently be used to describe the effect. The p'_c/p'_0 ratio of clay deposits of

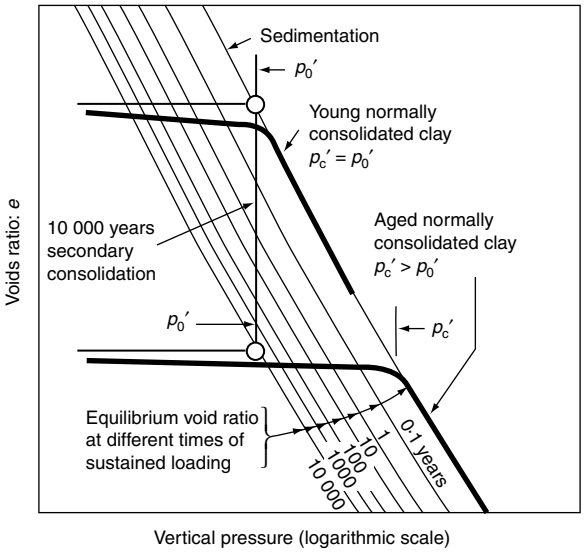

Fig. 5.13 Relationship between voids ratios–log effective pressure–time, after Bjerrum (1967)

the same age will increase with the amount of secondary consolidation which the clay has undergone under the existing over burden pressure. Because secondary consolidation increases with the plasticity of the clay, the p_c'/p_0' ratio will increase with the plasticity index. Fig. 5.14 shows the correlation between p_c'/p_0' ratio and the plasticity index observed in some normally consolidated clays, which have all aged over a period of thousands of years.

It is of considerable importance to distinguish between pre-consolidation pressure owing to (a) over-consolidation as a result of removal of overburden pressure, or ground water level fluctuations or chemical and weathering effects, and (b) delayed consolidation. There is some evidence to indicate that for the first category, clays can be loaded up very close

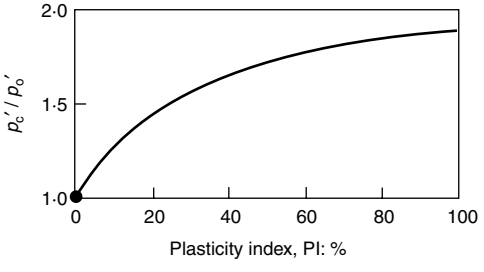

Fig. 5.14 Relationship between p_c'/p_0' and plasticity index, after Bjerrum (1967)

Table 5.3 Observed 20 year settlements for structures in Norway related to $\Delta p/(p'_c - p'_0)$ *and* $\Delta p/s_u$*, after Simons (1974)*

Structure	Settlement at 20 years (mm)	$\frac{\Delta p}{p'_c - p'_o}$	$\frac{\Delta p}{s_u}$
Skoger Sparebank	40	37%	0.6
Scheitliesgate 1	200	58%	0.9
Skistadbygget	c.230	72%	1.0
Konnerudgate 12	250	74%	1.6
Turnhallen. Light	360	68%	1.8
Konnerudgate 16	400	80%	1.8
Danvikgate 3	460	80%	1.8
Turnhallen. Heavy	600	123%	3.5

to the preconsolidation pressure with small resulting settlements (e.g. Vargas (1955)). If p'_c is due to delayed compression, however, then significant settlements, probably too large to be considered acceptable, develop when the applied pressure exceeds 50% of $p'_c - p'_0$ (Bjerrum, 1967), and as shown in Table 5.3.

It can be seen from Table 5.3 that settlements after 20 years amounting to about 200 mm may be expected for values of $\Delta p/(p'_c - p'_0)$ of 58% (Scheitliesgate 1), increasing to 400–460 mm (Konnerudgate 16 and Danvikgate 3) for $\Delta p/(p'_c - p'_0)$ about 80%.

A completely different picture emerges from the original studies carried out in Sweden by Nordin and Svensson (1974). At Margretelund, Lidköping, the measured settlement is less than 9 mm (and appears to be virtually complete) with a $\Delta p/(p'_c - p'_0)$ value of about 0.5, while at Lilla Torpa, Vänersborg, the observed settlements are up to 16 mm, with very little more expected, and here the net increase in stress due to the building loads and anticipated groundwater lowering, is nearly equal to $p'_c - p'_0$. At the present time, laboratory studies alone will not allow accurate settlement predictions to be made. Long term regional studies are vitally necessary to determine, in particular:

- Whether in the field, primary consolidation and/or secondary settlements will develop over a long period of time, and
- Whether a threshold level exists, below which acceptable settlements develop and above which large and potentially dangerous settlements will be experienced.

Regional studies of the type reported by Vargas (1955) for the Sao Paulo clay; Bjerrum (1967) for the Drammen clay; Jarrett, Stark and Green (1974) for the Grangemouth area; and Nordin and Svensson (1974) for Lidköping and Vänersborg, are therefore of considerable significance.

It should be stressed that, at the present time, it has been shown that very few clays exhibit a pre-consolidation pressure due to delayed consolidation (Brown, 1968).

Berre and Bjerrum (1973) have shown from a series of triaxial and simple shear laboratory tests that the development of a quasi pre-consolidation pressure may be associated with a critical shear stress; if the applied shear stress together with the initial shear stress is less than this value, then only relatively small deformations will be experienced. If the critical stress is exceeded, however, appreciable deformations will occur. This concept is confirmed by the behaviour of test embankments at Åsrum, Mastemyr and Sundland, in Norway.

Further confirmation is given by the settlement observations of various structures in Drammen and the relevant data are summarized in Table 5.3. It can be seen that there is a correlation between the 20 year observed settlement and the ratio of $\Delta p/s_u$ (Δp being the net applied foundation pressure on the surface of the clay layer, and s_u the undrained shear strength); the greater $\Delta p/s_u$, the greater the observed settlement.

Rate of settlement

The observed rate of settlement of structures is almost invariably very much faster than that calculated using one-dimensional consolidation theory based on oedometer tests carried out on small samples. Rowe (1968, 1972) showed that the drainage behaviour of a deposit of clay depends on the fabric of the soil. Thin layers or veins of sand and silt, or rootholes, can result in the overall permeability of the clay in situ being many times greater than that measured on small samples. An hydraulic oedometer (Rowe and Barden, 1966), was developed to enable more reliable measurements of c_v to be made. Sample diameters of up to 250 mm with heights of up to 125 mm can be accommodated, with either vertical or horizontal drainage. The loading is applied hydraulically, and pore water pressures, volume changes and axial deformations can be measured.

In situ permeability measurements, coupled with laboratory measurements of compressibility (which are not so sensitive to sample size) give values of c_v in fair agreement with field performance, and with the results from large samples tested in the hydraulic oedometer at similar stress levels. Reference can be made to the proceedings of the conference on 'In situ Investigations in Soils and Rocks', held in London (1970), and to the symposium on 'Field Instrumentation in Geotechnical Engineering' held in London (1973).

Recourse to theories of three-dimensional consolidation, coupled with reliable determinations of c_v taking account of orientation and stress level, is necessary if it is important to obtain reasonably accurate predictions of rates of settlement.

Table 5.4 Observed 20 year settlements greater than 200 mm, after Simons (1974)

Structure	δ_{20} (mm)	Reference
Skistadbygget, Drammen	c.230	Engesgaar (1972)
Konnerudgate 12, Drammen	250	Bjerrum (1967)
Masonic Temple, Chicago	250	Skempton, Peck & McDonald (1955)
Cold Stores, Grimsby	c.300	Cowley, Haggar and Larnach (1974)
Silo, Russi	c.300	Vefling (1974)
Konnerudgate 16, Drammen	400	Bjerrum (1967)
Monadnock Block, Chicago	450	Skempton, Peck & MacDonald (1955)
Danvikgate 3, Drammen	460	Bjerrum (1967)
Skabo Office Block, Oslo	460	Simons (1957)
Jernbanetollsted, Drammen	500	Andersen & Frimann Clausen (1974)
Auditorium Tower, Chicago	540	Skempton, Peck & MacDonald (1955)
Turnhallen, Drammen	600	Simons (1957)
Tower City Hall, Drammen	670	Bjerrum (1967)
Apartment Building, Oslo	c.700	Hutchinson (1963)
Residential Building, Nantua	c.1200	Sanglerat, Girousse & Gielly (1974)

Note: δ_{20} = observed or extrapolated maximum settlement at 20 years.

In situ permeability tests have to be conducted at relatively low stress levels and therefore at least a few laboratory consolidation tests on large samples should be carried out to investigate the influence of stress level on c_v. The field rate of consolidation is of particular importance when the design of road, rail or runway embankments on soft clay is being considered.

Secondary settlement

Secondary settlement is generally considered to be the settlement which develops following changes in effective stress. After many years of research work into secondary consolidation, no reliable method is yet available for calculating the magnitude and rate of such settlement, for which the necessary soil parameters can be obtained fairly simply, and which also takes into account the various factors, for example the principal effective stress ratio, the load increment ratio, temperature, and time effects, which are known to affect secondary settlement significantly. For this reason, if estimates of secondary consolidation are required in practice, they are generally based on empirical procedures.

Contrary to the view which has sometimes been expressed that secondary settlement is often of little practical consequence so far as structures are concerned, several case records are available which show clearly that in certain circumstances a large part of the observed settlement has occurred after full dissipation of excess pore-water pressure, for example, Foss (1969). Satisfactory prediction of secondary settlement is therefore certainly a matter of practical importance.

When considering secondary settlement it should be noted that two different factors may influence this process. The first is reduction in volume at constant effective stress and the second is vertical strain resulting from lateral movements in the ground beneath the structure. Terzaghi (1948) pointed out that these two factors may be expected to result in completely different types of settlement. The relative importance of these factors will vary from structure to structure, depending on the stress level, type of clay, and the geometry of the problem, and for any given structure will vary with the location of any deforming soil element, and with time.

No great accuracy can therefore be expected from predictions of secondary settlement and caution should be exercised when attempting to extrapolate the results from one particular investigation to another set of conditions.

Investigations into secondary settlement can be considered to fall into three categories:

- Laboratory work
- Empirical approaches based on field and laboratory results
- Theoretical analyses based on rheological models.

Laboratory work

Many workers have carried out various types of laboratory test to investigate various aspects of secondary consolidation behaviour. Important points to emerge are that:

- organic soils show pronounced secondary effects,
- many soils exhibit a linear relationship between settlement and log time for a considerable period, although this relationship cannot hold indefinitely,
- isotropic consolidation results in less secondary effect than consolidation with no lateral yield,
- secondary settlement is more pronounced at stresses below the preconsolidation pressure, for small load increment ratios, with increasing temperature, with decrease in the length of the drainage path, and for small factors of safety,
- instability may occur, that is, the rate of settlement may increase temporarily after a long period of time.

Empirical approaches

Generally, these approaches are based on the assumption that secondary settlements can be approximated by a straight line on a settlement versus logarithm of time plot (Buisman, 1936; Koppejan, 1948; Zeevaert, 1957, 1958). While there is much evidence to indicate that such a simple extrapolation cannot in general be expected to give reliable predictions

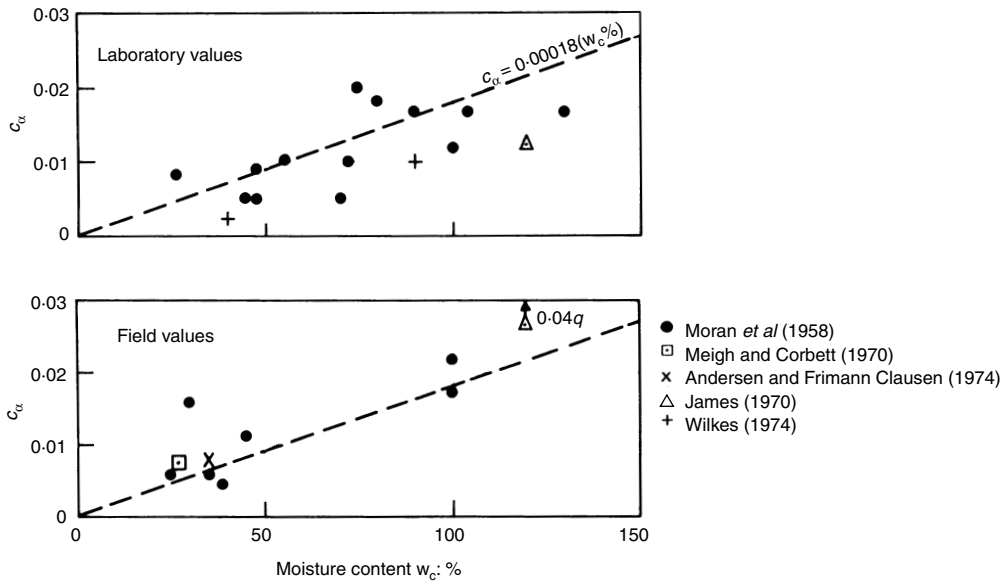

Fig. 5.15 Values of c_α, the coefficient of secondary consolidation plotted against moisture content, after Simons (1974)

in field problems, this approach is often adopted in practice and, it must be admitted, there is as yet no theoretical solution available which takes into account all the factors which are known to affect secondary compression and in which the relevant soil parameters can be fairly easily obtained.

Use has been made of c_α, the coefficient of secondary consolidation, defined as the secondary settlement per unit height per log cycle of time. Values of c_α are shown in Fig. 5.15.

Bjerrum (1967) presented his model to represent instant and delayed compression on a plot of void ratio versus the logarithm effective vertical pressure, Fig. 5.13, and Foss (1969) applied this approach to predicting the secondary settlements of four structures in Drammen. It must be noted, however, that the predictions are based on the assumptions that:

- the relative positions of the lines representing field void ratios at different loading times from 24 hours to 3000 years are available,
- if $\Delta p < p'_c - p'_0$, no primary consolidation settlement will occur, and, the clay under a structure will follow these relationships.

While Foss found good agreement between calculated and observed rates of secondary settlement, further comprehensive laboratory data for other clays are an urgent requirement. The data should be similar to those available for Drammen, and supported by settlement records of structures on these clays.

Theoretical approaches

A helpful summary of various theoretical approaches has been made by Clayton (1973). Possibly the most useful contribution of these approaches has been to study the effects of variables in order to suggest – qualitatively – differences between laboratory testing and field performance of clays. Garlanger's mathematical model (Garlanger, 1972) combined with finite difference techniques appears at the present time, to be the most powerful tool available in the prediction of the time-settlement behaviour of loaded soil in the field. This model takes into account the effects of drainage path length on the stress–strain behaviour of clays, and it can be adapted to reflect the effects of the variation of pressure increment that occurs beneath structures on deep deposits.

Long-term settlement records

Although secondary settlements are of significance for many structures, there are also a number of cases where settlement records show small or negligible secondary effects. Three such illustrative examples are, the apartment building at Økernbråten, Oslo (Simons, 1963), the trial embankment at Avonmouth (Murray, 1971), and the multi-storey buildings in Glasgow (Somerville and Shelton, 1972). Typical settlement–log time curves are shown in Fig. 5.16.

At Økernbråten, a nine-storey block of flats founded on strip foundations transmitting 226 kPa to the underlying firm to stiff, becoming soft with depth, clays, at least 20 m thick, experienced a maximum settlement of 18 mm and the settlements stopped completely about 3.5 years after the end of construction.

At Avonmouth, the square embankment with a maximum height of 9.2 m, a width at the base of 67 m and side slopes of 1 in 2, constructed of pulverized fuel ash of average bulk unit weight 13.4 kN/m^3 on highly compressible alluvial soils containing peat, about 13 m in thickness with undrained shear strengths ranging generally from about 40 kPa to about 90 kPa, experienced a maximum settlement of about 780 mm some 1000 days after the start of construction of the embankment, 90% of primary consolidation occurring 300 days after the start of construction. The rate of movement is now quite small and appears to be reducing with time.

At Glasgow, six blocks of fifteen storey flats were constructed in the Parkhead and Bridgeton districts, which are underlain by deep alluvial deposits of firm laminated clays and silts with deeper deposits of sands, gravels and glacial drifts, followed by productive coal measures. Raft foundations were adopted, with net bearing pressures of about 53.5 kPa. The time–settlement curves show very slow rates of settlement only 1 to 2 years after the end of construction, with maximum settlements ranging from 30 to 60 mm.

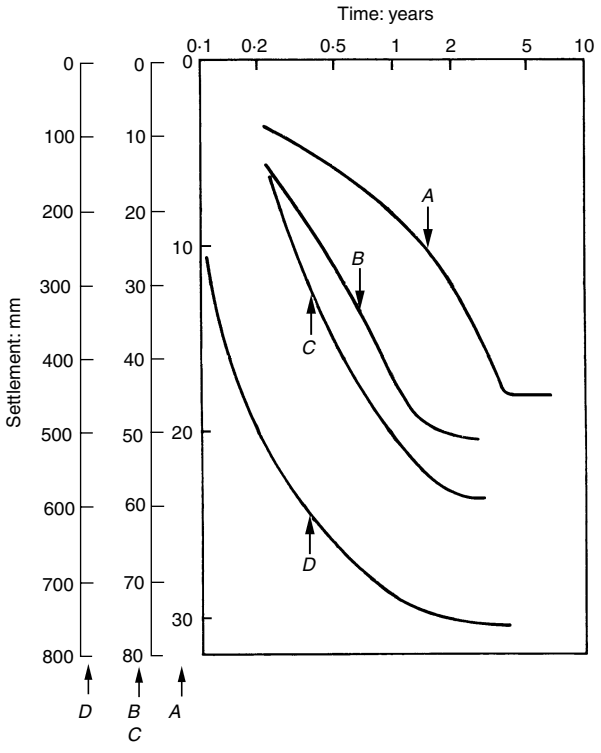

Fig. 5.16 Settlement–log time curves indicating terminating settlement, after Simons (1974).
CASE A. Økernbråten, Oslo, Simons (1963)
CASE B. Point 9, Block C, Bridgeton, Somerville and Shelton (1972)
CASE C. Point 19, Block C, Parkhead, Somerville and Shelton (1972)
CASE D. Avonmouth, Murray (1971)

Clearly, there is a need to be able to distinguish between cases where settlement continues over many years, as illustrated in Fig. 5.17 for Norwegian and Swedish clays, and cases where the rate of settlement virtually stops a few years after the end of construction, as shown in Fig. 5.16.

The complexity of the problem is shown in Fig. 5.18, which gives the settlement–log time plots for the three well-known Chicago structures, namely, the Masonic Temple, the Monadnock Block, and the Auditorium Tower (Skempton, Peck and MacDonald, 1955). The behaviour of the Masonic Temple is quite different from that of the other two, with more than 90% of the total final settlement developed after five years. The corresponding figures for the Monadnock Block and the Auditorium Tower are 47 and 62%. Furthermore, after 10 years the settlement of the Masonic Temple was virtually complete, but for the other two structures, settlements were still taking place after 30 years.

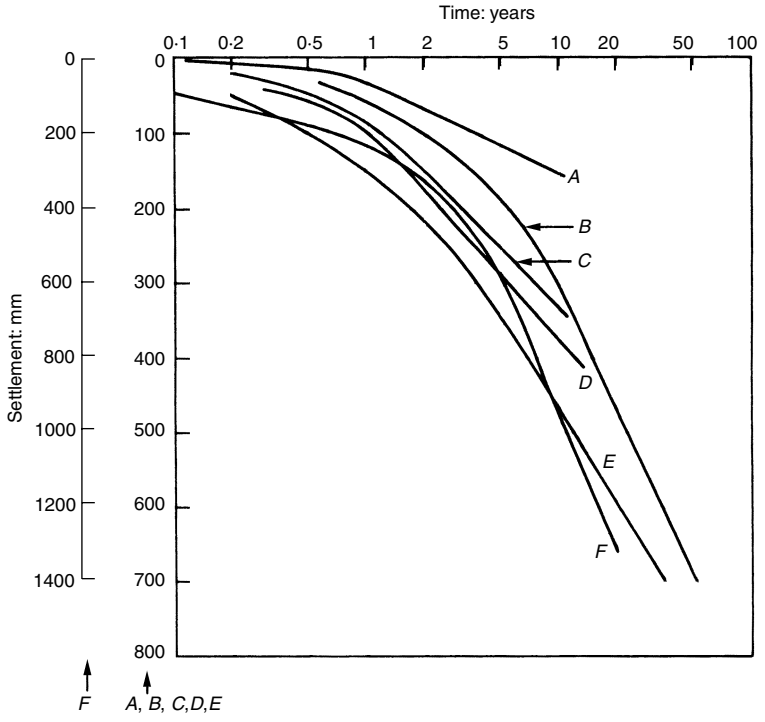

Fig. 5.17 Settlement–log time curves indication non-termination settlement, after Simons (1974)
CASE A. Scheitliesgate 1, Drammen, Bjerrum (1967)
CASE B. Jernbanetollsted, Oslo, Anderson and Frimann Clausen (1974)
CASE C. Konnerudgate 16, Drammen, Bjerrum (1967)
CASE D. Skabo office block, Oslo, Simons (1957)
CASE E. Turnhallen, Drammen, Simons (1957)
CASE F. Test fill. Vasby, Sweden, Chang, Broms and Peck (1973)

Investigations into the geochemistry of the soils, work on micropaleontology, or electron microscope analysis, might be necessary, as well as the determination of engineering properties, in order to classify clays with regard to their long term settlement behaviour.

Settlement observations taken on structures and embankments should be continued over a sufficient period of time for the long term trends to be indicated. To halt observations at a time when excess pore water pressures have just dissipated, for example, may well result in an incomplete picture emerging of the true settlement–time performance.

A final point to be noted is that structures subjected to large variations in live load, for example, silos, storage tanks and high structures under wind action, may be expected to experience appreciably larger secondary

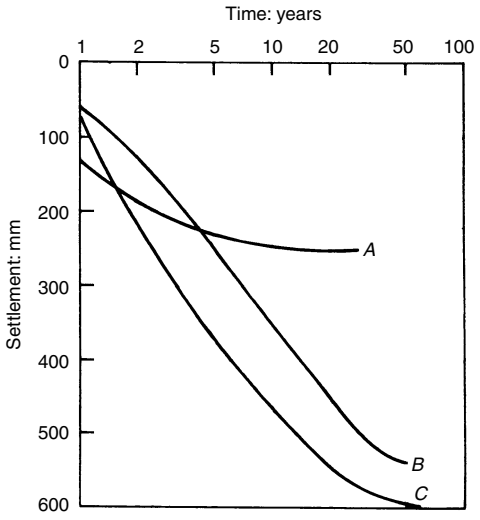

Fig. 5.18 Settlement–log time curves for three structures in Chicago, after Skempton, Peck and MacDonald (1955)
CASE A. Masonic temple
CASE B. Monadnock block
CASE C. Auditorium Tower

settlements than would be the case for non-varying loading conditions (Bjerrum, 1964, 1968).

Other methods of predicting settlement

Some other approaches which have been suggested for predicting the deformations of structures are outlined below.

Centrifugal models

Recent developments in testing centrifugal models demonstrate that this method of predicting ground displacements is a practical tool. The results obtained by Wroth and Simpson (1972) in predicting the deformations of the trial embankment at King's Lynn (Wilkes, 1974) are particularly encouraging. Reference may be made to Craig *et al.* (1988), Croce *et al.* (1988), Taylor (1995) and Okamura *et al.* (1998).

Janbu's deformation modulus

Settlement calculations are usually based on the parameters C_c or m_v. Janbu (1963, 1969) proposed basing computations on the tangent modulus, being equal to $d\sigma/d\varepsilon$, as a suitable measure of the compressibility of soils, ranging from sound rock to plastic clays. The tangent modulus depends on stress conditions and stress history and can be considered to represent a resistance against deformation. The calculation procedure

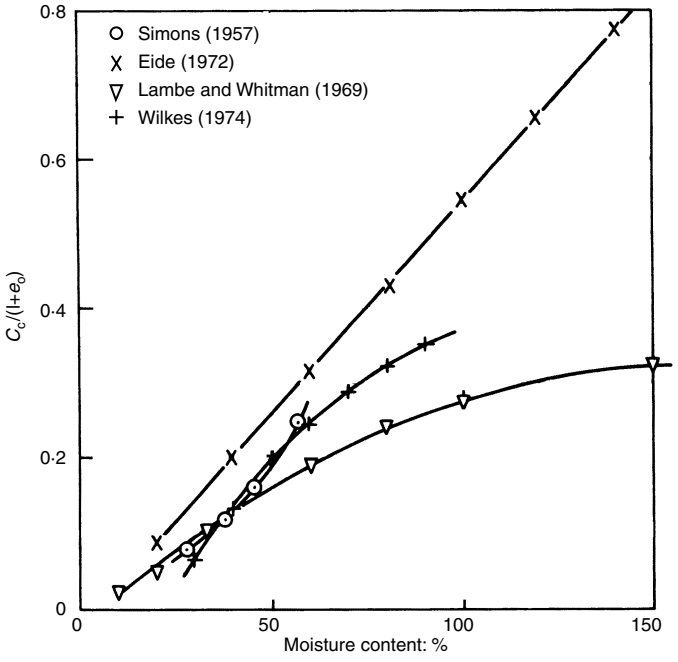

Fig. 5.19 Relationship between $C_c/(1+e_o)$ and natural moisture content, after Simons (1974)

based on the tangent modulus concept is very simple, and virgin loading, unloading and reloading conditions can be taken into account.

Dutch cone sounding apparatus

As an approximate method to estimate settlement, the use of the static cone sounding apparatus has been proposed (Gielly, Lareal and Sanglerat, 1970; Sanglerat, 1972) based on correlations between compressibility and the cone resistance. No accurate settlement forecast can be expected for reasons which have been discussed, but it appears that the cone resistance can give a useful first approximation of compressibility (Meigh and Corbett, 1970).

Correlation of compression index with moisture content

Another first approximation to compressibility for normally consolidated clays is based on correlations between $C_c/(1+e_o)$ and the moisture content. Various such correlations have been plotted on Fig. 5.19 and a fairly narrow band results only for moisture contents less than about 70%.

Elastic method

Butler (1974) describes the use of the so-called elastic method to predict the consolidation settlement of structures founded on the heavily

over-consolidated London clay. By assuming that $E' = 130s_u$, and taking Poisson's ratio = 0.1, reasonably good agreement between calculated and observed settlements was obtained. Use of this method, however, for general application to any clay requires a knowledge not only of Poisson's ratio, ν, and the elastic modulus E_v in the vertical direction, but also the elastic modulus, E_h, in the horizontal direction. This latter value is known to affect very significantly the value of the vertical displacement. For example, Simons, Rodrigues and Hornsby (1974) found that for $E_h = 1.8E_v$ (a typical value for London clay) the calculated settlements amounted to about 60% of those calculated for $E_h = E_v$. Use of the elastic method must therefore be restricted to those cases where reliable knowledge of E_h, E_v and ν is available and where comparisons between predicted and observed settlements can be made.

The prediction of settlements on granular deposits

Introduction

For granular soils, it has been indicated in Chapter 4, that, apart from very narrow, shallow footings on loose materials with a high water table, the allowable pressure which may be applied to a foundation will be governed by considerations of settlement, rather than of the shear strength of the soil. For this reason, accurate prediction of the settlement of structures founded on granular materials is of considerable practical importance.

Because of the high permeability of granular materials, most of the settlement will develop during application of the foundation loading. After the end of construction, therefore, only minor settlements due to creep are likely to occur, unless very large foundations are concerned or the granular soil is silty, or the foundation is subjected to fluctuating loads, for example, wind, machinery vibrations, and the filling and emptying of silos and oil tanks.

It is known from studies of case records of structures founded on granular soils that the differential settlement between adjacent footings can on occasions approach the total settlement (Skempton and MacDonald, 1956; Bjerrum, 1963; Terzaghi and Peck, 1967), partly because granular soils tend to be less homogeneous than clays. On average, however, the differential settlements are about $\frac{2}{3}$ the maximum settlement, whereas for clays the corresponding figure is about $\frac{1}{3}$. Thus for clays, for a given maximum settlement, a relatively smaller differential settlement will generally be experienced.

It is expensive and difficult, and in many cases impossible, to obtain undisturbed samples of granular soils. Even recompacting granular soil back to exactly the same relative density as in the field will not guarantee that stress–strain relationships obtained in the laboratory will be equal to

those pertaining in the field because the effects of over-consolidation, if any, lateral stresses in the field, and the structural arrangement of the grains will not be properly reproduced. Therefore, the methods generally used to predict settlements are based on field tests, namely, the plate loading test, the standard penetration test and the Dutch cone test. Very occasionally, laboratory tests have been used, for example, oedometer tests and stress path triaxial tests (D'Appolonia *et al.*, 1968).

Plate loading tests

For plate loading tests to be applicable at all, they must be carried out on soil which is representative of the soil to be stressed by the prototype foundation. Thus, plate tests should ideally be carried out at different depths and at different locations and the position of the groundwater table will have to be taken into consideration. Care must be taken to avoid disturbing the soil immediately below the plate, and to reduce bedding errors to a minimum.

Local minor variations in density will greatly affect the results of plate tests, but will have lesser influence on the settlement of the full size foundation. A sufficient number of tests should be carried out in order to obtain a reliable average value. Preferably, plates of different size should be used, so that a better extrapolation up to full size can be made.

An interesting development of the plate loading test is the screw plate, which can be rotated into the ground, a loading test carried out, and rotated further to a greater depth for another loading test. In this way, no excavation is required and tests can be carried out without difficulty below the water table (Kummeneje, 1955).

It is then necessary to extrapolate from the results of the plate loading tests to the settlement of the prototype foundation.

Terzaghi and Peck (1948) proposed the following relationship between the settlement of a footing of width B m and the settlement, δ_b, of a 0.3 m square test plate, loaded to the same loading intensity.

$$\frac{\delta_B}{\delta_b} = \left(\frac{2B}{B+0.3}\right)^2 \tag{5.16}$$

It should be noted that for large B, the ratio tends to a maximum value of four. The relationship is plotted in dimensionless form in Fig. 5.20.

Bjerrum and Eggestad (1963), from a study of case records, indicated that there can be an appreciable scatter in the correlation between settlement and the dimension of the loaded area, and, more important, that settlement ratios very much larger than four could occur. They suggested that the correlation was also dependent on density, and made the proposals shown in Fig. 5.20. It has been suggested that the correlation is also influenced by the grading of the sand (Meigh, 1963); coarse,

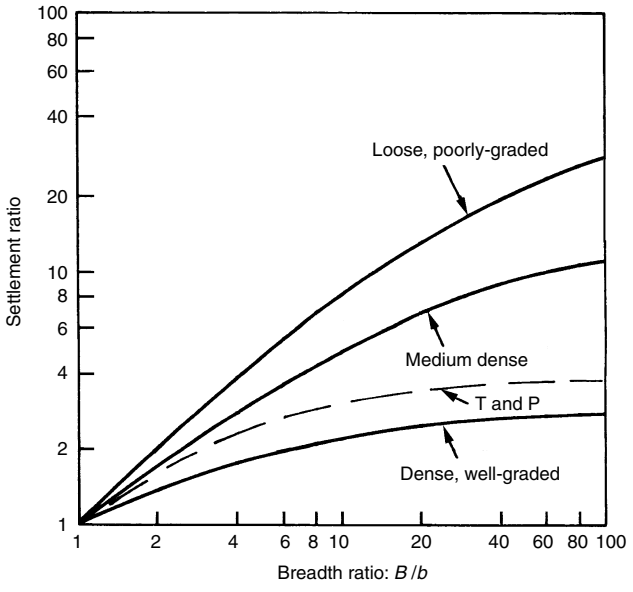

Fig. 5.20. Relationship between settlement ratio and foundation to plate size ratio, after Terzaghi and Peck (1948) and Bjerrum and Eggestad (1963)

well-graded soils have low settlement ratios, and fine uniformly graded soils, have high settlement ratios.

D'Appolonia *et al.* (1968) found settlement ratios greater than 10 for dense fine uniformly graded sands.

Dutch cone test

In this test, a 60° degree cone with a cross-sectional area of 10 cm^2 is forced into the ground at a reasonably constant rate of strain, and provision is made to measure independently the point resistance, and the resistance due to side friction. The test was first devised to assess the bearing capacity of piles, but is now used to predict the settlement of structures on sands. Originally, prediction procedures were developed by de Beer and his co-workers, but more recently Schmertmann has proposed a different approach. A practical problem associated with the test is that on occasions it is difficult to penetrate overlying harder layers.

If C_r is the static cone point resistance and p'_0 the effective overburden pressure at the depth the test is carried out, then de Beer and Martens (1957) proposed that the compressibility coefficient, C, is given by

$$C = \frac{1.5C_r}{p'_0} \tag{5.17}$$

The settlement is then given by

$$\delta = \frac{H}{C}\log_e \frac{p'_0 + \Delta p}{p'_0} \tag{5.18}$$

where Δp is the increase in stress due to the net foundation pressure at the centre of the layer of thickness H under consideration.

It has been found that this procedure generally overestimates the observed settlement. For example, de Beer (1965) found by comparing calculated and observed settlements for about 50 bridges that, on average, the calculated settlements were about twice as high as those observed. Because of this overestimate, the less conservative relationship of

$$C = \frac{1.9C_r}{p'_0} \tag{5.19}$$

suggested by Meyerhof (1965) has been more widely used. These methods strictly only apply to normally loaded sands; if a sand has been pre-loaded, subsequent settlements will be small, but it is, of course, difficult to determine the degree of over-consolidation of a granular deposit.

Schmertmann (1970 and 1978) proposed a different approach to the use of cone penetration tests in the calculation of the settlement of footings on sands. He made the point that the distribution of vertical strain under the centre of a footing on a uniform sand is not qualitatively similar to the distribution of the increase in vertical stress, the greatest strain occurring at a depth of about $B/2$.

Schmertmann gives the following equation for calculating settlement:

$$\delta = C_1 C_2 \Delta p \sum_0^{2B} \left(\frac{I_z}{E}\right) \Delta z \tag{5.20}$$

where, $\Delta p =$ increase in effective overburden pressure at foundation level; $\Delta z =$ thickness of layer under consideration; $C_1 =$ depth embedment factor; $I_z =$ strain influence factor given in Fig. 5.21.

$$C_1 = 1 - 0.5\left(\frac{p'_0}{\Delta p}\right) \tag{5.21}$$

where $p'_0 =$ initial effective pressure at foundation level and an empirical creep factor based on work by Nonweiller (1963) is

$$C_2 = 1 + 0.2\log_{10}\left(\frac{t}{0.1}\right) \tag{5.22}$$

where t is the period in years for which the settlement is to be calculated.

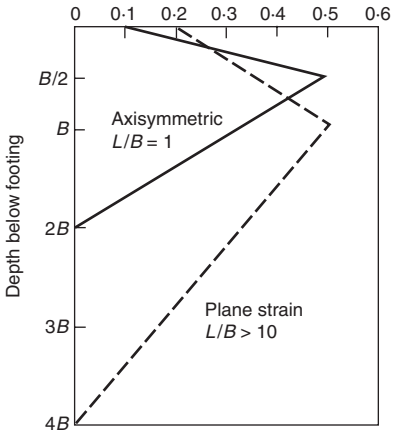

Fig. 5.21 Variation of strain influence factor with depth, after Schmertmann et al. (1978)

For plane strain, the deformation modulus is related to cone penetration resistance by

$$E = 2C_r \tag{5.23}$$

Schmertmann claims that not only is his method simple to apply but also that its use leads to more accurate estimates of settlement than the de Beer procedure. On average for 16 sites where a comparison has been made, settlements calculated using de Beer's method were about 50% greater than those obtained by the Schmertmann method.

Schmertmann (1975) modified his method to include non-plane strain cases.

Hence for $L/B = 1$, I_z is given by

$$I_z = 0.1 + 0.8z/B \text{ for } z < B/2$$

$$I_z = (2 - z/B)/3 \text{ for } z > B/2$$

For $L/B > 10$, I_z is given by

$$I_z = 0.2 + 0.6z/B \text{ for } z < B/2$$

$$I_z = (4 - z/B)/7 \text{ for } z > B/2$$

The procedure is to superimpose the profile of cone resistance C_r on top of the strain influence diagram, divide the soil below foundation level into a series of layers or strips, and calculate the vertical strain of each strip. The relationship between E and C_r is assumed to be $E = 2.5C_r$ (square footing) and $E = 3.5C_r$ (rectangular footing).

The method is best illustrated by a worked example.

WORKED EXAMPLE

Calculate the settlement for the loading condition illustrated in Fig. 5.22. The calculations are given below.

Net increase in pressure at foundation level (Δp) is:

$182 - 2 \times 16 = 150\,\text{kPa}$

Layer	Δz (mm)	C_r (kPa)	$E\ (= 2C_r)$	I_z	$I_z.\Delta z/E$
A	1000	2500	5000	0.20	0.0400
B	300	3500	7000	0.43	0.0184
C	1700	3500	7000	0.38	0.0923
D	500	7000	14000	0.25	0.0089
E	1000	3000	6000	0.15	0.0250
F	700	8500	17000	0.05	0.0021
					Sum = 0.1867

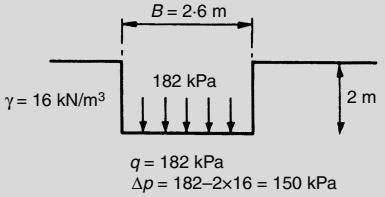

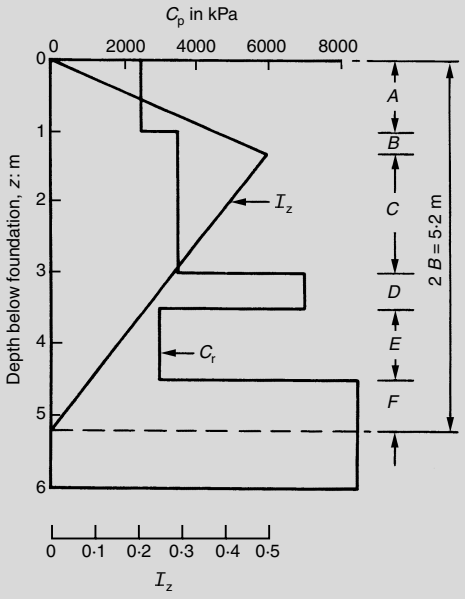

Fig. 5.22 Example of settlement calculation following Schmertmann (1970)

$$C_1 = 1 - 0.5\left(\frac{p_0'}{\Delta p}\right), \text{ from equation 5.21}$$

$$= 1 - 0.5\left(\frac{32}{150}\right) = 0.89$$

Taking a 5-year creep period,

$$C_2 = 1 + 0.2\log_{10}\left(\frac{t}{0.1}\right), \text{ from equation 5.21}$$

$$= 1 + 0.2\log_{10} 50 = 1.34$$

$$\delta = C_1 C_2 \Delta p \sum \frac{I_z \Delta z}{E}, \text{ from equation 5.20}$$

$$= 0.89 \times 1.34 \times 150 \times 0.1867$$

$$= 33.4\,\text{mm}$$

Correlation between standard penetration test (SPT) and Dutch cone tests

On occasions, it can be useful to estimate the equivalent SPT 'N' value from the results of Dutch cone point resistance, and vice versa.

Meyerhof (1956) attempted to correlate the results of the two tests and suggested the following relationship:

$$C_r = 4N \tag{5.24}$$

where, C_r = static cone point resistance in ton/ft^2 or kg/cm^2.

Further work (Meigh and Nixon, 1961; Rodin, 1961; Sutherland, 1963) showed that this simple relationship was not in general sufficiently accurate for all granular soils and that the correlation depended on grain size as shown in Table 5.5; in this case the units of C_r are in kPa.

Table 5.5 Ratio of cone point resistance to SPT N value, after Meigh and Nixon (1961)

Soil description	C_r/N
Sandy silt	250
Fine sand and silty fine sand	400
Fine to medium sand	480
Sand with some gravel	800
Medium and coarse sand	800
Fine to medium sand	1000
Gravelly sand	800–1800
Sandy gravel	1200–1600

Standard penetration test

The standard penetration test (SPT) is an empirical dynamic penetration test, developed in the USA in the 1920s, and was usually carried out in 50 to 100 mm diameter wash borings. In the UK it is almost always performed in shell borings of diameter 150 to 200 mm. This procedure increases the risk of disturbance of the soil immediately below the borehole due to suction as the shell is withdrawn. To minimize this effect, it is considered good practice to require that the outside shell diameter shall not be more than 90% of the internal diameter of the casing and that it should be withdrawn slowly from the hole.

The test consists of driving into the ground a standard split spoon sampler by a 63.6 kg weight failing 762 mm. The spoon sampler has a 50 mm outside diameter, a 35 mm inside diameter and a length of 0.8 m. After proper cleaning of the hole, the penetrometer on the end of the boring rods is lowered to the bottom of the hole and driven an initial 150 mm and the blow count recorded.

The penetrometer is then driven a further 300 mm and the blow count for this latter drive is called the SPT N value. It is considered good practice to record the blow count for each of six 75 mm increments, as this allows a better assessment of the depth of any disturbance. In very dense materials, the blow count necessary to achieve full penetration may be excessive and tests are often terminated after reaching a blow count of 50 and the penetration achieved is recorded.

Tests are generally carried out at depth intervals of 1.5 m. In gravel, a special solid 60° cone is used to avoid damage to the spoon, and work by Palmer and Stuart (1957) and Rodin (1961) showed that the solid cone tended to give slightly higher results.

If the soil consists of very fine or silty sand below the water table, a correction is made when the measured N is greater than 15, because excess pore water pressures set up during driving cannot dissipate. The results are affected as follows:

$$N_{\text{corrected}} = 15 + 0.5(N_{\text{measured}} - 15) \tag{5.25}$$

A granular deposit can be classified as shown in Table 5.6.

An approximate correlation between the N value and the angle of shearing resistance has been proposed by Peck, Hanson and Thornburn (1974) and is shown in Fig. 5.23.

Terzaghi and Peck (1948) were the first to propose a correlation between the N value and allowed pressure by presenting a relationship between the size of a footing, the N value, and the applied pressure to give a settlement of 25 mm for a deep groundwater table (depth greater than $2B$ below the underside of a footing of width B). This correlation is shown in Fig. 5.24. If the groundwater table is at foundation level, the

Table 5.6 Correlation of SPT N value with relative density for granular soils after Terzaghi and Peck (1948)

SPT *N* value	Relative density
0–4	Very loose
4–10	Loose
10–30	Medium dense
30–50	Dense
50	Very dense

allowable pressure should be halved. A further correction factor, C_D, for the depth of embedment of the footing was also introduced. C_D varies from 1 to 0.75 as the level of the base of the footing varies between ground level and a depth B below ground level, thus the deeper the footing the less the settlement.

This standard Terzaghi and Peck procedure is generally recognized as being conservative and as experience was gained, various different

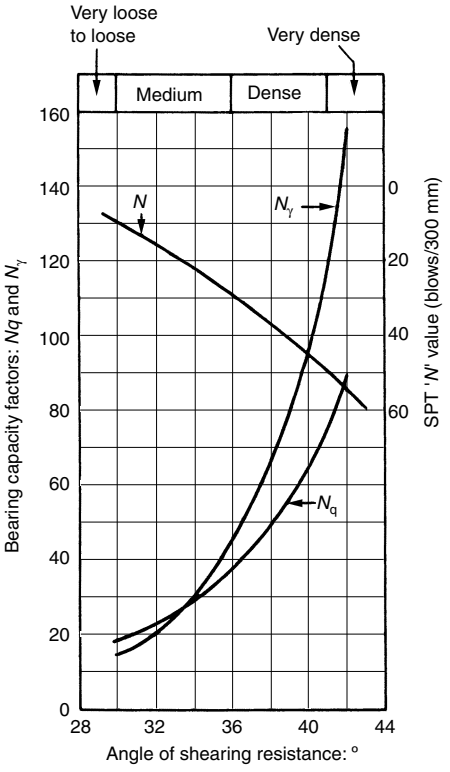

Fig. 5.23 Relationship between SPT 'N' value and ϕ', N_q and N_γ, after Peck, Hanson and Thorburn (1974)

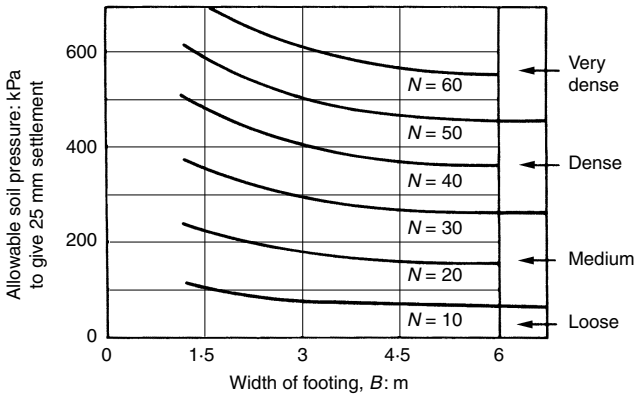

Fig. 5.24 Correlation of allowable bearing pressure to give 25 mm settlement to SPT 'N' value, after Terzaghi and Peck (1948)

procedures have been proposed to predict the settlements of structures founded on granular materials, based on N values. Some of these procedures are outlined below.

Following Meyerhof (1965), settlements can be calculated using the following relationships:

$$\delta = \frac{1.9q}{N} \text{ for } B < 1.25\,\text{m}$$

$$\delta = \frac{2.84q}{N}\left(\frac{B}{B+0.33}\right)^2 \text{ for } B > 1.25\,\text{m}$$

$$\delta = \frac{2.84q}{N} \text{ for larger rafts}$$

where q = applied foundation pressure.

N is averaged over a depth equal to the width of the footing. These equations correspond roughly to the standard Terzaghi–Peck settlement chart, given in Fig. 5.24.

Meyerhof (1965) also suggested that no allowance need be made for the groundwater table, as its presence should be reflected by the SPT results, and, in addition, that the allowed pressures can be increased by 50%. Meyerhof's proposals have been confirmed by the work of D'Appolonia *et al.* (1968).

The penetration resistance reflects both the in situ relative density and the effective stress at the depth at which the test is carried out, and therefore an infinite number of combinations of stress level and relative density will result in the same measured N value, and relationships have been developed to correct the measured blow count for the in situ vertical effective stress. A simple correction chart has been proposed by Tomlinson (1969) based on the work by Gibbs and Holtz (1957) and is reproduced

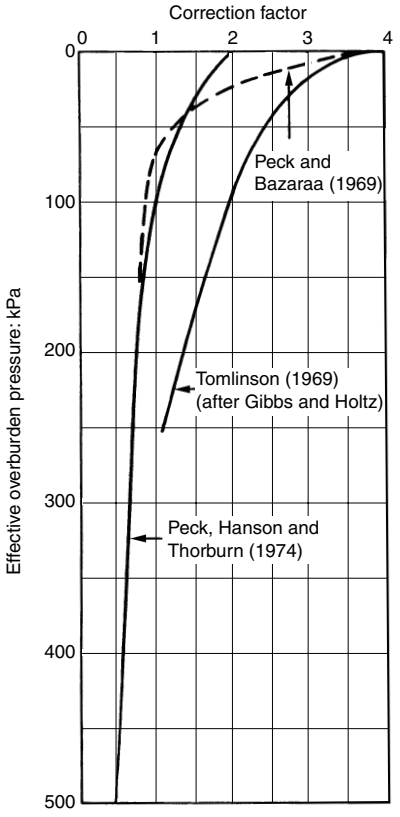

Fig. 5.25 Correction factor for influence of effective overburden pressure on SPT 'N' value, after Tomlinson (1969), Peck and Bazaraa (1969) and Peck, Hanson and Thorburn (1974)

in Fig. 5.25. The differences between the corrected and measured blow counts are most marked for tests carried out at shallow depths. Tomlinson's chart indicates that the measured N should be increased up to four times for very shallow depths, but a correction of this magnitude should be applied with caution.

Peck and Bazaraa (1969) recognized that the original Terzaghi and Peck proposals were too conservative, and proposed three modifications. First, the allowable soil pressures indicated in Fig. 5.24 should be increased by 50% as proposed by Meyerhof (1965). Second, they agreed that the measured N values should be corrected for overburden pressure, but considered that the application of the Gibbs and Holtz values lead to overcorrection, and, therefore proposed the curve marked Peck and Bazaraa in Fig. 5.25. This leads to smaller correction factors than do Tomlinson's proposals. Third, they proposed a slightly different correction for the groundwater position. They recommended that when the water table is at a

distance D_w below the base of a shallow footing of width B, then the settlement δ' may be estimated from $\delta' = K\delta$ where δ is the settlement of the same footing when the sand is dry. K is the ratio of the effective overburden pressure at a depth $0.5B$ below the base of the footing when the sand is dry to that at the same depth when the water table is present.

A further approach to the calculation of the settlements of footings on granular soils, again based on the work of Bazaraa (1967) is outlined by Peck, Hanson and Thornburn (1974). The influence of the effective overburden pressure on the measured N value is taken into account using the curve marked Peck, Hanson and Thornburn in Fig. 5.25. A correction for the water table position is given as:

$$C_w = 0.5 + 0.5\left(\frac{D_w}{D_f + B}\right) \tag{5.26}$$

where D_f is the depth of the footing and D_w the depth of the groundwater table, both measured from the ground surface. A maximum value for C_w of unity should be taken for D_w greater than $(D_f + B)$. These values are then used in a new chart relating N values, breadth of footings and allowable bearing pressure to give 25 mm settlement, shown in Fig. 5.26.

Parry (1971) proposed a simple empirical method for calculating settlement assuming that settlement is a function of the width of the loaded area, the magnitude of the bearing pressure and the deformation modulus of the soil. The equation to be used is:

$$\delta = \frac{aqB}{N} C_D C_w C_T \tag{5.27}$$

where δ = settlement in mm; a = constant = 200 in SI units; q = applied pressure in MPa; B = foundation width in m; N = measured average N value; C_D = factor for the influence of excavation; C_w = factor for the influence of the water table; C_T = factor for the thickness of the compressible layer.

N is taken as the measured value at a depth equal to $3B/2$ below foundation level if the N values vary consistently with depth. If otherwise, then:

Take the average value of N between foundation level and a depth of $3B/4$ and multiply by three giving $3N_1$.

Take the average value of N between depths $3B/4$ and $3B/2$ and multiply by two giving $2N_2$.

Take the average value of N between $3B/2$ and $2B$ giving N_3.

Then,

$$N = \frac{3N_1 + 2N_2 + N_3}{6} \tag{5.28}$$

C_D takes into account the fact that excavation for the foundation alters the stress system in the ground and hence the N values measured before

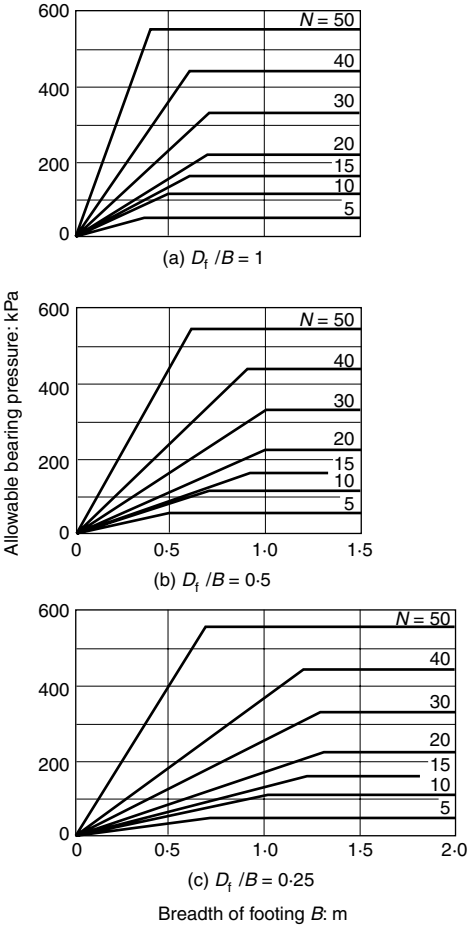

Fig. 5.26 Correlation of allowable bearing pressure to give 25 mm settlement to SPT 'N' value, after Peck, Hanson and Thorburn (1974)

excavation require modification. C_D is obtained from Fig. 5.27. C_D is unity if the foundation is placed on a completely backfilled excavation.

C_w corrects for the influence of the water table. Assuming that the water table has an influence only within a depth of $2B$ below foundation level, and taking D as the depth of the excavation and D_w the depth of the water table below ground surface.

$$C_w = 1 + \frac{D_w}{D + 3B/4} \text{ for } 0 < D_w < D \tag{5.29}$$

or

$$C_w = 1 + \frac{D_w(2B + D - D_w)}{2B(D + 0.75B)} \text{ for } D < D_w < 2B \tag{5.30}$$

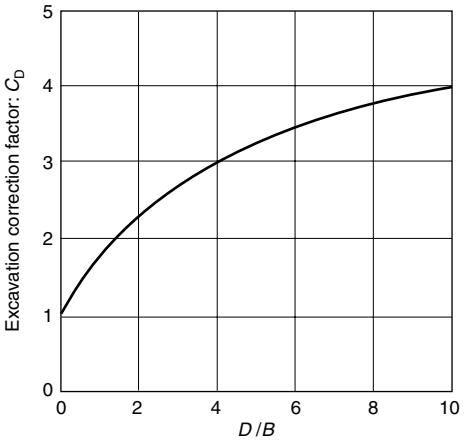

Fig 5.27 Excavation correction factor, C_D, after Parry (1971)

No correction is applied for surface footings or footings in backfilled excavations if the water table does not rise after the site excavation and during the life of the structure. If it is expected to rise, the measured N values should be reduced in direct proportion to the change in effective overburden pressure in the field.

The thickness, T, of the compressible sand stratum below the foundation is taken into account using the factor C_T, given in Fig. 5.28. When deriving the curve for C_T, it was assumed that in a uniform soil, half the settlement occurs within a depth $3B/4$ below foundation level and the remaining half within a depth range $3B/4$ to $2B$ below foundation level.

Burland and Burbidge (1985) base their method on a statistical analysis of over 200 case records of foundation settlement. An important feature of the method is the assessment of a zone of influence which extends to a depth of z_I beneath foundation level. Soil properties in this zone have the biggest influence on foundation settlement. The zone of influence appears to be a function of foundation width B alone, and is determined from a graph.

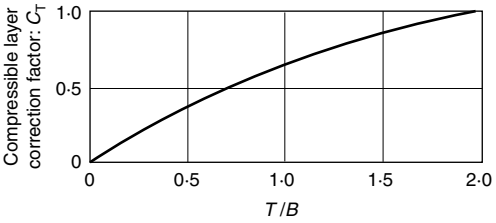

Fig. 5.28 Correction factor for thickness of compressible material, after Parry (1971)

They define an influence coefficient:

$$I_c = 1.71/N^{1.4}$$

where N is the average SPT value in the zone of influence.

Note:

- the method does not correct N for position of water table,
- if the soil is either very fine sand or silt, use adjusted SPT value $N' = 15 + 0.5(N - 15)$, if $N > 15$,
- if soil is gravel or sandy gravel, increase measured N by 25%, i.e. $N' = 1.25 \times N$.

For normally consolidated sands and gravels, immediate settlement is given by

$$\rho_i = \Delta q' \times B^{0.7} \times I_c \,\text{mm}$$

where $\Delta q'$ is the net applied foundation pressure.

For overconsolidated sands and gravels, immediate settlement is given by

$$\rho_i = (\Delta q' - \tfrac{2}{3}\sigma_{vo})B^{0.7} \times I_c \,\text{mm}$$

where σ_{vo} is the previous maximum effective overburden pressure experienced by the soil.

When $\Delta q'$ is less than σ_{vo} the above expression becomes

$$\rho_i = \Delta q' \times B^{0.7} \times I_c/3 \,\text{mm}$$

Burland and Burbidge found that the D/B ratio was unimportant for $D/B < 3$. The L/B ratio, however, did appear to have a significant influence on foundation settlement and they proposed a shape correction factor given by:

$$f_s = [(1.25L/B)/(L/B + 0.25)]^2$$

Another factor that appeared important was the thickness of the sand or gravel layer beneath the foundation, H_s. If $H_s < z_I$, then a further correction factor should be applied given by:

$$f_1 = (H_s/z_I)(2 - H_s/z_I)$$

Finally, an estimate of time-dependent movement, t years after construction, may be estimated by the use of a time factor thus:

$$f_t = \rho_t/\rho_i = (1 + R_3 + R_3 \log t/3)$$

For static loads $R_3 = 0.3$ and $R_t = 0.2$; for fluctuating loads values of R_3 and R_t are 0.7 and 0.8, respectively.

WORKED EXAMPLE

Using various methods of predicting settlement

The various methods outlined above have been used to calculate the settlement for the example illustrated in Fig. 5.29. The footing is founded on sand.

de Beer and Martens

$$\delta = \frac{H}{C}\log_e \frac{p'_0 + \Delta p}{p'_0} \text{ (equation 5.18)}$$

The calculations are given in Table 5.7.

de Beer and Martens, but taking

$$C = 1.9\frac{C_r}{p'_0}$$

The calculated settlement is

$$36.2 \times \frac{1.5}{1.9} = 28.6\,\text{mm}$$

Schmertmann. The influence factor I_z is obtained from Fig. 5.30.

$$\delta = C_1 C_2 \Delta p \sum \frac{I_z}{E} H \text{ (equation 5.20)}$$

The calculations are given in Table 5.8

$$C_1 = 1 - 0.5\left[\frac{p'_0}{\Delta p}\right] = 1 - 0.5\frac{20}{80} = 0.875$$

$$C_2 = 1 + 0.2\log_{10}\left[\frac{t}{0.1}\right] = 1 + 0.2\log_{10} 50 = 1.34$$

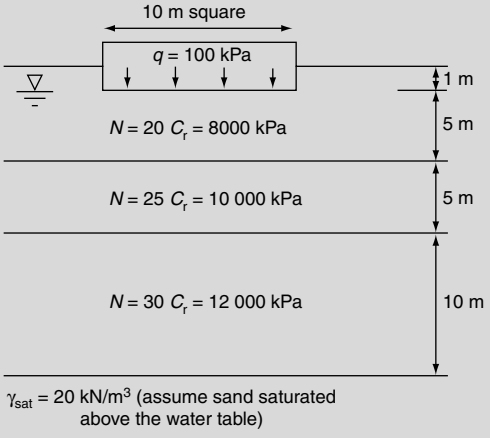

Fig. 5.29 Example used for settlement calculation

Table 5.7 Results of settlement calculations, following de Beer and Martens (1957)

Layer (m)	C_r (kPa)	p'_0 (kPa)	$C = \frac{3}{2}\frac{C_r}{p'_o}$	$p'_0 + \Delta p$	$\frac{p_0 + \Delta p}{p'_0}$	$\log_e \frac{B'_o + \Delta p}{p'_0}$	H (mm)	δ (mm)
0–5	8000	45	267	119.8	2.66	0.978	5000	18.3
5–10	10000	95	158	133.4	1.40	0.336	5000	10.6
10–20	12000	170	106	184.4	1.08	0.077	10000	7.3
							Total =	36.2

assuming a 5-year creep period. Therefore

$$\delta = 0.875 \times 1.34 \times 80 \times 0.2455 = 23.03\,\text{mm}$$

Terzaghi–Peck original proposal (from Fig. 5.24).

N	B (m)	q for 25 mm (kPa)	δ (mm)
22.5	10	95 (high groundwater table)	26.3

Meyerhof (1955)

$$\delta = \frac{2.84q}{N}\left[\frac{B}{B+0.33}\right]^2 = \frac{2.84 \times 100}{22.5}\left[\frac{10}{10.33}\right]^2 = 11.8\,\text{mm}$$

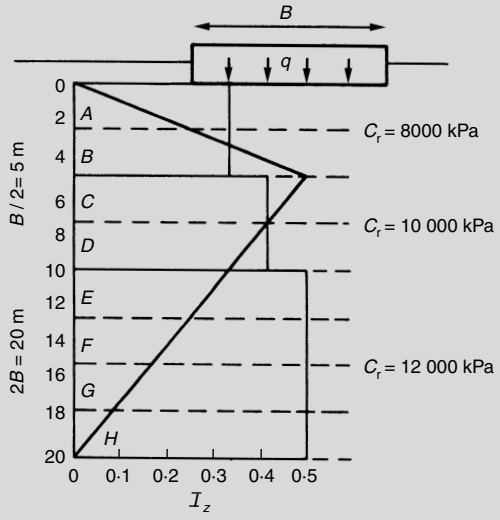

Fig. 5.30 Determination of Schmertmann's influence factor

Table 5.8 Results of settlement calculations, following Schmertmann (1975)

Layer	H (mm)	C_r (kPa)	$E = 2C_r$	I_z	$\frac{I_z}{E}H$
A	2500	8000	16000	0.12	0.0188
B	2500	8000	16000	0.35	0.0547
C	2500	10000	20000	0.45	0.0563
D	2500	10000	20000	0.36	0.0450
E	2500	12000	24000	0.30	0.0313
F	2500	12000	24000	0.21	0.0219
G	2500	12000	24000	0.12	0.0125
H	2500	12000	24000	0.05	0.0052
					Sum = 0.2455

Terzaghi–Peck modified by Meyerhof (1965)

N	B (m)	q for 25 mm (kPa)	δ (mm)
22.5	10	190×1.5	$\frac{25 \times 100}{285} = 8.8$

Terzaghi–Peck using Tomlinson's correction for p_0'

N	p_0' (kPa)	Correction factor	N_{cor}	q for 25 mm (kPa)	δ (mm)
22.5	70	2.2	49.5	450	5.6

Peck and Bazaraa

N	p_0' (kPa)	Factor for p_0'	Factor for water table	q for 25 mm (kPa)	δ (mm)
22.5	70	1.0	$\frac{6 \times 20}{20 + 5 \times 10} = 1.7$	$190 \times 1.5 = 285$	$\frac{100}{285} \times 1.7 \times 25 = 14.9$

Parry

$$\delta = \frac{aqB}{N_m} C_D C_w C_T \text{ (equation 5.27)}$$

N_m	B (m)	T (m)	D (m)	C_D	C_T	q (kPa)
25	10	20	1.0	1.1	1.0	0.1

Table 5.9 Calculated settlements by 10 methods for example in Fig. 5.29

Method	Calculated settlement	Field test
de Beer and Martens	36	Cone test
de Beer and Martens with $C = 1.9C_r/p'_o$	29	Cone test
Schmertmann	23	Cone test
Terzaghi–Peck	26	SPT
Meyerhof	12	SPT
Terzagi–Peck modified by Meyerhof	9	SPT
Terzaghi–Peck modified by Tomlinson	6	SPT
Peck and Bazaraa	15	SPT
Parry	10	SPT
Burland and Burbidge	7	SPT

$$D_w = 1.0\,\text{m}, \qquad C_w = 1 + \frac{D_w}{D + 3B/4} = 1 + 0.118 = 1.118$$

$$\delta = \frac{200 \times 0.1 \times 10}{25} \times 1.1 \times 1.118 \times 1.0 = 9.8\,\text{mm}$$

Burland and Burbidge

N	$\Delta q'$ kPa	B (m)	$B^{0.7}$	$I_c = 1.71/N^{1.4}$	$\rho_i = \Delta q' \times B^{0.7} \times I_c$ mm
22.5	$100 - 2 \times 20 = 60$	10	5.01	2.19×10^{-2}	6.6

The calculated settlements according to the various methods are collected together in Table 5.9

It can be seen that widely differing predictions result from the various methods. It must be stressed that in other situations, although a scatter in predicted settlements must be expected, the relative differences between the methods may well be quite different.

Simons, Rodrigues and Hornsby (1974) used eight of the above methods to predict the settlements of six structures for which settlements have been observed. The results are summarized in Table 5.10. It can be seen that although Schmertmann's method using the Dutch static cone gives the best agreement with observed settlements on average, the ranges of calculated to observed settlement are very wide indeed and hence in any single case, the calculated settlement may be quite different from that actually experienced

This is perhaps not surprising as neither the SPT nor the Dutch cone test measures soil compressibility directly, and in particular, the test results

Table 5.10 Calculated settlements by eight methods for six structures where settlements have been observed

Method	$\frac{\delta_{calc}}{\delta_{obs}}$ average	$\frac{\delta_{calc}}{\delta_{obs}}$ range
de Beer and Martens	3.22	1.0–4.8
Schmertmann	1.48	0.2–4.0
Terzaghi and Peck	1.89	0.5–3.2
Terzaghi and Peck, modified by Meyerhof	0.70	0.2–1.1
Terzaghi and Peck, modified by Tomlinson	0.31	0.1–0.6
Peck and Bazaraa	0.63	0.3–1.4
Parry	0.72	0.1–1.3

will not indicate whether a granular deposit is normally or over-consolidated, and this is one important factor which will influence the settlement which will develop. The use of in situ plate loading tests which at least measure soil compressibility would seem to lead to more reliable predicted settlements.

Modern seismic methods for stiffness profiling, however, such as cross-hole, down-hole, SASW (spectral analysis of surface waves) and CSW (continuous surface wave) methods offer a logical and lower cost alternative to plate loading tests (refer to Chapter 3 and also see, for example, Matthews *et al.*, 1996, and Matthews *et al.*, 2000).

Allowable settlements

The allowable settlement of a structure, that is, the amount of settlement a structure can tolerate, depends on several factors, for example the type of structure, its height, rigidity, function, and location; and the magnitude, rate and distribution of settlement.

It is important to distinguish between:

- Total settlement, which may cause damage to the services of the structure
- Differential settlement as a result of tilt which may be noticeable in high buildings
- Differential settlement due to shear distortion, which may lead to structural damage.

The foundation engineer, ideally, is required to predict the amount of differential settlement, due to tilt or distortion, which a structure can tolerate, and then to predict the differential settlement which will actually occur resulting from the structural loading and the ground conditions.

In reality it is difficult – if not impossible – to make this prediction, because of the difficulty of taking into account the interaction of the various structural elements, the redistribution of load as the structure settles differentially, and the time factor. The slower the settlements develop, the greater will be the settlements a structure is able to withstand without damage, because of creep in the structure, and hence the settlement criteria are different for buildings on sand and on clay. In addition, it is not possible in practice to determine with any degree of accuracy the variations in thickness and compressibility of the various strata underlying a structure. Finally, it is necessary to take into account that types of

Table 5.11. Classification of visible damage to walls with particular reference to ease of repair of plaster and brickwork or masonry (Burland et al. 1977).

Degree of damage	Description of typical damage†	Approximate crack width (mm)
1. Very slight	Fine cracks which can easily be treated during normal decoration. Perhaps isolated slight fracture in building. Cracks in external brickwork visible on close inspection.	Not greater than 1*
2. Slight	Cracks easily filled. Re-decoration probably required. Several slight fractures showing inside of building. Cracks are visible externally and some re-pointing may be required externally to ensure watertightness. Doors and windows may stick slightly.	Not greater than 5*
3. Moderate	The cracks require some opening up and can be patched by a mason. Recurrent cracks can be masked by suitable linings. Repointing of external brickwork and possibly a small amount of brickwork to be replaced. Doors and windows sticking. Service pipes may fracture. Weathertightness often impaired.	5 to 15* or a number of cracks greater than 3
4. Severe	Extensive repair work involving breaking-out and replacing sections of walls, especially over doors and windows. Windows and door frames distorted, floors sloping noticeably. Walls leaning or bulging noticeably, some loss of bearing in beams. Service pipes disrupted.	15 to 25* but also depends on number of cracks
5. Very severe	This requires a major repair job involving partial or complete rebuilding. Beams lose bearing, walls lean badly and require shoring. Windows broken with distortion. Danger of instability.	Usually greater than 25* but depends on number of cracks.

† In assessing the degree of damage, account must be taken of its location in the building or structure.
* Crack width is only one aspect of damage and should not be used on its own as a direct measure of it.

cracks inevitably appear in all buildings due to other causes, requiring maintenance expenses independent of whether or not cracks result from settlement.

For these reasons observation has been used as a basis for suggesting tolerable limits to settlements (Skempton and MacDonald, 1955; Bjerrum, 1963a, b).

Because maximum settlements can be predicted with some accuracy (but not differential settlements) it is usual to relate allowable settlements to maximum settlements.

Skempton and MacDonald (1955) suggested the following design limits for maximum settlements:

- Isolated foundations on clay: 65 mm
- Isolated foundations on sand: 40 mm
- Rafts on clay: 65 to 100 mm
- Rafts on sand: 40 to 65 mm.

The smaller limits placed on foundations on sand are due partly to the time factor discussed previously, and also to the fact that granular soils tend to be less homogeneous than clays.

Burland *et al.* (1977) refer to basically three criteria which have to be satisfied when considering limiting movements. These are visual appearance, seviceability or function, and stability. They conclude with Skempton and MacDonald (1956) that, for the majority of buildings the allowable settlement is governed more by architectural damage than by overstressing of the structure. They define classifications of visible damage as shown in Table 5.11.

CHAPTER SIX

Piled foundations

Introduction

The following aspects of pile design are considered:

- types of pile
- piles in cohesive soils
- piles in granular soils
- group action of piles
- negative skin friction
- piles under lateral loads
- testing of piles.

Three design criteria should be kept in mind:

- The pile material itself must not be over-stressed.
- There must be an adequate factor of safety against a shear failure.
- The settlements must be within tolerable limits.

It should be noted that piles are required for a variety of reasons, for example, to:

- Transfer load to a stronger and/or less compressible stratum.
- Carry horizontal forces from bridge abutments or retaining walls.
- Increase the stability of tall buildings.
- Carry uplift forces.
- Avoid scour damage.
- Compact loose sands.

In any situation, the type of pile chosen and the design method used will be influenced by the factors which governed the decision to use piles in the first place.

It should be emphasized that although in the following sections the methods outlined for predicting the bearing capacity of piles are based on field and laboratory tests, pile loading tests should be carried out whenever circumstances permit, as a check on the computations.

Types of pile

Piles may be classified in a number of ways. Following the Code of Practice for Foundations, BS 8004:1986, which is based on the effect the

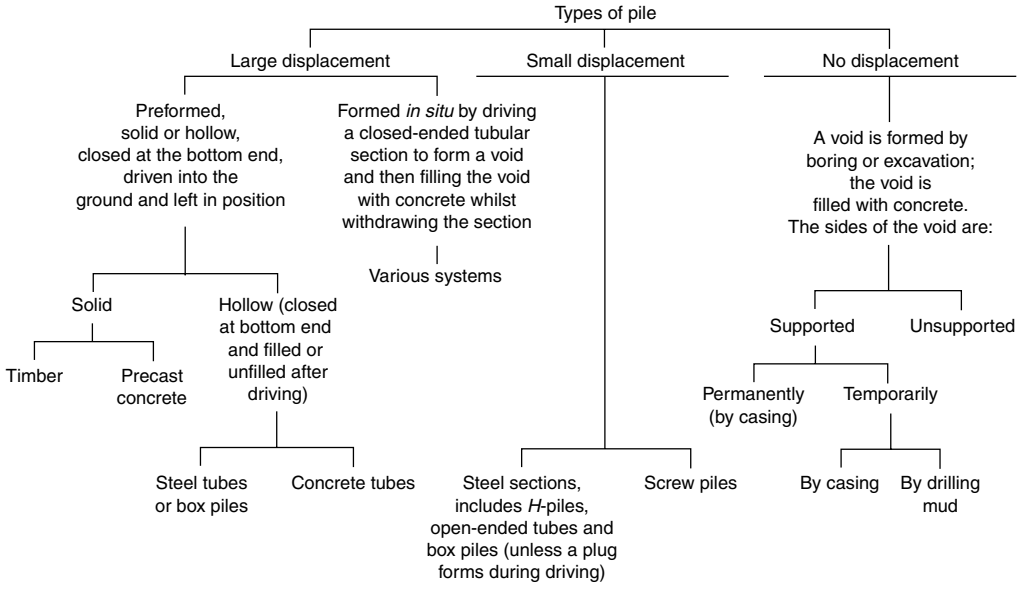

Fig. 6.1 Classification of piling systems

pile has on the soil during installation, piles are considered to fall into three main classes: very large displacement, small displacement, and non-displacement, with further sub-divisions as shown in Fig. 6.1.

There are numerous types of pile, either proprietary or non-proprietary, in the above groups. Considering the technical factors listed below narrows the choice to two or three types and the final choice is generally made on overall cost, although the reputation of a particular piling contractor may well prove to be a decisive influencing factor.

Factors governing the choice of pile type

Vital factors to be taken into consideration when determining the type of pile to be used are:

- The location and type of structure.
- Ground conditions, including the position of the ground water table.
- Durability in the long term. Timber piles are subject to decay, particularly above the water table, and to attack by marine borers. Concrete is liable to chemical attack in the presence of salts and acids in the ground, and steel piles may suffer from corrosion if the specific resistivity of the clay is low and the degree of depolarization is high.
- Overall cost to the client. The cheapest form of piling is not necessarily the cheapest pile per metre run. Delays to the contract owing to lack of experience or lack of appreciation of a particular problem by the piling

contractor may add considerably to the total cost of a project. The cost of pile testing should be considered if the piling contractor has insufficient experience to establish the required pile length or diameter. In particular, heavy additional costs to the contract may be incurred if piles fail under test load. It is advantageous to use a reputable firm with good local experience. It should be stressed that most delays and troubles on piling contracts can be avoided by carrying out a thorough site investigation at as early a stage as possible.

Large displacement piles

Driven and cast-in-place

The advantages are:

- Can be driven to a predetermined set.
- Pile lengths are readily adjustable.
- An enlarged base can be formed which can increase the relative density of a granular founding stratum leading to much higher end bearing capacity.
- Reinforcement is not determined by the effects of handling or driving stresses.
- Can be driven with a closed end so excluding the effects of ground water.
- Noise and vibration can be reduced in some types, for example, by driving on a plug at the bottom of the pile.

The disadvantages are:

- Heave of neighbouring ground surface, which could affect nearby structures or services.
- Disturbance of the soil, which could lead to reconsolidation and the development of negative skin friction forces on piles.
- Displacement of nearby retaining walls.
- Lifting of previously driven piles, where the penetration at the toes of the piles into the bearing stratum has not been sufficient to develop the necessary resistance to upward forces.
- Tensile damage to unreinforced piles or piles consisting of green concrete, where forces at the toe have been sufficient to resist upward movements.
- Damage to piles consisting of uncased or thinly cased green concrete due to the lateral forces set up in the soil, for example, necking or waisting.
- Concrete cannot be inspected after completion.
- Concrete may be weakened if artesian flow pipes up shaft of piles when tube is withdrawn.

- Light steel sections or precast concrete shells may be damaged or distorted by hard driving.
- Limitation in length owing to lifting force required to withdraw casing.
- Noise, vibration and ground displacement may cause a nuisance or may damage adjacent structures.
- Cannot be driven with very large diameters nor can very large end bulbs be formed.
- Cannot be driven where headroom is limited.
- Pile lengths of up to 24 m and pile loads of about to 1500 kN are common.

Driven precast reinforced or prestressed concrete piles

The advantages are:

- Can be driven to a predetermined set.
- Stable in squeezing ground, for example, soft clays, silts and peats.
- Pile material can be inspected before piling.
- Can be redriven if affected by ground heave.
- Construction procedure unaffected by ground water.
- Can be driven in long lengths.
- Can be carried above ground level, for example, through water for marine structures.
- Can increase the relative density of a granular founding stratum.

The disadvantages are:

- Heave and disturbance of surrounding soil may cause difficulties, as discussed above for driven and cast-in-place piles.
- Cannot readily be varied in length.
- May be damaged due to hard driving.
- Reinforcement may be controlled by handling and driving requirements rather than by stresses caused by structural loads.
- Cannot be driven with very large diameters or in conditions of limited headroom.
- Noise, vibration and ground displacements may cause difficulties.

Pile lengths up to 27 m and pile loads up to 1000 kN are usual.

Timber piles

Timber piles are light, easy to handle and, in some countries, cheap. They can be joined together and can be provided with driving points. Timber piles are liable to decay and attack by marine borers and generally are only used below the water table but can be pressure impregnated to provide protection above the water table. They are usually used as friction piles but, on occasions, can be used as point bearing piles. In this case,

care must be taken to avoid damage owing to overdriving. The danger of damaging the pile during driving can be reduced by limiting the drop and the number of blows of the hammer. The weight of the hammer should at least be equal to the weight of the pile for hard driving conditions and not less than half the weight of the pile for easy driving. Pile lengths up to 20 m and loads up to 600 kN are usual.

Small displacement piles

Examples of these piles are rolled steel sections, screw piles, or open-ended tubes and hollow sections where the soil is removed during penetration. Some of the remarks listed for large displacement piles apply.

Rolled steel section piles are easily handled and can be driven hard. They can be driven in very long lengths and the pile length can be readily varied. They can carry heavy loads and can be successfully anchored in steeply sloping rock surfaces (Bjerrum, 1957). The piles are liable to corrosion which can be allowed for in design or can be treated using cathodic protection, or the piles can be coated.

Screw piles are valuable in marine works because they can resist both tensile and compressive forces.

In general, small displacement piles are particularly useful if ground displacements and disturbance must be severely curtailed.

Rolled steel section piles are used up to 36 m in length with pile loads of up to 1700 kN, and with screw piles, lengths of up to 24 m with working loads up to 2500 kN are possible.

Bored and cast-in-place non-displacement piles

Advantages

- No risk of ground heave.
- Length can be readily varied.
- Soil can be inspected and compared with site investigation data.
- Can be installed in very long lengths, with very large diameters, and end enlargements of up to two or three pile diameters are possible in clays and soft rocks.
- Reinforcement is not dependent on handling or driving conditions.
- Can be installed without appreciable noise or vibration, and under conditions of limited headroom.

Disadvantages

- Boring methods may loosen sandy or gravelly soils or change soft rocks to a slurry, for example, chalk or marl.
- Susceptible to waisting or necking in squeezing ground.
- Difficulties with concreting under water. The concrete cannot subsequently be inspected.

- An inflow of water may cause damage to the unset concrete in the pile or may cause a disturbance to the surrounding ground leading to reduced pile bearing capacity.
- Enlarged ends cannot be formed in granular soils.

Concrete should be placed as soon as possible after boring the hole, to avoid softening of the ground. It is important to have adequate workability, so that the concrete can flow against the walls of the shaft. In practice, this means that the concrete slump should be in the range of 100 mm to 150 mm. To avoid segregation, honeycombing, bleeding and other defects resulting from high water content, the use of a plasticizing additive may be beneficial. In general, the concrete should contain not less than 300 kg of cement per cubic metre.

Pile lengths of up to 45 m with loads of up to 10 000 kN are not unusual.

Piles in cohesive soils

Piles in cohesive soils, apart from short under-reamed piles of large diameter, generally carry most of the load on the pile shaft. The bearing capacity is usually predicted on the basis of undrained shear strength data, although an effective stress approach has been proposed (Burland, 1973).

The failure load Q_f, of a pile is given by:

$$\begin{aligned} Q_f &= \text{load carried on the shaft} + \text{load carried on the base} \\ &= sc_s A_s + (N_c A_b s_u + \gamma D A_b) \end{aligned} \tag{6.1}$$

where A_s = area of pile shaft; A_b = area of base of pile; s_u = undrained shear strength at base of pile; c_s = average adhesion between shaft and clay; N_c = bearing capacity factor; D = length of pile; γ = bulk unit weight of clay; s = shape factor, which is 1.0 for a plain shaft and 1.2 for a tapered pile.

The weight of a pile is approximately equal to $\gamma D A_b$. Thus, the load, P_f causing failure of a pile is given by:

$$P_f = N_c A_b s_u + sc_s A_s \tag{6.2}$$

The allowable load, P_a, is given by:

$$P_a = \frac{N_c A_b s_u}{F_1} + \frac{sc_s A_s}{F_2} \tag{6.3}$$

or

$$P_a = \frac{N_c A_b s_u}{F_1} + \frac{s\bar{s}_u a A_s}{F_2} \tag{6.4}$$

where $\bar{s}_u$ = average undrained shear strength over the length of the pile

and the adhesion factor is

$$\alpha = c_s/s_u \tag{6.5}$$

The first term presents no difficulty because N_c can be taken as being equal to nine. For large diameter short piles a reduced value from Fig. 4.9 can be used. The undrained shear strength can be obtained with sufficient accuracy if the factors outlined in Chapter 2 are taken into account. In addition, the load carried on the base is generally small compared with that carried on the shaft and so an error in the estimation of the base load is of less significance. The major problem, therefore, is the determination of the adhesion mobilized between the shaft and the clay.

Driven piles

Driving piles into cohesive soils causes radical changes to the soil strength, and phenomena like remoulding, ground heave, the formation of an enlarged hole, and strain softening affects the adhesion developed between pile and clay.

With the passage of time, reconsolidation of the clay around the pile will occur and hence the adhesion will depend on the time elapsed between pile driving and pile loading or testing. Experience has shown that at least 30 days should elapse between driving and testing in order to allow equilibrium conditions to be re-established in the clay. With some clays, 90 days may be more suitable. It should also be noted that on any one site the adhesion factor may vary to a certain extent from pile to pile.

The problem of the variation of the adhesion factor has been studied by Tomlinson (1957), Peck (1958), Nordlund (1959), Woodward *et al.* (1961), Flaate (1968) and Tomlinson (1970, 1971).

Figure 6.2, after Tomlinson (1969), shows the variation of the adhesion factor with the undrained shear strength of the clay. The drop in adhesion factor with increasing strength of the clay is most marked.

It should be noted that Fig. 6.2 can only be expected to give an approximate indication of the failure load of a driven pile in clay because of the large variation in the adhesion factors for any given shear strength.

Flaate (1968), after a comprehensive analysis of a number of pile-loading tests suggested that α depended not only on the average undrained shear strength of the clay, but also on the plasticity index and made the proposals shown in Fig. 6.3. It should be noted that very few tests were analysed in the firm to stiff range of clay strength.

The work of Tomlinson (1957, 1970, 1971), has greatly clarified the position regarding adhesion factors for piles driven into stiff clays. Piles driven into stiff to hard cohesive soils without any soft or loose overburden cause a heave of the ground surface around the pile. Radial cracks develop and a gap is formed between the pile and the soil. Tomlinson (1957) noted the

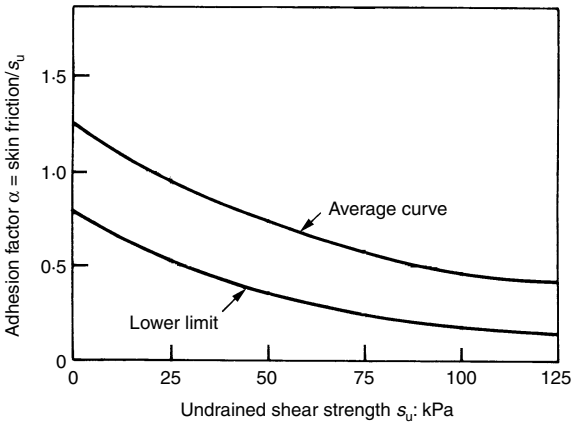

Fig. 6.2 Relationship between adhesion factor for driven piles and undrained shear strength of clay, after Tomlinson (1969)

significance of this gap in reducing the skin friction of piles in clays and stated that it was probably due to lateral vibrations or 'whip' of the piles during driving. Perhaps even more important, Tomlinson (1970, 1971), showed that the adhesion factor is influenced by the presence of other soils overlying the stiff London clay. Overlying soft clay results in smaller adhesion factors, whereas overlying granular soils give greater factors. He observed that driven piles generally give higher adhesion factors than jacked piles.

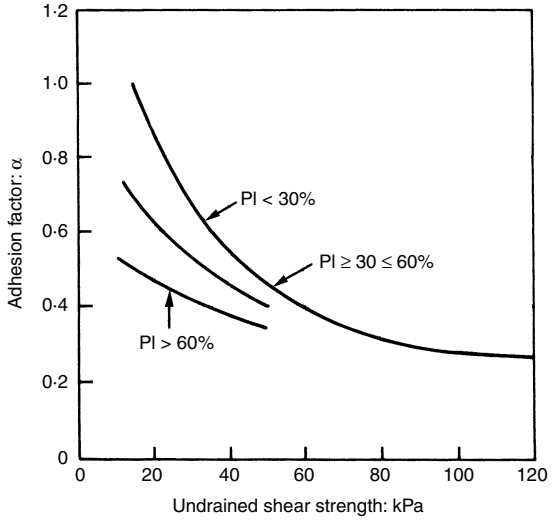

Fig. 6.3 Relationship between adhesion factor for driven piles and undrained shear strength of clay, after Flaate (1968)

Important conclusions resulting from Tomlinson's work are as follows:

- Where piles are driven through sands or sandy gravels, these soils are carried down to a limited depth forming a skin of compacted sand or sand/clay mixture around the shaft. This skin has a high skin friction value such that piles driven to penetrations of less than 20 diameters into the stiff cohesive soils can have an ultimate skin frictional resistance exceeding 1.25 times the undrained shear strength of the soil. For greater penetrations, the effect of the skin of granular material becomes progressively less and the adhesion factor tends to decrease with increasing shear strength of the soil.
- Where piles are driven through soft clays or silts into stiff to very stiff cohesive soils, a soft skin is carried down, again to a limited depth, but the skin gains somewhat in shear strength owing to consolidation. The soft skin has a considerable weakening effect on the frictional resistance on the shaft where the pile penetrates the stiff cohesive soil by less than 20 diameters. An adhesive factor of 0.4 should be used for these conditions subject to a minimum penetration of eight diameters. Beyond 20 diameters penetration, the adhesion factor appears to be fairly constant for undrained shear strengths between 70 and 140 kPa at an average value of 0.70.

Piles driven into stiff to very stiff cohesive soils extending from the surface downwards cause a gap to form around the upper part of the shaft such that skin friction cannot be assumed to act over this part. The gap is of considerable significance where piles are driven to a penetration of less than 20 diameters, where an adhesion factor of 0.4 may be adopted for penetrations between eight and 20 diameters. For piles driven deeper than 20 diameters the adhesion factor is governed by the shear strength of the soil, decreasing from unity for undrained shear strengths up to 90 kPa to 0.4 at a strength of 170 kPa.

For the case of steel H-piles, the adhesion is usually calculated on a perimeter equal to twice the flange width plus twice the web depth, and the end bearing on the gross cross-sectional area, that is, the flange width times the web depth.

An overall factor of safety of 2.5 is often used, and it has been suggested that partial factors of safety are appropriate, for example, 3 on end bearing and, say, 1.5 on shaft resistance. This is in an attempt to take into account the fact that the shaft resistance may be fully mobilized at a deformation of the order of 2–7 mm whereas the base resistance requires a greater deformation for full mobilization.

The material of the pile does not appear to be of any great significance, although it is commonly believed that timber and concrete piles should have higher adhesion factors than smooth steel piles. For examples, the

Code of Practice of the Danish Society of Engineers (1966) suggests multiplying the calculated adhesion by unity for timber and concrete piles and by 0.7 for steel piles. If the pile material is coated by bitumen, for example, greatly reduced adhesion will result. An interesting case has been described by Hutchinson and Jensen (1968). Reinforced concrete test piles driven into soft silty clays at Khorramshar failed to reach their predicted carrying capacity by quite a wide margin. In a subsequent investigation of the difficulties, Hutchinson and Jensen made the interesting observation that the skin friction at the pile/soil interface had been considerably weakened by the 1–2 mm, thick coating of soft bitumen applied to the piles to protect them from acid attack. The skin friction developed on the coated piles was only 30 to 80% of that on the uncoated piles.

Cast in situ bored piles

The process of boring a hole for a pile seriously disturbs the clay in the immediate neighbourhood of the hole. Placing the concrete causes water to be absorbed by the clay surrounding the pile, leading to softening and reduced strength. The base resistance and adhesion of bored piles in the London clay has been extensively studied (Skempton, 1959; Burland *et al.*, 1966; Whitaker and Cooke, 1966; Butler and Morton, 1971; Burland and Cooke, 1974).

Skempton (1966) has suggested *first approximation design rules,* which are given below.

The load on the shaft, P_s, is given by:

$$P_s = A_s \times 0.45 \times \bar{s}_u \tag{6.6}$$

The load on the base, P_b, is given by:

$$P_b = A_b \times 9 \times w \times s_u \tag{6.7}$$

where $w = 0.8$ for $B < 1\,\text{m}$ and 0.75 for $B > 1\,\text{m}$; A_s = area of shaft; A_b = area of base; $\bar{s}_u$ = average undrained shear strength along the shaft; s_u = undrained shear strength at the base.

These undrained shear strengths are based on traditional 38 mm diameter triaxial tests on U-4 open drive samples using average values. If the strength is measured in a different way, that is, using plate loading tests or larger samples, then different coefficients of correlation will result.

The working load (WL) is then given as follows:

$$\text{For plain shafts, WL} = \frac{\text{Total}}{2} \tag{6.8}$$

For belled piles

$$\text{(i) WL} = \frac{\text{Total}}{2.5} \text{ with } B < 2\,\text{m} \tag{6.9}$$

or

$$\text{(ii) WL} = \frac{\text{Shaft}}{1.5} + \frac{\text{Base}}{3} \tag{6.10}$$

For $B > 2$ m, the working load is to be evaluated from settlement considerations. Finally, the settlements of the structure should be checked.

For the case of short-bored piles in London clay, where the clay may be heavily fissured at a shallow depth, the adhesion factor should be taken as 0.3.

It must be stressed that the adhesion factor of 0.45 is an average value and may vary from site to site and may also vary on any one site, if the workmanship and the method of construction are allowed to vary. The adhesion factor may be lower for belled piles because of the greater time involved in constructing such piles. The time elapsed between drilling and correcting is important. Generally, piles should be concreted immediately after they are drilled. Water added to assist the drilling operations may lead to lower values of the adhesion factor.

For belled piles, it has been suggested that the shaft resistance should be ignored for a distance of two base diameters above the top of the under-ream.

Based on research carried out by the Building Research Station, UK, Burland and Cooke (1974) have proposed a simple and logical method for determining the allowable working loads for piles in stiff clays having a wide range of dimensions. Using their approach, the corresponding settlements are likely to be acceptable for most common structures and they further indicate how the immediate settlements for a single pile can be estimated with tolerable accuracy. The discussion which follows draws heavily on their paper.

The significance of pile geometry on pile behaviour was not appreciated until tests on bored piles were carried out in which the shaft and base components of resistance were separated. Whitaker and Cooke (1966) have tested bored piles with load cells incorporated in each shaft immediately above the base, and so it was possible to measure the development of shaft and base forces separately as the applied load was increased and the pile settled. The results presented by Whitaker and Cooke show that the two components are mobilized at entirely different rates of settlement. For most practical purposes the load-settlement relationships for the shaft and the base are independent of each other. The frictional resistance on the shaft develops rapidly and almost linearly with settlement and is generally fully mobilized when the settlement is about 0.5% of the shaft diameter. Thereafter, it either remains sensibly constant, or decreases slightly as the settlement is increased further. On the other hand, the base resistance is seldom fully mobilized until the pile settlement reaches

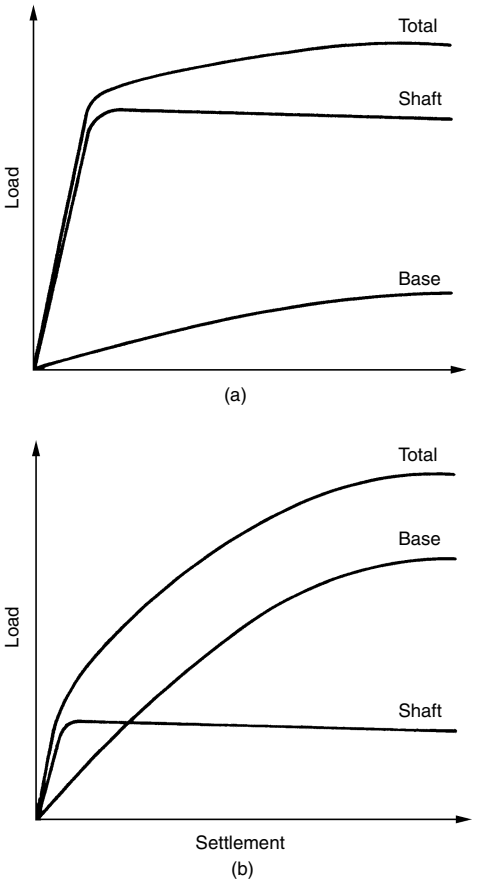

Fig. 6.4(a) Load settlement relationship for long straight shafted bored pile in London clay; (b) load settlement relationship for short under-reamed bored pile in London clay, after Burland and Cooke (1974)

10 to 20% of the base diameter. The load–settlement relationship is normally far from linear although it is often convenient to assume that it is linear for loads less than about one-third of the ultimate base resistance.

The shape of the total load settlement curve for a bored pile depends on the relative load contributions of the shaft and the base. A test on a long straight shafted pile will result in a total settlement curve of the form shown in Fig. 6.4(a), while relatively short piles with large under-reams exhibit behaviour of the form illustrated in Fig. 6.4(b).

If piles are designed to carry a working load equal to $\frac{1}{3}$ to $\frac{1}{2}$ the total failure load, it can be seen from Fig. 6.4(b) that for piles with large under-reams there is every likelihood of the shaft resistance being fully

mobilized at the working load. This has an important bearing on design which is discussed later.

It has been shown that the behaviour of a bored pile can lie anywhere between that of a friction pile (i.e. long straight shafted pile) and that of a deep footing (i.e. a short under-reamed pile). A load factor criterion for design is therefore required which is applicable over the complete range. It has already been stressed that the deflections required to mobilize end bearing are much larger than those required to mobilize the full shaft adhesion. Thus, if the base is operating at a reasonable factor of safety, the shaft adhesion will be at, or very close to, its ultimate value. Therefore, Burland *et al.* (1966) suggested two simple stability criteria which impose a minimum overall load factor, F, with the additional proviso that a factor of safety in end bearing, F_b, is not exceeded. This proviso will normally only apply when the shaft friction is fully mobilized. These conditions may be written:

$$P_a \leq \frac{L_B + L_s}{F} \tag{6.11}$$

and

$$P_a \leq L_s + \frac{L_B}{F_B} \tag{6.12}$$

where P_a = working load; L_B = ultimate base load; L_s = ultimate shaft load; F = overall load factor, often taken as 2.0; F_B = factor of safety in end bearing, usually taken as 3.0.

Methods for evaluating L_B and L_s have already been described. Put simply, equation 6.11 ensures overall stability and equation 6.12 guards against local over-stressing. Equation 6.12 only applies when the base diameter, D, is large compared with the shaft diameter, d.

To predict the short-term undrained behaviour of a bored pile, the procedure outlined by Burland *et al.* (1966) is suggested. It is based on the assumption that the load settlement curve for the pile shaft is linear up to full mobilization which takes place at a settlement of 0.5% of the shaft diameter. As far as the base is concerned, Burland *et al.* found that, to a good approximation:

$$\frac{\delta}{D} = K\frac{q}{q_s} \tag{6.13}$$

where δ = settlement of the base; D = base diameter; q = applied pressure; q_s = ultimate pressure; K = factor varying from 0.01 to 0.02.

In any problem, K can be determined from a large in situ plate loading test, or if this is not possible, can be taken conservatively as 0.02.

The method of design is illustrated by an example which is reproduced from Burland and Cooke (1974).

WORKED EXAMPLE

Test pile, P, Whitaker and Cooke (1966)

Details: Length of shaft = 14.5 m
Diameter of shaft = 0.94 m
Diameter of base = 1.86 m
$\bar{s}_u = 128$ kPa
$s_u = 150$ kPa

Required: With $F = 2$ and $F_b = 3.0$, find the maximum safe working load and draw the load settlement diagram up to working load. It is assumed that the shear strength values quoted are representative for the clay in situ.

$$L_s = a\bar{s}_u A_s$$
$$= 0.45 \times 128 \times \pi \times 0.94 \times 14.5$$
$$= 2466\,\text{kN}$$

$$L_B = 9 \times s_u \times A_b$$
$$= 9 \times 150 \times \pi/4 \times 1.86^2$$
$$= 3668\,\text{kN}$$

Now, from equation 6.11 (overall stability),

$$P_a = \frac{2466 + 3660}{2} = 3063\,\text{kN}$$

and, from equation 6.12 (over-stressing of base),

$$P_a = 2466 + \frac{3660}{3} = 3686\,\text{kN}$$

Therefore, the working load is 3063 kN.

It is assumed that the settlement will be large enough to mobilize the full shaft adhesion, i.e. $L_s = 2466$ kN.

Therefore, the load on the base is $(3063 - 2466) = 597$ kN.

Now, from equation 6.13,

$$\delta = D \times \frac{Q}{Q_u} \times K$$
$$= 1.86 \times \frac{597}{3668} \times 0.02$$
$$= 6\,\text{mm}$$

The settlement required to mobilize fully the shaft friction is $(0.5/100) \times 940 = 4.7$ mm. Thus the assumption of full mobilization is valid.

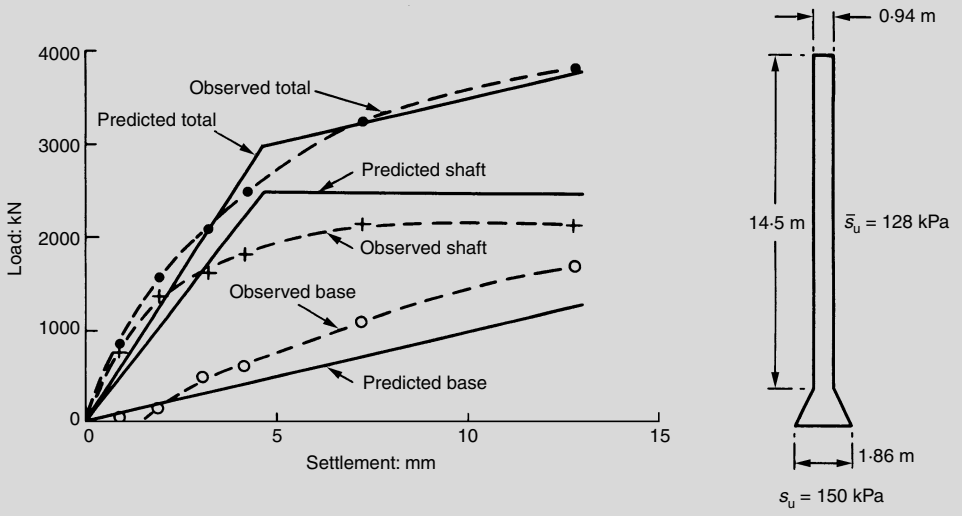

Fig. 6.5 Predicted load–settlement relationship for a bored pile in London clay, after Burland and Cooke (1974)

Figure 6.5 from Burland and Cooke (1974) shows the load–settlement curves for the shaft, the base and the complete pile (being the sum of the previous two), together with the results of an incremental load test. The analysis is in remarkable agreement with the observations, and this must to some extent be considered fortuitous.

Burland and Cooke (1974) also describe a method for preparing simple design charts which greatly facilitate design decision making because the effects of changing pile dimensions, founding levels or working levels can be determined at a glance.

There is little published data on adhesion factors appropriate to other types of clay. Tomlinson (1969) quotes 0.1 in very stiff to hard Lias clay, while Woodward *et al.* (1961) have quoted values of 0.49 to 0.52 for clays in California having shear strengths of about 100 kPa.

In all cases, of course, the most reliable estimates of pile bearing capacity will result from pile loading tests. It is, however, vital that the test piles are bored and constructed in the same way as the piles under the structure. Account must also be taken of time effects.

Piles in granular soils

Parallel-sided piles in granular soils act mainly as end bearing piles, with only a relatively small proportion of the load being carried on the shaft.

Pile bearing capacity can be predicted on the basis of:

- bearing capacity theory
- Dutch cone test
- standard penetration test
- pile driving formulae
- correlation with special sounding tests, for example, driving rods, pushing and pulling rods, rotating rods.

Bearing capacity theory

$$P_f = A_b p'(N_q - 1) + A_s K p'_{ave} \tan \delta' \tag{6.14}$$

where p' = effective overburden pressure at base of pile; p'_{ave} = average effective overburden pressure over the length of pile; K = a coefficient of earth pressure; δ' = angle of wall friction; A_b = base area of pile: A_s = shaft area of pile; N_q = bearing capacity factor; P_f = failure load on pile.

The above expression neglects the $\frac{1}{2}\gamma' B N_\gamma$ term since it is small compared with the N_q term, and assumes that the bulk unit weight of the soil is equal to the unit weight of the pile.

There are many relationships which have been proposed between N_q and ϕ'. Tomlinson (1969) has suggested, for pile design, using the work of Berezantsev (1961) and this relationship is given in Fig. 6.6. It should, however, only be used provided the pile can be driven into the granular stratum for a depth equal to about five times the pile width. For shallow penetrations, the values approach Terzaghi's solution for shallow foundations.

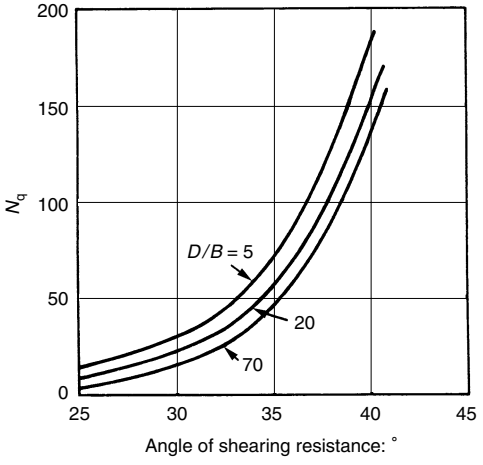

Fig. 6.6 Relationship between N_q and ϕ', after Berezantsev (1961)

Since N_q is sensitive to ϕ', a relatively small error in estimating ϕ' will lead to a much larger error in N_q. Of particular difficulty is the assessment of the effect of pile driving operations on ϕ'. Meyerhof (1959) suggests that the bearing capacity of piles driven into loose sands can be doubled owing to compaction.

Broms (1965b) suggested the following values for K in granular soils:

Type of pile	*Loose*	*Dense*
Steel	0.5	1.0
Concrete	1.0	2.0
Timber	1.5	3.0

Aas (1966) proposed the following values of δ', which are perhaps somewhat on the safe side:

Steel piles	$\delta' = 20^\circ$
Concrete piles	$\delta' = \frac{3}{4}\phi'$
Timber piles	$\delta' = \frac{2}{3}\phi'$

Dutch cone test

The failure load on the base of the pile is simply

$$P_b = A_b C_{KD} \tag{6.15}$$

where C_{KD} is the cone point resistance averaged over a distance extending from about $4B$ above the pile tip to $1B$ below. With a factor of safety of $2\frac{1}{2}$, the pile is unlikely to settle more than 12 mm under working load. The skin friction can either be calculated from bearing capacity, theory, above, or as follows (Meyerhof, 1965).

For displacement piles, the ultimate unit skin friction

$$c_s = \frac{C_{KD\,ave}}{200}\ \text{kPa} \tag{6.16}$$

or for H-piles, the ultimate unit skin friction

$$c_s = \frac{C_{KD\,ave}}{400}\ \text{kPa} \tag{6.17}$$

where $C_{KD\,ave}$ = average cone point resistance over the length of the pile in kPa.

Standard penetration test

This can only be used in an indirect manner as follows:

- Estimating ϕ' from N and then using bearing capacity theory.
- Estimating C_{KD} from N and then proceeding as for Dutch cone test.

Pile driving formulae

Many attempts have been made to determine the relationship between the dynamic resistance of a pile during driving and the static load-carrying capacity of the pile. These intended relationships are called pile-driving formulae and have been established empirically or theoretically. Much discussion has been generated, for example, ASCE (1951), Chellis (1941), Cummings (1940), and Greulich (1941). Conflicting opinions have been expressed.

The relationship between dynamic and static resistance of a pile as expressed by a pile driving formula should be independent of time if the formula is to have any validity. This is clearly not the case with clays and, therefore, pile driving formulae should not, in general, be applied to cohesive soils, but only to granular soils, that is, sands and gravels.

Of the many pile driving formulae which have been proposed, the authors suggest that the Janbu formula and the Hiley formula are convenient to use and give reasonable predictions of the ultimate bearing capacity of driven piles in granular soils.

The Janbu formula (Janbu, 1953)

$$Q_u = \frac{1}{K_u}\frac{\eta WH}{s} \tag{6.18}$$

where Q_u = ultimate load capacity; WH = input energy; s = final set (penetration/blow)

$$K_u = C_d\left[1 + \left(1 + \frac{\lambda_e}{C_d}\right)^{1/2}\right] \tag{6.19}$$

$$C_d = 0.75 + 0.15\frac{W_p}{W} \tag{6.20}$$

$$\lambda_e = \frac{\eta WHL}{AEs^2} \tag{6.21}$$

where L = length of pile; A = cross-sectional area; E = modulus of elasticity of pile material; W = weight of hammer; W_p = weight of pile; H = drop of hammer. Fig. 6.7 eases the computation.

The efficiency factor, η, is dependent on the pile driving equipment, the driving procedure adopted, the type of pile, and the ground conditions. Values of η can be chosen as follows:

$\eta = 0.70$ for good driving conditions

$\eta = 0.55$ for average driving conditions

$\eta = 0.40$ for difficult or bad conditions.

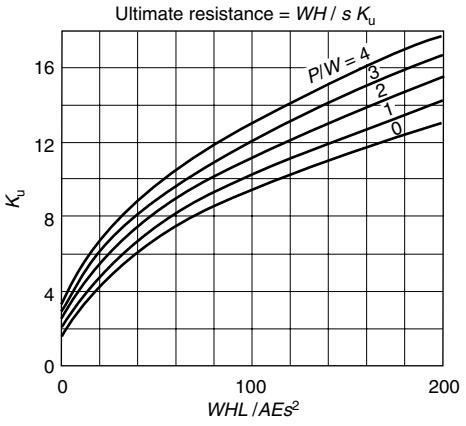

Fig. 6.7 Design chart for the Janbu pile driving formula

The Hiley formula (Hiley, 1925)

$$Q_u = \frac{KWH\eta}{s + c/2} \tag{6.22}$$

where η = efficiency of the blow; K = hammer coefficient; c = sum of the temporary elastic compression of the pile c_p, the pile head c_c and the ground c_q.

Values of K, η, c_c, c_p and c_q can be obtained from Table 6.1 and Figs 6.9 to 6.13, although it is preferable to measure c_p and c_q directly in the field.

It should be noted that η depends on the coefficient of restitution, e, which is given in Table 6.2, η then being obtained from Fig. 6.8.

Comparison of formulae

A detailed investigation into the validity of pile-driving formulae in granular soils (Flaate, 1964) suggests that there is little to choose between the Hiley and the Janbu formulae. In order to obtain a minimum factor of

Table 6.1 Values of hammer coefficient K, after BSP Pocket Book (1969)

Hammer	*K*
Drop hammer, winch operated	0.8
Drop hammer, trigger release	1.0
Single-acting hammer	0.9
BSP double-acting hammer	1.0*
McKiernan–Terry diesel hammers	1.0†

* Instead of *WH* in the Hiley formula use manufacturer's rated energy per blow, at actual speed of operation of hammer, the hammer speed must be checked when taking the final set.
† For *WH* substitute manufacturer's rated energy per blow, corresponding to the stroke of the hammer at the final set.

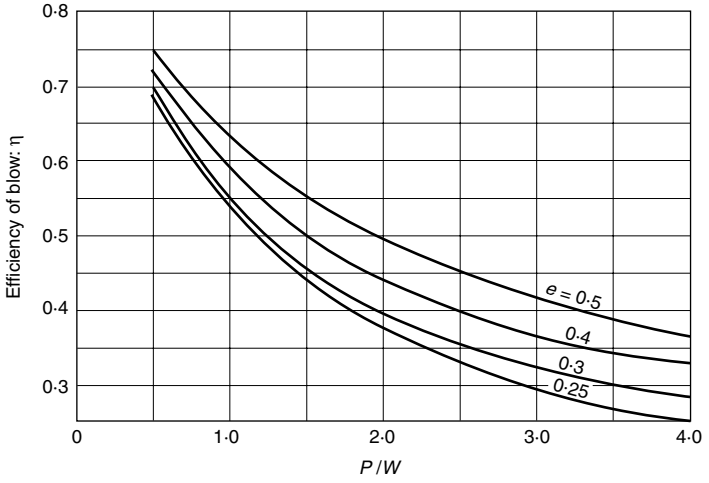

Fig. 6.8 Determination of efficiency factor, η, for use in the Hiley pile driving formula, after BSP Pocket Book (1969)

safety of 1.75 for any one pile, Flaate showed that it is necessary to use $F = 2.7$ with the Hiley formula and $F = 3.0$ with the Janbu procedure. Janbu's formula gave a slightly better correlation between tested and calculated bearing capacity and also the lowest arithmetic mean value of the factor of safety.

An example on the use of these formulae is given below:

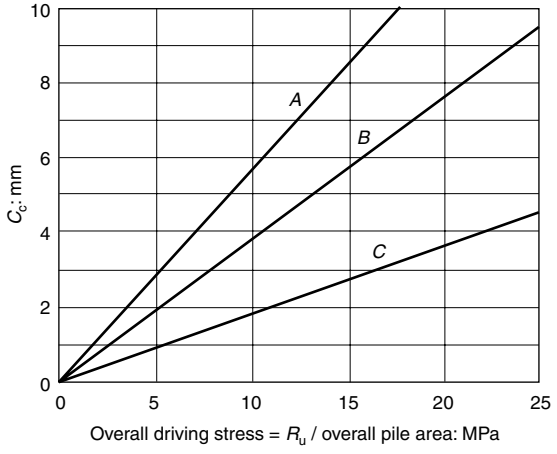

Fig. 6.9 Determination of temporary elastic compression C_c, after BSP Pocket Book (1969) Key: A = concrete pile, 75 mm packing under helmet; B = concrete or steel pile, helmet with dolly or head of timber pile. C = 25 mm pad only on head of RC piles

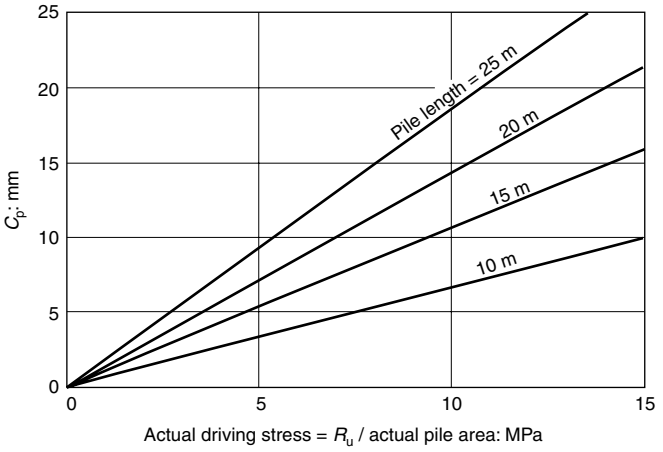

Fig. 6.10 Determination of temporary elastic compression C_p, for concrete piles, after BSP Pocket Book (1967)

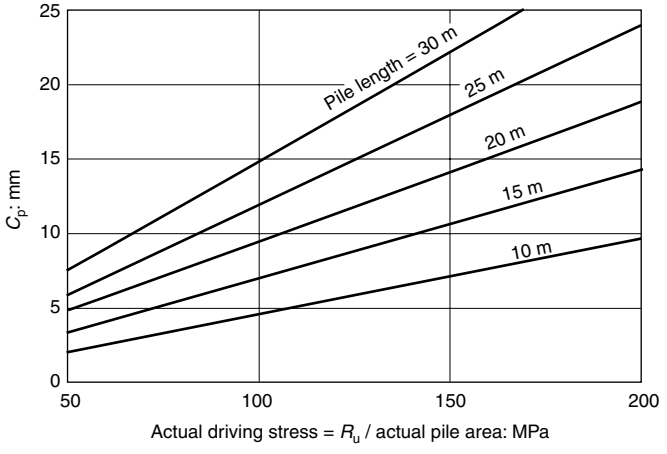

Fig. 6.11 Determination of temporary elastic compression C_p, for steel piles, after BSP Pocket Book (1969)

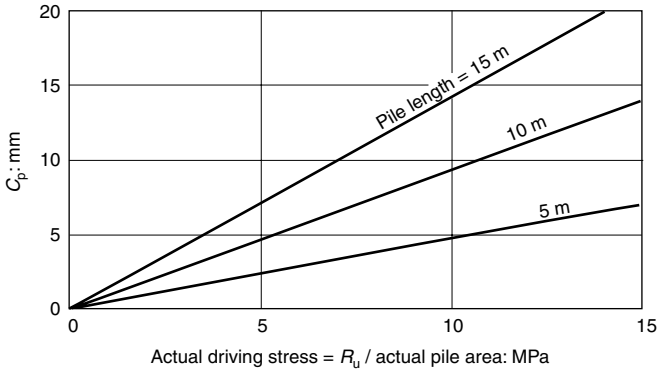

Fig. 6.12 Determination of temporary elastic compression C_p, for timber piles, after BSP Pocket Book (1967)

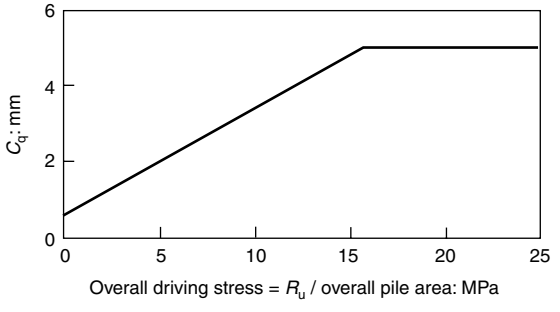

Fig. 6.13 Determination of temporary elastic compression C_q, after BSP Pocket Book (1969)

Table 6.2 Values of the coefficient of restitution, e, after BSP Pocket Book (1969)

Type of pile	Head condition	Single-acting or drop-hammer or diesel hammer	Double-acting hammer
Reinforced	Helmet with composite plastic or Greenheart	0.4	0.5
Concrete	Dolly and packing on top of pile		
	Helmet with timber dolly (not Greenheart) and packing on top of pile	0.25	0.4
	Hammer directly on pile with pad only		0.5
Steel	Driving cap with composite plastic or Greenheart dolly	0.5	0.5
	Driving cap with timber (not Greenheart) dolly	0.3	0.3
	Hammer directly on pile		0.5
Timber	Hammer directly on pile	0.25	0.4

WORKED EXAMPLE

A 400 mm × 400 mm reinforced concrete pile 20 m long is driven through loose materials and then into dense gravel to a final set of 3 mm/blow using a 30 kN single-acting hammer with a stroke of 1.5 m. Determine the ultimate driving resistance of the pile if it is fitted with a helmet, plastic dolly and 50 mm of packing on top of the pile. The weight of the helmet and dolly is 4 kN.

Weight of pile = 74 kN

Weight of helmet and dolly = 4 kN

Total weight, $P = 78$ kN

Weight of hammer, $W = 30$ kN

Therefore, $P/W = 78/30 = 2.6$. Using the Hiley formula

$e = 0.4$ (Table 6.2), hence $\eta = 0.39$ (Fig. 6.8).

H = effective height of fall of hammer

$= 0.9 \times 1.5$ m (Table 6.1)

$= 1.35$ m $= 1350$ mm

Assume a value for the ultimate driving resistance $Q'_u = 1250$ kN. Then

$$\text{Overall driving stress} = \frac{1250}{0.4 \times 0.4}$$

$$= 7813 \text{ kPa}$$

$$= 7.8 \text{ MPa}$$

If $c_c = 5.8$ mm (Fig. 6.9, $\frac{2}{3}A + B$), $c_p = 11.0$ mm (Fig. 6.10), $c_q = 2.8$ mm (Fig. 6.13).

Total $c = c_c + c_p + c_q = 19.6$ mm.

$$Q_u = \frac{WH\eta}{s + c/2} = \frac{30 \times 1350 \times 0.39}{3 + \frac{1}{2} \times 19.6}$$

$$= 1234 \text{ kN}$$

This is nearly equal to the assumed value of 1250 kN and hence the calculation need not be repeated.

Using the Janbu formula

$$\frac{\eta WHL}{AEs} = \frac{0.70 \times 30 \times 1.5 \times 20}{0.16 \times 14 \times 10^6 \times 0.003^2} = 0.3$$

$K_u = 7.1$

Then

$$Q_u = \frac{\eta WH}{sK_u}$$
$$= \frac{0.70 \times 30 \times 1.5}{0.003 \times 7.1} = 1479\,\text{kN}$$

It can be seen that in this case the Janbu formula predicts a greater ultimate pile capacity than the Hiley formula.

The corresponding working loads are:

- for the Hiley formula, $\frac{1234}{2.7} = 457\,\text{kN}$
- for the Janbu formula, $\frac{1479}{3} = 493\,\text{kN}$

Correlation with special sounding tests

Provided sufficient experience is available, that is, comparisons with pile loading tests, special sounding tests can be extremely useful, for example, driving rods, pushing and pulling rods, rotating rods, light Swedish rotary sounding apparatus.

Overdriving of piles

It is sometimes necessary to drive piles through dense sands and gravels, for example, either to penetrate an underlying clay layer, or because of the possibility of scour in river beds. Damage to the pile due to over-driving must be avoided, both when penetrating an overlying hard layer or when driving into the bearing stratum to develop the full bearing capacity. In this connection, it should be remembered that a penetration of up to five pile diameters into dense granular material may be necessary to develop fully the end bearing capacity.

The Hiley formula can be used to determine the failure, load, Q_u, and then the peak driving stress, P_d, is given by

$$P_d = \frac{Q_u}{A}\left(\frac{2}{\sqrt{\eta}} - 1\right) \tag{6.23}$$

Janbu (1953) suggests that the driving energy, $(WH)_c$, needed to avoid damage is limited by:

$$(WH)_c = \left(\frac{L}{2500} + 2s\right)\sigma_0 A \tag{6.24}$$

where L = pile length; s = set; A = cross-sectional area of the pile; σ_0 = half-compressive strength.

Group action of piles

Spacing

Upheaval of the ground surface caused by driving closely spaced piles into dense or incompressible material should be minimized and hence a minimum pile spacing is necessary. If the spacing is too large, on the other hand, uneconomic pile caps may result. When driving piles in sands or gravels, it is advisable to start driving at the centre of a group and then to work outwards, in order to avoid difficulty with 'tightening-up' of the ground. BS 8004:1986 suggests the following minimum pile spacing:

Type of pile	Minimum spacing
Friction	Perimeter of the pile
End bearing	Twice the least width
Screw piles	$1\frac{1}{2}$ times diameter of screw blades

The Norwegian Code of Practice on Piling, Den Norske Pelekomitè (1973), gives the following minimum pile spacing:

Length of pile	Friction piles in sand	Friction piles in clay	Point bearing piles
Less than 12 m	3 *d*	4 *d*	3 *d*
12 to 24 m	4 *d*	5 *d*	4 *d*
Greater than 24 m	5 *d*	6 *d*	5 *d*

Note: *d* is the pile diameter or largest side – the pile spacing is measured at pile cut-off level, unless raking piles are used, in which case the spacing is measured at an elevation 3 m below pile cut-off level.

Settlement of pile groups in clays

It is clear that settlement of a group of piles in clay cannot be predicted from the results of a loading test on a single pile. This is because time effects, remoulding of the soil owing to pile driving and scale effects are quite different for the single test pile from the pile group. The action of the piles is to transfer the load to some lower stratum and various suggestions have been proposed as to how to include this load transfer in settlement calculations. Once a load transfer is assumed, then settlement calculations can be made in the usual manner.

The following assumptions have been used:

(1) An equivalent raft at two-thirds the pile length over the area enclosed by the piles at that depth.
(2) An equivalent raft at two-thirds the pile length over a larger area, because of side friction on the group of piles. A spread of one horizontal to four vertical may be reasonable.

(3) An equivalent raft at the base of the piles over the area enclosed by the piles at this depth.
(4) An equivalent raft at the base of the piles over a larger area.

The differences between these assumptions are clearly appreciable. Comparing (1) and (3) above, which appear to be those in most common use, a design using assumption (1) would provide piles 50% longer than one using assumption (3) for the same allowable maximum settlement. This is clearly illogical. For displacement piles, assumption (1) would seem to be a suitable choice, as it would, in general, give a greater computed settlement than (3), and so would in some measure allow for the disturbance caused by pile driving. For bored piles, particularly if they are closely spaced, assumption (3) seems realistic.

Settlement of pile groups in granular soils

It should be possible to calculate the settlement of a group of piles in granular soils in a manner similar to that employed for pile groups in clay. This is to assume some form of distribution of load and then to calculate the settlements using the results of Dutch cone or standard penetration tests. This procedure is not generally adopted, however, and it is usual to base settlement predictions for pile groups on the results of loading tests on individual piles.

Skempton (1953) has compared the settlements of a number of pile groups with the settlements of corresponding individual piles. He has proposed the following relationship between the settlement, δ_B, of a pile group of width B m, and the observed settlement δ_s, of a single pile at the same load intensity:

$$\frac{\delta_B}{\delta_s} = \left(\frac{4B+3}{B+4}\right)^2 \tag{6.25}$$

Care should be taken when piles are driven into sands and gravels which are underlain by clays. This is because the stresses transferred to the clays from the pile group may result in over-stressing or excessive consolidation. The factor of safety against a bearing capacity failure in the clay can be assessed by assuming a spread of load onto the surface of the clay in a similar manner as indicated in Fig. 4.5. The settlement in the underlying layer can be computed in the normal way by first determining the distribution of stress throughout the clay layer, using, for example, Fig. 3.3.

An interesting case record has been described by Terzaghi (1939). Timber piles for a hospital in New Orleans were driven through clay to virtual refusal into a sand deposit. There were no measurable settlements under a pile test load of 15 tons, and the piles were designed to carry this loading. During construction, a settlement of 100 mm occurred, which

increased to 300 mm after 2 years. This was due to a compressible clay layer underlying the sand.

Bearing capacity of pile groups in clay

It has been recognized for some time that a group of piles may fail as a block under a loading less than the sum of the bearing capacity of the individual piles.

In an interesting series of model experiments carried out at the Building Research Establishment (Whitaker, 1970), it was shown that a group of piles in clay could either fail as individual piles or as a block. A block failure occurred for pile spacings of the order of two diameters. For wider spacings the piles failed individually but the efficiency ratio (equal to the average load per pile in the group at failure divided by the failure load of a single comparable pile) only reached unity at a spacing of about eight diameters.

The stability of a group of piles may be checked using Terzaghi and Peck's block failure hypothesis, where the failure load of a pile group, Q_g is given by:

$$Q_g = N_c \times A_b \times s_u + A \times \bar{s}_u \tag{6.26}$$

where, N_c = bearing capacity factor; A_b = base area enclosed by the pile group; $\bar{s}_u$ = undrained shear strength at base of pile group; A_s = perimeter area of pile group; s_u = average undrained shear strength around the perimeter of the piles.

In addition to checking block failure, Tomlinson (1969) has suggested taking an efficiency ratio of 0.7 for a spacing of two diameters increasing to unity at a spacing of eight diameters.

Bearing capacity of pile groups in granular soils

The action of driving pile groups into granular soils will tend to compact the soil around the piles. In addition, because of the greater equivalent width of a pile group as compared with a single pile, the ultimate failure load will tend to increase. For these reasons, the efficiency ratio of a group of piles in granular soils will be greater than unity, or for large pile spacings equal to unity.

It is unusual to take this into account in design.

Care must be taken, of course, to ensure that no weaker or more compressible soil layers occur within the zone of influence of the pile group.

When driving piles into dense granular soils, care must be taken to ensure that previously driven piles are not lifted by the driving of other piles.

For further discussion on group action, reference can be made to Tomlinson (1969) and Whitaker (1970).

Negative skin friction

When piles are driven through strata of soft clay into firmer materials, they will be subjected to loads caused by negative skin friction in addition to the structural loads, if the ground settles relative to the piles. Such settlement may be due to the weight of superimposed fill, to ground water lowering, or a result of disturbance of the clay caused by pile driving (particularly large displacement piles in sensitive clays leading to reconsolidation of the disturbed clay under its own weight).

This additional loading due to negative skin friction may be so large as to cause over-stress of the pile material or may lead to large settlements, or even failure, in the underlying supporting soil.

An interesting example of the development of negative skin friction forces has been described by Johannessen and Bjerrum, (1965). A hollow steel pile was driven through about 40 m of soft blue clay to rock, and 10 m of fill was placed around the pile. After $2\frac{1}{2}$ years, the ground surface had settled nearly 2 m and the pile had shortened by 15 mm. The compressive stress induced at the pile point, resulting only from negative skin friction, was 200 MPa. It was also found that the adhesion developed between the clay and the steel pile was equal to $0.2 \times$ (the effective vertical stress) and was also approximately equal to the undrained shear strength of the clay, measured by the in situ vane test, before pile driving.

The load transferred to the pile depends on:

- the pile material
- the type of soil
- the amount and rate of relative movement between the soil and the pile.

It appears that only a small relative movement, of the order of 10 mm is necessary for full negative skin friction to occur.

The maximum extra load per pile in a pile group due to negative skin friction, Q_{ns} is given by:

$$Q_{ns} = A_s \times \bar{s}_u \times \alpha \tag{6.27}$$

or

$$Q_{ns} = \frac{A_g X \bar{s}_u + W}{n} \tag{6.28}$$

whichever is smaller, where A_s = circumferential area of a pile; A_g = circumferential area of the pile group; $\bar{s}_u$ = average undrained shear strength along length of pile; α = adhesion factor; W = buoyant weight of soil within pile group; n = number of piles.

To reduce negative skin friction, the following measures have been used:

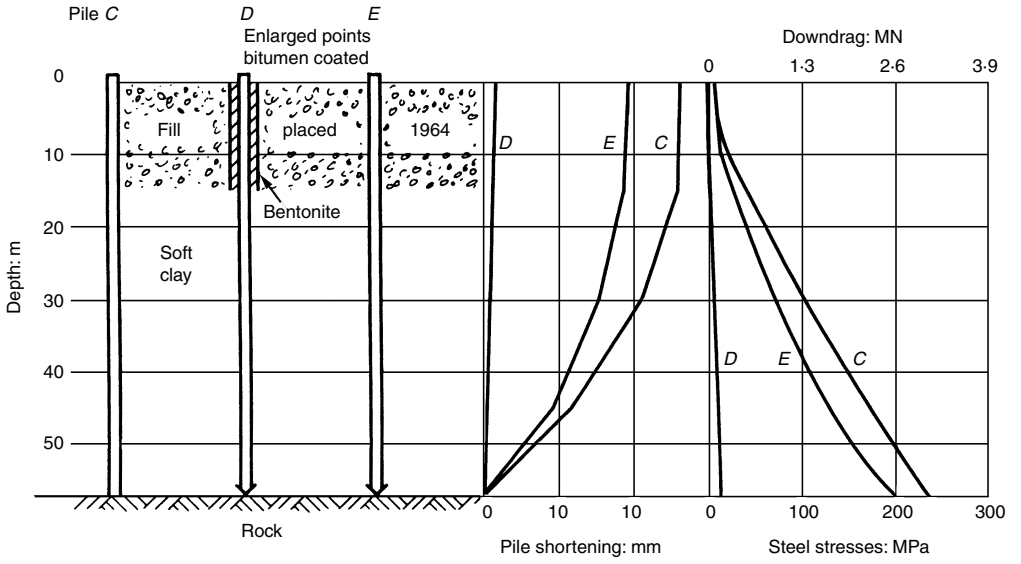

Fig. 6.14 Examples of the effects of negative skin friction on the behaviour of piles, after Bjerrum, Johannessen and Eide (1969)

- In Holland, for example, using precast concrete piles with shafts of small cross-sectional area compared with the points (Plantema and Nolet, 1957).
- Driving piles inside a casing with the space between pile and casing filled with a viscous material and the casing withdrawn (Golder and Willeimier, 1964).
- Coating the piles with bitumen.

An example of the successful use of bitumen coating on piles has been given by Bjerrum *et al.* (1969). At Sørenga, Norway, three test piles *C*, *D*, *E* were installed in 1966 through about 15 m of fill consisting of rock fill and boulders placed in 1964, overlying about 40 m of soft marine clay. The test piles were full-scale steel tube piles with a diameter of 500 mm and a wall thickness of 8 mm.

Pile *C*, see Fig. 6.14, was the reference untreated pile, and piles *D* and *E* were both coated by a 1 mm thick layer of bitumen and were driven with an enlarged point of diameter 690 mm. In order to protect the bituminous coating on pile *D* from being damaged during driving through the fill, an outer casing of diameter 630 mm was driven down through the fill with the pile section, and the space between the pile and the casing was filled with bentonite slurry. No precautions other than the enlarged point were undertaken to protect the bitumen on pile *E* when it was driven through the fill.

About a year after driving the test piles, the negative friction on the reference pile, pile *C*, amounted to about 3000 kN just above the point with a corresponding steel stress of 226 MN/mm^2. The pile top had settled more than 50 mm, of which 25 mm was due to the penetration of the pile point into rock. Pile *D* was coated with bitumen and driven with the outer casing as protection against the fill, and showed at that time a negative skin friction load of about 150 kN. The necessity of using a casing through the fill to protect the bitumen was clearly illustrated by the observations on pile *E.* In spite of its bitumen coating, the load due to negative skin friction amounted to 2600 kN. These results are illustrated in Fig. 6.14. It can be concluded that a bitumen coating provides a most efficient means of reducing negative skin friction loads, provided the integrity of the coating is ensured when driving the pile through coarse overlying fill material.

Results of measurements of negative skin friction on piles have been presented by Gant *et al.* (1958), Fellenius and Broms (1969), Endo *et al.* (1969), Walker and Darval (1973). Theoretical expressions for the design of pile foundations taking into consideration negative skin friction have been developed by Buisson *et al.* (1960), Zeevaert (1960), Brinch Hansen (1968), Paulos and Mattes (1969) and Sawaguchi (1971).

Bjerrum (1973) drew attention to the fact that the adhesion developed between a pile and clay was dependent not only on the pile material, the type of clay, the time elapsed between installing the pile and testing it, and the presence or otherwise of other material overlying the clay, but also on the rate of relative deformation between the pile and the soil. For soft compressible clays, it is known that the lower the rate of relative deformation, the smaller will be the developed adhesion. For cases where the rate of relative movement is high, the procedure outlined above may be used to estimate the magnitude of the negative skin friction forces. When the rate movement is small, Bjerrum suggested that the negative skin friction, s_α, could be estimated from the simple equation:

$$s_\alpha = Kp'_0 \tag{6.29}$$

where,

$K = 0.25$ for very silty clay,

$= 0.20$ for low plasticity clays,

$= 0.15$ for clays of medium plasticity,

$= 0.10$ for highly plastic clays.

Although a bitumen coating on piles can lead to great reductions in negative skin friction forces, it must be ascertained that the integrity of the coating will be maintained during the period of the relative movement between soil and pile. A case in Perth, Western Australia was discussed by

Simons (1971b). The ground conditions consisted of about 20 m of soft, normally consolidated clay on which embankments up to 18 m high were placed, leading to settlements of up to 7 m. Four unloaded steel test piles were put down, two coated with bitumen and two were uncoated. The uncoated piles soon picked up a large negative skin friction load, whereas the bitumen-coated piles initially showed little load pick-up. After some months, the loads on the coated piles began to increase, eventually reaching the same order of magnitude as the loads on the uncoated piles. This was apparently due to bacteriological action in the clay attacking the bitumen coating. Caution must therefore be exercised when transferring experience from one part of the world to another.

If piles subjected to negative skin friction forces are founded in granular material, then not only must the additional pile loading be taken into account in design, but also the reduction in bearing capacity of the granular material, due to the decrease in the effective overburden pressure on the surface of the granular soil, brought about by the transfer of load to the pile.

Based on a bearing capacity equation put forward by Brinch Hansen (1968), which takes into consideration the penetration of a foundation into the bearing stratum, Simons and Huxley (1975) have presented a series of solutions incorporating as variables:

- pile diameter
- pile penetration into the granular material
- angle of shearing resistance of the granular material
- effective overburden pressure on the surface of the granular material.

These solutions allow the bearing capacity of a pile to be read-off, once the friction angle and reduction in effective overburden pressure on the surface of the granular material due to negative skin friction, have been assessed.

An example is given in Fig. 6.15, and it can be seen that for small penetrations and small effective overburden pressures, the calculated failure load in the granular material is less than the allowable load which the concrete in the pile can carry.

It should be noted that a solution to this problem was proposed by Zeevaert (1960). This solution did not consider the effect of pile penetration into the bearing stratum and is somewhat unrealistic as it follows logically from this limitation that the bearing capacity of any pile driven into granular material occurring at the ground surface, is zero.

The Norwegian Code of Practice on Piling, Den Norske Pelekomitè (1973) recommends:

- That negative skin friction be calculated to a depth D where the ground settles 5 mm more than the piles.

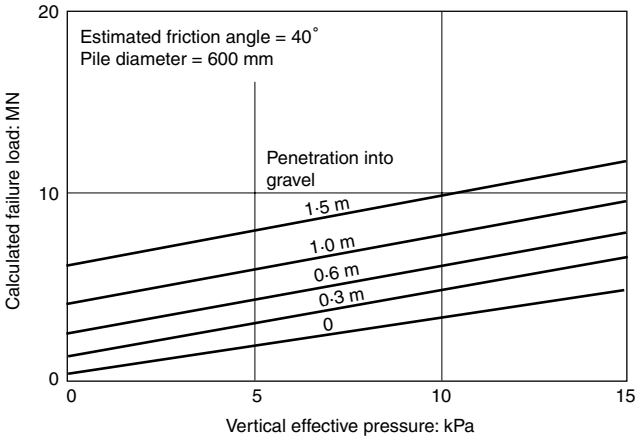

Fig. 6.15 Effect of negative skin friction forces on the bearing capacity of piles founded in granular soils, after Simons and Huxley (1975)

- If displacement piles are driven at close centres leading to ground displacements and the establishment of excess pore-water pressures, and the subsequent ground settlement is due only to these factors, and not due to nearby filling, then a reduced value of negative skin friction load can be adopted, for example by using half the undrained shear strength for soft clays, or assuming the adhesion is equal to 0.1 times the vertical effective stress.
- An upper limit to the submerged weight of soil which can be transferred to a group of piles of plan area $B \times L$ is obtained by considering a volume of soil equal to $D \times (B + D/4) \times (L + D/4)$.
- It is considered satisfactory to operate with the minimum calculated value for negative skin friction load.
- Bitumen coating of piles leads to significant reduction in negative skin friction forces. Measurements show that bitumen coatings have reduced adhesions of 50 to 60 kPa for uncoated piles to 5 to 15 kPa for coated piles.
- For steel piles, a bitumen coating thickness of 1 mm should be used, and for concrete piles, a thickness of 2 mm is suggested.
- Provision must be made to avoid damage to the coating during pile driving, using, for example, enlarged pile points or driving inside a casing if overlying granular material is present.

Lateral loads on piles

Lateral loads applied to groups of piles can be carried either by the horizontal components of raking piles or by the lateral resistance of the soil surrounding vertical piles. If vertical piles are subjected to substantial horizontal forces, then the upper levels of the ground should be able to

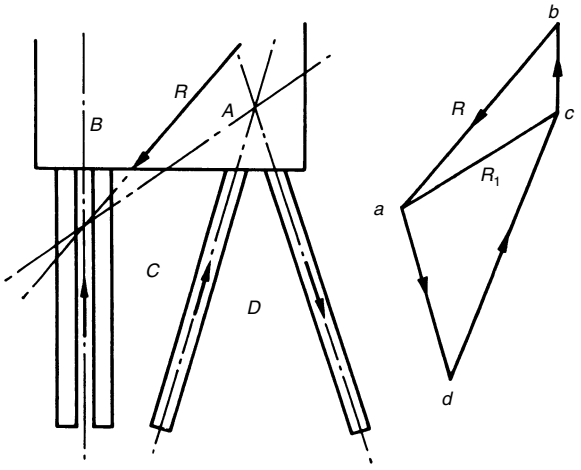

Fig. 6.16 Graphical procedure for determining the distribution of loads for a group of vertical and raking piles

resist these forces without excessive lateral movement occurring. It may be necessary to connect pile caps with horizontal beams to obtain sufficient resistance. If these measures are insufficient, then raking piles should be used.

Lateral loads on raking piles

The computation of the forces and moments transmitted to a group of vertical and raking piles presents an extremely difficult problem to which no satisfactory solution exists at present.

It is usual to base the analysis on severe simplifying assumptions, for example, that the piles are axially loaded, that Hooke's law is obeyed, that the lateral restraint to the piles from the soil can be ignored, and that the piles are hinged top and bottom.

A simple graphical procedure is illustrated in Fig. 6.16.

Lateral loads on vertical piles

A guide to the allowable horizontal forces that may be applied at ground level to the tops of vertical piles is given in Table 6.3 for short term loading of timber and concrete piles in clay. Table 6.4 gives allowable long term loads for timber and concrete piles in clay, silt and sand. For the short term case, the maximum bending moment occurs at a depth of between 0.5 and 1.5 m, and for the long term case the critical depth is between 1 and 1.5 m.

There are three design considerations:

- The pile must be able to carry the bending moments.

Table 6.3 Guide to allowable horizontal force applied to the top of a timber or concrete pile for short term loading, in clays, after Den Norske Pelekomitè (1973)

		Allowable short term lateral load in clays (kN)		
Pile area (m^2)	Max bending moment (m kN)	$s_u = 10$ kPa	$s_u = 25$ kPa	$s_u = 50$ kPa
0.04	4.5	7	15	20
0.06	8.5	10	20	30
0.09	15.0	15	30	40

Table 6.4 Guide to allowable horizontal force applied to the top of a timber or concrete pile for long term loading, after Den Norske Pelekomitè (1973)

		Allowable long term lateral load (kN)		
Pile area (m^2)	Max bending moment (m kN)	Clay $\tan\phi' = 0.5$	Silt $\tan\phi' = 0.7$	Sand $\tan\phi' = 0.9$
0.04	4.5	5	6	7
0.06	8.5	8	10	12
0.09	15.0	13	16	19

- The soil must be able to support the loading.
- The lateral deflections must be tolerable.

For a group of vertical piles carrying an inclined eccentric load, R, as shown in Fig. 6.17, the vertical load, P_v, on any one pile is given by:

$$P_v = \frac{V}{n} + \frac{Ve\bar{x}}{\bar{x}^2} \tag{6.30}$$

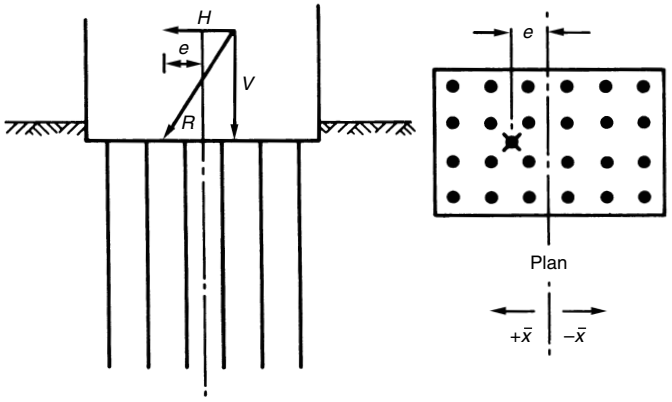

Fig. 6.17 Group of vertical piles under an inclined eccentric load

where V = total vertical load on the group; n = number of piles in the group; e = eccentricity of the load; $\bar{x}$ = distance from centre line of a pile to the neutral axis of the pile group; it is positive when measured in the same direction as e, and negative when in the opposite direction.

The procedures outlined below, to calculate horizontal loads on vertical piles, follow the proposals suggested by Broms (1964a, 1964b, 1965a) which are based on simplifying assumptions which are questionable. The reasonably good agreement obtained between the methods proposed and the results of field tests indicates, however, that the assumptions are justified.

Single piles in cohesive soils

Ultimate lateral resistance

Possible failure mechanisms for short and long unrestrained piles are shown in Fig. 6.18 and for short and long restrained piles in Fig. 6.19. Short piles imply that failure is governed by the soil strength, and with long piles, failure is governed by the moment of resistance of the pile.

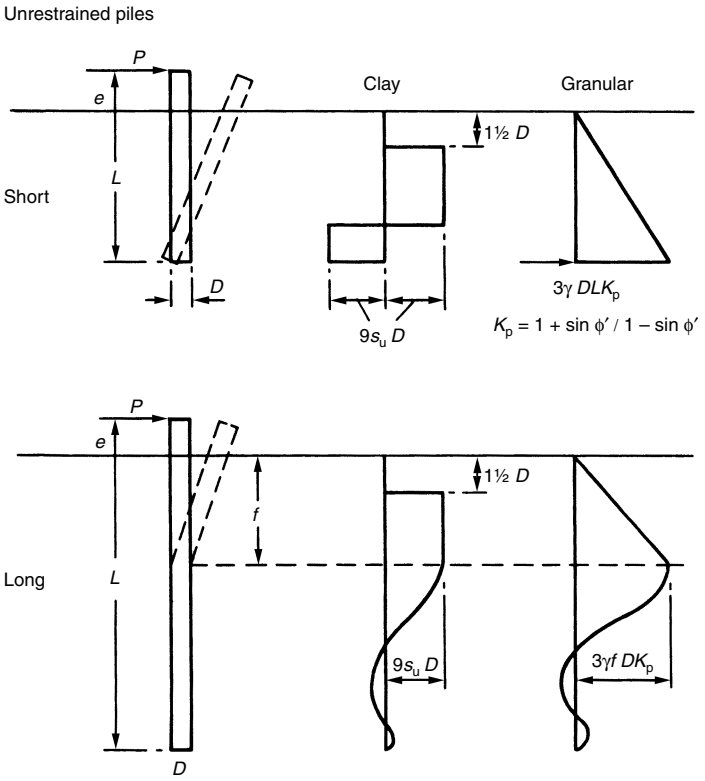

Fig. 6.18 Failure mechanisms for short and long unrestrained piles, after Broms (1965)

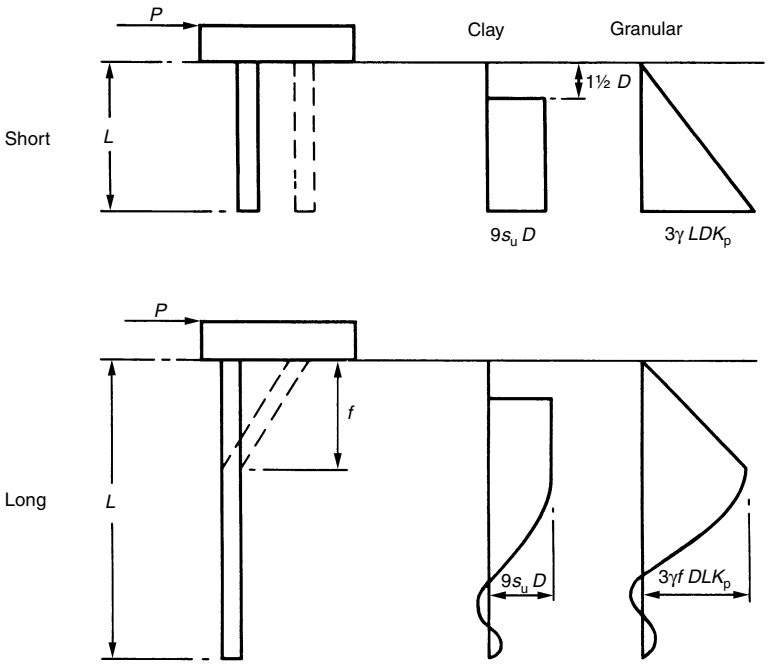

Fig. 6.19 Failure mechanisms for short and long restrained piles, after Broms (1965)

The ultimate value of soil resistance against a laterally loaded pile appears to vary between eight and 12 times s_u and there is some evidence to suggest that the value is somewhat smaller to a depth of about three pile diameters below the surface. Broms suggested, therefore, an assumed distribution of soil reaction of zero from the surface to a depth of 1.5 pile diameters and a constant value of $9\,s_u$ below this depth, as required.

Based on these assumptions, solutions are given in dimensionless form in Fig. 6.20 for short piles and Fig. 6.21 for long piles. For the case of restrained piles, it should be noted that the solutions imply that moment restraint from the pile cap, equal to the moment in the pile just below the cap, is available. In any particular case, the procedure is to determine from Fig. 6.20 that adequate penetration into the soil is obtained and then from Fig. 6.21 to check that the available moment of resistance of the pile section is not exceeded.

Lateral deflections

The calculation of lateral deflections is based on the coefficient of subgrade reaction, k, defined by the equation:

$$p = ky \tag{6.31}$$

where p is the applied pressure causing a deflection y.

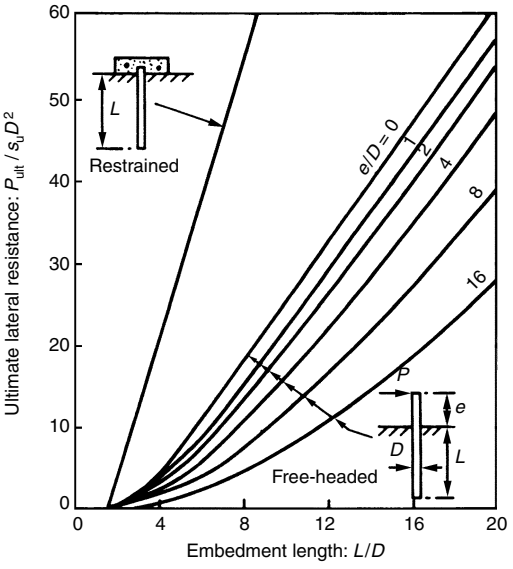

Fig. 6.20 Ultimate lateral resistance for short piles in cohesive soils, after Broms (1965)

It should be noted that the value of k depends not only on the nature of the soil but also on the size, shape and stiffness of the foundation which carries the load. It is extremely difficult to obtain values for k and hence only very approximate predictions of the magnitude of the lateral deflections of a laterally loaded pile can be expected.

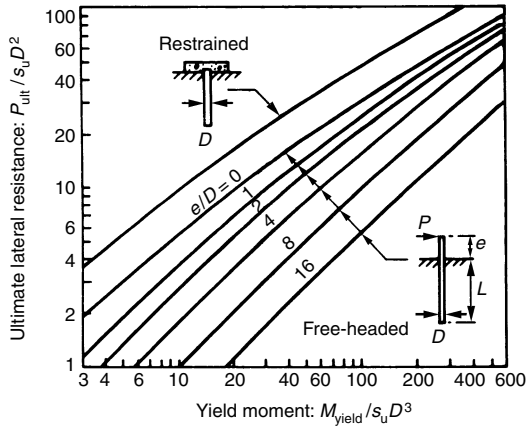

Fig. 6.21 Ultimate lateral resistance for long piles in cohesive soils, after Broms (1965)

Table 6.5 Values of k for cohesive soils

Undrained strength of clay, s_u (kPa)	50 to 100	100 to 200	200 to 400
k (kN/m^3)	8000	16 000	32 000

The deflections depend primarily on the dimensionless length βL where

$$\beta = \left(\frac{k_h B}{E_p I_p}\right)^{1/4} \tag{6.32}$$

where $E_p I_p$ is the stiffness of the pile section, B is the diameter or width of the laterally loaded pile in metres and k_h is the coefficient of horizontal subgrade reaction for the pile and depends on the deformation properties of the soil and on the dimensions and stiffness of the laterally loaded pile.

For long piles, $\beta L > 2.25$, the value of k_h to be used is obtained from:

$$k_h = 0.4\frac{k}{B} \tag{6.33}$$

where k is the coefficient of subgrade reaction, applicable to a square plate of breadth equal to 1 m.

Values of k can be estimated from Table 6.5.

For short piles, $\beta L < 2.25$, the value of k_h may be taken equal to:

$$k_h = \left(\frac{1L + 3B}{5L}\right)\frac{k}{B} \tag{6.34}$$

Preferably, the coefficient of horizontal subgrade reaction may be estimated from the results of lateral load tests on piles.

The lateral deflection at ground surface, y_0 is obtained from Fig. 6.22.

It is sufficient to consider variations in k_h to a depth of $\beta L = 2$ for restrained piles and $\beta L = 1$ for free-headed, when the piles are long.

For short piles, if k increases with depth, the value at a depth of $0.25L$ for a free-headed pile, and at a depth of $0.5L$ for a restrained pile, may be taken as the equivalent uniform value.

Single piles in granular soils

Ultimate lateral resistance

Possible failure mechanisms for unrestrained piles are shown in Fig. 6.18 and for restrained piles in Fig. 6.19. The following assumptions are made in the analysis:

- The active earth pressure acting on the back of a laterally loaded pile may be neglected.
- The distribution of passive pressure along the front of the pile is equal to three times the calculated Rankine earth pressure.

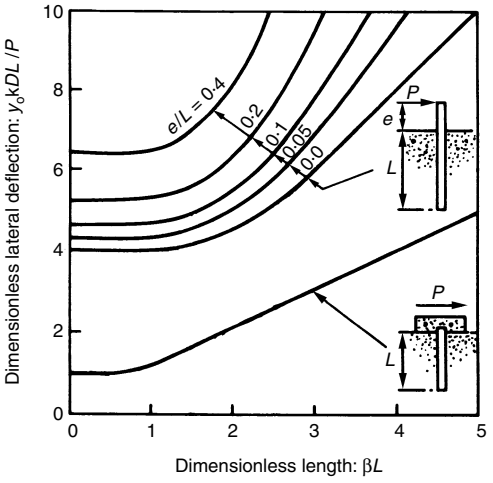

Fig. 6.22 Lateral deflections at ground surface for piles in cohesive soils, after Broms (1965)

- The shape of the pile section has no influence on the ultimate lateral resistance or the earth pressure distribution.
- The full lateral resistance is mobilized at the movements considered.

Based on these assumptions, solutions are given in Fig. 6.23 for short piles and Fig. 6.24 for long piles.

K_p is the coefficient of passive pressure

$$= \frac{1 + \sin \phi'}{1 - \sin \phi'}$$

and γ is the unit weight (submerged for high groundwater table).

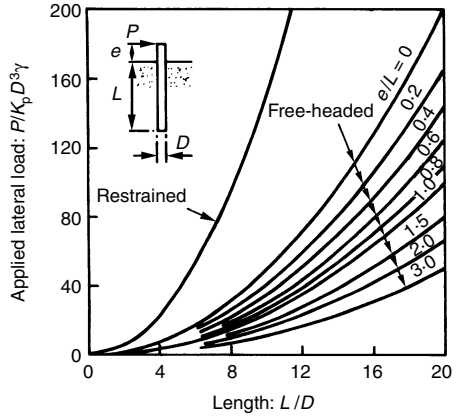

Fig. 6.23 Ultimate lateral resistance for short piles in granular soils, after Broms (1965)

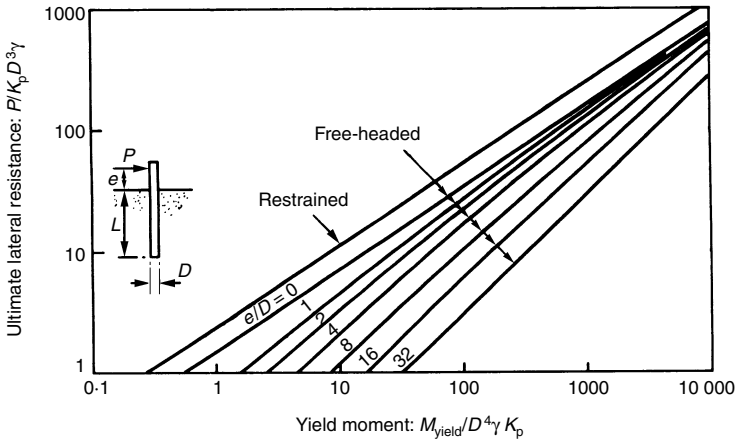

Fig. 6.24 Ultimate lateral resistance for long piles in granular soils, after Broms (1965)

Lateral deflections

The solution is again based on the use of a coefficient of subgrade reaction k_h which is assumed to be proportional to depth,

$$k_h = n_h \frac{z}{B} \tag{6.35}$$

The deflections depend on the dimensionless length, ηL where

$$\eta = \left(\frac{n_h}{E_p I_p} \right)^{1/5} \tag{6.36}$$

and values of n_h are given in Table 6.6.

The dimensionless lateral deflection $y_o(E_pI_p)^{3/5}(n_h)^{2/5}$ is plotted against the dimensionless length ηL in Fig. 6.25.

It should be noted that the lateral deflections may be larger than those indicated in Fig. 6.25, if jetting has been used.

The lateral deflections at ground surface for relatively short piles have been found to be mainly a function of the penetration depth and the deformation properties of the surrounding soil. The lateral deflections at the ground surface of a relatively long pile, however, are independent of the penetration depth but dependent on the stiffness of the pile section.

Table 6.6 Values of n_h for granular soils

Relative density of sand	Loose	Medium	Dense
n_h (dry or moist) (kN/m^3)	750	2250	6000
n_h (submerged) (kN/m^3)	400	1500	3600

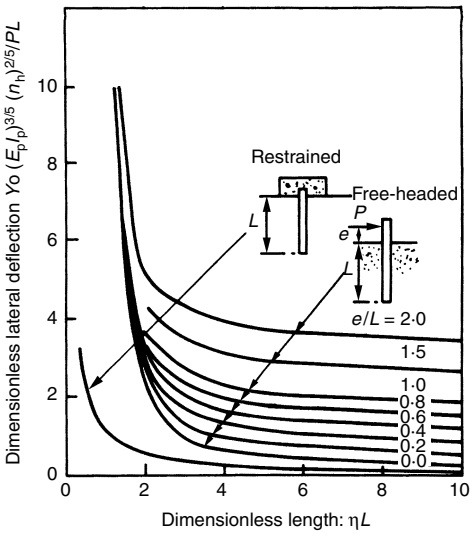

Fig. 6.25 Lateral deflections at ground surface for piles in granular soils, after Broms (1965)

The ultimate lateral resistance of short piles has been found to be governed by the penetration depth of the pile and to be independent of the pile section. The ultimate lateral resistance of long piles is governed by the ultimate bending resistance of the pile section and is independent of the penetration depth.

It should be pointed out that the ultimate lateral resistance of a pile group may be less than the ultimate lateral resistance calculated as the sum of the ultimate resistances of the individual piles. This effect is likely to be more pronounced for clays than for sands. Little or no reduction may be expected when the pile spacing is greater than four pile diameters. If the pile spacing is two pile diameters, then the piles and the soil within the pile group may behave as a unit.

General comments

- If raker piles have to be placed at the perimeter of a heavily loaded area in soil subject to significant settlement, then the risk of overstressing these piles is considerable, and heavy reinforcement may be necessary. Under such conditions, it may well be preferable to avoid using raking piles.
- It should be emphasized that because of variations in alignment of raker piles, the effects of differential settlement of a pile group, the stiffness of the pile cap, and the difficulty in determining with any precision the magnitude of the horizontal loads to be carried, the loads on individual raking piles may well vary quite substantially

from those obtained by analysis. A conservative approach should therefore be used.

- The performance of a vertical pile when subjected to a horizontal load is mainly controlled by the properties of the soil near the surface, for example, the upper 3 to 5 m. Seasonal variations in moisture content may therefore be of significance. It may be beneficial to remove poor surface soil and replace it with well compacted gravel.
- Repeated load applications may increase the lateral deflection to about twice that for constant loading.
- If piles are driven into granular soils the soil stiffness is increased and thus the lateral soil resistance is increased.
- There is considerable interaction between closely spaced piles in a group. For maximum lateral restraint, widely spaced piles are advisable, up to eight pile diameters in the direction of the load and about four pile diameters normal to the load.
- The lateral deflections resulting from restrained piles are much smaller than those from similar free headed piles.
- Further reference can be made to McNulty (1956), Clapham (1963), Reese and Matlock (1956), Broms (1964a, b), Broms (1965a), and Poulos (1971).

Pile testing

In this section, a brief review is given of methods which can be used to test piles. Pile loading tests are first discussed, followed by integrity testing.

Pile loading tests

Pile loading tests are carried out for the following reasons:

- To determine the settlement under working load.
- To determine the ultimate bearing capacity.
- As proof of acceptability.

There are two types of loading test which can be carried out, viz., the maintained load (ML) test, in which the loading is applied incrementally, and the constant rate of penetration (CRP) test.

In the ML test, the maximum load to be applied should be determined in advance, and the stages of the incremental loading, and unloading, should be prescribed. It is convenient to use increments of about 25% of the working load up to working load, with smaller increments thereafter. Each increment of load should be applied as smoothly and expediently as possible and simultaneous readings of time, and the load and settlement gauges are taken at convenient intervals as the load increases. For each loading increment, the loading should be held constant, and settlement

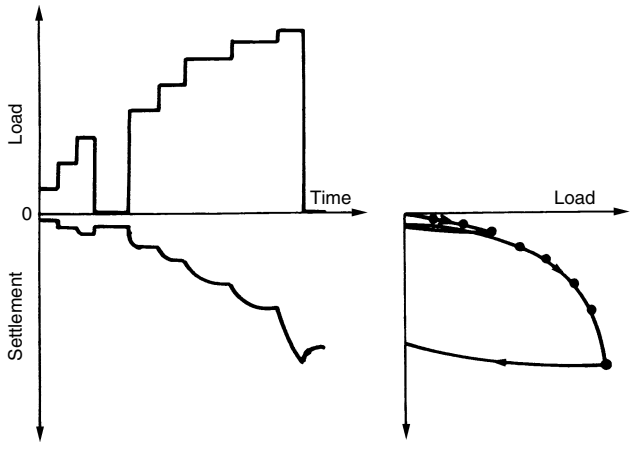

Fig. 6.26 Results of a maintained load pile test

readings taken at intervals of time which may be made progressively longer. A plot of settlement against time should be made as the test proceeds and the trend of the curve will indicate when movement has decreased to an acceptably small rate, which according to CP200 4:1972 may be taken as 0.1 mm in 20 minutes. It is usual to include unloading stages in the programme and one unloading stage, from the working load, is often specified. It is desirable to hold the working load for a period of 24 hours.

The results of a maintained load test are shown in Fig. 6.26, giving the curves of load and settlement versus time and of load versus the maximum settlement reached at each stage. The unloading stage is also plotted.

The maintained load test is commonly used to determine the ultimate bearing capacity of a pile. In practice, a well-defined failure load is not necessarily obtained and the following definitions of failure are often adopted:

- The failure load is that which causes settlement equal to 10% of the pile diameter, making allowance for the elastic shortening of the pile itself which may be significant for long piles.
- The failure load is that at which the rate of settlement continues undiminished without further increment of load, unless, of course, the rate is so slow as to indicate that it is due to consolidation of soil.
- The failure load is the load where the load settlement curve has its minimum radius of curvature.
- Drawing tangents to the initial and final portions of the load settlement curve and taking the point of intersection as the failure load.
- The failure load is that load which gives double the settlement for 0.8 of the failure load.

The ML test is time-consuming (because of having to wait until the rate of settlement drops to an acceptable value) and often the failure load is not clearly defined.

The CRP test has the advantage that it is quick and often results in a well-defined failure load. It has the disadvantage that it does not give the elastic settlement under the working load, which is of significance in determining whether or not there has been plastic yield of the soil at working load.

In the CRP test, the pile is jacked continuously into the soil, with the load being adjusted to give a constant rate of penetration. In this connection a pacing ring has been used to advantage. Failure is defined either as the load at which the pile continues to move downward without further increase in load, or the load at which the penetration reaches a value equal to 10% of the pile base diameter. It is important that the jack should have a travel greater than the sum of the final penetration of the pile and the upward movement of the reaction system. The movement of the reaction system may be about 75 mm if kentledge is used and about 25 mm with tension piles. In an end bearing pile the penetration in a test may reach as much as 25% of the pile base diameter and for a friction pile about 10% of the shaft diameter. A rate of penetration of about 0.75 mm/min has been found suitable for friction piles in clay, for which the penetration to failure is likely to be less than 25 mm. For end bearing piles in granular soils, where larger movements are necessary, rates of penetration of 1.5 mm/min may be required. Tests have shown that the actual rate of penetration, provided it is steady, may be half or twice these values without significantly affecting the result.

During the test, a plot of load against settlement should be made. The curve for a friction pile will be similar to those shown in Fig. 6.27,

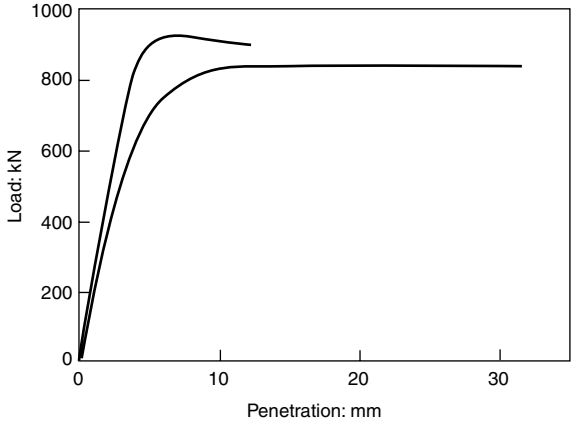

Fig. 6.27 Load settlement curve for a friction pile

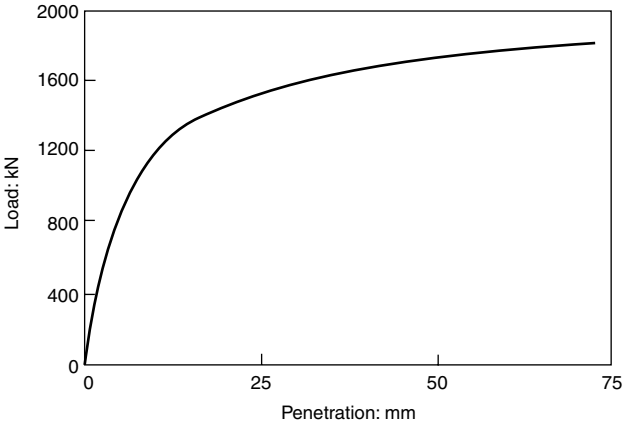

Fig. 6.28 Load settlement curve for an end bearing pile

usually a well-defined failure load at a small penetration, and for an end bearing pile as shown in Fig. 6.28, a poorly-defined failure load at a large penetration.

The reaction for the loading can be applied either (a) using kentledge applied directly to the pile, (b) by jacking against kentledge supported above the pile, or (c) by jacking against a beam tied down to tension piles. The supports in method (b) should be preferably more than 1.25 m away from the test pile. In method (c) any anchor pile should be at least four test pile diameters from the test pile, centre to centre, and in no case less than 1.5 m. When testing piles with enlarged bases, the spacing should be twice the base diameter or four times the test pile shaft diameter, whichever is larger, from the centre of the test pile to the centre of any anchor pile.

With kentledge, loads of up to 5000 kN can be applied. It is important to ensure that the arrangement is stable and safe. The set-up should be properly designed, and inspected regularly during load application for signs of distress. Observations of horizontal movement of the system may give an early indication of instability. Kentledge normally cannot be used to test raking piles, and care should be taken when building up kentledge on sloping ground.

Using tension piles, loads of up to 15 000 kN have been applied, and for large loads in particular, tension piles may well provide a more economical solution than kentledge. It is difficult to line-up accurately two tension piles with a test pile, but the system may be stabilized by cross-braces. It may be preferable to use three or four tension piles per test pile. Working piles are not normally used as tension piles.

When measuring loads, it is advisable to use an hydraulic capsule (up to 4500 kN) or a load measuring column (up to 10 000 kN) or a proving ring.

The height of the load measuring system should be kept as small as possible and the loading must be applied concentrically to the pile. A check on the load, for gross errors, may be obtained from the pressure gauge reading of the jack. Bourdon gauges are of low accuracy and should be regularly calibrated in a testing machine.

The settlements may be measured in the following ways.

(a) Direct levelling using a surveyor's level and staff to determine the movement of the pile head with reference to fixed datum. Preferably a check to a second datum should be carried out. A precision of reading of at least 1 mm is generally required

(b) Using dial gauges measuring off glass plates related to a reference beam supported on two foundations which are sufficiently far from the test pile and the reaction system to be unaffected by ground movement. The distance should not be less than three test pile diameters, or in no case less than 2 m. Readings should be taken to an accuracy of 0.02 mm and observations taken on at least two or preferably four points to check on any tilting.

(c) Using a strained high tensile wire, which is positioned against a scale fixed to the pile and the movement of the scale relative to the wire is determined to any accuracy of 0.5 mm.

Where methods (b) and (c) are used, protection of the beam or wire from sun and wind should be made. Regular temperature observations during the loading test should be carried out.

It is important that test piles are representative of the working piles, that is, they should be constructed in exactly the same manner as working piles. Furthermore, when evaluating test pile results, the fact that the soil conditions may well vary across the site should be considered. Finally, attention must be paid to time effects; sufficient time must be allowed between installation and testing for the soil conditions to be re-established around the pile, and it should be remembered that pile load tests are short-term, undrained tests, while working piles are loaded much more slowly. In this connection, reference can be made to Eide *et al.* (1961) who discussed the results of a long-term test loading of a friction pile in clay.

Integrity testing

There is increasing interest in methods which have been used to test the integrity of piles. Basically, methods are available which either test the pile material itself, or test the pile and soil together. Again, some methods require prior measures, whereas others do not. Some of the methods which are available are described in this section.

Pile loading tests

These have been discussed in some detail in the preceding sections. From the point of view of integrity testing, they suffer from the following disadvantages (Davis and Dunn, 1974):

(a) They are expensive and time-consuming.
(b) Because of (a), only a small number of piles is usually tested and this number is often not large enough to give statistically significant results.
(c) Because of (b), load tests can be regarded as measuring the performance of test piles only and do not serve to locate faulty piles.
(d) Test piles are seldom loaded up to failure.
(e) They are seldom carried out to determine the relative contributions of end resistance and skin friction.
(f) The test yields no information as to the actual dimensions of the pile under the ground; it only confirms that the pile is structurally strong enough to carry the test load without giving any measure of concrete quality.
(g) More care may be taken by the contractor in installing test piles than other piles. Hence results can be misleading.
(h) The pile is usually discarded after test and not included as part of the foundation.

Pile coring

Coring is the traditional method to check a suspect pile, by drilling using a diamond drill. Cores are collected from the axis of the pile and the composition of the cores examined to establish structural homogeneity. The process requires highly skilled and systematic workmanship and is expensive both in terms of time and money. To core drill a 10 m length of pile takes about two days. A caliper log of the drilled hole can also be made.

A much faster method, nowadays often used, is to drill holes in the pile by percussion equipment and then to examine the inner structure physically by lowering a television camera and watching the transmission on a screen. A 100 mm diameter hole, or perhaps a clean 50 mm diameter hole, is required. During drilling, the integrity of the pile can be roughly determined by the drill resistance and the composition and colour of the material blown out. The camera is necessary for confirmation and for those cases when the extent of discontinuity is small. The method is quick and about six 10 m long piles can be drilled and tested in a day.

Excavation

A well-established method used to examine piles is to set up headings under a foundation slab and observe the piles in situ. Timbering is

required and care must be taken not to damage piles during excavation. A major disadvantage is that in general piles are only exposed down to the groundwater level. If groundwater lowering is contemplated, thought must be given to possible effects of settlement or negative skin friction, which may be induced. Exposed piles should be measured and photographed and the pile material thoroughly examined.

Stressing internally cast rods or cables (Moon, 1972)

In principle, the method is that of applying a compressive force over the length of the pile by the stressing of internally cast, and recoverable, rods or cables. If the pile is significantly weakened by any form of fault, this becomes apparent by a downward movement of the top, in the case of a fault near the top, or by greater elongation of the stressing element than that due to stressing alone, indicating an upward movement of a lower section in the case of faulting nearer the base. A pile may have imperfections, but satisfactory application of a test load equal to or greater than the required capacity would prove them insufficient to require the condemning of the pile. It has been estimated that the test would increase the cost of a bored pile by some 12%.

Vibration testing (Gardner and Moses 1973; Davis and Dunn, 1974)

Vibration testing of piles has been developed by the Centre Experimental de Recherches et d'Etudes du Bâtiment et des Travaux Publiques (CEBTP) of France and the technique has been used on a number of sites in the UK.

A generator supplies a sinusoidal current of frequency f which can be varied from 0 to 1000 Hz. This current drives an electrodynamic motor of mass M which is installed at the head of the pile. The motor vibrates vertically and exerts a force F on the head of the pile.

$$F = F_0 \sin wt = M\gamma \tag{6.37}$$

where $\gamma = \gamma_0 \sin wt$ is the acceleration of the mass M. A signal from the motor feeds a regulator which keeps γ_0 constant. The head of the pile vibrates at the same frequency as the motor. The force constant F_0 can be determined by measuring the amplitude of F at a known frequency f. If the instantaneous velocity of the pile head V is measured continuously, the value of the velocity constant V_0 for any frequency can be determined from:

$$V = V_0 \sin wt + K \tag{6.38}$$

V_0/F_0 is called the modulus of mechanical admittance.

During the test the frequency is varied from 20 to 1000 Hz and an automatic plotter records the variation of V_0/F_0 with f. The shape of the resulting graph depends upon the soundness of the pile, the rigidity of the end

bearing and also the lateral restraint provided by the soil surrounding the pile.

The vibration method does not require any special provision to be made in the piles during casting. The pile heads require some preparation; the pile head must be level with the ground surface, and must be horizontal and smooth. The test will not detect minor defects but it is claimed that it will establish that a sound end bearing has been achieved and that the pile is free from major defects. Limitations on the use of the vibration test include a limiting length to diameter ratio of 20 and the requirement for the pile to be a right cylinder, although end bearing piles through soft alluvial deposits can be successfully tested with L/d ratios up to 30. It is necessary to test with no extraneous vibrations caused by site plant, which means testing at night on some sites. Also, if bulbs are formed at depth, it is usually impossible to learn anything about the state of the pile concrete below the bulb. The testing schedule need not interrupt the site programme, because between 25 and 40 piles can be tested per day, from pile ages of 4 days upwards.

It is claimed that the method can check or give a measure of:

- The pile length, or depth to first major discontinuity.
- The weighted average pile cross-section.
- The mass of the pile.
- The damping effect of the soil surrounding the pile.
- The apparent stiffness of the pile.

Sonic testing (Levy, 1970; Gardner and Moses, 1973)

The test is based on the measurement of time taken to pass sonic pressure waves horizontally between a transmitter and receiver. The transmitter and the receiver, which are made of piezoelectric ceramics, move within two (or three, for large piles) parallel, vertical, 42 mm diameter tubes cast into the pile. The tubes are first filled with water to ensure acoustic coupling and the transducers are raised within the tubes by a winch to keep them in the same horizontal plane. The difference in propagation times of the sound waves between the two tubes is represented as a linear trace on the oscilloscope. A zone of weak concrete is detected by a marked fainting of the signals and a sudden lengthening of the travel time. A Polaroid camera attached to the oscilloscope is used to obtain a permanent record of the results.

Radiometric logging (Forrester,1974)

These techniques give information on properties of materials at the atomic level. Measurements are unaffected by the way in which constituent atoms are bound together. It is possible by the measurement of

attenuation or scattering of gamma-rays that arise from radioactive sources to derive the density of concrete. The water content can be determined by the amount of moderation of fast neutrons by hydrogen.

Assuming that instrumental errors are small and that they can be kept to within 1%, the precision of density measurements by gamma-ray attenuation through concrete thicker than 200 mm depends on the distance of the source from the detector, the thickness of the concrete, the magnitude of the reading and the compaction of the concrete.

The measurement of the density of the concrete in a pile is a measure of its integrity. Measurement by attenuation of a gamma-ray involves the positioning of two vertical parallel tubes in the pile on a diameter. A source and a detector are lowered to the same level and the amount of attenuation of the radiation in the concrete is measured. This attenuation can be related to the density of the concrete. A 3% error in the density can arise from the variability of the source intensity and compositional changes in the solid component of the concrete examined can produce an apparent density error of 24%.

With the back-scatter technique the source and deduction are separated in a tubular probe by a lead block. The probe is lowered into a single tube pre-positioned vertically in the pile. Radiation from the source only reaches the detector by being scattered back from the tube and the concrete surrounding it. A sphere of concrete 100–150 m in diameter is surveyed by this technique and the errors in the estimation of the density can be up to 10%.

Excess water in the concrete can affect the estimation of the density because the attenuation and scattering of the gamma-rays by hydrogen is not in the same relative proportion as for other elements.

Water measurements by neutron moderation are carried out by a probe in a single tube. A radioactive isotope–light metal source generates fast neutrons and the slow neutrons produced by the interaction with hydrogen are measured by a selective detector. The probe has the generator and detector in one piece and the volume of concrete examined is a sphere of between 100–150 m in diameter. The precision of measurement can be within 10%

Safety in handling these devices is covered by their having to comply with the standards prescribed in the *Ionising Radiations (sealed sources) Regulations, 1969*.

Offshore pile design: total stress and effective stress approaches

Background

Pelletier *et al.* (1993) pointed out that the axial capacity of piles has been the subject of many studies over the past five decades of active offshore

development. Design methods during this period were based on static load tests, static design equations (using laboratory sample strength data or estimated skin friction), and/or dynamic driving formulas. Offshore practice was largely an extension of onshore practice.

Prior to the 1950s, onshore pile design capacities were most commonly based on dynamic-driving formulae such as the Engineering News Formula. A number of static load test programs were performed by various investigators during this period that gradually shifted design practice more towards the use of static design equations. Initially, estimated values of skin friction based on general descriptions of various soil types and consistencies were used with this equation. Later, laboratory strength data played a more important role in establishing design parameters.

Total stress design of axially loaded piles in clay

With the static method of analyses, the ultimate pile capacity is computed by adding the shaft friction resistance, Q_f, to the point or end bearing capacity, Q_p. The shaft friction is computed by integrating the unit skin friction, f, over the embedded surface area of the pile. There are a number of different methods for estimating the unit skin friction, and it is these methods that give rise to the primary controversy for piles in clay. Both effective stress methods, with f being a function of the soil friction angle, overburden stress, etc., and total stress methods, with f being a function of undrained shear strength, overconsolidation ratio, etc., have been proposed. There is a reasonable agreement that the unit end bearing is,

$$q = N_c s_u \tag{6.39}$$

where N_c is the bearing capacity factor, usually assumed equal to 9, and s_u is the undrained shear strength of the soil at the pile tip. This value is integrated over the area of the pile tip if the pile is considered plugged, or over the pile annulus if it is unplugged. The internal plug capacity is usually calculated using the formulation for external skin friction.

Prior to the mid 1950s, the static method specified that f be equal to s_u, if the design s_u value did not exceed 1000 psf (47.8 kPa). This approach was used to design piles for platforms installed in the Gulf of Mexico between 1946 and 1956. In 1956 McClelland Engineers formalized this procedure for offshore pile design.

Additional studies of pile load test data were conducted in the late 1950s to correlate the ratio of average unit skin friction (f_{ave}) to s_u. The ratio of $(f_{ave})/s_u$ was termed the friction ratio, α, whence skin friction is:

$$f_{ave} = \alpha s_u \tag{6.40}$$

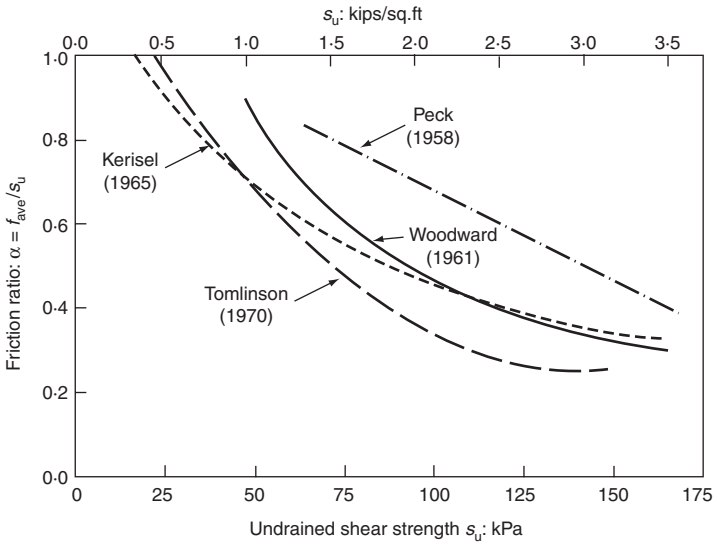

Fig. 6.29 Correlations of friction ratio, α, with undrained shear strength, s_u (after McClelland, 1974)

Most of these studies stated that α decreases with increasing s_u. The study by Tomlinson (1957) showed that α reduced substantially below 1.0 when f exceeded 0.50 kips/sq. ft. (23.9 kPa) as shown in Fig. 6.29. Other studies conducted by Peck (1958), Woodward *et al.* (1961), and Kerisel (1964), confirmed that lower values of α exist for large values of s_u as also shown in Fig. 6.29.

In 1962, McClelland Engineers modified their design practice for offshore piles such that f would be assumed equal to s_u for penetrations less than 100 ft (30.5 m) for normally consolidated clays. In overconsolidated clays, f would be limited to 1000 psf (47.8 kPa) or the s_u value expected at that depth for a normally consolidated clay of the same plasticity, whichever is greater (McClelland Engineers 1967). Similar concepts were later published by McClelland *et al.* (1969), and McClelland (1972). In a subsequent discussion to McClelland's 1972 paper, Wroth (1972) generalized this idea, stating that α values, plotted against overconsolidation ratio (OCR), would have a similar trend as those plotted against s_u. Later, McClelland (1974) concluded, 'that α would have a value of 1.0 in a deep normally consolidated clay which was stiff by virtue of large overburden pressures rather than from some source of overconsolidation'. Therefore, α would have a value of 1.0 for deep normally consolidated clays. The design criterion of McClelland Engineers (1967) was routinely included as Appendix C in McClelland's site investigation reports used for offshore pile design.

Effective stress design of axially loaded piles in clay

Throughout the 1970s, a number of other studies were conducted to improve the empirical correlations for computing the unit skin friction resistance as described by Focht (1988). Vijayvergiya and Focht (1972) published the λ-method that correlates f to both s_u and the vertical effective stress σ'_v by:

$$f = \lambda(\sigma'_v + 2s_u) \tag{6.41}$$

Various forms of the so-called β-method were proposed in which f was correlated to the estimated lateral elective stress by

$$f = K\sigma'_v \tan\delta = \beta\sigma'_v \tag{6.42}$$

where δ is the effective angle of friction between the clay and the pile shaft, and K relates the effective overburden pressure, σ'_v, to the horizontal effective stress σ'_h by

$$\sigma'_h = K\sigma'_v \tag{6.43}$$

It can be seen that β is similar to the empirical factor α, the important difference being that β is related to the fundamental effective stress parameters K and δ (Burland 1973).

This *effective stress* approach to shaft friction of piles in clay was first published by Burland (1973) with subsequent versions by Meyerhof (1976), Parry and Swain (1977), Flaate and Selnes (1977), and Janbu (1976). Various theoretically based, effective stress approaches were also developed during this period, as described by Esrig *et al.* (1977) and Esrig and Kirby (1979).

Randolph and Murphy (1985) used equations 6.40 and 6.42 to relate α and β via the strength ratio (s_u/σ'_v) as:

$$\beta = \alpha(s_u/\sigma'_v) \tag{6.44}$$

In this way, effective and total stress approaches were combined. Using equations developed from effective stress methods to estimate α, they proposed an incremental analysis to compute the ultimate shaft capacity. They derived peak skin friction at any depth to be:

$$\tau_s = [(s_u/\sigma'_v)_{nc}]^{0.5} s_u{}^{0.5} \sigma'_v{}^{0.5} \quad \text{for } (s_u/\sigma'_v) \leq 1.0 \tag{6.45}$$

and

$$\tau_s = [(s_u/\sigma'_v)_{nc}]^{0.5} s_u{}^{0.75} \sigma'_v{}^{0.25} \quad \text{for } (s_u/\sigma'_v) > 1.0 \tag{6.46}$$

where the subscript 'nc' stands for the normally consolidated state.

They verified their method by using a database of over one thousand axial load tests on piles that had been assembled under the auspices of the American Petroleum Institute (API).

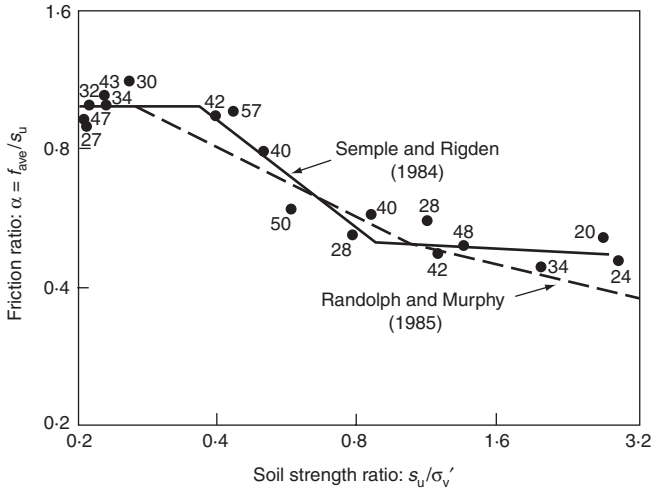

Fig. 6.30 Correlations of friction ratio, α, with strength ratio, s_u/σ_v', for $L/D < 60$ (after Young, 1991)

Semple and Rigden (1984) correlated peak values of α on relatively rigid piles to the over-consolidation ratio of the soil as reflected by the strength ratio, (s_u/σ_v') as shown in Fig. 6.30. The pile embedment ratio L/D, was used as a convenient simplification of pile stiffness for assessing the length effects associated with progressive strain-softening at the pile-soil interface and pile whip during driving. Semple and Rigden point out that the correlation of α with the degree of overconsolidation was previously recommended by McClelland (1974) and Wroth (1972). Thus an α value of unity is suggested for normally consolidated clays, regardless of s_u, and smaller α values are proposed for overconsolidated clays. The close agreement between the computed values obtained by the Semple and Rigden and Randolph and Murphy methods is shown in Fig. 6.30.

Since s_u/σ_v' is an implicit measure of soil overconsolidation ratio, highly overconsolidated soils have low α values. Conversely, normally consolidated soils have α values close to or equal to unity (Pelletier *et al.* 1993).

Design of axially loaded piles in sand

The basic design method for axially loaded piles in sand is similar to that for clays in that total pile capacity, Q, is the sum of the shaft resistance, Q_f, and the toe resistance or 'end bearing', Q_p. The shaft resistance is the integral over the embedded pile area of the unit skin friction value, f, which, for cohesionless soils is taken as:

$$f = K\sigma_v' \tan\delta \leq f_{max} \tag{6.47}$$

where K is a dimensionless earth pressure coefficient, σ'_v is the effective overburden pressure, δ is the friction angle between the pile and the soil and f_{max} is a maximum or limiting value of f. The toe resistance is taken as the unit end bearing, q, acting over all or part of the pile tip, which for cohesionless soils is taken as:

$$q = \sigma'_v N_q \leq q_{max} \tag{6.48}$$

where N_q is a dimensionless bearing capacity factor and q_{max} is a maximum or limiting value. If the pile is open ended the soil plug will develop frictional resistance on the internal pile wall that can be added to the end bearing of the pile annulus with the constraint that the total end bearing remains less than q times the tip area.

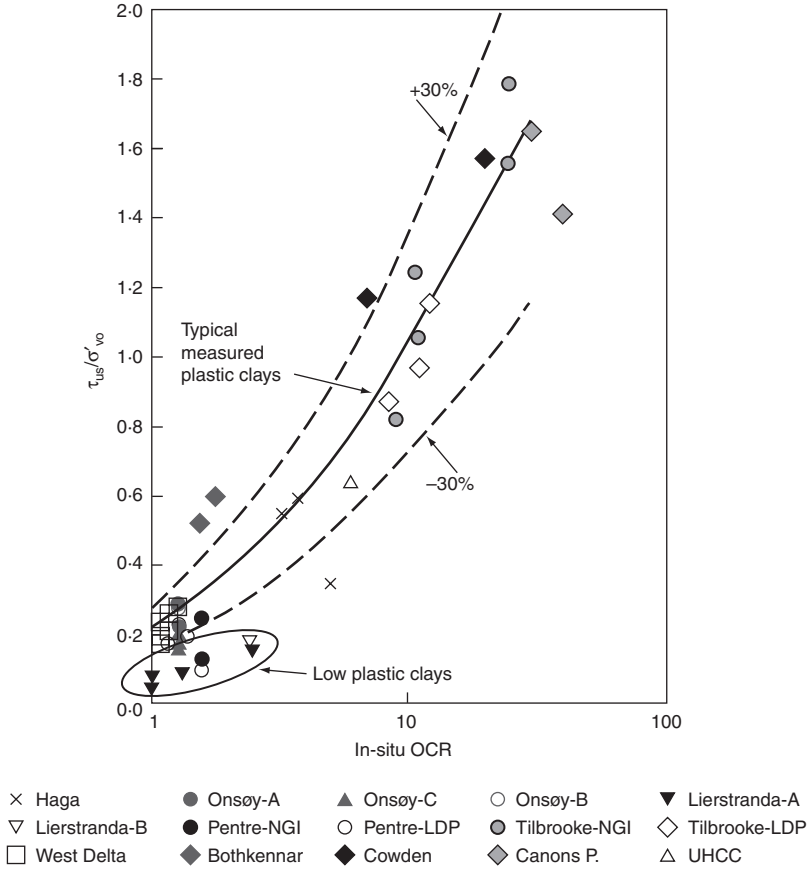

Fig. 6.31 β-plot for various test sites (after Karlsrud, 1999)

Overview

The main point with regard to the so-called 'total stress' and 'effective stress' methods for estimating shaft friction of piles is that they are both correlations. The total stress correlation for shaft friction is against s_u (friction $f = \alpha s_u$). The effective stress correlation for shaft friction is against σ'_v (friction $f = \beta\sigma'_v$). Given the way most plots are drawn, the correlation with s_u (α-plot) works better for soft clays, purely because the correlation with σ'_v (β-plot) is concentrated down at $\beta \leq 0.2$ for low plasticity clays, with a steep gradient against over-consolidation ratio as shown in Fig. 6.31 (Karlsrud, 1999). The crucial importance of plasticity is shown in Fig. 6.32 (Karlsrud, 1999).

The main advance in offshore pile design has been to plot either α or β as a function of the strength ratio, s_u/σ'_v (see Fig. 6.30), rather than against absolute strength or stress (or over-consolidation ratio). It is still a correlation based on statistical analyses of many field and lab tests (e.g. see Kolk

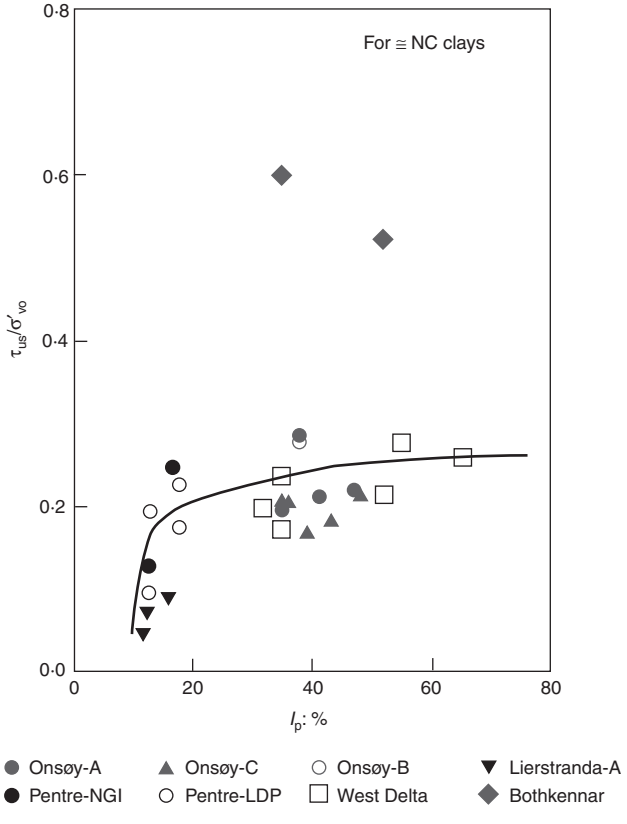

Fig. 6.32 Pile shafts friction correlation with effective over-burden pressure and plasticity index (after Karlsrud, 1999)

and van der Velde, 1996), but on a much better basis. This is because the method draws together existing total and effective stress approaches for calculating pile capacity in a manner that *reduces the sensitivity of the calculation to the measured shear strength of soil* (Randolph and Murphy, 1984; Randolph, 1999).

Design guides

An important design manual is the *New Design Methods for Offshore Piles* by R. J. Jardine and F. C. Chow (1996) of the Department of Civil Engineering, Imperial College. It is published by MTD (The Marine Technology Directorate Ltd) and is available from them as follows:

MTD
Tel.: +44 (0)20 8464 3870
e-mail: MTD.rwb@btinternet.com

The Norwegian Geotechnical Institute have embodied their 'NGI-method' in their Publication Nr.188 (1992). This contains five papers principally by Karlsrud, and also by Lacasse and Kalsnes among others. NGI Publication Nr.188 is available from:

Norwegian Geotechnical Institute
Tel.: +47 22 02 30 00
Fax: +47 22 23 04 48
e-mail: ngi@ngi.no
Web: www.ngi.no

For an overview of specifically European practice, reference may be made to De Cock and Legrand (1997) and to De Cock *et al.* (1999).

WORKED EXAMPLES

1. A bridge pier has a plan area of 15 m × 6 m and carries a load of 30 MN. The soil profile comprises the following succession:

0–3 m: recently placed loose sand fill,
3–10 m: soft clay of undrained shear strength $s_u = 30$ kPa,
10 m – great depth: dense sand, average cone point resistance = 15 000 kPa.
Provide a design solution for supporting the pier which uses driven precast reinforced concrete piles.
Try a square pile 0.3 m × 0.3 m, driven to the dense sand.
Area of end bearing is $A_b = 0.09\,m^2$.
Failure load = 0.09 × 15 000 = 1350 kN.
Take factor of safety of $F = 2.5$, which gives a working load = 540 kN.

Through the clay, the negative skin friction will be
$4 \times 0.3\,\text{m} \times 7\,\text{m} \times (\alpha = 1) \times 30(s_u) = 252\,\text{kN}$
Therefore the structural load capacity per pile is $540–252 = 288\,\text{kN}$.
Number of piles to support total load is therefore $30\,000/288 = 104$.
Try $7 \times 15 = 105$ piles.
Spacing is $5.7/6 = 0.95\,\text{m}$ and $114.7/14 = 1.05\,\text{m}$ which is OK as it is approximately three times the pile diameter.

2. A test pile failure load is 3200 kN. The pile is of uniform diameter 600 mm. The length of pile below ground is 115 m. The soil is clay of undrained shear strength $s_u = 75\,\text{kPa}$ at the surface increasing linearly to 275 kPa at 20 m.
What is the failure load for an under-reamed pile 15 m long with a shaft diameter of 11 m and a base diameter of 2 m? What is the allowable load?
Noting that the ultimate load is made up of bearing plus side friction we have

$$q_{ult} = N_c \times s_u \times A_b + s_{uav} \times \alpha \times A_s$$

For the test pile:

$$3200 = 9 \times 225 \times \pi/4 \times 0.6^2 + 150 \times \alpha \times 15 \times 0.6 \times \pi$$

i.e. $\alpha = 0.62$.
For the under-reamed pile:
Assume skin friction is acting on a pile length of 12.5 m. The load at failure is

$$\begin{aligned} Q_f &= 9 \times 225 \times \pi + 0.62 \times 137.5 \times 12.5 \times \pi \\ &= 6362 + 3348 \\ &= 9710\,\text{kN} \end{aligned}$$

The allowable load is

$$\begin{aligned} Q_a &= 9710/2.5 \\ &= 3884\,\text{kN} \end{aligned}$$

or

$$\begin{aligned} Q_a &= 6362/3 + 3348/1.5 \\ &= 4353\,\text{kN} \end{aligned}$$

3. Design a bored pile in stiff fissured clay to carry 3500 kN. The undrained shear strength $s_u = 100$ kPa at the surface increasing linearly to 400 kPa at 30 m.
Try length $L = 20$ m, diameter $D = 1$ m. Take $w = 0.75$ and $\alpha = 0.45$.

$$Q_u = \pi/4 \times 1^2 \times 9 \times 0.75 \times 300 + \pi \times 1 \times 20 \times 0.45 \times 200$$
$$= 7253 \text{ kN}$$

Take $F = 2$, and so

$$Q_a = 3626 (\text{OK}, > 3500 \text{ kN})$$

Challenge

The following is an assignment we set our final year undergraduate students. You may wish to attempt this.

Part I: A reinforced concrete framed office building having a plan of 15 m × 30 m is to be constructed on a site where the soil profile is a heavily overconsolidated fissured silty clay from the ground surface to great depth. The overall gross bearing pressure is 150 kPa. The engineering properties of the clay are given in the table following:

Depth (m)	s_u (kPa)	E (MPa)	m_v m^2/MN	γ kN/m^3
0	50	15	0.200	19
5	100	30	0.100	19
10	150	45	0.067	19
15	200	60	0.050	19
20	240	72	0.042	20
25	280	84	0.036	20
30	310	93	0.032	20
35	340	102	0.029	20
40	370	111	0.027	20

Consider three possible founding alternatives.

(a) a raft (without piles) at a founding depth of 1.5 m.
(b) a deep raft with basements at a founding depth of 6 m.
(c) a piled shallow raft.

For each possibility, determine the likely settlement and the factor of safety against a bearing capacity failure.

State which solution you would adopt and give reasons for your choice.

You may find that the settlement for the deep raft is less than the settlement for the piled shallow raft!

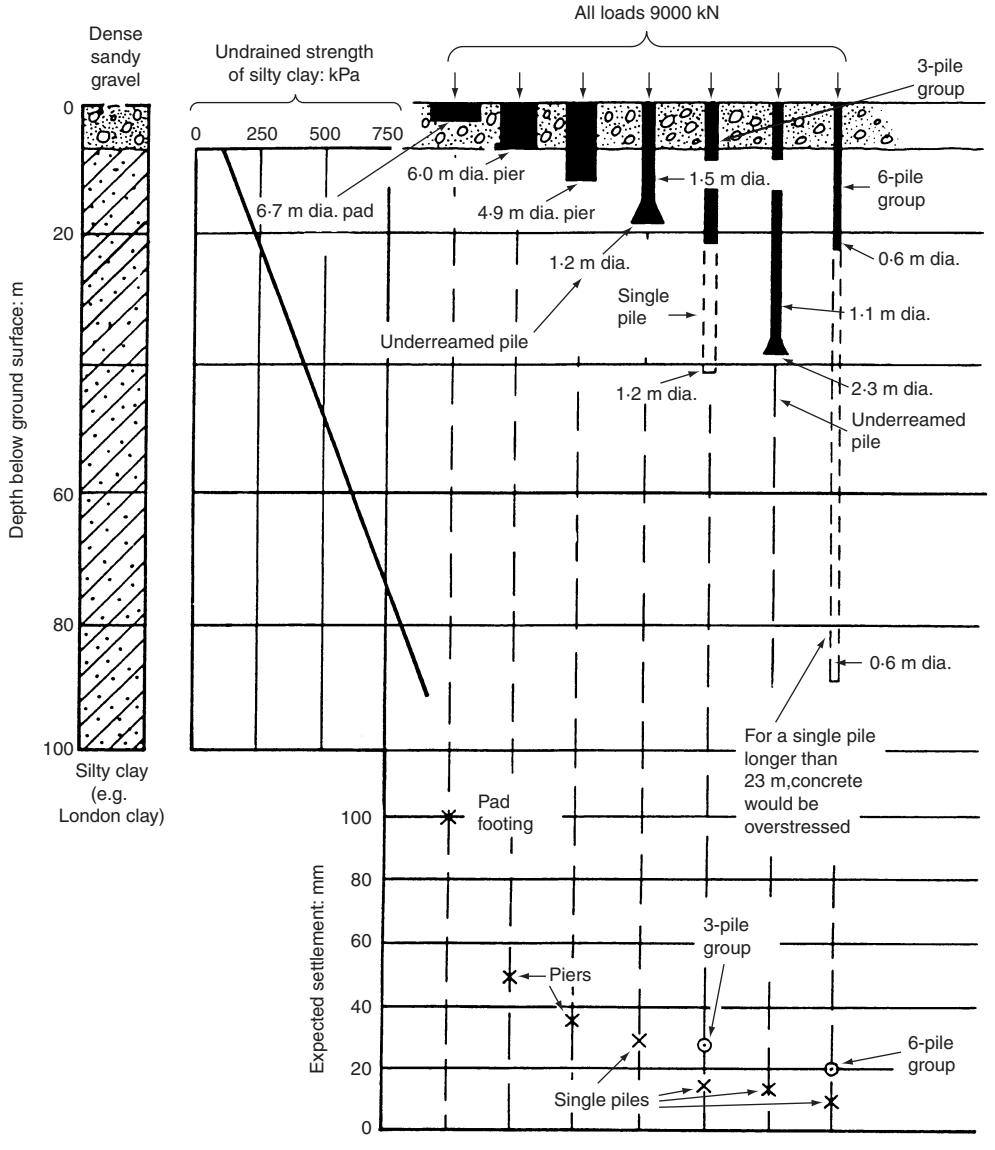

Fig. 6.33 Methods of supporting a 9000 kN load (after Cole, 1989)

Part II: Referring to Fig. 6.33, give design calculations verifying the various methods of supporting a 9000 kN load together with their associated expected settlements. Make any appropriate assumptions.

References and bibliography

ASCE (1951). The Committee on the Bearing Value of Pile Foundations. Pile Driving Formulae. Progress Report, *Proc. ASCE,* **67** (5), 853–866.

Aas, G. (1966) Baerceevne av peler i frisksjonsjordarter. *Norsk Geoteknisk Forening Stipendium,* (1956–66). Oslo, NGI.

Aldrich, H. P. (1952). *Importance of net load to the settlement of buildings in Boston. Contributions to Soil Mechanics,* (1941–53). Boston Society of Civil Engineers.

Anderson, K. H. and Frimann Clausen, C. J. (1974). A 50-year settlement record of a heavy building on compressible clay. *Proceedings Conference on Settlement of Structures, Cambridge*. Pantech Press, London, pp. 71–78.

Arthur, J. R. F. and Menzies, B. K. (1968). Correspondence on: A new soil testing apparatus. *Géotechnique*, **18**, 271–272.

Arthur, J. R. F. and Menzies, B. K. (1972). Inherent anisotropy in a sand. *Géotechnique,* **22** (1), 115–128.

Arthur, J. R. F. and Phillips, A. B. (1972). Discussion on: Inherent anisotropy in a sand. *Géotechnique,* **22** (1), 537–538.

Atkinson, J. H. (1973). The deformation of undisturbed London clay. PhD Thesis. University of London.

Atkinson, J. H. (1974). Discussion on Session 4: The interpretation of field observations. *Field Instrumentation in Géotechnical Engineering*. Part 2, Butterworths, London, pp. 677–679.

Ballard, R. F. and McLean, F. G. (1975) Seismic field methods for in situ moduli. *Proc. Conf. on In situ Measurement of Soil Properties.* Speciality Conference of the Geotechnical Engineering Division ASCE, Raleigh, North Carolina, 1, pp. 121–150.

Bauer, C. E. A., Scott, J. D. and Shields, D. H. (1973). The deformation properties of a clay crust. *Proc. 8th Int. Conf. Soil Mech. & Fdn Engng*, USSR National Society of Soil Mechanics and Foundation Engineering, **1.1**, pp. 31–38.

Bazaraa, A. R. S. S. (1967). Use of the standard penetration test for estimating settlement of shallow foundations on sand. PhD Thesis, University of Illinois.

Bell, A. L. (1915). Lateral pressure and resistance of clay. *Min. Proc. Instn Civ. Engrs,* **1** (99), 233–272.

Berezantsev, U. G. (1961). Load bearing capacity and deformation of piled foundations. *Proc. 5th Int. Conf. Soil Mech. & Fdn Engng*, *Paris*, DUNOD, Paris, **2**, pp. 11–12.

Berre, T. (1973). *Sammenheng Mellom Tid, Deformasjoner og Spenninger for Normal–Konsoliderte Marine Leire*r. Publication No. 97, Norwegian Geotechnical Institute, Oslo , pp. 1–14.

Berre, T. and Bjerrum, L. (1973). Shear strength of normally consolidated clays. *8th Int. Conf. Soil Mech. & Fdn Engng, Moscow*, USSR Nat. Soc. Soil Mech. & Fdn Engng, **1.1**, pp. 39–49.

Berre, T., Schjetne, K. and Sollie, S. (1969). Sampling disturbance of soft marine clays. *7th Int. Conf. Soil Mech. & Fdn Engng, Mexico*, Scociedad Mexicana de Mecanica de Suelos, Special Session 1, pp. 21–24.

Bishop, A. W. (1958a). Test requirements for measuring the coefficient of earth pressure at rest. *Conf. Earth Pressure Problems*, *Brussels*, **1**.

Bishop, A. W. (1958b). Test requirements for measuring the coefficient of earth pressure at rest. *Conf. Earth Pressure Problems*, *Brussels*, 2–14.

Bishop, A. W. (1959). The principle of effective stress. Text of lecture to NGI 1955, *Teknisk Ukeblad,* **106** (39), 859–863.

Bishop, A. W. (1966a). *Soils and soft rocks as engineering materials.* Inaugural lecture, Imperial College of Science and Technology, London.

Bishop, A. W. (1966b). Sixth Rankine Lecture: The strength of soils as engineering materials. *Géotechnique,* **16** (1), 89–130.

Bishop, A. W. (1973a). The influence of an undrained change in stress on the pore pressure in porous media of low compressibility. *Géotechnique,* **23** (3), 435–442.

Bishop, A. W. (1973b). The influence of the undrained change in stress on the pore pressure in porous media of low compressibility. *Géotechnique*, **23** (3), 435–442

Bishop, A. W. and Bjerrum, L. (1960). The relevance of the triaxial test to the solution of stability problems. *Proc. Res. Conf. Strength of Cohesive Soils. Boulder, Colorado*, ASCE, pp. 437–501.

Bishop, A. W., Garga, C. E., Andresen, A, and Brown, J. D. (1971). A new ring shear apparatus and its application to the measurement of residual strength. *Géotechnique,* **21**, 273–328.

Bishop, A. W. and Henkel, D. J. (1953). Pore pressure changes during shear in two undisturbed clays. *3rd Int. Conf. Soil Mech. & Fdn Engng*, *Zurich*, ICOSOMEF, Zurich, **1**, pp. 94–99.

Bishop, A. W. and Henkel, D. J. (1962). *The Measurement of Soil Properties in the Triaxial Test.* Edward Arnold (Publishers) Ltd, London.

Bishop, A. W. and Wesley, L. D. (1975). A hydraulic triaxial apparatus for controlled stress path testing. *Géotechnique,* **25** (4), 657–670.

Bjerrum, L. (1957). Norwegian experiences with steel piles to rock. *Géotechnique,* **7** (1), 24.

Bjerrum, L. (1963a). Generelle Krav til Fundamentering av Forskjellige Byggverk; Tillatte Setninger. *NIF Kurs in Fundamentering*, Oslo, pp. 17.

Bjerrum, L. (1963b). Discussion on Section 6. *Proc. Eur. Conf. Soil Mech & Fdn Engng*, *Wiesbaden*, **2**, pp. 135–137. (Also NGI, Publication No. 98).

Bjerrum, L. (1964). Relasjon Mellom Målte og Beregnede Setninger av Byggverk på Leire og Sand. N. G. F. Foredraget, 1964. Norwegian Geotechnical Institute, Oslo, pp. 92.

Bjerrum, L. (1967). Engineering geology of Norwegian normally consolidated marine clays as related to settlements of buildings. 7th Rankine Lecture, *Géotechnique,* **17**, 81–118.

Bjerrum, L. (1968). Secondary settlements of structures subjected to large variations in live load. *NGI Publication No. 73,* Norwegian Geotechnical Institute, Oslo.

Bjerrum, L. (1972a). Embankments on soft ground. *ASCE specialty conference on performance of earth and earth supported structures*, *Purdue University, Lafayette, Indiana*, pp. 1–54.

Bjerrum, L. (1972b). The effect of rate of loading on the p'_c value observed in consolidation tests on soft clay. *Publication No. 95,* Norwegian Geotechnical Institute, Oslo.

Bjerrum, L. (1973). Problems of soil mechanics and construction on soft clays. *Proc. 8th Int. Conf. Soil Mech. & Fdn Engng, Moscow*, USSR Nat. Soc. Soil Mech & Fdn Engng, **3**, pp. 111–159.

Bjerrum, L. and Eggestad, A. (1963). Interpretation of loading tests on sand. *Proc. Eur. Conf. Soil Mech. & Fdn Engng*, *Wiesbaden*, **1**, pp. 199–204.

Bjerrum, L. and Eide, O. (1966). Anvendelse av Kompensert Fundamentering i Norge. *Publication No. 70,* Norwegian Geotechnical Institute, Oslo.

Bjerrum, L. and Øverland, A. (1957). Foundation failure of an oil tank in Frederikstad, Norway. *Proc. 4th Int. Conf. Soil Mech. & Fdn Engng*, *London*, Butterworth, London, **1**, pp. 287–290.

Bjerrum, L. and Simons, N. E. (1960). Comparison of shear strength characteristics of normally consolidated clays. *Proceedings of Research Conference on Shear Strength of Cohesive Soils*, Boulder, Colorado. ASCE, pp. 711–724.

Bjerrum, L., Johannessen, I. J, and Eide, O. (1969). Reduction of negative skin friction on steel piles to rock. *Proc. 7th Int. Conf. Soil Mech. & Fdn Engng, Mexico*, Scociedad Mexicana de Mecasica de Suelos, **2**, pp. 27–34.

Bjerrum, L., Simons, N. E. and Torblaa, I. (1958). The effect of time on the shear strength of a soft marine clay. *Proc. Conf. Earth Pressure Problems*, *Brussels*, **1**, pp. 148–158.

Boussinesq, J. (1876). Essai théorique sur l'équilibre d'élastité des massifs pulveruients. *Mem. Savante etrangere, Acad. Belgique*, **40**, 1–80.

Boussinesq, J. (1885). *Application des Potentiels a l'étude de l'équilibre et du Mouvement des Slides Elastiques*, Gauthier–Villard, Paris.

Bratchell, G. E., Leggatt, A. J, and Simons, N. E. (1974). The performance of two large oil tanks founded on compacted gravel at Fawley, Southampton, Hampshire. *Proc. Conf. Settlement of Structures*, *Cambridge*. Pantech Press, London, pp. 3–9.

Brinch, Hansen J. (1955). Simpel Beregning av Fundamenters Baereevne. *Ingeniøren,* **4**, pp. 95–100.

Brinch, Hansen J. (1968). A revised and extended formula for bearing capacity. *Bulletin No. 28*, Danish Geotechnical Institute.

British Standards Institution. *BS 8004: 1986. British standard code of practice for foundations*. BSI, London.

British Steel Piling Company, Ltd. (1969). *The BSP pocket book*.

Broms, B. B. (1964a). Lateral resistance of piles in cohesive soils. *Proc. ASCE J Soil Mech. & Fdn Engng*, (SM2), 27–63.

Broms, B. B. (1964b). Lateral resistance of piles in cohesionless soils. *Proc. ASCE J Soil Mech. & Fdn Engng,* (SM3), 123–156.

Broms, B. B. (1965a). Design of laterally loaded piles. *Proc. ASCE J. Soil Mech. & Fdn Engng,* (SM3), 79–99.

Broms, B. B. (1965b) Methods of calculating the ultimate bearing capacity of piles: a summary. *Sols–Soils*, **5** (18–19), 21–32.

Brown, J. D. (1968). General Report. *Proceedings Bolkesjø Symposium on shear strength and consolidation of normally consolidated clays*, pp. 2–8.

Buisman, A. S. K. (1936). Results of long duration settlement tests. *Proc. 1st Int. Conf. Soil Mech. & Fdn Engng, Cambridge, Mass*, Harvard University, **1**, pp. 100–106.

Buisson, M., Ahee, J. and Habil, P. (1960). Le Frottement Négatif Institut Technique de bâtiment et des les, Travaux Publics. *Annales*, **13** (145), Supplement, pp. 30–46.

Burland, J. B. and Lord, J. A. (1970). The load–deformation behaviour of Middle Chalk at Mundford, Norfolk: a comparison between full-scale performance and in-situ and laboratory measurements. *Proc. Conf. In situ Investigations in Soils and Rocks*, British Geotechnical Society, ICE, London, pp. 3–15.

Burland, J. B. and Cooke, R. W. (1974). The design of bored piles in stiff clays. *Ground Eng.,* **7** (4), 28–35.

Burland, J. B. and Hancock, R. J. R. (1977). Underground car park at the House of Commons, London: geotechnical aspects. *Struct. Engr,* **55** (2), 87–100.

Burland, J. B. and Wroth, C. P. (1974). General Report – session 5. *Proc. Conf. Settlement of Structures*, Cambridge. Pantech Press, London.

Burland, J. B. and Burbidge, M. C. (1985). Settlement of foundations on sand and gravel. *Proc. Instn Civ. Engrs*, Part 1, 1985, 78, Dec., 1325–1381.

Burland, J. B., Butler, F. G. and Dunican, P. (1966). The behaviour and design of large diameter bored piles in stiff clay. *Large Bored Piles*. ICE, London, pp. 51–71.

Burland, J. B., Sills, G. C. and Gibson, R. E. (1973). A field and theoretical study of the influence of non-homogeneity on settlement. *Proc. 8th Int. Conf. Soil Mech. & Fdn Engng*, *Moscow*, USSR Nat. Soc. Soil Mech. & Fdn Engng, **1.3**, pp. 39–46.

Burland, J. B., Broms, B. B. and De Mello, V. F. B. (1977). Behaviour of foundations and structures. *Proc. 9th Int. Conf. Soil Mech. & Fdn Engng. Tokyo*. Japanese Soc. Soil Mech. & Fdn Engng.

Burland, J. F. (1973). Shaft Friction of Piles in Clay: A Simple Fundamental Approach, *Ground Engineering*, **6** (3), 30–32, 37–42.

Butcher, A. P. and Tam, W. S. A. (1994). An example of the use of Rayleigh waves to detect the depth of a shallow land fill. *Modern Geophysics in Engineering Geology*, (Eds. D. M. McCann, M. Eddleston, P. J. Fenning and G. M. Reeves). Geol. Soc. Engng Geol. Special Publication No. 12, Geol. Soc., London.

Butler, F. G. (1974). General Report and State of the Art Review, Session 3: Heavily over-consolidated clays. *Proc. Conf. Settlement of Structures*, Cambridge. Pantech Press, London.

Butler, F. G. and Morton, K. (1971). Specification and performance of test piles in clay. *Conf. Behaviour of Piles*, ICE, London, pp. 17–26.

Calladine, C. R. (1985). *Plasticity for engineers*. Ellis Horwood Ltd, Chichester.

Calhoon, M. L. (1972). Discussion on D'Appolonia, Poulos and Ladd (1971). *Proc. ASCE J. Soil Mech. & Fdn Engng,* **98** (SM3), 306–308.

Carrier, W. D. and Christian, J. T. (1973). Rigid circular plate resting on a non-homogeneous elastic half-space. *Géotechnique,* **23** (4), 67–84.

Casagrande, A. (1936). The determination of the pre-consolidation load and its practical significance. *Proc. 1st Int. Conf. Soil Mech. & Fdn Engng*, *Cambridge, Mass*, Harvard University, **3**.

Casagrande, A. (1936). Characteristics of cohesionless soils affecting the stability of slopes and earth fills. *J. Boston Soc. of Civ. Engrs*, **23**(1), 13–32.

Casagrande, A. and Fadum, R. E. (1942). Application of soil mechanics in designing building foundations. *Proc. ASCE*, **68**, 1487–1520.

Casagrande, A. and Carillo N. (1944). Shear failure of anisotropic materials. *Proc. Boston Soc. of Civ. Eng.,* **31**, 74–87.

Chang, Y. C. E., Broms, B. and Peck, R. B. (1973). Relationship between the settlement of soft clays and excess pore pressure due to imposed loads. *Proc. 8th Int. Conf. Soil Mech. & Fdn Engng, Moscow*, USSR Nat. Soc. Soil Mech. & Fdn Engng, **1.1**, pp. 93–96.

Chellis, R. D. (1941) Discussion on pile driving formulae. Progress Report, Committee on the bearing value of pile foundations. *Proc. ASCE*, **67** (8), 1517–1537.

Christian, J. T. and Carrier, W. D. (1978). Janbu, Bjerrum and Kjaernsli's chart reinterpreted. *Can. Geotech. Jnl.* **15**, 123–128.

Clapham, H. G. (1963). *The effect of lateral loads on embedded piles*. DIC Dissertation, University of London.

Clayton, C. R. I. (1973). *The secondary compression of clays*. MSc Thesis, Imperial College, London.

Clayton, C. R. I. (1991). The mechanical properties of the Chalk. Keynote Address, *International Chalk Symposium*, Brighton. Thomas Telford, London.

Clayton, C. R. I., Edwards, A. and Webb, J. (1991). Displacements in London clay during construction. *Proc. 10th Eur. Conf. on Soil Mech. and Fdn Engng*. Florence, **2,** pp.791–796.

Clayton, C. R. I., Gordon, M. A. and Matthews, M. C. (1994) Measurements of stiffness of soils and weak rocks using small strain laboratory testing and geophysics. *Proc. Int. Symp. on Pre-failure Deformation Characteristics of Geomaterials*, Balkema, Rotterdam, **1**, pp. 229–234.

Clayton, C. R. I., Simons, N. E. and Instone, S. J. (1988). Research on dynamic penetration testing in sands. *Proc. 1st Int. Conf. on Penetration Testing*. Florida, 415–422.

Clayton, C. R. I. and Heymann, G. (in press) The stiffness of geomaterials at very small strains. Submitted to *Géotechnique*.

Clayton, C. R. I., Matthews, M. C., Gunn, M. J., Foged, N. and Gordon, M. A. (1995) Reinterpretation of surface wave test for the Øresund crossing. *Proc. 11th Eur. Conf. on Soil Mech. and Found. Engng*, Copenhagen, Danish Geotechnical Society, Copenhagen, **1**, pp. 141–147.

Cole, K. W. (1989). *Foundations*. ICE Construction Guide Series. Thomas Telford, London.

Cole, K. W. and Burland, J. B. (1972). Observations of retaining wall movements associated with a large excavation. *Proc. 5th Eur. Conf. on Soil Mech. and Found. Engng*, *Madrid*, **1**, pp. 445–453.

Cowley, B. E., Haggar, E. G. and Larnach, W. J. (1974). A comparison between the observed and estimated settlements of three large cold stores in Grimsby. *Proc. Conf. Settlement of Structures*, *Cambridge*. Pantech Press, London, pp. 79–90.

Craig, W. H., Schofield, A. N. and James, R. G. (eds) (1988). *Centrifuges in soil mechanics*. A. A. Balkema, Rotterdam.

Croce, P., Ko, H.-Y., Schiffman, R. L. and Znidarcic, D. (1988). The influence of vertical drains on consolidation. *Proc. Int. Conf. Centrifuge 88*, Boulder, Colorado, 171–180.

Cuellar, V., Monte, J. L. and Valerio, J. (1995) Characterization of waste land fills using geophysical methods. *Proc. 11th European Conf. on Soil Mech. and Found. Engng*, *Copenhagen*, Danish Geotechnical Society, Copenhagen, **2**, pp. 33–38.

Cummings, A. E. (1940). Dynamic pile driving formulae. *Contributions to soil mechanics*, (1925–1940). *J. Boston Soc. of Civ. Engrs*, 392–413.

De Cock, F. and Legrand, C. (1997). *Design of axially loaded piles – European practice.* Proc. ERTC3 Seminar, Brussels. Balkema, Rotterdam.

De Cock, F., Legrand, C. and Lehane, B. (1999). (eds) *Survey report on the present-day design methods for axially loaded piles. European practice.* Published on the occasion of the XIIth Eur. Conf. Soil Mech. Fdn Eng. Amsterdam, 56 pp.

D'Appolonia, D. J., D'Appolonia, E. and Brisette, R. F. (1968). Settlement of spread footings on sand. *Proc. ASCE J Soil Mech. & Fdn Engng*, SM3, pp. 735–760.

D'Appolonia, D. J. and Lambe, T. W. (1971). Floating foundations for control of settlement *Proc. ASCE J. Soil Mech. & Fdn Engng*, **97**, SM6, pp. 899–915.

D'Elia, B. and Grisolia, M. (1974). On the behaviour of a partially floating foundation on normally consolidated silty clays. *Proc. Conf. Settlement of Structures*, *Cambridge*, Pantech Press, London, pp. 91–98.

Davis, A. G. and Dunn, C. S. (1974). From theory to field experience with the non-destructive vibration testing of piles. *Seminar on concrete pile testing*. C and CA, Fulmer.

Davis, E. H. and Poulos, H. G. (1968). The use of elastic theory for settlement prediction under three dimensional conditions. *Géotechnique,* **18** (1), 67–91.

de Beer, E. E. (1965). Bearing capacity and settlement of shallow foundations on sand. *Proc. Symposium on Bearing Capacity and Settlement of Foundations.* Duke University, pp. 15–33.

de Beer, E. E. and Martens. A. (1957). Method of computation of an upper limit for the influence of heterogeneity of sand layers on the settlement of bridges. *Proc. 4th Int. Conf. Soil Mech. & Fdn Engng, London*, Butterworth, London, **1**, pp. 275–281.

Den Norske Pelekomite (1973). *Veiledning ved pelefundamentering*. Veiledning No. 1, Norwegian Geotechnical Institute, Oslo.

Eide, O Hutchinson, J. N. and Landva, A. (1961). Short and long term test loading of a friction pile in clay. *Proc. 5th Int. Conf. Soil Mech. & Fdn Engng*, *Paris,* DUNOD, Paris.

Eide, O. (1972). Personal communication.

Endo, M., Minau, A., Kawaski, T. and Schibata, T. (1969). Negative skin friction acting on steel pipe pile in clay. *Proc. 7th Int. Conf. Soil Mech. & Fdn Engng*, Mexico, Scociedad Mexicana de Mecanica de Suelos, **2**, pp. 85–92.

Engesgaar, H. (1970). *Resultater av to Belastningsforsøk på Sundland i Drammen*. Publication No. 84, Norwegian Geotechnical Institute, Oslo.

Engesgaar, H. (1973). 15-storey building on plastic clay in Drammen, Norway. *Proc. 8th Int. Conf. Soil Mech. & Fdn Engng*, *Moscow*, USSR Nat. Soc. Soil Mech. & Fdn Engng, **1.3**, pp. 75–80.

Esrig, M. E. and Kirby, R. C. (1979) Advances in general effective stress method for the prediction of axial capacity for driven piles in clay. *Proc. 11th Offshore Technology Conferenc*e, Houston, Texas, **1**, Paper No. 3406, pp. 437–448.

Esrig, M. E., Kirby, R. C., Bea, R. G. and Murphy, B. S. (1977). Initial development of a general effective stress method for the prediction of axial capacity for driven piles. *Proc. 9th Offshore Technology Conference, Houston, Texas,* **3**, Paper No. 2943, pp. 495–506.

Fadum, R. E. (1948). Influence values for estimating stresses in elastic foundations. *Proc. 2nd Int. Conf. Soil Mech. & Fdn Engng*, *Rotterdam*, **3**, pp. 77–84.

Fellenius, B. H. and Broms, B. B. (1969). Negative skin friction for long piles driven in clay. *Proc. 7th Int. Conf. Soil Mech. & Fdn Engng, Mexico*, Scociedad Mexicana de Mecanica de Suelos, **2**, pp. 92–98.

Fillunger, P. (1915). Versuche ober die zugfestigkeit beiailsetigen wassersruck. *Osterr. Wochenschr Offentlich Band ienst*. Vienne. pp. 443–448.

Flaate, K. (1964). An investigation of the Validity of Three Pile Driving Formulae in Cohesionless Materials. *NGI Publication No. 56*, pp. 11–22.

Flaate, K. (1968). *Baereevne av Friksjonspeler i Leire; om Beregning av Baereevne på grunnlag av Geotekniske Undersøkelser*. Oslo, Veglaboratoriet, 38 pp, mimeographed.

Flaate, K. and Selnes, P. (1977) Side Friction of Piles in Clay, *Proc. 9th Int. Conf. Soil Mech. & Fdn Engng*, *Tokyo*, Japanese Soc. Soil Mech. & Fdn Engng, **1**, pp. 517–522.

Focht, J. A., Jr. (1988). Axial capacity of offshore piles in clay, *Proc. Shanghai Symp. on Marine Geotechnology and Nearshore Structures*, *Shanghai, China*.

Forrester, J. (1974). Radiometric logging. *Seminar on concrete pile testing*, C and CA, Fulmer.

Foss. I. (1969). Secondary settlements of buildings in Drammen, Norway, *Proc. 7th Int. Conf. Soil Mech. & Fdn Engng, Mexico*, Scociedad Mexicana de Mecanica de Suelos, **2**, pp. 99–106.

Fox, E. N. (1948). The mean elastic settlement of uniformly loaded area at a depth below ground surface. *Proc. 2nd Int. Conf. Soil Mech. & Fdn Engng*, *Rotterdam*, **1**, p. 129.

Frimann Clausen, C. J. (1969). Loading test, Mastemyr. *Proc. Bolkesjø symposium on shear strength and consolidation of normally consolidated clays*, pp. 42–44.

Frimann Clausen, C. J. (1970). Resultater av et Belastningsforsøk på Mastemyr i Oslo. *Publication No. 84*, Norwegian Geotechnical Institute, Oslo, pp. 29–40.

Gant, E. V., Stephens, J. E, and Moulton, L. K. (1958). Measurement of forces produced in piles by settlement of adjacent soil. *Highway Research Board Bulletin,* **173**, pp. 20–45.

Gardner, R. P. M. and Moses, G. W. (1973). Testing bored piles formed in laminated clays. *Civ. Eng. and Public Works Rev.,* pp. 60–63.

Garlanger, J. E. (1972). The consolidation of soils exhibiting creep under constant effective stress. *Géotechnique,* **2** (2), 141–161.

Gazetas, G. (1982) Vibrational characteristics of soil deposits with variable velocity. *Int. J for Numerical and Analytical Methods in Geomechanics*, **6**, 1–20.

Gibbs, H. J. and Holtz, W. G. (1957). Research on determining the density of sands by spoon penetration testing. *Proc. 4th Int. Conf. Soil Mech. & Fdn Engng*, *London*, Butterworth, London, **1**, pp. 35–39.

Gibson, R. E. (1967). Some results concerning displacements and stresses in a non-homogeneous elastic half-space. *Géotechnique,* **17**, 58–67.

Gibson, R. E. (1974). Fourteenth Rankine Lecture: The analytical method in soil mechanics. *Géotechnique,* **24** (2), 113–140.

Gibson, R. E. and Sills, G. C. (1971). Some results concerning the plane deformation of a non-homogeneous elastic half-space. *Proc. Roscoe Memorial Symposium on Stress–Strain Behaviour of Soils*, G. T. Foulis, Henley-on-Thames, pp. 564–572.

Gielly, L., Lareal, P. and Sanglerat, G. (1970). Correlations between in situ penetrometer tests and the compressibility characteristics of soils. *Proc. Conf. In situ Investigations in Soils and Rocks*, ICE, London, pp. 167–172.

Golder, H. Q. (1965). State of the art of floating foundations. *Proc. ASCE J. Soil Mech. & Fdn Engng,* **31**, SM2, Proceeding Paper 4278, pp. 81–88.

Golder, H. Q. and Willeimier, G. C. (1964). Design of the main foundations of the Port Mann Bridge, *Eng. J. Canad,* **47** (8), 22–29.

Gordon, M.A. (1997). *Applications of field seismic geophysics to the measurement of geotechnical stiffness parameters*. PhD Thesis, University of Surrey, Guildford.

Gordon, M. A., Clayton, C. R. I., Thomas, T. C. and Matthews, M. C. (1995). The selection and interpretation of seismic geophysical methods for site investigation. *Proc. ICE Conf. on Advances in Site Investigation Practice*, March 1995.

Greulich, G. G. (1941). Discussion on pile driving formulae, Progress report, Committee on the Bearing Value of Pile Foundations, *Proc. ASCE*, **67** (7), 1391–1396.

Heymann, G. (1998). *The stiffness of soils and weak rocks at very small strains*. PhD Thesis, University of Surrey, Guildford.

Heymann, G., Clayton, C.R.I. and Reed, G.T. (1997). Laser interferometry to evaluate the performance of local displacement transducers. *Géotechnique,* **47** (3), 399–405.

Hiley, A. E. (1925). A rational pile driving formula and its application in practice explained. *Engineering*, **119**, 657.

Hobbs, N. B. (1971). The Menard pressuremeter – *in situ* loading tests in soils and rocks. Summer school in foundation engineering, University of Surrey.

Høeg K., Andersland, O. B. and Rolfsen, E. N. (1969). Undrained behaviour of quick clay under load tests at Åsrum. *Géotechnique,* **19** (1), 101–115.

Hooker, P. (1998) Seismic solution: Ground improvement. *Ground Engineering*. London.

Hope, V. S. (1993). *Applications of seismic transmission tomography in civil engineering.* PhD Thesis, University of Surrey, Guildford.

Hutchinson, J. N. (1963). Settlements in soft clay around a pumped excavation in Oslo. *Eur. Conf. Soil Mech. & Fdn Engng*, *Wiesbaden*, **1**, pp. 119–126.

Hutchinson, J. N. and Jensen, E. V. (1968). Loading tests on piles driven into estuarine clays at Port of Khorramshav, and observations on the effect of bitumen coatings on shaft bearing capacity. *Publication No. 78,* Norwegian Geotechnical Institute, Oslo.

Izumi, K., Ogihara, M. and Kamaya, H. (1997). Displacements of bridge foundations on sedimentary soft rock: a case study on small-strain stiffness. *Geotechnique,* **47** (3), 619–632.

James, P. M. (1970). The behaviour of a soft recent sediment under embankment loadings. *J. of Eng. Geology,* **3**, 41–53.

Janbu, N. (1953). Une analyse energetique du battage des pieux a l'aide de paramètres sans dimension. *Institut Technique du Batiment et des Travoux Publics. Annales*, No. 63–64. (also *NGI Publication No. 3*).

Janbu, N. (1963). Soil compressibility as determined by oedometer and triaxial tests. *Eur. Conf. Soil Mech. & Fdn Engng*, *Wiesbaden*, **1**, pp. 19–25.

Janbu, N. (1969). The resistance concept applied to deformations of soils. *Proc. 7th Int. Conf. Soil Mech. & Fdn Engng, Mexico*, Scociedad Mexicana de Mecanica de Suelos, **1**, pp. 191–196.

Janbu, N. (1976) Static bearing capacity of friction piles *Proc. 8th Int. Conf. Soil Mech. & Fdn Engng*, *Moscow,* USSR Nat. Soc. Soil Mech. & Fdn Engng, **1**, pp. 479–488.

Janbu, N., Bjerrum, L. and Kjaernsli, B. (1956). Veiledning ved Løsning av Fundamenteringsoppgaver. *NGI Publication No. 16*, Norwegian Geotechnical Institute, Oslo, 93 p.

Jardine, R. J. and Chow, F. C. (1996). *New design methods for offshore piles*. Publication 96/103, Marine Technology Directorate, 48 pp.

Jardine, R. J., Potts, D. M., Fourie, A. B. and Burland, J. B. (1986). Studies of the influence of non-linear stress–strain characteristics in soil–structure interaction. *Géotechnique*, **36** (3), 377–396.

Jarrett, P. M., Stark, W. G. and Green, J. (1974). A settlement study within a geotechnical investigation of the Grangemouth area. *Conf. Settlement of Structures*, *Cambridge*, Pantech Press, London, pp. 99–105.

Johannessen, I. J. and Bjerrum, L. (1965). Measurement of the compression of a steel pile to rock due to settlement of the surrounding clay. *Proc. 6th Int. Conf. Soil Mech. & Fdn Engng, Montreal*, University of Toronto Press, **2**, pp. 261–264.

Jones, R. B. (1958). In situ measurement of the dynamic properties of soil by vibration methods. *Géotechnique*, **8** (1), 1–21.

Jones, R. B. (1962). Surface wave technique for measuring the elastic properties and thickness of roads: theoretical development. *J Appl. Physics*, **13**, 21–29.

Karlsrud, K. (1999). *Lessons learned from instrumented axial pile load tests in clay*. Lecture presented at the 1999 Offshore Technology Conference, Austin, Texas. Published in Norwegian Geotechnical Institute Report 525211-1.

Kee, R. and Clapham, H. G. (1971). An empirical method of foundation design in Chalk. *Civ. Eng. and Public Wks Rev*.

Kerisel, J. (1964). Vertical and horizontal bearing capacity of deep foundations in clays. *Bearing Capacity and Settlement of Foundations*. Proc. Conf., Duke University, Durham N. C. pp. 45–51.

Kolk, H. J. and van der Velde, E. (1996). A reliable method to determine friction capacity of piles driven into clays, OTC 7993, *Proc. Offshore Technology Conf.,* Houston, Texas, pp. 337–346.

Koppejan, A. W. (1948). A formula combining the Terzaghi load–compression relationship and the Buisman secular time effect. *Proc. 2nd Int. Conf. Soil Mech. & Fdn Engng, Rotterdam,* **3**, pp. 32–37.

Kurnmeneje, O. (1955). Fundamentering av oljetank i Drammen. *Bygg*, **3** (9), 239–243. (also *NGI Publication No. 12*).

Ladd, C. C. (1964). Stress–strain modulus of clay in undrained shear. *Proc. ASCE J Soil Mech. & Fdn Engng*, **90** (SM5), 103–132.

Ladd, C. C. (1969). The prediction of *in situ* stress–strain behaviour of soft saturated clays during undrained shear. *Bolkesjø symposium on shear strength and consolidation of normally consolidated clays*, Norwegian Geotechnical Institute, Oslo, pp. 14–19.

Lambe, T. W. (1964). Methods of estimating settlement. *Proc. ASCE J Soil Mech. & Fdn Engng*, **90** (SM5), 43–67.

Lambe, T. W. (1973a). Predictions in soil engineering. *Géotechnique,* **23** (2), 151–202.

Lambe, T. W. (1973b). Up-to-date methods of investigating the strength and deformability of soils. *Proc. 8th Int. Conf. Soil Mech. & Fdn Engng*, *Moscow*, USSR Nat. Soc. Soil. Mech. & Fdn Engng, **3**, 3–43.

Lambe, T. W. and Whitman, R. V. (1969). *Soil Mechanics.* John Wiley and Sons, Inc.

Laughton, A. S. (1955). *The compaction of ocean sediments*. PhD Thesis, University of Cambridge.

Levy, J. F. (1970). Sonic pulse method of testing cast *in situ* concrete piles. *Ground Engineering,* **3** (3), 17–19.

Liu, T. K. and Dugan, J. P. (1974). Elastic settlement behaviour of three steel storage tanks. *Proc. Conf. Settlement of Structures*, *Cambridge*, Pantech Press, London, pp. 106–109.

Lo, K. Y. (1965). Stability of slopes in anisotropic soils. *Proc. ASCE J. Soil Mech. & Fdn Engng*, **91** (SM4), 85–106.

Lyall, C. (1871). *Students elements of geology*. Murray, London, pp. 41–42.

Lysmer, J and Duncan, J. M. (1972). *Stresses and Deflections in Foundations and Pavements.* Department of Civil Engineering, University of California, Berkeley, 5th Edition.

Madhloom A. A. W. A. (1973). *The undrained shear strength of a soft silty clay from Kings Lynn, Norfolk*. MPhil. Thesis, University of Surrey.

Marsland, A. (1971a). Large *in situ* tests to measure the properties of stiff fissured clays. *Proc. 1st Australia–New Zealand Conf. on Geomechanics, Melbourne*, pp. 180–189.

Marsland, A. (1971b). The shear strength of stiff fissured clays. *Proceedings of Roscoe Memorial Symposium on Stress–strain Behaviour of Soils*, *Cambridge*, G. T. Foulis, Henley-on-Thames, pp. 59–68.

Marsland, A. (1971c). Laboratory and *in situ* measurements of the deformation moduli of London clay. *Proc. Symp. Interaction of Structure and Foundation*, Midland Soil Mechanics and Foundation Engineering Society, Department of Civil Engineering, University of Birmingham, pp. 7–17.

Matthews, M. C. (1993). *Mass compressibility of fractured chalk*. PhD Thesis, University of Surrey, Guildford.

Matthews, M. C. (1994). The use of geophysics in settlement prediction. *Proc. 6th Int. Congress of Int. Assoc. Eng. Geol.* Amsterdam. Balkema, Rotterdam, **5**, pp. 3337–3339.

Matthews, M. C., Hope, V. S. and Clayton, C. R. I. (1996). The use of surface waves in the determination of ground stiffness profiles. *Proc. Instn Civ. Engrs (Geotech. Engng),* **119**, April, 84–95.

Matthews, M. C., Hope, V. S. and Clayton, C. R. I. (1997). The geotechnical value of ground stiffness determined using seismic methods. *Modern Geophysics in Engineering Geology*, (Eds. D. M. McCann, M. Eddleston, P. J.

Fenning and G. M. Reeves). Geol. Soc. Engng Geol. Special Publication No. 12, 113–124.

Matthews, M. C., Clayton, C. R. I. and Own, Y. (2000). The use of field geophysical techniques to determine geotechnical stiffness parameters. *Proc. Instn Civ. Engrs (Geotech. Engng)*, **143** Jan, 31–42.

McClelland Engineers, Inc. (1967). *Appendix C, Criteria for Predetermining Pile Capacity* Report section included for clients of offshore geotechnical investigations.

McClelland B. (1972). Design and performance of deep foundations. *Proc. ASCE Speciality Conf. on Performance of Earth and Earth Supported Structures. Lafayette, Indiana*, **2**, pp. 111–145.

McClelland, B. (1974). Design of Deep Penetration Piles for Ocean Structures *Proc. ASCE J. Soil Mech. & Fdn Engng*, **100** (7), 705–747.

McClelland, B., Focht, I. A. and Emrich, W. J. (1969). Problems in design and installation of offshore piles. *Proc. ASCE J. Soil Mech. & Fdn Engng*, **95** (SM6), 1491–1514.

McNulty, J. F. (1956). Thrust loading on piles. *Proc. ASCE J. Soil Mech. & Fdn Engng*. Paper 940 (SM2).

Meigh, A. C. (1963). Discussion on settlements on granular soils. *Proc. Eur. Conf. Soil Mech. & Fdn Engng, Wiesbaden*, **2**, pp. 71–72.

Meigh, A. C. and Nixon, I. K. (1961). Comparison of *in situ* tests for granular soils. *Proc. 5th Int. Conf. Soil Mech. & Fdn Engng*, *Paris*, DUNOD, Paris, **1**, pp. 499.

Meigh, A. C. and Corbett, B. O. (1970). A comparison of *in situ* measurements on a soft clay with laboratory tests and the settlement of oil tanks. *Proc. Conf. In situ Investigations in Soil and Rocks*, ICE, London, pp. 173–179.

Menzies, B. K. (1988). A computer controlled hydraulic triaxial testing system. *Advanced Triaxial Testing of Soil and Rock*. ASTM STP 977, 82–94.

Menzies, B. K. (1997). Applying modern measures. *Ground Engng*, July, London.

Menzies, B. K. (2000). Near surface site characterisation by ground stiffness profiling using surface wave geophysics. *H. C. Verma Commemorative Volume*. Indian Geotechnical Society, New Delhi.

Menzies, B. K. and Hooker, P. (1992). PC and local microprocessor controlled geotechnical testing systems. *Proc. Int. Conf. Geotechnics and Computers. Paris*.

Menzies, B. K., Sutton, H. and Davies, R. E. (1977). A new system for automatically simulating K_0 consolidation and K_0 swelling in the conventional triaxial cell. *Géotechnique,* **27** (4), 593–596.

Meyerhof, G. G. (1953). The bearing capacity of foundations under eccentric and inclined loads. *Proc. 3rd Int. Conf. Soil Mech. & Fdn Engng*, *Zurich*, ICOSOMEF, Zurich, **1**, pp. 440–445.

Meyerhof, G. G. (1956). Penetration tests and bearing capacity of cohesionless soils. *Proc. ASCE J. Soil Mech. & Fdn Engng*, **82** (SM1).

Meyerhof, G. G. (1959). Compaction of sands and bearing capacity of piles. *Proc. ASCE J. Soil Mech. & Fdn Engng*, (SM6), 1–29.

Meyerhof, G. G. (1965). Shallow foundations. *Proc. ASCE J. Soil Mech. & Fdn Engng*. **91** (SM2), 21–31.

Meyerhof, G. G. (1976) Bearing Capacity and Settlement of Pile Foundations *Proc. ASCE J. Soil Mech. & Fdn Engng*, **102** (3), 1–29.

Moon, M. R. (1972). A test method for the structural integrity of bored piles. *Civ. Eng. and Public Works Rev.,* 476–480.

Moran, Proctor, Meuser, and Rutledge (1958). Study of deep soil stabilization by vertical sand drains. *Report for Bureau of Yards and Docks*. Department of the Navy.

Murray, R. T. (1971). Embankments constructed on soft foundations; settlement study at Avonmouth. *Report No. 419*, TRL Crowthorne, 26 pp.

Nazarian, S. and Stokoe, K. H. (1984). In situ shear wave velocities from spectral analysis of surface waves. *Proc. 8th World Conf. on Earthquake Engineering*, 3**,** 31–38.

Newmark, N. M. (1942). *Influence charts for computation of stresses in elastic soils*. University of Illinois, Eng. Experimental Station Bulletin. No. 338.

NGI Publication No. 188, Norwegian Geotechnical Institute, Oslo 1992:

Karlsrud, K. and Nadim, F. Axial capacity of offshore piles in clay.

Lacasse, S. and Goulois, A. Uncertainty in API parameters for prediction of axial capacity of piles in sand.

Karlsrud, K., Hansen, S. B., Dyvik, R. and Kalsnes. NGI's pile tests at Tilbrooke and Pentre – review of testing procedures and results.

Nowacki, F., Karlsrud, K. and Sparrevik. Comparison of recent tests on OC clay and implications for design.

Karlsrud, K., Kalsnes, B. and Nowacki, F. Response of piles in soft clay and silt deposits to static and cyclic axial loading based on recent instrumented pile load tests.

Nordin, P. Q. and Svensson, L. (1974). Settlements of buildings founded on lightly over-consolidated clay in Western Sweden. *Proc. Conf. Settlement of Structures, Cambridge*, Pantech Press, London, pp. 116–122.

Nordlund, R. L. (1959). Bearing capacity of piles in cohesionless soils. *Proc. ASCE J Soil Mech. & Fdn Engng.* (SM3), 1–35.

Okamura, M., Sahara, F., Takemura, J. and Kusakabe, O. (1998). Load settlement behaviour of shallow footings on compressible sand deposits. *Proc. Int. Conf. Centrifuge 98*, Tokyo, 435–440.

Palmer, D. J. and Stuart, J. G. (1957). Some observations on the standard penetration test and a correlation of the test with a new penetrometer. *Proc. 4th Int. Conf. Soil Mech. & Fdn Engng*, *London*, Butterworth, London, **1**, pp. 231–236.

Parry, R. H. G. (1971). A direct method of estimating settlements in sands from SPT values. *Proc. Symp. Interaction of Structure and Foundations*, Midlands Soil Mech & Fdn Engng Soc., Birmingham, pp. 29–37.

Parry, R. H. G. and Swain, C. W. (1977). Effective Stress Methods of Calculating Skin Friction on Driven Piles in Soft Clay. *Ground Engineering,* **10** (3), 24–26.

Peck, R. B. (1958) A study of the comparative behaviour of Friction Piles. *Highway Research Board Special Report No. 36*. Washington, DC: National Research Council.

Peck, R. B. (1962). Art and science in subsurface engineering. *Géotechnique,* **12**, 60–68.

Peck, R. B. and Bazaraa, A. R. S. S. (1969). Discussion. *Proc. ASCE J. Soil Mech. & Fdn Engng*. **95** (SM3), 305–309.

Peck, R. B., Hanson, W. E. and Thornburn, T. H. (1974). *Foundation Engineering,* John Wiley and Sons, Inc., 514 pp.

Pelletier, J. H., Murff, J. D. and Young, A. C. (1993). Historical development and assessment of the current API design methods for axially loaded piles. OTC 7157, *Proc. 25th Offshore Technology Conf., Houston, Texas*, pp. 253–281.

Plantema, G. and Nolet, C. A. (1957). Influence of pile driving on the sounding resistances in a deep sand layer. *Proc. 4th Int. Conf. Soil Mech. & Fdn Engng*, London, Butterworth, London, **2**, pp. 52–55.

Poulos, H. G. (1971). Behaviour of laterally loaded piles. *Proc. ASCE J. Soil Mech. & Fdn Engng*. (SM5), 711–731 (Part 1, single piles); 733–751 (Part 2, pile groups).

Poulos, H. G. and Davis, E. H. (1974). *Elastic Solutions for Soil and Rock Mechanics.* John Wiley & Sons, New York.

Poulos, H. G. and Mattes, N. S. (1969). The analysis of downdrag in end bearing piles. *Proc. 7th Int. Conf. Soil Mech. & Fdn Engng*, *Mexico*, Scociedad Mexicana de Mecanica de Suelos, **2**, pp. 203–209.

Powrie, W. (1997) *Soil Mechanics: Concepts and Applications*. E & FN Spon, London. 420 pp.

Randolph, M. F. (1999). Private communication.

Randolph, M. F. and Murphy, B. S. (1985). Shaft capacity of driven piles in clay. *Proc. 17th Annual Offshore Technology Conference*, *Houston*, **1**, pp. 371–378.

Raymond, G. P., Townsend, D. L. and Lojkasek, M. J. (1971). The effect of sampling on the undrained soil properties of a Leda soil. *Canadian Geotechnical J.*, **8**, 546–557.

Reese, L. C. and Matlock, H. (1956). Non-dimensional solutions for laterally loaded piles with soil modulus assumed proportional to depth. *8th Texas Conf. Soil Mech. & Fdn Engng* Special Publication No. 29, University of Texas.

Reynolds, O. (1886). Experiments showing dilitancy, a property of granular material. *Proc. Royal Inst.,* **11**, 354–363.

Rodin, S. (1961). Experiences with penetrometers with particular reference to the stand ard penetration test. *Proc. 5th Int. Conf. Soil Mech. & Fdn Engng*, *Paris*, DUNOD, Paris, **1**, p. 517.

Rodrigues, J. S. (1975). *The development and application of a finite element program for the solution of geotechnical problems*. PhD Thesis, University of Surrey, Guildford.

Roscoe, K. H., Schofield, A. N. and Wroth, C. P. (1958). On the yielding of soils. *Géotechnique*, **8** (1), 22–52.

Rowe, P. W. (1968). The influence of geological features of clay deposits on the design and performance of sand drains. *Proc. Instn Civ. Engrs*, Supplement Paper 70585, 72 pp.

Rowe, P. W. (1972). The relevance of soil fabric to site investigation practice. 12th Rankine Lecture. *Géotechnique,* **22** (2), 195–300.

Rowe, P. W. and Barden, L. (1965). Closure to discussion on: Importance of free ends in triaxial testing. *Proc. ASCE J. Soil Mech. & Fdn Engng*. **91**, 105–106.

Rowe, P. W. and Barden, L. (1966). A new consolidation cell. *Géotechnique,* **16**, 162–170.

Rutledge, P. C. (1944). Relation of undisturbed sampling to laboratory testing. *Trans. ASCE,* **109**.

Sanglerat, G. (1972). *The Penetrometer and Soil Exploration*. Elsevier, 464 pp.

Sanglerat, G., Girousse, H. and Gielly, J. (1974). Unusual settlements of a building at Nantua (France). *Proc. Conf. Settlement of Structures*, *Cambridge*, Pantech Press, London, 123–131.

Sawaguchi, M. (1971). Approximate calculation of negative skin friction of a pile. *Soils and Foundations,* **2** (3), 31–49.

Schmertmann, J. H. (1953). Estimating the true consolidation behaviour of clay from laboratory test results. *Trans. ASCE.*, **79**, Separate No. 311.

Schmertmann, J. H. (1955). The undisturbed consolidation behaviour of clay. *Trans. ASCE*. No. 120, Paper 2775, pp. 1201–1233.

Schmertmann, J. H. (1970). Static cone to compute static settlement over sand. *Proc. ASCE J. Soil Mech. & Fdn Engng*. **98** (SM3), 1011–1043.

Schmertmann, J. H., Hartman, J. P. and Brown, P.R. (1978). Improved strain influence factor diagrams. *Proc. ASCE J. Soil Mech. & Fdn Engng*, **104** (GT8), 1131–1135.

Semple, R. M. and Rigden, W. J. (1984) Shaft capacity of driven pipe piles in clay. *Proc. Symp. on Analysis and Design of Pile Foundations*. ASCE Nat. Convention, San Francisco.

Serota, S. and Jennings, R. A. J. (1959). The elastic heave of the bottom of excavations. *Géotechnique,* **9** (1), 62–70.

Simons N. E. (1957). Settlement studies on two structures in Norway. *Proc. 4th Int. Conf. Soil Mech. & Fdn Engng*, London, Butterworth, London, **1**, pp. 431–436.

Simons, N. E. (1963). Settlement studies on a nine-storey apartment building at Økernbråten, Oslo. *Eur. Conf. Soil Mech. & Fdn Engng Wiesbaden*, **1**, pp. 179–191.

Simons N. E. (1967). Discussion, *Proc. Geotech. Conf. Oslo*, Session 2: shear strength of stiff clay, pp. 159–160.

Simons. N. E. (1971a). The stress path method of settlement analysis applied to London clay. *Proceedings Roscoe Memorial Symposium on Stress–Strain Behaviour of Soils*, *Cambridge*, G. T. Foulis, Henley-on-Thames, pp. 241–252.

Simons, N. E. (1971b). Discussion, *Conference on Behaviour of Piles*, ICE, London, p. 94.

Simons, N. E. (1974). General Report, Session 2, *Proc. Conf. Settlement of Structures*, *Cambridge*, Pantech Press, London.

Simons, N. E. and Som, N. N. (1969). The influence of lateral stresses on the stress deformation characteristics of London clay. *Proc. 7th Int. Conf. Soil Mech. & Fdn Engng*, *Mexico City*, Scociedad Mexicana de Mecanica de Suelos, **1**, pp. 369–377.

Simons, N. E. and Som, N. N. (1970). Settlement of structures on clay with particular emphasis on London clay. *Constr. Industry Research Institute Assoc. Report 22*, 51 pp.

Simons, N. E. and Menzies, B. K. (1974). A note on the principle of effective stress. *Géotechnique* **24**, 259–261.

Simons N. E. and Huxley, M. A. (1975). *The effect of negative skin friction on the bearing capacity of piles in granular soils*. Private communication.

Simons, N. E, Rodrigues, J. and Hornsby, P. A. (1974). Discussion. *Proc. Conf. Settlement of Structures*, *Cambridge,* Pantech Press, London.

Skempton, A. W. (1951). The bearing capacity of clays. *Building Research Congress*, England.

Skempton, A. W. (1953). Discussion, *Proc. 3rd Int. Conf. Soil Mech. & Fdn Engng*, *Zurich*, ICOSOMEF, Zurich, **3**, p. 172.

Skempton, A. W. (1954). The pore pressure coefficients A and B. *Géotechnique,* **4**, 143–147.
Skempton, A. W. (1959). Cast *in situ* bored piles in London clay. *Géotechnique,* **9** (4), 153–173.
Skempton, A. W. (1960). Significance of Terzaghi's concept of effective stress. *From Theory to Practice in Soil Mechanics*. John Wiley. New York.
Skempton, A. W. (1961). Horizontal stresses in over-consolidated Eocene clay. *Proc. 5th Int. Conf. Soil Mech. & Fdn Engng*, *Paris*, DUNOD, Paris, **1**, pp. 351–357.
Skempton, A. W. (1964). Fourth Rankine Lecture: Long-term stability of clay slopes. *Géotechnique,* **14**, 77–101.
Skempton, A. W. (1966). Summing-up. *Proc. Symp. on Large Bored Piles*, ICE, London, pp. 155–157.
Skempton, A. W. and Bishop, A. W. (1954). *Soils, Building Materials, their Elasticity and Inelasticity*. Ch. 10. North Holland Publishing Company, Amsterdam.
Skempton, A. W. and MacDonald, D. H. (1956). The allowable settlement of buildings. *Proc. Instn Civ. Engrs*, **5 (**3), 737–784.
Skempton, A. W. and Bjerrum, L. (1957). A contribution to the settlement analysis of foundations on clay. *Géotechnique,* **7** (4), 168–178.
Skempton, A. W. and Sowa, V. A. (1963). The behaviour of saturated clays during sampling and testing. *Géotechnique,* **13**, 269–290.
Skempton, A. W., Peck, R. B., and MacDonald, D. H. (1955). Settlement analyses of six structures in Chicago and London. *Proc. Instn Civ. Engrs*, Part 1, **4** (4), 525.
Som, N. N. (1968). *The effect of stress path on the deformation and consolidation of London clay*. PhD Thesis, University of London.
Somerville, S. H. and Shelton, J. C. (1972). Observed settlement of multi-storey buildings on laminated clays and silts in Glasgow. *Géotechnique,* **22**, 513–520.
Steinbrenner, W. (1934). Tafeln zur Setzungberechnung. *Die Strasse*, **1**, 121.
Sutherland, H. B. (1963). The use of *in situ* tests to estimate the allowable bearing pressure of cohesionless soils. *Struct. Eng.,* **41** (3).
Sutherland, J. B. (1974). General Report. Session 1, *Proc. Conf. Settlement of Structures*, Cambridge.
Tatsuoka, F. and Shibuya, S. (1992). *Deformation characteristics of soils and rocks from field and laboratory tests*. Report of the Institute of Industrial Science, The University of Tokyo, **37** (1), 1–136.
Taylor, D. W. (1948). *Fundamentals of soil mechanics*. John Wiley, New York, 700 p.
Taylor, R. N. (ed) (1995). *Geotechnical centrifuge technology*. Blackie Academic & Professional, Chapman and Hall, London.
Telford, W. M., Geldart, L. P. and Sheriff, R. E. (1990). *Applied Geophysics*. 2nd Edition, Cambridge University Press, Cambridge, 770 pp.
Terzaghi, K. (1 936). The shearing resistance of saturated soils. *Proc. First Int. Conf. Soil Mech., Cambridge, Mass*, Harvard University, **1**. pp. 54–56.
Terzaghi, K. (1936). Settlement of structures. *Proc. 1st Int. Conf. Soil Mech. & Fdn Engng, Cambridge, Mass*, Harvard University, **3**, pp. 79–87.
Terzaghi, K. (1939). Soil mechanics – a new chapter in engineering science. James Forrest Lecture. *Journal Instn Civ. Engrs,* No. 7, pp. 106–141.

Terzaghi, K. (1941). Undisturbed clay samples and undisturbed clays. *J. Boston Soc. of Civ. Eng,* **28** (3), 211–231.

Terzaghi, K. (1943). *Theoretical Soil Mechanics.* John Wiley and Sons Ltd., 510 pp.

Terzaghi, K. (1948). Closing Discussion on: Foundation pressure and settlements of buildings on footings and rafts. *Proc. 2nd Int. Conf. Soil Mech. & Fdn Engng*, *Rotterdam,* **6**, p. 118.

Terzaghi, K. and Redulic, L. (1934). Die wirksame Flächenprosität des Bretons. Zeit, öster. *Ing. Orch. Ver.*, **86**, pp. 1–9.

Terzaghi, K. and Peck, R. B. (1948). *Soil Mechanics in Engineering Practice.* 1st edition, New York, Wiley.

Terzaghi, K. and Peck, R. B. (1967). *Soil Mechanics in Engineering Practice.* 2nd edition, Wiley, New York, 729 p.

Timoshenko, S. and Goodier, J. N. (1951). *Theory of Elasticity,* McGraw Hill.

Tokimatsu, K., Kuwayama, S., Tamura, S. and Miyadera, Y. (1991). V_s determination from steady state Rayleigh wave method. *Soils and Foundations*, **31**(2), 153–163.

Tomlinson, M. J. (1957). The adhesion of piles driven in clay soils. *Proc. 4th Int. Conf. Soil Mech. & Fdn Engng.*, *London*, Butterworth, London, **2**, pp. 66–71.

Tomlinson, M. J. (1969). *Foundation Design and Construction.* Pitman Publishing, 2nd edition, p. 785.

Tomlinson, M. J. (1970). *Research on the Skin Friction of Piles Driven into Stiff Clays.* CIRIA Research Report.

Tomlinson, M. J. (1971). Some effects of pile driving on skin friction. *Proc. Conf. Behaviour of Piles*, ICE, London, pp. 107–114.

Vargas, M. (1955). Foundation of structures on over-consolidated clay layers in Sao Paulo. *Géotechnique,* **5**, 253–266.

Vefling, G. (1974). Settlements of three heavy sugar silos in Italy. *Proc. Conf. Settlement of Structures, Cambridge*, Pantech Press, London, pp. 132–138.

Vijayvergiya, Y. N. and Focht, J. A. (1972). A new way to predict capacity of piles in clay. *Proc. 4th Annual Offshore Technology Conference*, **2**, OTC Paper 171 8, Houston, Texas, May 1–3, pp. 865–874.

Wakeling, T. R. M. (1970). A comparison of the results of standard site investigation methods against the results of a detailed geotechnical investigation in Middle Chalk at Mundford, Norfolk. *Proc. Conf. on In situ Investigations in Soils and Rocks*, British Geotechnical Society, ICE, London, 17–22.

Walker, L. K. and Darval, P. L. P. (1973). Dragdown on coated and uncoated piles. *Proc. 8th Int. Conf. Soil Mech. & Fdn Engng, Moscow*, USSR Nat. Soc. Soil Mech. & Fdn Engng, **2.1**, pp. 257–262.

Ward, W. H. (1971). Some field techniques for improving site investigations and engineering design. *Proc. Roscoe Memorial Symposium on Stress–Strain Behaviour of Soils*, pp. 676–682.

Ward, W. H., Burland, J. B. and Gallois, R. W. (1968). Geotechnical assessment of a site at Mundford, Norfolk, for a large proton accelerator. *Géotechnique,* **18**, 399–431.

Ward, W. H. (1961). Displacements and strains in tunnels beneath a large excavation in London. *Proc. 5th Int. Conf. Soil Mech. & Fdn Engng*, *Paris*, DUNOD, Paris, **2**, pp. 749–753.

Westerberg, N. (1926). Jordtryck i Kohesionara jordarter. *Tek. Tidsk. Vag. o. Vatten,* **51**, pp. 25–29.

Whitaker, T. (1970). *The Design of Piled Foundations.* Pergamon Press, 188 pp.

Whitaker, T. and Cooke, R. W. (1966). An investigation of the shaft and base resistance of large bored piles in London clay. *Proc. Conf. Large Bored Piles*. ICE, London, pp. 7–49.

Wilkes, P. F. (1974). *A geotechnical study of a trial embankment at Kings Lynn*. PhD Thesis, University of Surrey.

Woodward, R. J., Lundgren, R. and Boitano, J. D. (1961). Pile loading tests in stiff clays. *Proc. 5th Int. Conf. Soil Mech. & Fdn Engng*, *Paris*, DUNOD, Paris, **2**, pp. 177–184.

Wroth, C. P. and Simpson, B. (1972). An induced failure of a trial embankment. Part 2: finite element computations. *Conference on Performance of Earth and Earth Supported* Structures, Purdue, **1.1**, pp. 65–79.

Wroth, C. P. (1972). Discussion on the design and performance of deep foundations. *Conference on Performance of Earth and Earth Supported Structures*, *Purdue*, ASCE. **3**, pp. 231–234.

Young, A. G. (1991). Marine foundation studies. *Handbook of Coastal and Ocean Engineering*, **2**, Ch. 7. John B. Herbich, Ed. Gulf Publishing Co. pp. 446–596.

Zeevaert, L. (1957). Foundation design and behaviour of Tower Latino Americana in Mexico City. *Géotechnique,* **7**, 115–133.

Zeevaert, L. (1958). Consolidation of Mexico City's volcanic clay. *Proc. Conf. Soils for Engineering Purposes*, ASTM, STP, No. 232, p. 28.

Zeevaert, L. (1960). Reduction of point bearing capacity of piles because of negative friction. *Proc. 1st Pan American Conf. Soil Mech.*, Mexico, **3**, pp. 1145–1152.

Index

Note: page numbers in *italics* represent figures.